Assessing indicators of population size and causes of extinction in late Quaternary megafauna

By

Nicholas George Spano

A dissertation submitted in partial satisfaction of the

requirements for the degree of

Doctor of Philosophy

in

Integrative Biology

in the

Graduate Division

of the

University of California, Berkeley

Committee in charge:

Professor Anthony D. Barnosky, Chair
Professor Cynthia V. Looy
Professor Thomas Bruns

Spring 2020

Abstract

Assessing indicators of population size and causes of extinction in late Quaternary megafauna

By

Nicholas George Spano

Doctor of Philosophy in Integrative Biology

University of California, Berkeley

Professor Anthony D. Barnosky, Chair

Megafauna are ecologically important. They are ecosystem engineers that substantially modify modern ecosystems, and likely did so for prehistoric ecosystems prior to the Late Quaternary extinction (LQE) event as well. The LQE resulted in the loss of ~65% of all large mammals during an age of global climate change and human population expansion. This means that understanding the causes and ecological impacts of megafauna preceding, during, and following the LQE is important for better understanding megafauna ecology and conservation today.

To further this understanding, here I 1) explore the developing body of indicators used for inferring historic and prehistoric megafauna abundances; 2) investigate the environmental conditions surrounding human arrival and megafauna extirpation in Brazil, and; 3) test how sensitive the *Sporormiella* megafauna indicator is to temperature and humidity, as these factors could confound megafaunal population-size estimates based on *Sporormiella* abundances.

The first chapter reviews the many different population-size indicators used in megafauna paleoecology. and finds all have their pros and cons regarding their applicabilities towards reconstructing megafauna populations depending on the depositional environment and other taphonomic factors. A widely used indicator of relative megafauna population size is the abundance of the dung fungus *Sporormiella* in sediment records, despite the need for more taphonomic work necessary to more robustly relate spore abundance to megafauna abundance.

The second chapter untangles the relationship between climate, vegetation changes, human population growth, and megafauna decline surrounding the LQE in Brazil as a case study. I found that combinations of anthropogenic, climatic, and vegetational changes are likely implicated as causal factors, but the tree factors vary in their importance for different regions of Brazil. However, human population growth prior to the megafauna extirpation stands out as most notable.

The third chapter reports results of an experiment that tested the effects of temperature and relative humidity on *Sporormiella* growth. I found that humidity above 89% does not notably affect *Sporormiella* growth but temperature in the range of 10-40°C is important.

In sum, this means that there is room for development of megafauna indicators, nuances between how different LQE causes can be distinguished at finer spatial scales, and reason to suggest that past climate change may bias *Sporormiella*-based reconstructions of megafauna populations.

Chapter 1: A review of terrestrial vertebrate paleo-presence and -abundance indicators

Spano, N.[1, 2]
[1]Department of Integrative Biology, University of California, Berkeley, Berkeley, California, United States of America
[2]University of California Museum of Paleontology, University of California, Berkeley, Berkeley, California, United States of America
E-mail: spano@berkeley.edu

Abstract

Terrestrial vertebrate paleo-presence and -abundance indicators are indirect measures of past vertebrate occupation at or around a depositional site. They include a broad set of indicators that have been used for various archaeological, paleoecological, and historic applications, but an integrated review of their pros, cons, and efficacy has been lacking. Here I provide such a review that includes fungal spores, steroidal biomarkers, paleoenvironmental DNA, pollen and plant spore types associated with vertebrates, radiometric date clusters from bone records, invertebrate remains, and other miscellaneous past vertebrate population density indicators. Although much remains unknown about the taphonomy and fidelity of these vertebrate population indicators, this review highlights a great potential for actualistic experiments, advances in identification tools, and additional applications to further our understanding of these novel sources of information about past vertebrate populations.

Introduction

Terrestrial vertebrate paleo-population-density indicators (PDIs) are indirect markers of past vertebrate population densities, in contrast to more direct observational methods that can be applied to living biota. This is a precise definition that encompasses a group of indicators that have been reviewed separately (e.g., Rawlence et al., 2014; Perrotti & van Asperen, 2019) but not yet in an integrated way. Evaluating these indicators together provides a better understanding about their potential applications, including: reconstructing Quaternary faunal communities (Lydolph et al., 2005); reconstructing historic pastoral landscapes (Chepstow-Lusty et al., 2019; Etienne et al., 2015; Giguet-Covex et al., 2014; Guillemot et al., 2015); pinpointing Hannibal's path through the Alps en route to invading Italy (Mahaney et al., 2017); and the timing of extinctions during the Quaternary. These latter applications include both Holocene insular extinctions (Wood et al., 2011; Graham et al., 2016; Burney, Robinson, & Burney, 2003) and late Pleistocene examples (Halligan et al., 2016). Along with determining the timing of Quaternary extinctions, some studies have applied these PDIs to document ecological state-shifts following Quaternary defaunation (Gill et al., 2009; Rule et al., 2012; Barnosky et al., 2016; Robinson, G. S., Pigott Burney, L., & Burney, 2005).

PDIs and paleoenvironmental indicators are commonly preserved alongside each other and can thus provide complementary sources of information for more complete paleoenvironmental reconstructions. For example, by combining records of dung fungal spores with pollen records, we can better understand the establishment of animal husbandry practices through time (Setyaningsih et al., 2019) and the evolution of pastoral landscapes (Guillemot et al., 2015; López-Merino et al., 2009; Schofield & Edwards, 2009). These synoptic studies can also help to inform debates regarding the causes of late-Quaternary extinctions by more precisely timing vertebrate last appearances in comparison with environmental changes (e.g., Fiedel, 2018). In associated research areas, PDIs can help inform long-term perspectives on landscape restoration and ecological baseline assessment through enabling inferences about vertebrate paleo-population-densities with their associated habitats (Bradshaw, Hannon, & Lister, 2003; Vera, 2000; Birks, 2005). PDIs can also potentially provide insights regarding pre-Quaternary terrestrial vertebrate-ecosystem dynamics, as many of these PDIs were present before the Quaternary (e.g., Davis & Ellis, 2010; Andreev et al., 2014)

Survey methodology

My literature search included three queries through Web of Science with all available databases and articles published from 1864 - 2019 and the following search terms on 16 October 2019:

For indicator fungal spores:

TS=(((pal$eo* OR arch$eolog* OR histor*) AND (((dung OR coprophilous OR keratin*) AND fung* AND spore$) OR sporormiella)))

For indicator plant spores/pollen:

TS=(((pal$eo* OR arch$eolog* OR histor*) AND (palyno* OR pollen$) AND (livestock OR pastor* OR megafauna$ OR grazer$) AND (indicator$ OR proxy OR proxies)))

This query returned 144 articles on the *Sporormiella* (synonym: *Preussia*) indicator. The bibliographies of relevant publications were then mined to further identify pertinent articles. Here I generally cite only the most comprehensive or recent articles, but many additional relevant references can be found in review articles cited within this review (e.g., Perrotti & van Asperen, 2019; Evershed & Bethell, 1996; Rawlence et al., 2014; and references therein).

Defining terrestrial vertebrate paleo-population-density indicators

Although this review focuses on terrestrial vertebrate paleo-population-density indicators, some of those covered here (e.g., steroidal biomarkers, pollen types associated with vertebrates, radiometric date clusters from bone records, and helminth (parasitic worm) eggs) have so far only been applied to infer vertebrate presence. Complications in using these indicators to infer vertebrate population density include taphonomic pathways that may be largely unknown and that can bias the population estimate unduly. Thus, I provide this caveat that many of the indicators discussed here are still largely undeveloped, but may well reflect terrestrial population densities and have the potential to be further refined.

I limit this review to terrestrial vertebrates because the field of aquatic vertebrate paleo-population-density indicators is relatively unestablished, aside from historical quantitative studies that use fisheries records to infer fish population densities (see Jackson & McClenachan, 2017). Similarly, relatively little information is available about non-vertebrate paleo-population-density indicators relative to the situation for vertebrates. However, paleoenvironmental DNA (PalEnDNA) studies could provide insights for reconstructing populations of invertebrate and plant communities (Rawlence et al., 2014).

In the context of this paper, the "paleo" in PDIs is more of a methodological definition than a temporal one, given that the temporal extent of included studies ranges from centuries (e.g., Etienne et al., 2015) to potentially more than 65 million years (e.g., Schweiger & Svenning, 2018). Regarding population density, all paleo-indicators are spatially- and temporally-averaged to some

degree, so to reflect this, I use the term population density to indicate the average number of individuals per unit area instead of overall population size. I refer to these remains as indicators instead of proxies because proxies are assumed to be direct substitutes for their given forcing variable(s) (Cohen, 2003, p. 4). Many of these indicators have not yet been tested enough to be *bona fide* direct substitutes for terrestrial vertebrate paleo-population densities. My intent in this review is to provide an overview of the PDIs, taphonomic considerations that may affect them, and future directions to potentially strengthen these indicators towards better reconstructing terrestrial vertebrate paleo-population densities.

Indicators

This review focuses on a broad set of organic remains that can be preserved in sediments, including fungal spores, steroidal biomarkers, paleoenvironmental DNA (PalEnDNA), pollen types associated with vertebrates, radiometric date clusters from bone records, invertebrate remains (including those from dung beetles, dung-inhabiting mites, and helminth eggs), and other miscellaneous PDIs (Fig. 1). Summarized information regarding their population density fidelities, taxa each indicator has been associated with, host-taxon precisions, depositional environments, relative preservation potentials, and applications is available in the literature (see Table 1 for an overview).

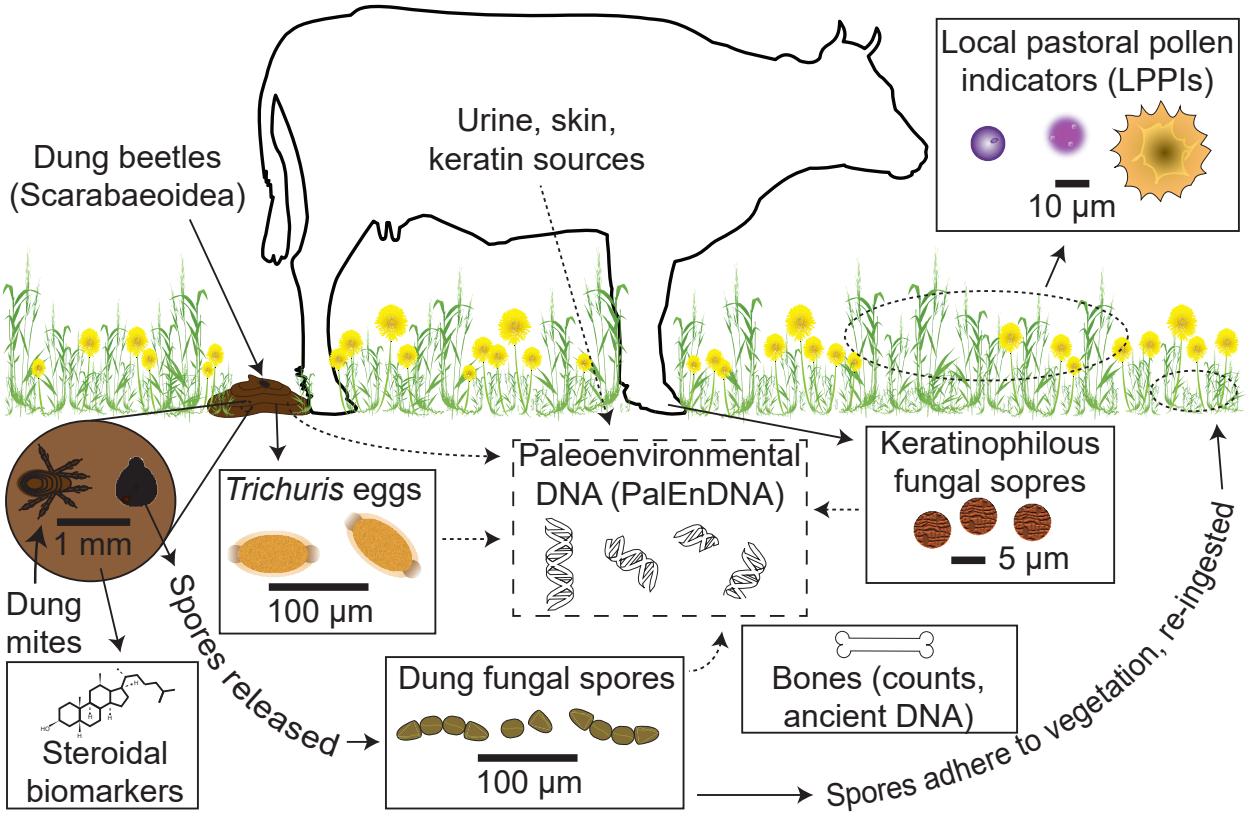

Figure 1: Terrestrial vertebrate paleo-presence and -abundance indicators mentioned in the text.

Table 1: Characteristics of terrestrial vertebrate paleo-population density indicators

General indicator	Population density fidelity	Taxa the indicator has been associated with	Host-taxon precision	Depositional environments	Relative preservation potential	Paleo applications	References
Coprophilous fungi (*Sporormiella* (syn: *Preussia*), *Sordaria*, *Podospora*)	Assumed to be high but requires more understanding	Mammals and birds	Medium-high	Lacustrine sediments, peatland sediments, marine sediments, soils, and dung	High	Linking late-Quaternary extinctions with environmental change; reconstructing pastoral landscapes	Aptroot & van Geel, 2006; Baker, Bhagwat, & Willis, 2013; Chepstow-Lusty et al., 2019; Davis, 1987; Ekblom & Gillson, 2010; Graham et al., 2016; Guillemot et al., 2015; Ledger et al., 2014; Perrotti & van Asperen, 2019; and references therein

Keratinophilous fungi	Unknown	Mammals, arthropods, and birds	Unknown or low	Caves, cold sediments, marine sediments, and archaeological soils	Unknown or low to medium-low	Proposed megafaunal indicator associated with mammoth, bison, and horse DNA in permafrost; proposed indicator of anthropogenically-altered Medieval settlements in Russia and Kazakhstan	Cano & Guarro, 1990; Ginarte et al., 1996; Hayes, 2012; Howard, 2002; Ivanova & Marfenina, 2015; Presbury & Young, 1978; Van Oorschot & Connie, 1980; Zhang et al., 2006; Zimmermann, 2008
Steroidal biomarkers	Unknown	Mammals	Medium	Dung, soils, mire sediments, and aquatic sediments	Medium to high	Identifying fecal material in archaeological soils; lipid analysis of a ground sloth coprolite; timing Hannibal's invasion of Italy; documenting historic fecal pollution in lake sediments; testing a putative 14,000 year-old human coprolite from Oregon; reconstructing a	Evershed, 1993; Evershed & Bethell, 1996; Gill et al., 2009; Guillemot et al., 2015; Mahaney et al., 2017; Müller et al., 1979; Sistiaga et al., 2014; and references therein

						pastoral landscape from Greenland	
Paleoenvironmental DNA (PalEnDNA)	Unknown	Many	Medium	Many	Medium	Reconstructing paleoenvironmental histories; timing megafaunal extirpations; taxonomic surveys; reconstructing pastoral landscapes	Etienne et al., 2015; Graham et al., 2016; Hadly et al., 2004; Parducci et al., 2017; Rawlence et al., 2014; Ramakrishnan et al., 2005; and references therein
Pastoral pollen indicators (PPIs)	Unknown	Mammalian livestock	Unknown	Soils	High	Reconstructing pastoral landscapes	Florenzano et al., 2015; Gauthier et al., 2010; Ledger et al., 2014; Ledger, Edwards, & Schofield, 2015; Mercuri & Carter, 2013; Qiu et al., 2014; van Geel et al.,

							2003; Velázquez & Burry, 2012
Fossil bones	Medium to good, depending on sample size, taxa, and taphonomy	Many	Large vertebrates: Poor to medium Small vertebrates: Medium to high (depending on depositional system)	Coastal, fluvial/deltaic, lacustrine, volcanigenic, eolian, *et al*	High	Linking late-Quaternary extinctions with environmental change	Barnosky, ed., 2004; Damuth et al., 1992; Guthrie, 2006; Kidwell & Flessa, 1996; Shapiro et al., 2004; Western & Behrensmeyer, 2009
Dung beetles	Unknown	Extinct megafauna (inferred) and domesticated mammals	Unknown	Dung, soils	Low	Landscape shifts following Quaternary large herbivore extinctions in the UK; environmental reconstruction of a Roman archaeological site in the Netherlands	Sandom et al., 2014; van Geel et al., 2003
Mites (Orders: Oribatida and Gamasina)	Unknown	Humans, livestock, and poultry	Medium (Gamasina) or unknown	Pasture soils, lake sediments, and archaeological dung deposits	Medium	Identifying archaeological dung deposits; timing the rise and fall of the Inca empire with	Baker, 2009; Chepstow-Lusty et al., 2007, 2019; Leng et al.,

						lake sediments	2007; Schelvis, 1987, 1990, 1992
Helminth eggs	Unknown	Sheep, goats, cattle, and humans	Unknown	Archaeological latrines	Medium	Paleo-parisitological surveys in archaeological contexts	Ejarque, Miras, & Riera, 2011; Reinhard et al., 1986

Fungi

Many fungi produce spores with thick, chitinous cell walls that presumably lend them to being well preserved in sediment records (e.g., van Geel et al., 2003; Cook et al., 2011). The thick walls of these spores likely makes dormancy possible, meaning that these spores would remain in such a state and not germinate after deposition into sediment records. A subset of these fungi utilize dung or keratin as nutrient sources, which puts them in direct association with animal hosts. Those that utilize dung (coprophilous fungi) have a well-characterized life history (Newcombe et al., 2016), including: (1) ingestion by terrestrial vertebrates; (2) defecation; (3) germination; (4) and spore ejection from the fungal fruiting bodies on the dung's surface to new substrates. If that substrate is more forage, the fungi may repeat the cycle, being ingested once more (Richardson, 2001). Spores that become incorporated into sediment records are thought to do so through short-distance wind dispersal or sticking to clayey soil particles and then washing into basins through surface runoff (Etienne et al., 2013). It has been hypothesized that the evolution of endothermy was important for the origination of coprophilous fungi, as only a few dung fungi are found on the dung of invertebrates or ectothermic vertebrates (Krug, Benny, & Keller, 2004).

The three dung fungal spore types thought to be the most reliable as PDIs are those of *Podospora, Sordaria,* and *Sporormiella* (Baker, Bhagwat, & Willis, 2013). These fungi have been applied as PDIs more than any other group. Most of these applications focus on *Sporormiella* because it can be relatively easily identified by its distinct gumdrop-shaped tetrad spores and sigmoid-shaped germination slits (see Fig. 1 and Bell, 2005). These applications include: documenting the rise and fall of the Inca (Chepstow-Lusty, Frogley, & Baker, 2019); dating the extinction of moas in New Zealand (Wood et al., 2011); discovering the earliest known evidence of buffalo husbandry and rice cultivation in Sumatra (Setyaningsih et al., 2019); assessing the causes of Australian Pleistocene large mammal extinctions (van der Kaars et al., 2017) and their ecological consequences (Rule et al., 2012); similarly, estimating the timing of North American Pleistocene large mammal extinctions (Halligan et al., 2016) and their ecological consequences (Barnosky et al., 2016; Gill et al., 2009; Robinson, Burney, & Burney, 2005); reconstructing pastoral landscapes (López-Merino et al., 2009; Innes & Blackford, 2003; Bowes et al., 2015; Orbay-Cerrato et al., 2017; and references therein); and investigating sediment records for the ecological consequences of historic herbivore introductions to islands (Wood et al., 2016). Other fossil dung fungal spores have been applied as PDIs too, including those of *Chaetomium*, *Cercophora*, *et al*, but their usefulness remains relatively unknown (Baker et al., 2013).

The usefulness of *Podospora, Sordaria, and Sporormiella* has also come under scrutiny, with recent studies questioning the fidelities of these fungi to terrestrial vertebrate dung, environmental factors affecting spore production, and sedimentary factors affecting spore preservation. Although these fungi have been referred to as obligate to dung, this is not entirely true. For example, *Sordaria fimicola* and *Sporormiella* can sexually reproduce on *Bromus tectorum* (cheatgrass) (Newcombe et al.,

2016) and may do so on other plants too. Also, *Sporormiella* can be found growing in Brazilian black and white pepper (*Piper nigrum*) (Freire, Kozakiewicz, & Paterson, 2000). This is not to say that these fungi are not indicative of dung and thus terrestrial vertebrates, but more accurately, that these fungi are commonly but not always encountered on dung. However, it is unknown how frequent these non-dung-growth cases are and how spore production from these fungi growing on substrates other than dung could be contributing to sediment records. In sum, the application of these PDIs as mostly direct substitutes for terrestrial vertebrates should be done cautiously given these alternative growth habits.

Environmental factors might also affect the utility of dung fungal spores as PDIs. These factors include how (in)tolerant dung fungi are to different climate conditions and how dung fungal communities differ between habitats. Both of these suggest that factors other than population densities (e.g., temperature, precipitation, nearby vegetation, etc.) could drive dung fungal spore quantities and mask a vertebrate population signal. For example, *Sporormiella* appears late after other dung fungi in dung fungal successional sequences (Angel & Wicklow, 1983) and is relatively tolerant of low water content (Kuthubutheen & Webster, 1986b), which occasionally may give *Sporormiella* a competitive advantage. However, a high water concentration may cause *Sporormiella* to be out-competed by other coprophilous fungi (van Asperen, 2017). This, combined with the fact that in temperate latitudes, dung fungal diversity is higher in wetter, cooler seasons and lower *vice versa* suggests that there may be a seasonality to dung fungal PDIs. In temperate latitudes, persistently warm and dry weather may therefore cause a lack of dung fungi, even when the terrestrial vertebrate dung that would otherwise host them is abundant. It is also known from experimental work that these dung fungi do not grow well under extreme conditions of temperature or humidity (Perrotti & van Asperen, 2019). More broadly, climate can have a significant influence on dung fungal presence and further studies are needed to address how (paleo)climate may confound interpretations of dung fungal spore assemblages as PDIs.

Significant differences in dung fungal communities between habitats can complicate the use of these fungi as PDIs too. For example, the abundance and diversity of fungal spores is much higher in peatlands than lake watersheds assumedly because these fungi are dispersal-limited and can grow directly on the peatland localities (Cook et al., 2011). This means that PDI records from peat cores could portray a much different paleoenvironmental story than those from lake sediments. Similarly, Wood & Wilmshurst (2012) found that *Sporormiella* spore abundances from cores sampled in dry habitats in New Zealand correlate well with known histories of livestock introduction and population density. However, the relationship between livestock and *Sporormiella* assemblages in wetter New Zealand habitats is less clear (Wood & Wilmshurst, 2012). Remains of testate amoebae, wetland herb pollen types, and moisture-sensitive moss spores from these wetter locations suggest that wetland soil moisture introduces a strong confounding factor for the *Sporormiella* indicator (Wood & Wilmshurst, 2012).

Spore dispersal and sedimentation are two taphonomic factors that may affect dung fungal PDI representation and utility (see taphonomic factors in Fig. 2). Regarding spore dispersal, the

spores of *Sordaria* and *Sporormiella* can be found at least 15 m above ground in meteorological samples (Haskouri et al., 2016; Hernández Trejo et al., 2012). This suggests that wind may be a more significant dung fungal spore dispersal agent than previously suggested. Also, given dung fungal PDIs take weeks to germinate and produce spores from a dung sample, defecation directly into water (e.g., from animals cooling off at a lake shore) likely contributes very few spores to these records. For ambient spores washed into these basins though, significant changes in dung fungal spore assemblages through time may be caused by changes in watershed transport and sedimentation regimes. For example, studies by Raper & Bush (2009) and Parker & Williams (2012) argued that coring proximity to shoreline is a significant predictor of *Sporormiella* quantities in lake sediments. Given that dung-fungal spores are thought to enter basins mostly through surface runoff, the idea here is that these spores are settling closer to shorelines than they are to deeper parts of lakes. However, a study by Etienne et al. (2013) did not find this to be a significant predictor, instead finding a significant correlation between lake inlet stream proximity and spore quantities. In all of these cases, changes in hydrologic regimes can significantly affect spore quantities by changing where the spores are deposited and how close the vertebrates in question are to a given shoreline at any given time (Fig. 2 & 3). Therefore changes in relative percentages of spores through a core should be matched carefully with sedimentary history to ensure that changes in percentages are not possibly attributable to changes in the position of inlets.

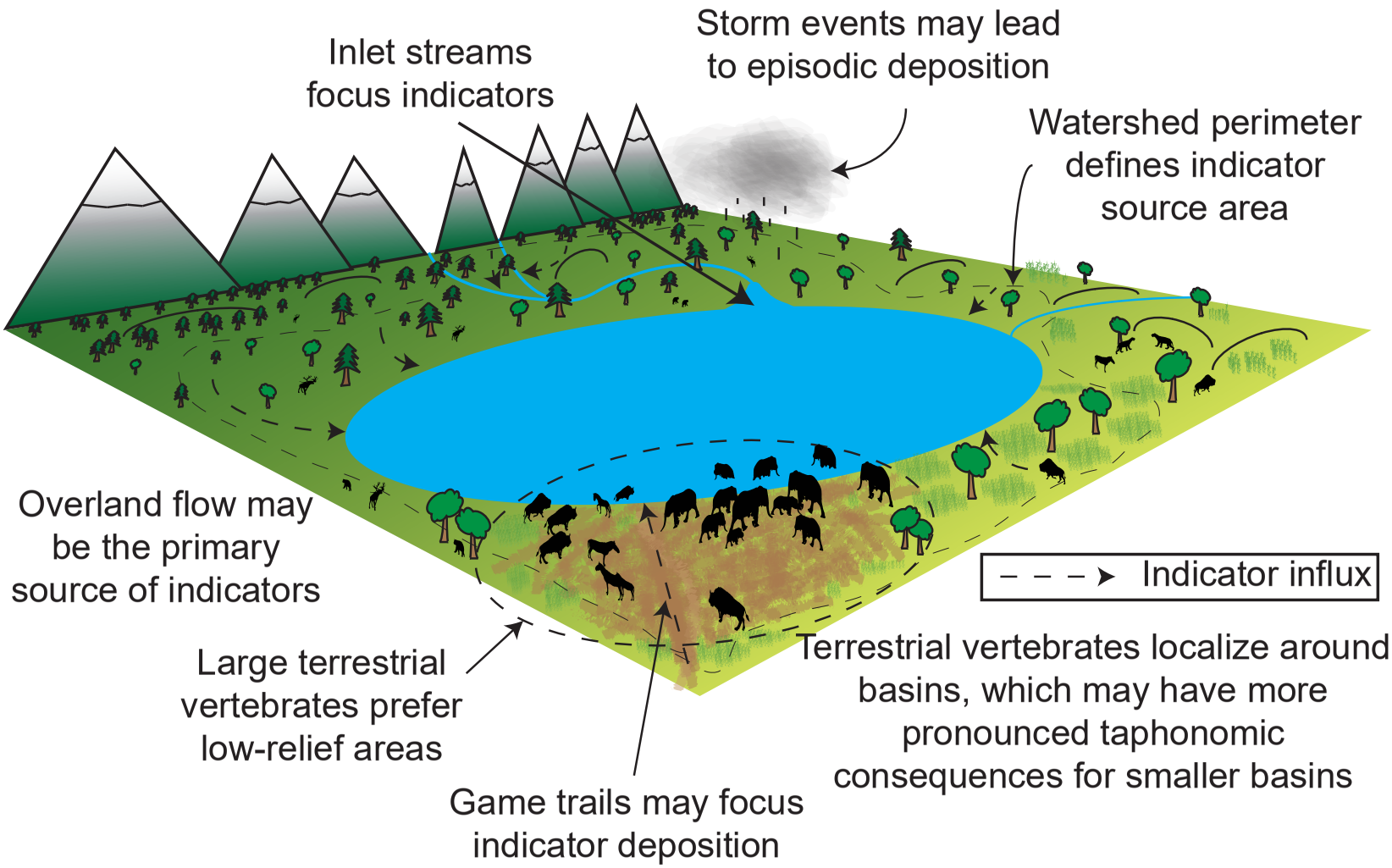

Figure 2: Taphonomic factors that may affect terrestrial vertebrate paleo-presence and -abundance indicators.

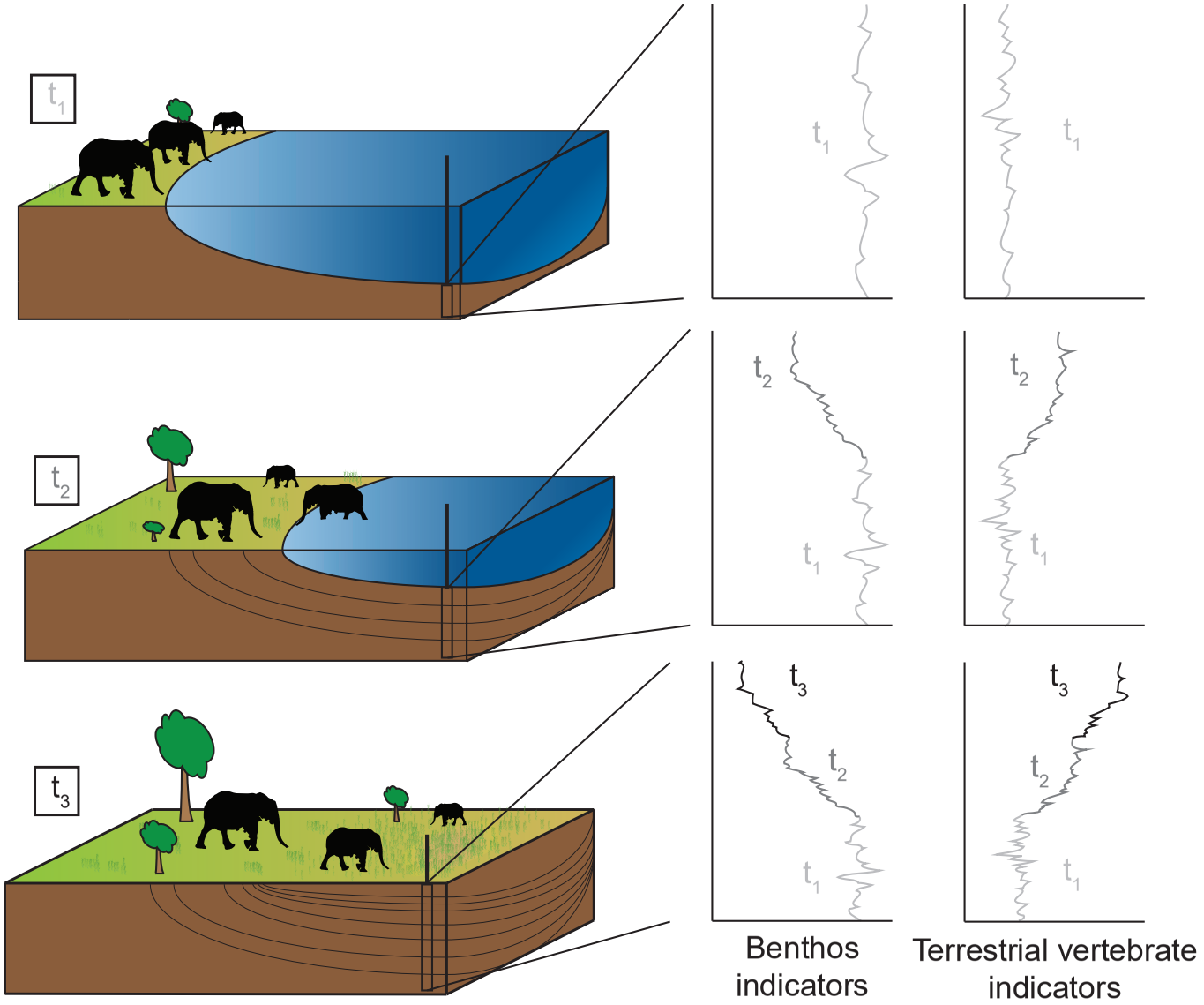

Figure 3: Decreases in terrestrial vertebrate paleo-presence and -abundance indicators can be due to changes in lake levels, independent of changes in terrestrial vertebrate densities.

Lastly for dung fungal spores, work by van Asperen, Kirby, & Hunt (2016) showed that different palynological preparation techniques can yield significantly different spore quantities, highlighting the importance of sample processing in PDI interpretations. To account for this, Perrotti & van Asperen (2019) recommended the development of a more standardized dung fungal spore processing procedure, which would make comparisons between studies easier. This method would ideally involve minimal acetolysis to reduce spore degradation and sieving and separation by heavy liquids to maximize dung fungal spore retention (van Asperen, Kirby, & Hunt, 2016).

In summary, the factors that can significantly affect counts of dung fungal spores in cores include their fidelity to dung, their sensitivity to weather and climate, and how they are transported and deposited into sediment records. Further studies investigating how different dung fungal PDIs associate with different substrates (e.g., soils, plant tissues, different dung types) and how viable they are on each could provide insights regarding the relative importance of each substrate as a dung fungal PDI source. Actualistic studies linking temperature and humidity to dung fungal growth (e.g., Asina, Jain, & Cain, 1977; Kuthubutheen & Webster, 1986a, 1986b) in controlled lab and field settings could highlight the significance of these variables to dung fungal spore abundances, including diurnal and seasonal variability, species-specific responses to weather differences, and so forth. Tests that would be appropriate for assessing the importance of transport and deposition are highlighted below in the **Future directions** section.

Fungi that utilize keratin as a carbon source (keratinophilous fungi) have not been as well studied as coprophilous fungi, but have potential for further development as PDIs. These fungi grow on hair, nails, and skin (Lydolph et al., 2005), and their spores are presumably transported by surface runoff into depositional settings as well. Most work with keratinophilous fungi has focused on humans or archaeological sites, but a handful of studies note their incidence associated with non-human vertebrates, including mammoths, bison, horses, penguins, seals, birds, shrews, and voles (Table 1). Some of these fungi, including *Aphanoascus keratinophilous* (Cano & Guarro, 1990), *Chrysosporium tropicum*, and *C. pannicola* (Oorschot, 1980), have relatively thick spore cell walls, which might lend them to being well preserved in sediment records. However, the only evidence of keratinophilous fungi that have been associated with Pleistocene large mammals is PalEnDNA sequences of *Phialopora* and *Geomyces pannorum* (Lydolph et al., 2005).

Other fungal remains that might have potential as PDIs but have been even less studied include parasitic plant fungi recovered from dung and fungi that grow in or on vertebrate epithelial tissues. *Urocystis* is a genus of smut fungi which parasitizes many plant families. Members of this taxon may be found in cattle dung (Ejarque, Miras, & Riera, 2011) and thus through association with this terrestrial vertebrate, have potential as a PDI. The extent to which *Urocystis* and other parasitic plant fungi (e.g., *Clasterosporium caricinum, Sphaerodes*, and *Arthrinium* cf. *luzulae*) (Ejarque, Miras, & Riera, 2011) are consumed by terrestrial vertebrates and thus may be good PDIs is unknown, but is an area of future potential research. For fungi associated with vertebrate epithelial tissues—including lungs (Summerbell, 2004) and rumens (Wubah, 2004)—to become incorporated into sediment records, they need to be effectively transported outside of the vertebrate body. While it is unknown

how often this happens with fungi that grow in vertebrate lungs, the symbiotic rumen fungi *Neocallimastix, Piromyces, Orpinomyces,* and *Caecomyces* have been found as viable spores in fecal smears isolated from cattle (Wubah, 2004). The general extent to which these other fungi may be preserved as body fossils or provide PalEnDNA sequences (see below) is currently unknown.

Steroidal biomarkers

Steroidal biomarkers are organic compounds with four carbon rings that can remain unaltered in sediments for potentially millions of years (Bethell et al., 1994), making them a robust group of PDIs. Two groups of steroidal biomarkers found in sediments—5β-stannols and cholic (or bile) acids—are mostly metabolic products of digestion in vertebrates (Evershed, 1993). The 5β-stannols commonly applied include 24β-ethyl-5β-cholestano-3β-ol (5β-stigmastannol) and 5β-cholestan-3β-ol (coprostanol/coprosterol). 5β-stigmastannol is the gut-microbially-reduced form of the plant sterol sitosterol, which is derived from plant cell membranes. Because 5β-stigmastannol is only known to be formed from this pathway originating from plants, it may be an indicator obligate to plant matter or herbivore dung (Sistiaga et al., 2014). Similarly, coprostanol is the gut-microbially-reduced form of cholesterol (derived from animal cell membranes), differing from cholesterol only by a reduced double bond between $C_{5\text{-}6}$ (Walker, Wun, & Litsky, 1982). Coprostanol has been primarily applied as an indicator of human fecal pollution (Jeng, & Han, 1994; Müller et al., 1979; Sherwin et al., 1993; Walker, Wun, & Litsky, 1982). Coprostanol breaks down quicker in the water column than some other organic molecules (e.g., petroleum production byproducts) (LeBlanc et al., 1992) and much more quickly in aerobic conditions than anaerobic conditions (Elhmmali, Roberts, & Evershed, 1997). However, coprostanol might adsorb to sediments and become relatively stable once bound (LeBlanc et al., 1992).

The diversity of these fecal steroids is due to differences in vertebrate metabolic pathways and diets, meaning that they can be applied to identify vertebrate taxa with a relatively high degree of precision (Table 1). Some 5β-stannols can be created from microbial epimerization outside of vertebrate intestines though, meaning the presence of 5β-stannols alone does not necessarily indicate vertebrate presence (Mahaney et al., 2017). Also, the concentration of 5β-stannols in sediments can increase with input of 5α-stannols not specific to vertebrate presence, confounding the relationship between 5β-stannols and vertebrate presences. To account for this, Bethell et al. (1994) recommended normalizing the concentration of coprostanol in sediments by the abundance of total 5β- and 5α-stannols. High values of this ratio represent fresh dung, whereas values of ~54-55% represent disseminated fecal input into sediments (Bethell et al., 1994). Similarly, the ratio of coprostanol to its byproduct isomer—5β-cholestan-3α-ol (epicoprostanol)—is known to vary between vertebrate taxa and can be used to distinguish human from marine mammal fecal inputs (Sherwin et al., 1993). A recent study by Harrault et al. (2019) demonstrated the power of these PDIs to distinguish multiple wild and domesticated Siberian mammals in an archaeological context.

They did so by comparing multiple 5β-stannols, four previously applied ratios between these 5β-stannols, and the correlation of these historic 5β-stannols with known values from recent dung samples using principal component analysis (PCA) and hierarchical clustering on principal components (HCPC). They suggest that using more 5β-stannols can resolve mammalian sources in archaeological contexts more precisely without added costs, as all of the 5β-stannols they tested can be analyzed in a single mass spectroscopy run. Although they were unable to distinguish 5β-stannol signatures from some samples using these techniques (e.g., humans and dogs with similar omnivorous diets), many taxa could be distinguished (e.g., horses from cattle, reindeer with lichen-rich winter diets vs. reindeer with lichen-poor summer diets, etc.) using these techniques. This highlights the rich potential of 5β-stannols to be further applied as PDIs.

The other group of steroidal PDIs—bile acids—are formed directly from cholesterol in the vertebrate digestive system (Evershed, 1993). They have been applied as PDIs to pinpoint the path Hannibal's army took through the Alps to invade Italy (Mahaney et al., 2017) and to document the establishment of pastoral landscapes in Southern Greenland (Guillemot et al., 2015). The primary bile acids produced in vertebrate livers are cholic acid and chodeoxycholic acid (Mahaney et al., 2017), which are then reduced by intestinal microbes into the secondary bile acids, deoxycholic acid and lithicholic acid, respectively (Evershed, 1993). After deposition, bile acids are more resistant to degradation than coprostanol (Elhmmali et al., 1997). Both primary and secondary bile acids are found in sediment records, and they are not known to be created outside of the vertebrate digestive system (Mahaney et al., 2017), making them fidelitous PDIs (Table 1). Because the concentrations of 5β-stannols and bile acids vary with digestive mechanisms (e.g., ruminants vs. monogastric mammals, herbivores vs. omnivores, etc.), the proportions of different 5β-stannols, different bile acids, and the two groups relative to each other can be very useful for differentiating terrestrial vertebrate presences from sediment records. For reference, Evershed & Bethell (1996) outline a very useful flow chart for using these proportions to distinguish human, ruminant, and porcine fecal inputs into sediments. The application of steroidal biomarkers in sediment records has been largely reserved for (zoo)archaeological and pollution studies, but holds a great potential for other vertebrates and prehistoric research.

Paleoenvironmental DNA (PalEnDNA)

Paleoenvironmental DNA (PalEnDNA) is ancient DNA (aDNA) from disseminated environmental materials (Rawlence et al., 2014). Direct sources of PalEnDNA can include bone, skin, muscle, urine, feces, eggshells, hair, teeth, gut contents, and saliva (Rawlence et al., 2014; Pedersen et al., 2015) (Fig. 1). Disseminated PalEnDNA-bearing environmental materials can include sediments, ice, soil, and tephra (Rawlence et al., 2014). Also, many reviews have focused specifically on PalEnDNA and aDNA (Rawlence et al., 2014; Parducci et al., 2017; and references therein), but few address the use of PalEnDNA as a PDI. Many terms have been applied to describe

disseminated DNA found in preserved environmental materials, including sedimentary ancient DNA (sedaDNA), dirt DNA, fossil DNA, and lake sediment DNA (lake sedDNA), but PalEnDNA succinctly and meaningfully includes all of them (Rawlence et al., 2014). As a PDI, PalEnDNA sequences have been applied to investigate the mid-Holocene extinction of the last known wooly mammoths (*Mammuthus primigenius*) on St. Paul Island (Graham et al., 2016) and over 5,000 years of pastoral landscape history in France (Giguet-Covex et al., 2014; Etienne et al., 2015). PalEnDNA has the distinct advantage over other PDIs for its ability to reconstruct population structures (Parducci et al., 2017), population bottlenecks (Chan, Anderson, & Hadly, 2006), and directly infer taxon-specific presences in paleoenvironments. PalEnDNA also provides a much more localized signal compared to classic indicators such as pollen and spores (Parducci et al., 2017). A more localized signal may be preferable for a given study, but should be compared with more regional signals for more synoptic paleoenvironmental reconstructions. Also, the upper age limit for which identifiable sequences of PalEnDNA can be identified is a product of temperature, pH, association with mineral surfaces, and oxygen availability (Parducci et al., 2017). Further taphonomic research on PalEnDNA—including experimental insights from modern environmental DNA—could enhance our understanding of PalEnDNA taphonomy for more informative PDI studies.

Pollen and spores

The distribution of vegetation is largely driven by climatic variables (Woodward, 1987). However, through selective browsing, trampling, and grazing (or non-grazing, in the case of *Nardus stricta* (Ejarque, Miras, & Riera, 2011)), herbivorous terrestrial vertebrates (especially ungulates) can also significantly affect and thus characterize plant communities (Gill, 2014). The scale at which this occurs can be studied in Quaternary sediment records through palynological analyses. Reconstructions of past plant communities can thus be used to infer population densities of herbivorous terrestrial vertebrates. The application of particular plant groups as PDIs can be roughly binned into two groups: pastoral pollen indicators (PPIs) and lawn grasses.

Pastoral pollen indicators (PPIs) are "a group of taxa strictly correlated to pastoral activities" (Bowes et al., 2015) (Fig. 1, Table 1). Local pastoral pollen indicators (LPPIs) are mainly entomophilous, do not disperse far from the parent plant, and are associated with pastoral landscapes through livestock disturbance regimes. These regimes include ungulate trampling/wallowing and agricultural disturbance, selective grazing, and removal or suppression of woody plants. Although they have been defined as strictly correlated to pastoral activities, the livestock behaviors that facilitate the abundances of these plants are found in modern wild terrestrial herbivores and were likely characteristic of (pre)historic wild animals too. This means that they may be found in pre-agrarian sediment records as indicative of wild, large mammalian herbivores.

Some examples of pollen types that have been applied as LPPIs include (of the Asteraceae): *Aster*, *Centaurea nigra*, *Carduus*, *Cirsium*, *Matricaria*, and Cichorieae (especially *Cichorium intybus* (Ejarque,

Miras, & Riera, 2011)); and of other groups: *Galium*-type, *Heracleum* cf., *Potentilla*, *Ranunculus*, and Ranunculaceae. An important taphonomic note for LPPIs is that substrate type and landscape openness independent of large herbivore behaviors can also correlate with the presence of LPPIs (Ejarque, Miras, & Riera, 2011), obscuring their fidelity as PDIs.

Regional pastoral pollen indicators (RPPIs) are also indicative of pastoral landscapes and thus grazing terrestrial vertebrates, but are dispersed more widely. These include pollen grains from *Artemisia*, Chenopodiaceae, *Plantago lanceolata,* and *Plantago major/media* (Mazier et al., 2006). Because these taxa are also anemophilous (see Clifford, 1962; Tkach et al., 2007; Borsch, 2009), their wider dispersal makes sense. As implied above, some of these pastoral indicators have also been verified as indicators of wild grazing ungulates, and it is often difficult to distinguish the effects of wild vs. domesticated grazers from pollen records. For example, the increased abundance of *Plantago lanceolata* before the Holocene elm decline in the English Lake District might have been caused grazing deer (Buckland & Edwards, 1984).

For some PPIs, it is unknown the extent to which they are more local vs. regional PDIs. These include *Urtica dioica* (stinging nettle) (López-Merino et al., 2009; Ejarque, Miras, & Riera, 2011), *Polygonum aviculare*, and Cerastium-type (Schofield & Edwards, 2011), and *Rumex* (Mazier et al., 2006). *Rumex,* however, is often found on the margins of wetlands, is only sporadically recovered from pastoral sites, and is thus not a reliable PPI (Mazier et al., 2006). Similarly, Cichorieae pollen types are commonly reported as LPPIs, but can be more commonly associated with Mediterranean river bed vegetation than pastoral landscapes (Florenzano et al., 2015), meaning that their fidelity to grazing terrestrial vertebrates is questionable. For pastoral landscapes, artificial mowing can result in pollen assemblages similar to those resulting from grazing behaviors, and it can thus be difficult to distinguish the two causes from a pollen assemblage alone. For example, *Ranunculus acris, Plantago lanceolata,* Cichorioideae, and Poaceae can be found in both artificially mown and naturally grazed landscapes (Hjelle, 1999). Also, Poaceae can include grasses that are more indicative of wetlands—such as reeds (e.g., *Phragmites*)—than grazing activities.

Some non-ruderal plants, including Scrophulariaceae, *Linaria*-type, *Sedum*, and Cyperaceae have been observed in livestock feces (Ejarque, Miras, & Riera, 2011) and thus might be valuable as PDIs. In areas where grasses were not present before human arrival, Poaceae can act as a livestock indicator (Ledger, Edwards, & Schofield, 2014), but this limited application is thus reserved for pastoral applications and is likely not meaningfully applicable as a PDI for wild vertebrates. Similarly, many of these pastoral plants can be found in human-disturbed habitats, independent of other terrestrial vertebrate activities. The degree to which these pastoral plants have recently become adapted to human- vs. herbivore-disturbed habitats is unknown, but may limit our ability to test the associations between these PDIs and actual terrestrial vertebrate population densities using modern studies. An interesting behavioral consideration that Hjelle (1999) observed is that some of these pastoral plants are grazed before flowering. These plants may be indicative of grazing behavior, but because their pollen dispersal can be suppressed by grazing, they might be underrepresented in pollen assemblages.

Along with PPIs, lawn grass taxa may also produce fossil assemblages indicative of terrestrial vertebrates. Lawn grass taxa are short statured plants that are grazing-adapted (Archibald et al., 2005). In areas of intense grazing such as the African savanna, lawn grass taxa can be found in abundance as grazing lawns—expanses of short grasses actively created and maintained by grazing (J.T. Verweij et al., 2006). Grazing lawns can also be found in western Alaska as swaths of *Carex subspathacea* (a sedge, not a grass) created by grazing black Brant geese (*Branta bernicula nigricans*) (Person et al., 2003). *Carex subspathacea* is an important indicator because it is only found in grazing lawn form, making it an obligate indicator of goose behavior and highlights the fact that large ungulates are not the only animals that can make grazing lawns. In general, these lawns can range from a few square meters to square kilometers, depending on the herbivores present, herbivore population densities, and landscape structure (Person et al., 2003). For example, hippos (*Hippopotamus amphibius*) and kob (*Kobus kob*) are known to maintain grazing lawns in different locations from each other (J.T. Verweij et al., 2006). It is important to note that swards, or expanses of even-statured (mostly defined as short-statured) grasses, can be also be classified as grazing lawns and include lawn grass taxa, but are not necessarily created by grazing. Likewise, some grazing lawns are facultatively created, but obligate lawns with plants that require regular grazing hold the highest potential as PDIs. Obligate grazing lawn plants from Africa are the best studied, and include the grasses *Andropogon greenwayii*, *Cynodon dactylon*, *C. plectostachys*, *Paspalum conjugatum*, *Pennisetum clandestinum*, and *Stenotaphrum secundatum*. (Hempson et al., 2015).

A major consideration for utilizing lawn grasses as PDIs is that they produce pollen grains that are visually distinct and preserve well. Distinguishing different grasses in pollen assemblages is notoriously difficult, but these lawn grasses may also produce distinct phytoliths that preserve well and could thus be utilized as PDIs. No known studies have yet actively sought to link pollen or phytolith assemblages with grazing lawns in sediment records, so this remains a potential area of further research. For pollen PDIs, the ability of fire to open landscapes and promote plants that favor open landscapes may produce pollen assemblages indistinguishable from those produced by terrestrial vertebrate herbivores. For example, *Pteridium aquilinum* and *Melampyrum* have been suggested as grazed forest indicators, but may also benefit from fires (Svenning, 2002). Also, significant changes in browse-plant quantities inferred from their pollen types could indicate changes in terrestrial vertebrate paleo-population densities. For example, an increase in the abundance of *Fraxinus nigra*-type and *Ostrya/Carpinus* pollen from Appleman Lake, Indiana, at 13.7 ka is thought to be from a loss of Pleistocene megaherbivores (Gill et al., 2009). Similarly, the spread of *Nothofagus* forests in southwestern Patagonia may have resulted from the loss of Pleistocene megaherbivores there (Barnosky et al., 2016).

Fossil bones

Extrapolating population densities of large mammals from fossil bone records is well known to be a questionable task (Bradshaw, Hannon, & Lister, 2003). Large-mammal bones tend to have wider distributions in space and time about a given environment; however, fossils of small mammals can be more localized in space and can provide valuable information on small-mammal population densities (Hadly, 1994; Barnosky, 2004; Terry, 2008). Some studies have attempted to utilize temporal clusters of radiocarbon dates from bones of large mammals as indicators of population density. The idea here is that if there are many vertebrates leaving their radiocarbon-datable bones on landscapes, we can infer from clusters of these dates that there were many individuals at that location at that time and that changes in these clusters may represent changes in population densities. For example, Pleistocene-Holocene radiocarbon date clusters of horse, wooly mammoth, bison, wapiti, moose, and human bones have been used to investigate the timing of large mammalian herbivore extirpation vs. human arrival in Siberia, Beringia, and northwest North America (Alaska and the Yukon Territory) (Guthrie, 2006; Zimov, Zimov, & Chapin, 2012). In a more sophisticated approach, Steele (2010) investigated the record of North American human radiocarbon dates to estimate initial Pleistocene-Holocene colonization speeds. By binning frequencies of radiocarbon first-appearance data (FADs) for humans in North America, Steele (2010) argued that this event frequency could be used as a proxy for population concentrations. Similarly, Goldberg, Mychajliw, & Hadly (2016) estimated the population density of South American humans throughout the Holocene by utilizing Bayesian- and likelihood-based models applied to radiocarbon FADs.

Although I include radiocarbon date clustering as a PDI, these studies have actually attempted to determine the spatial distributions of FADs and last-appearance dates (LADs). In general, clustering radiometric dates of bones to infer paleo-population densities is a very rough approach that involves a relatively high degree of time-averaging and has only been applied at regional scales. It may, however, provide insights regarding at least the presence and possibly the relative abundances of vertebrates through time. By applying this approach to more localized scales at localities with high-resolution vertebrate chronologies (e.g., select bone assemblages in caves), a closer sense of population density might be achievable.

Invertebrate remains

Some invertebrates are well-known to be associated with terrestrial vertebrates and have hard parts that preserve well. These include select dung beetles (Coleoptera: Scaraboidea in the families Geotrupidae, Aphodiinae and Scarabaeinae) (Raine & Slade, 2019), oribatid and gamasid mites (Class: Arachnida, Order: Oribatida; Order: Parasitiformes), and helminth (parasitic worm) eggs. Dung beetles in particular are intuitively associated with terrestrial vertebrates through

vertebrate dung. The chitinous remains of dung beetles can be found in archaeological deposits (van Geel et al., 2003), woodlands, pastures (Sandom et al., 2014), and tar pits and tar seeps (Miller, 1983) (Table 1). Although no studies have yet applied dung beetle assemblages to explicitly infer vertebrate paleo-population densities, their remains have been applied to argue that the loss of late-Pleistocene large mammals caused a decrease in dung beetle diversity in Great Britain (Sandom et al., 2014) and a downsizing of dung beetles throughout Europe (Schweiger & Svenning, 2018). Notably, dung beetle body size is well-known to be closely correlated to dung size, which in turn is closely related to dung-producer size (Hanski & Cambefort, 2014). Although this is not quite taxon-specific, it may mean that mean that the sizes of dung beetle remains in paleo-records could be used to infer the presences of some vertebrates over others (e.g., large dung beetles associated with proboscidean dung vs. smaller dung beetles associated with antelope dung). Some limitations behind applying dung beetle remains as PDIs include the fact that dung beetle macrofossils are better preserved in wet areas (Sandom et al., 2014) and their remains cannot be temporally resolved as well as microfossil PDIs can. Also, dung beetles can become associated with other hosts or become frugivorous if their dung-producing hosts disappear, as may have happened as part of the late-Quaternary extinction event (Raine & Slade, 2019). Thus, if dung beetles are to be applied as PDIs, they should be done so in conjunction with paleo-hydrological indicators (e.g., remains of diatoms, chironomids, testate amoebae) and other PDIs for comparison.

Regarding mites, the two groups that may be the most useful as PDIs are oribatids and gamasids. Oribatids are small (~1 mm), generally soil-dwelling detritivores that can be found in moist habitats on decaying vegetation, soil, and dung (Chepstow-Lusty et al., 2007). Most oribatids have a low dispersal ability (Gulvik, 2007) which may make them useful for inferring local terrestrial vertebrate paleo-population densities. They have been applied mostly as indicators of local plant communities and habitats (e.g., peat bogs vs. oligotrophic lakes) (Solhøy, 2001), but a few studies have focused on select taxa as dung, pasture, and large herbivore indicators (e.g., Baker, 2009; Chepstow-Lusty et al., 2007; and Schelvis, 1992). Studies by Chepstow-Lusty et al. (2007, 2019) are the only ones that have focused on these mites as indicators of vertebrate densities in a stratigraphic context, which highlights the untapped potential for further research.

Like oribatids, gamasids are generally characteristic of environments rich in decaying organic matter and have been found in deposits consisting almost entirely of human and animal feces. However, historic remains of mites can be difficult to identify because their diagnostic legs, genitalia, and other features do not preserve well (Schelvis, 1990). One benefit of working with mites as PDIs though is that mite researchers have compiled detailed tables of associations between mite taxa and vertebrate dung. For example, Table 1 from Baker (2009) has information on a diverse set of mites from coprolites from Brazil and the US, and a publication by Schelvis (1992) has multiple tables with associations between gamasids and host dung samples. Again, these tend to be focused on domesticated animals for zooarchaeological purposes, but there is the potential for non-domesticates as well.

Lastly for invertebrate PDIs, parasitic worm (helminth) eggs are commonly found in fresh dung samples and coprolites (e.g., Reinhard et al., 1986, Ejarque, Miras, & Riera, 2011). These eggs are ~100 μm long and ovoid with grainy textures (see Fig. 1). They are very resistant to decay, having multiple layers that resist desiccation, strong acids and bases, oxidation, reduction, detergents, and proteolytic compounds (Jimenez, 2007, Fairweather & Threadgold, 1981; Quilès, Balandier, & Capizzi-Banas, 2006). Reinhard et al. (1986) reported their abundances in a stratified medieval latrine, suggesting that they may be found in other stratigraphic contexts too. Ejarque, Miras, & Riera (2011) reported that helminth egg abundances in modern domesticated livestock feces are higher than those for non-domesticates, suggesting a degree of taxonomic specificity. For their use as archaeological indicators and by extension, PDIs, the eggs of Ascaridae, Capillaridae, Trichuridae (whiptail worms), Oxyuridae, and cestodes (e.g., tapeworms) have been proposed as particularly useful (Bouchet et al., 2003). Other helminth eggs—including those from *Hymenolepsis, Dicrocoelium dentriiicum,* and *Enterobius vermicularis*—have also been found in stratified archaeological contexts but their potential utility as PDIs is less known, especially for other contexts (e.g., lake and peat sediments, cave records, etc.). Also, although helminth eggs are relatively resistant to decay, they are still subject to taphonomic alteration, including fracturing possibly from frost wedging (Reinhard et al., 1986). Plus, while some archaeological sites have well-preserved helminth eggs, other sites with similar climates have poorly preserved or absent eggs for reasons unknown.

Given these eggs are commonly found in bulk sediments, some paleo-parasitologists have attempted to isolate them using palynological processing techniques, including acetolysis and separation by density (Reinhard et al., 1986). These methods are favorable because the eggs that survive this process are cleaned by it and are thus easier to identify. In general though, helminth egg identification is notoriously difficult. For example, some diagnostic features may be obscured by using density separation techniques, and some eggs can be commonly confused with fungal spores. Also, with density separation, many techniques have been proposed, but there is currently no 'catch-all' standard approach that works for most helminth eggs from most sites.

Other indicators

Lastly, δ^{15}N values and remains of aquatic macroinvertebrates may have potential as unexplored PDIs. Work by Foote and Hornung (2005) showed that dragonfly and damselfly (Order: Odonata) diversity and abundance negatively correlates with cattle grazing pressure in Alberta, Canada. If bodily remains or PalEnDNA sequences from these insects preserve well in aquatic sediments, they may have potential as PDIs. Also, Keatley et al. (2011) argued that δ^{15}N values in a lake sediment core profile closely matched the proximity of seabird colonies, as seabird nitrogenous wastes are δ^{15}N-enriched relative to terrestrial and freshwater sources.

General taphonomic considerations

Given all of these remains are indicators and not quite proxies, their absences in sediment records may not necessarily reflect actual terrestrial vertebrate absences and vice versa. Davis (1987) exemplified this in the case of livestock being present around ponds when *Sporormiella* was absent from those pond sediment records. In general, this calls for further taphonomic consideration and testing, including more actualistic experiments, studies of vertebrate behaviors regarding PDIs, research comparing PDI sedimentation with actual population density records, refined PDI identification methods, and improved analytical methods.

Actualistic experiments

The taphonomic uncertainties associated with these indicators all call for actualistic experiments to assess the effects of environmental factors on PDI quantities. However, while existing actualistic studies note the importance of modern factors affecting PDI quantities (e.g., temperature and humidity affecting dung fungal growth), it is largely unknown the extent to which these modern environmental determinants are 'washed out' as noise in sediment records. This is not to say that these studies are uninformative, but that it is difficult to determine *a priori* which modern factors are most important for PDI taphonomy. Particularly informative experiments could involve known terrestrial vertebrate population densities in defined areas such as zoos, reserves, and sanctuaries. For example, an exceptional study by Baker et al. (2016) compared population records of vertebrates at a preserve in The Netherlands around human-made ponds ~16-31 years old with influx/accumulation rates of dung fungal spores. This study showed a significant correlation between the population densities of these vertebrates and dung fungal spore influx/accumulation rates retrieved from the pond sediment records. More studies that have similar time-spans should be conducted to bridge known terrestrial vertebrate population densities with resultant PDI quantities in recent sediment records.

Vertebrate behaviors and representation in sediment records

Given that vertebrates are known to concentrate around watering holes (Deocampo, 2002) and defecate in select latrines regularly (Perrotti & van Asperen, 2019), these behaviors may result in localized hotspots of PDIs (Fig. 2). Also, some vertebrates may have migratory behaviors that lend them to only being occasionally present around a given depositional site (Fig. 2). In a sediment record with a high temporal resolution (e.g., varved lake sediments), this may be observable as a seasonal trend. However, with a given hydrologic regime during the season of vertebrate presence, select PDIs may not preserve well and could thus represent a false extirpation event. Lastly, some

dung-loving arthropods (e.g., dung beetles, dung fungal gnats, etc.) can be significant dung fungal spore dispersal agents, which may lead to spores being dispersed much further away from their vertebrate hosts than expected (Graf & Chmura, 2006). The extent to which this could affect dung fungal spore records is unknown.

Sedimentation vs. actual paleo-population density

As previously mentioned for dung fungal spores, the causes for changes in PDI quantities may be difficult to distinguish (Dodson & Field, 2018) (Fig. 3). These could include changing shoreline conditions, episodic deposition (e.g., storm events), and dispersal from the vertebrate source to the coring location (Fig. 2 & 3). This is a potential concern for all other indicators mentioned (except radiometric date clustering) as well.

In general, the relationship between mesic vs. xeric conditions and microfossil PDI sedimentation and preservation is unclear. Overland flow of these indicators may lead to increased influx/accumulation rates, but for a given coring site, a laterally-expanding lake margin would mean that these indicators are settling out of the water column further away from the coring site (opposite from Fig. 3). Alternatively, a storm event could cause increased runoff of PDIs into a basin, dispersing PDIs into areas they would not normally reach (Cook, 2009) (Fig. 2). This could be inaccurately inferred as an acute terrestrial vertebrate population density growth event. Also, the grain size of the surrounding sediment is known to be a significant determinant of spore concentrations (Holmes, 1994) and thus may be so for microfossil PDIs as well. For example, sandy layers in a sediment core may represent high-energy times where significantly smaller microfossil PDIs might have been washed away and thus not preserved. Relatedly, as mentioned above for fungal spores sticking to clayey particles, a lack of clay minerals may result in lower preservation rates of microfossil and molecular PDIs, as they would have less sticky sediment to adhere to.

The shape of a lake basin may also affect the relationship between sedimentation and actual terrestrial vertebrate population density. For example, there may be plenty of vertebrates around hypothetical pan lakes/playas, but given the shallow nature of these lakes, the PDIs would likely be eroded and not well preserved. There may also be plenty of vertebrates around low-altitude and steeply-deepening rift lakes, but given the relatively low sediment influx/accumulation rates of those lakes, the preservation potentials there may be sub-optimal to compare low-resolution PDI quantities with paleo-population densities. The bowl-like shapes of alpine lakes may be ideal for preserving PDIs, but large vertebrates may avoid high-altitude locations to conserve energy (Taylor, Caldwell, & Rowntree, 1972; Wall, Douglas-Hamilton, & Vollrath, 2006). With those considerations, kettle and impact crater lakes are likely the best depositional environments for both focusing terrestrial vertebrates and reducing the chance that PDIs will be eroded or bioturbated.

PDI identification difficulty

As previously mentioned for dung fungal spores and helminth eggs, microfossil identification can be notoriously difficult. A trained eye in microfossil identification may take years to acquire, and even then, some microfossil groups are notoriously difficult to differentiate yet are ecologically distinct and important as indicators. This can limit the ability of researchers to apply PDIs for more comprehensive paleoecological studies, as the utility of many microfossil indicators is limited by their ability to be taxonomically resolved. The ability to more precisely and completely identify microfossil indicators would allow for microfossil-vertebrate associations to be more thoroughly and rigorously applied towards questions of how specific vertebrates interact with landscapes through time. Similarly, the vertebrate taxonomic resolution available with these indicators is quite variable and dependent upon multiple factors. These factors include the ability to identify microfossils to the species-level, the preservation and quality of PalEnDNA sequences, and the relative fidelities between PDIs and their vertebrate sources. Each of these concerns should be addressed to more precisely understand the relationships between terrestrial vertebrates and their paleo-environments through time.

Analytical concerns

For quantifying microfossil PDIs, the pros and cons of using relative quantification/abundance (microfossil quantity as a proportion of a total microfossil sum), concentration (microfossils per unit mass or volume), and influx/accumulation rate (microfossils per unit time and catchment area) have been addressed in detail by Baker et al. (2013) and Perrotti & van Asperen (2019). Both of these studies recommend using accumulation/influx rates as the most accurate way to quantify microfossil PDIs. Also, inferring changes in PDI quantities is often not done in a statistically significant manner. This is a problem because visual differences may not be analytically or paleoecologically meaningful. Statistical change-point analyses for univariate time series—including break or "two-phase" regression, Bayesian, and likelihood approaches—are particularly informative for identifying significant changes across temporal scales in climatological time series (Mudelsee, 2014a) and may also be particularly useful for PDI studies. These change-point detection methods are currently under-developed within the paleo-sciences in general (Mudelsee, 2014a), but could be advanced with insights from the statistical literature.

Future directions

There are many potential directions that could be taken to advance PDIs, including improving the understanding of relationships between PDIs and climatic factors, understanding

transport into lacustrine settings, comparing indicators together, streamlining identification techniques, extracting PalEnDNA from the indicators themselves, and applying PDIs to pre-Quaternary records.

Understanding climatic influences on PDIs

As previously mentioned for dung fungal spores, weather and climate are known to directly affect PDI quantities. These factors likely affect other fungal PDIs and invertebrate PDIs, and are known to affect pollen PDI quantities. Weather and climate can also indirectly affect PDI quantities through hydrogeologic processes, including pulses into depositional basins from storm events (Fig. 2). For dung-based PDIs especially, environments that are too wet may cause the dung to wash away or become too runny before significant PDI inhabitation can occur (e.g., dung fungal growth, dung mite and beetle occupation, etc.). As mentioned above, cultivating these indicators under controlled lab and field conditions can elucidate our understanding of these factors. For example, experimental work showing how dung fungal spore production rates vary between treatments of temperature and humidity on shorter time scales (e.g., diurnal temperature fluctuations, artificial rainfall events, etc.) could aid our understanding of how these acute factors could affect dung-based PDI production. At longer time scales, field-based experiments in locations with variable temperatures, humidities, wind velocities, vegetation, physiographic conditions, etc. could help aid our understanding of how these broader environmental factors affect dung-based PDI production. This could be especially insightful for understanding situations where large mammalian herbivores are known to be present but recent sediment records do not capture PDIs to corroborate this.

Understanding transport mechanisms into lacustrine settings

As Figures 2 & 3 show, the pathway a PDI may take from a vertebrate to a lacustrine basin can be complicated by many factors. These hydrogeologic complications can obscure the relationship between population densities and PDI quantities. Thus, understanding how these processes affect these relationships can bring us closer to accurately inferring population densities. Ideally, a long-term study to get at these factors could involve an experimental lake basin with known terrestrial vertebrate population densities and terrestrial (e.g., Tauber, 1974) and aquatic sediment traps to compare population densities with PDI influx/accumulation rates over many years. Physiographic factors of a given watershed—including relief, slope, aspect, and game trails—could be accounted for in this study to determine their contributions to PDI sediment records. Also, flume-based studies could improve our understanding of PDI microfossil sedimentology, which could provide insights regarding associations between PDI quantities and changes in hydrogeologic regimes.

Comparing indicators together

To investigate the effects of other environmental variables on PDI quantities, other indicators should be included in the same studies. This is especially important because some PDIs can mismatch even in the same record, suggesting that at least one of them is not accurately representing population density. For example, Chepstow-Lusty (2019) found that quantities of *Sporormiella* and Oribatid remains did not correlate with each other, even when the study area was known to have thousands of camelids present at times. Also, many researchers interested in timing Quaternary megafaunal extinctions using radiocarbon LADs and *Sporormiella* have found discrepancies between *Sporormiella* declines and the most recent Pleistocene megafaunal radiocarbon dates. For example, Gill et al. (2009) found *Sporormiella* to decline ~1,000-2,000 years before Pleistocene megafaunal LADs determined from radiocarbon samples. As *Sporormiella* is thought to be a higher-resolution microfossil indicator of large herbivore population densities, Gill et al. (2009) suggested that this discrepancy represents an initial population decline inferred from the *Sporormiella*, and a final population crash inferred from the radiocarbon dates. However, the opposite pattern could hold true in other cases, where LADs from bone records could preceed *Sporormiella* declines due to a low bone preservation potential in a given region or landscape. For paleoenvironmental indicators other than PDIs, remains of diatoms, chironomids, and testate amoebae can act as paleo-water-level indicators, which could control for the effects of basin size changes on PDI quantities. Similarly, quantities of *Glomus*—an endomycorrhizal fungus that forms spores below the soil surface (Cook et al., 2011)—and x-ray fluorescence (XRF) measurements could be used to detect changes in erosional regimes through time.

Different PDIs should be investigated in conjunction to test for covariances between two or more PDIs. If the covariances between two or more PDIs match (i.e., they correlate) and if these covariances match potentially known population density values, this suggests that these PDIs accurately represent population densities. If the covariances between two or more PDIs do not match each other or potentially known population density values, this would suggest that there are taphonomic/fidelity concerns that are hindering the usefulness of one or more of these PDIs. Spearman's grade correlation coefficient (r_s)—a form of Spearman's rank correlation coefficient (ϱ_s) modified for continuous random bivariate distributions (Mudelsee, 2014b)—may be an appropriate metric for testing the correlation between two PDI series.

Methods to improve microfossil PDI identification

A growing number of microfossil morphotypes have been photographed and cataloged (Doyen & Etienne, 2017). If microfossil morphotypes can be identified through machine learning, this may ameliorate the time spent trying to identify morphotypes and the expertise required to do so. This may be especially helpful for distinguishing different species of coprophilous fungi, who

differ only by slight variations in their spore axis lengths (Bell, 2005). As different species of coprophilous fungi have different host dung preferences, this may open the door to accurately making more refined spore-host association claims with microfossils (Baker, Bhagwat, & Willis, 2013).

PalEnDNA of indicators

Although indirect compared to genetic sequences directly from focal vertebrates, all of the aforementioned indicators (except steroidal biomarkers and nitrogen values) are sources of PalEnDNA too. As with above, correlations between PDIs, PalEnDNA from focal vertebrates, and PalEnDNA from PDIs could highlight taphonomic discrepancies relating to DNA transport and preservation. This may be currently infeasible, however, given the difficulty behind extracting miniscule quantities of vertebrate PalEnDNA, let alone the PalEnDNA of PDIs.

Pre-Quaternary applications

Except for PalEnDNA which has yet to be preserved from pre-Quaternary sediments and radiocarbon date clustering which does not work for pre-Quaternary records, all of the aforementioned PDIs were likely present in pre-Quaternary depositional environments too. Thus, these indicators should be observable in pre-Quaternary sediments as well. For example, *Sporormiella* has been found in Pliocene (Andreev et al., 2014) and even ~11.5 million-year-old Miocene sediments (Davis & Ellis, 2010). Also, dung beetles might have originated with mid-Cretaceous angiosperms and would thus have been associated with large herbivorous dinosaurs, but are at least associated with Paleogene megafauna (Schweiger & Svenning, 2018). And similarly, if the life cycle of dung fungi mostly centers around large terrestrial herbivores, spores of these fungi may be present in Paleogene sediments—possibly indicative of the first large mammals. By further exploring Quaternary and pre-Quaternary sediment records for PDIs, we may be able to gain novel insights regarding the paleoecology of terrestrial vertebrates and their environments through time.

Chapter 2: Chronology of late Quaternary megafaunal extinction, paleoenvironmental change, and human arrival in Brazil

Spano, N.[1, 2]
[1]Department of Integrative Biology, University of California, Berkeley, Berkeley, California, United States of America
[2]University of California Museum of Paleontology, University of California, Berkeley, Berkeley, California, United States of America
E-mail: spano@berkeley.edu

Abstract

Much work has investigated the late-Quaternary extinction event at continental scales, but few studies have focused on regional scales. I sought to investigate the vertebrate paleontological, archaeological, vegetational, and climatic conditions surrounding the late-Quaternary extinction event in Brazil, an area of South America that had not previously been studied in such detail. To do so, I utilized pre-existing references for all known Brazilian Pleistocene archaeological and megafaunal radiocarbon dates, and used the distribution of the resulting 1,163 archaeological dates and 13 megafaunal dates to estimate the arrival and humans and extirpation of megafauna. These arrival and extirpation estimates were compared with nearby paleoclimate and paleovegetation records. For Brazil as a whole, I calculated a megafaunal extirpation age estimate of 12,656-11,696 Cal yr BP and a human arrival age estimate of 22,893-16,005 Cal yr BP. I found that humans, climate, and vegetation change correlate with Brazilian Pleistocene megafaunal extirpation, in the form of gradual human population growth, regional effective moisture changes, and regional vegetation change. This highlights the need for finer regional studies to investigate the chronologies of these events for synthetic comparisons between regions of Brazil.

Keywords

Brazil, Extinction, Quaternary, Megafauna, Paleoenvironment, GRIWM

Introduction

Over the past 50,000 years, about half the world's large mammal species have become extinct from a combination of human population pressures, climate change, and habitat loss (Brook

& Barnosky, 2012). These late-Quaternary extinctions (LQE) peaked around the end-Pleistocene, which was an age of significant global environmental change, including human population expansion, warming following the last glacial maximum (LGM; ~24-18 ka) (Clark et al., 2009), a brief cold snap during the Younger Dryas (~12.9-11.7 ka) (Fairbanks, 1989), and regional biome reconfigurations (Williams et al., 2004). All of these changes resembled ongoing and projected global changes, although they were of much lower magnitude and velocity. Nevertheless, the resemblance in the kinds of potential forcing factors of extinction makes understanding the LQE especially important for understanding the modern biodiversity crisis.

The causes of the LQE have been intensely debated for decades and have focused on anthropogenic vs. climatic mechanisms (Wroe, 2004; Koch & Barnosky, 2006; Bartlett et al., 2016; Araujo et al., 2017; Monjeau et al., 2017; Nagaoka, Rick, & Wolverton, 2018). Additionally, recent work has focused on the ecological consequences of the LQE (Johnson, 2009; Blois, McGuire, & Hadly, 2010; Gill, 2014; Pires et al., 2014, 2015, 2018; Smith et al., 2016; Galetti et al., 2018; DeSantis et al., 2019), which is shedding new light on the environmental changes and potential feedbacks that accompanied the extinction event. Identifying these consequences hinges upon whether habitat changes preceded or followed the LQE, which requires a robust chronology of the paleoenvironmental conditions surrounding the LQE. This is difficult to establish because the LQE was time-transgressive on a global scale and spread over thousands of years between continents. Most previous work has focused on these continental scales, but as both the amount of dated materials and precision in radiocarbon dating have increased, workers are becoming more able to discover intricacies between regions, taxa affected, and specific paleoenvironmental conditions surrounding the megafaunal losses.

A region of particular interest is Brazil, given that previous work has shown that at a continental scale, the LQE was the most severe in South America, with over 50 megafauna genera (~83%) seeing extinction (Koch & Barnosky, 2006; Borrero, 2009; Hubbe, Hubbe, & Neves, 2013; Martin & Borrero, 2017; Polotis et al., 2019). Lost forever were giant ground sloths (Mylodontidae, Megatheriidae), car-sized armadillos (Glyptodontidae), the rhino-like toxodons (Toxodontidae), and a proboscidean (*Notiomastodon platensis*). Other studies have highlighted regional trends for other parts of South America (e.g., Barnosky et al., 2016; Villavicencio et al., 2015), but the Brazilian paleoenvironmental record surrounding the LQE has yet to be similarly investigated. To more thoroughly investigate this record in relation to the LQE in Brazil, it is necessary to establish a refined, high-precision chronology of: 1) when humans first arrived; 2) how vegetation was changing around this time; 3) how climate was changing; and 4) how the chronologies of these events align with megafaunal extirpation.

To investigate this, I compiled a list of published radiocarbon dates for extinct Quaternary megafauna and archaeological sites in Brazil, estimated human arrival and megafaunal extirpation dates using the Gaussian resampled inversely-weighted McInerny et al. method (GRIWM) (Saltre et al., 2015), and compared the estimated arrival and extirpation dates to published paleo-vegetation and -climate records. The data were used to investigate four alternative working hypotheses:

1) Megafauna loss caused an ecological "ripple effect" on vegetation (i.e., a defaunation signal from changes in herbivory and/or seed dispersal) (e.g., Dirzo et al., 2014; Barnosky et al., 2016; Ripple et al., 2015; Young et al., 2016). Rejecting this hypothesis would require that the decline of megafauna postdated certain kinds of vegetation shifts.

2) Loss of habitat was a chief cause of megafauna extinction. Rejection requires that vegetation shifts occur before the megafaunal decline.

3) Climate change was the ultimate driver of megafaunal decline, possibly mediated through changes in the plant communities. If vegetation shifts and megafauna declines were concurrent and matched a pronounced paleoclimatological change, this would be consistent with climate change being the ultimate driver of extirpation. Rejecting this hypothesis would require a significant mismatch in the timing of climate change, vegetation change, and megafaunal loss.

4) Human pressures—direct, indirect, or a combination of both—were the chief driver of megafauna loss. If certain vegetation shifts (e.g., those consistent with aboriginal land management with fire and/or landscape modification for favored vegetation) and megafauna decline was concurrent but do not match a pronounced paleoclimatological change, this would be consistent with human population pressures causing both the extirpation and vegetation change. This hypothesis could be rejected if the nature of vegetation change was not consistent with aboriginal land-management practices, or if it could be demonstrated that human entry into the area or an increase in their population sizes did not coincide with the megafaunal decline and vegetation change.

(Paleo)climate of Brazil

Brazil is a large country with a heterogeneous climate, but generally is characterized as humid around the equator and along the Atlantic coast, and drier further south and inland. Over broad spatial scales, the intertropical convergence zone (ITCZ) and South American summer monsoon (SASM) are important climatic factors. The ITCZ is a band of high precipitation and temperatures spatially defined by the annual north-south migration of the meteoric equator about the geographic equator (Garrison, 2012). Ranging annually from 10° N in August to 1° S in March (Baker & Fritz, 2015), the ITCZ thus affects broad spatiotemporal climate patterns in tropical Brazil. The South American summer monsoon (SASM) brings significant moisture from the Atlantic Ocean to southeastern Brazil during the austral summer months (Cruz et al., 2005), whereas the ITCZ deposits rainfall further north. Also, although El Niño / Southern Oscillation (ENSO) is an important climatic factor for other South American regions, there is little support for it to explain modern and historical high amplitude, low frequency precipitation events in Brazil (Baker & Fritz, 2015). The ITCZ and SASM, however, have affected Brazil's climate throughout the Quaternary—even with changes in insolation—and were likely affected by end-Pleistocene global climatic events as well.

Paleoclimatically, both local and large-scale events are discernable from Brazil's prehistoric records, including relatively wet conditions in southeastern Brazil during the LGM and dry conditions in the early- to mid-Holocene (Baker & Fritz, 2015). Aside from a lake (Moro et al., 2004) and peat (Ledru et al., 2005) sediment record from southern Brazil and two marine sediment core records from northeastern Brazil (Nace et al., 2014), speleothem records from southeastern Brazil (e.g., Cruz Jr. et al., 2005; 2006)—especially those from Botuverá Cave—are the main paleoclimate archives for the country. All of these records suggest that precipitation response to climate change was not uniform across regions of Brazil. For example, southern Brazil became drier after the LGM,

then wetter at the start of the Holocene, followed by drying and several more effective moisture oscillations during the rest of the Holocene (Moro et al., 2004). Conversely, northeastern Brazil became wetter after the LGM, followed by a sharp decrease in effective moisture ~14-14.5 ka, then a sharp increase in effective moisture ~14-12 ka, and finally gradual drying throughout the Holocene (Nace et al., 2014). These differences highlight how paleoclimatic changes in Brazil cannot be generalized for the entire country and must be examined by region to understand their effects on Brazilian Pleistocene megafauna.

Bioregions of Brazil

As directly affected by Brazil's climate, Brazil's vegetation can be categorized into seven distinct bioregions with ecotones between them: the Pampas, the *Araucaria* Plateaus, the Atlantic Rainforest, the Pantanal, the Amazon Rainforest, the Cerrado, and the Caatinga (see Figs 4 and 5 for overview maps).

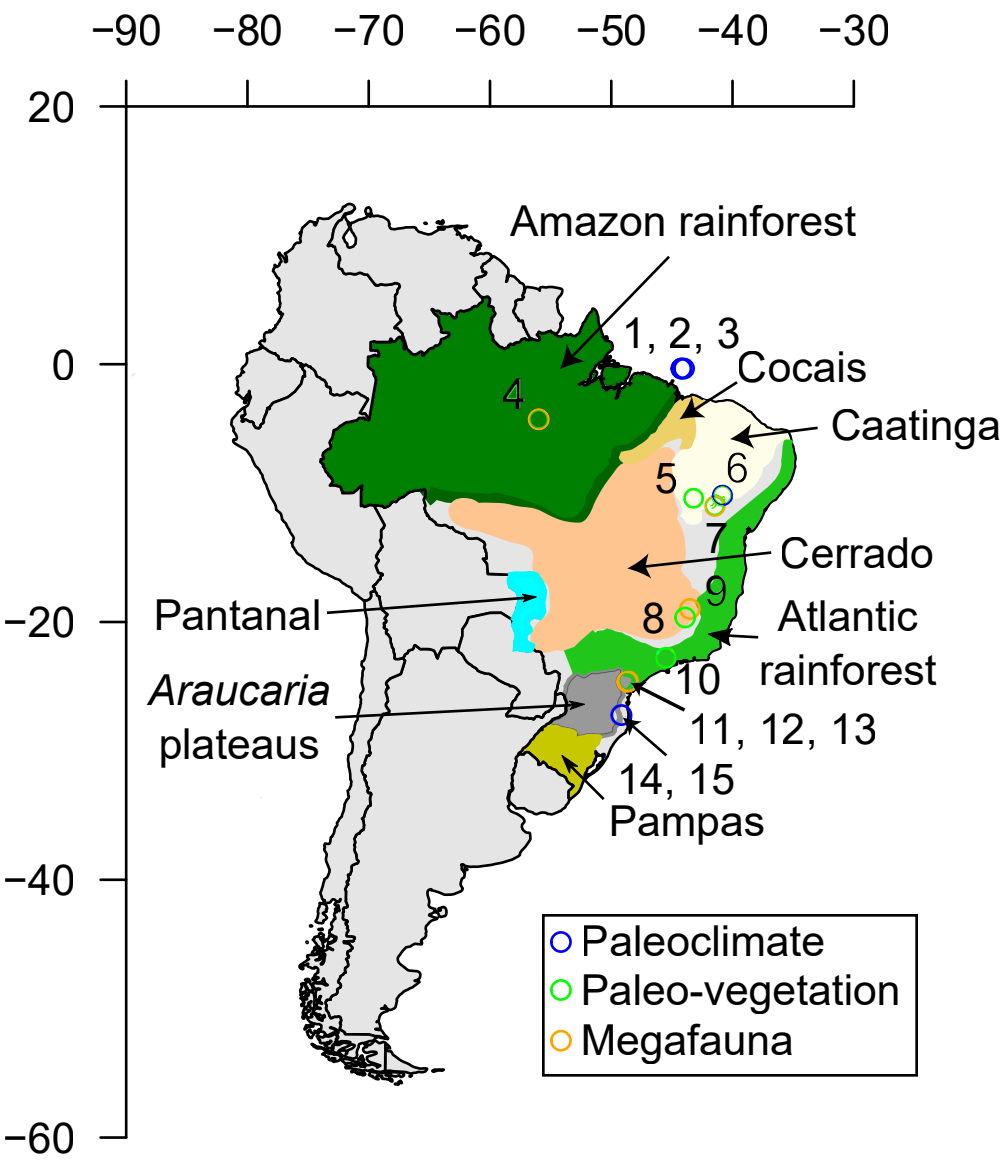
−90
−80
−70
−60
−50
−40
−30
20
0
−20
−40
−60
Amazon rainforest
1, 2, 3
Cocais
Caatinga
4
5
6
7
Cerrado
Pantanal
8
9
Atlantic
rainforest
10
Araucaria
plateaus
11, 12, 13
14, 15
Pampas
Paleoclimate
Paleo-vegetation
Megafauna

Fig 4. Map of Brazilian paleoclimate, paleo-vegetation, and Pleistocene megafaunal localities. This map is a Mercator projection, meaning that there is equal spacing between latitude lines and likewise for longitude. Axes show latitude and longitude in degrees. Color coding for bioregions in other parts of this manuscript is based on that in this map. Numbers represent paleoclimate, paleo-vegetation, and megafauna localities from Table 1 as follows: 1, 2, 3 = marine sediment cores BC 82, CDH 86, and GGC 81, respectively; 4 = Itaituba Quarry; 5 = Saquinho; 6 = Bahia; 7 = Gruta dos Brejoes; 8 = Lagoa Olhos D'Agua; 9 = Lapa dos Tatus); 10 = Morro de Itapeva (MDI); 11, 12, 13 = Abismo do Fossil Cave, Abismo do Iguatemi Cave, and Ribeira do Iguape, respectively; 14 = Botuverá Cave.

Table 2: Brazilian Paleo-vegetation, Paleoclimate, and Pleistocene Megafauna Localities. Color coding follows that of Figure 4.

Site number on Fig. 4	Site name	Site latitude, longitude (°)	Deposit category	Deposit type	Bioregion	References
1	CDH 86	-0.33766, -44.2095	Paleoclimate	Marine sediments	Amazon Rainforest	Nace et al., 2014
2	BC 82	-0.33776, -44.00036	Paleoclimate	Marine sediments	Amazon Rainforest	Nace et al., 2014
3	GGC 81	-0.33776, -44.2095	Paleoclimate	Marine sediments	Amazon Rainforest	Nace et al., 2014
4	Itaituba Quarry	-4.2761, -55.9836	Megafauna	Dung	Amazon Rainforest	Rossetti et al., 2004; Hubbe et al., 2013
5	Saquinho	-10.4, -43.21	Paleo-vegetation	Fluvial sediments	Caatinga	De Oliveira, Barreto, & Sugio, 1999
6	Bahia	-10.16, -40.83	Paleoclimate	Speleothem	Caatinga	Wang et al., 2004
7	Gruta dos Brejoes	-10.9891048, -41.4646824	Megafauna	Bone	Caatinga	Auler et al., 2006
8	Lagoa Olhos D'Agua	-19.648677, -43.9098	Paleo-vegetation	Lake sediments	Cerrado	Raczka et al., 2013
9	Lapa dos Tatus	-18.984329, -43.524324	Megafauna	Bone	Cerrado	Barnosky & Lindsey, 2010
10	Morro de Itapeva	-22.78, -45.53	Paleo-vegetation	Peat	Atlantic Rainforest	Behling, 1997

11	Abismo do Fossil Cave	-24.58, -48.59	Megafauna	Bone	*Araucaria* Plateaus	Hubbe et al., 2013
12	Abismo do Iguatemi Cave	-24.58, -48.59	Megafauna	Bone	*Araucaria* Plateaus	Hubbe et al., 2013
13	Ribeira do Iguape	-24.6439, -48.6856	Megafauna	Bone	*Araucaria* Plateaus	Neves, Hubbe, & Karmann, 2007; Hubbe et al., 2013
14	Lagoa Dourada	-25.2408, -50.0422	Paleoclimate	Lake sediments	*Araucaria* Plateaus	Moro et al., 2004
15	Botuvera Cave	-27.2233, -49.1555	Paleoclimate	Speleothem	*Araucaria* Plateaus	Cruz Jr. et al., 2005; 2006; 2007; Baker & Fritz, 2015

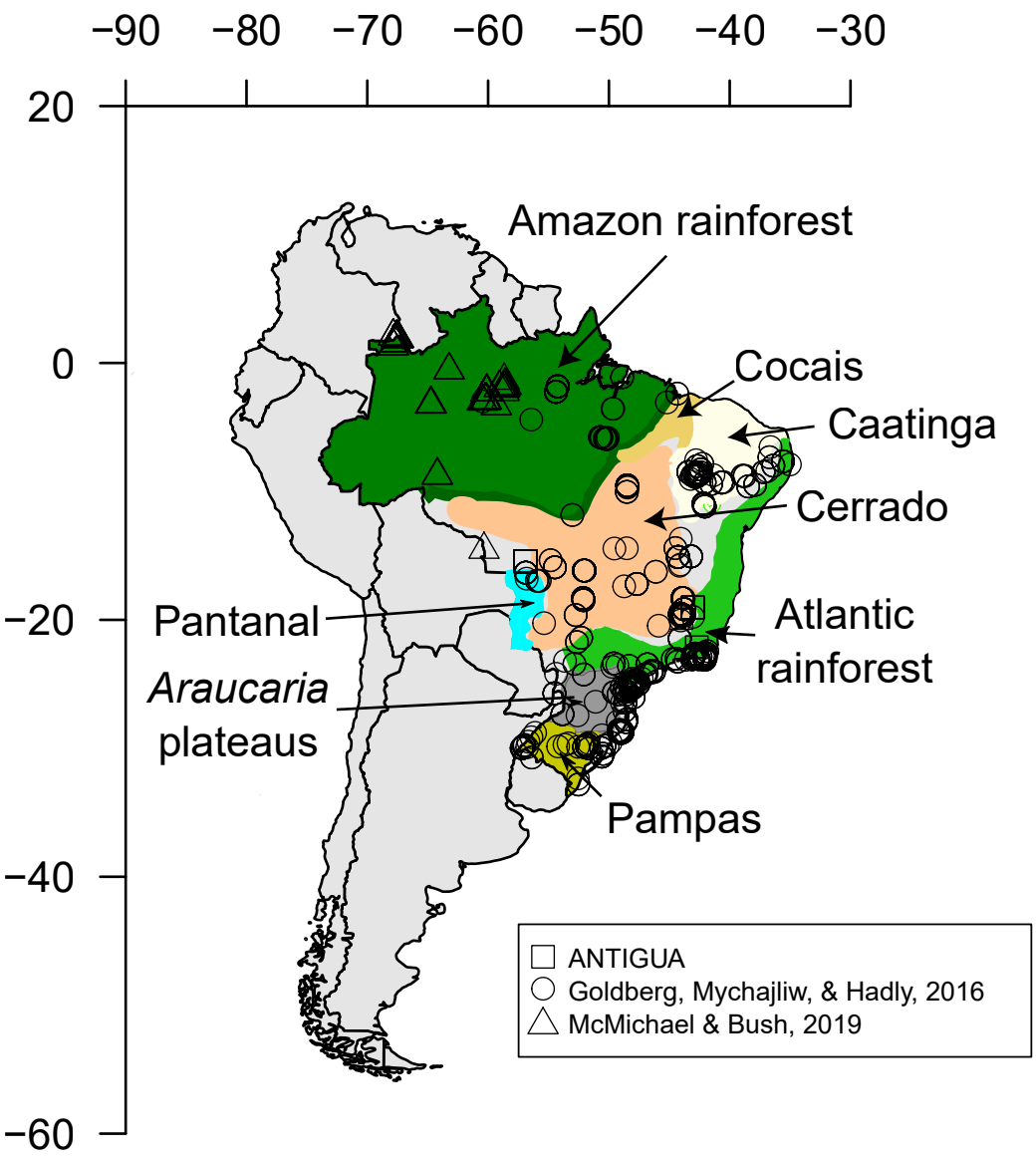
−90
−80
−70
−60
−50
−40
−30
20
0
−20
−40
−60
Amazon rainforest
Cocais
Caatinga
Cerrado
Pantanal
Atlantic
rainforest
Araucaria
plateaus
Pampas
ANTIGUA
Goldberg, Mychajliw, & Hadly, 2016
McMichael & Bush, 2019

Fig. 5: Map of Brazilian archaeological localities. This map is a Mercator projection, meaning that there is equal spacing between latitude lines and likewise for longitude. Axes show latitude and longitude in degrees. Color coding for bioregions in this figure is based on that of Fig. 4. Squares represent ANTIGUA localities, circles represent Goldberg, Mychajilw, & Hadly (2016) localities, and triangles represent McMichael & Bush (2019) localities.

The Pampas

The Pampas is a region of low-relief, subtropical grasslands in south-southwestern Brazil and large parts of Argentina and Uruguay (Salgado, Santos, & Paisani, 2019). The grassland vegetation here is mostly herbaceous and shrubby plants (e.g., *Aristida jubata*; Family: Poaceae) thought to reflect a mixture of Cerrado and Argentinian steppe communities whose ranges have advanced and retreated in response to paleoclimatic changes (Verdum et al., 2019). Along with those herbs and shrubs, the Pampas also has riparian forests mostly made of palms (e.g., *Butia lallemantii*), leguminous trees (e.g., *Prosopis nigra*, *Vachellia caven*, and *Prosopis affinis*), and ironwood capons (e.g., *Myrachodruon balansae;* Family: Anacardiaceae) (Verdum et al., 2019). Average annual temperature and precipitation of the Pampas ranges from 17-23 °C and 1400-1800 mm, respectively (Verdum et al., 2019).

The *Araucaria* Plateaus

The *Araucaria* Plateaus line the southeastern Brazilian coast and have average annual temperatures of 12-18 °C (Gu et al., 2017). The higher-altitude areas of these plateaus, which have average winter temperatures of 15 °C and mean annual rainfall of 1700 mm (Ledru et al., 2005), host Brazil's *Araucaria* forests. These plateau forests are dominated by the conifers*Podocarpus lambertii* and *Araucaria angustifolia* (Salgado, Santos, & Paisani, 2019), and the angiosperms *Mimosa scabrella,* and *Ilex* (Gu et al., 2018). *A. angustifolia*—also known as the Brazilian pine (although not part of the Pinaceae Family)—is a long-lived conifer that reaches adult heights of 50 m and widths of 3 m (Salgado, Santos, & Paisani, 2019). It only tolerates well-drained sandy soils, so areas of the *Araucaria* Plateaus that have poorly-drained riparian forests are instead dominated by *Sebastiania commersoniana*—a leafy euphorb that can make up 80% of the individuals along these streams (Salgado, Santos, & Paisani, 2019).

At higher altitudes from these riparian forests, the montane communities in this bioregion are rich in *A. angustifolia* and *P. lambertii*, and these forests then transition to high montane steppes dominated by grasses (Salgado, Santos, & Paisani, 2019). In general, the vegetation of the Araucaria Plateaus is currently controlled by altitudinal gradients: differences in altitude translate to differences in groundwater and climatic regimes, which result in differences in plant communities. Also, there are many natural wetland reservoirs in this bioregion, which means that paleo-vegetation changes are well documented in palynological records from here (e.g., Ledru et al., 2005; Gu et al., 2017; 2018; Behling & Oliveira, 2018; and references therein).

The Atlantic Rainforest

The Atlantic Rainforest is just north of the *Araucaria* Plateaus in a 50-200 km wide strip (Gu et al., 2017) along the Atlantic coast of Brazil (Salgado, Santos, & Paisani, 2019), from the equator to 30° S (Ledru et al., 2005). Spanning this wide latitudinal range, the Atlantic rainforest also covers a broad spectrum of climates, from a more seasonal precipitation regime in the north, to a lack of dry season in the south (Ledru et al., 2005). Mean annual temperature ranges from 19-26 °C, mean summer highs range from 25-34 °C, and mean winter lows range from 14-18 °C (Kamino et al., 2019). Mean annual rainfall ranges from 1800-2400 mm along the coast to over 3600 mm further inland at higher elevations (Kamino et al., 2019). The Atlantic rainforest is also seasonally influenced

by both the ITCZ and ENSO: the former influences the length of the rainy season while the latter affects rainfall magnitude (Kamino et al., 2019). This forest is currently isolated from the Amazon rainforest by a drier strip of Caatinga, Cerrado, and Pampas, but was possibly connected to the Amazon in the past (see the 'Pleistocene arc hypothesis' below).

The plant community of this region is dominated by angiosperms from the families Orchidaceae, Fabaceae, Asteraceae, Bromeliaceae, Poaceae, Myrtaceae, Melastomataceae, Euphorbiaceae, Rubiaceae, and Apocynaceae, which mostly make up ombrophilous and seasonal vegetation (Kamino et al., 2019). Parts of these ombrophilous forests at elevations above 1,700 m have high abundances of *A. angustifolia* as well (Kamino et al., 2019). Some of this region's seasonal forests are defined by significant winter drought and intense summer rainfall, while others are defined by consistent annual rainfall and cold winters (mean monthly temperature < 15 °C) (Kamino et al., 2019). In these seasonal forests, 20-50% of the trees are deciduous (Kamino et al., 2019).

The Pantanal

The Pantanal is a relatively small (~150,000 km^2), semi-arid bioregion of western Brazil that is well known for its extensive seasonal flooding during the austral summer (Boin et al., 2019). Mean annual rainfall of the Pantanal is only 1500 mm and is evenly distributed throughout the year, but the tributaries of the Paraguay River have marked upstream spikes in discharge rates between December and April. This leads to flooding from January to March (Boin et al., 2019). Being mostly inland, the Pantanal's temperature follows a relatively high amplitude pattern throughout the year, with temperatures ranging from average summer highs over 38 °C to average winter lows around 18 °C (Boin et al., 2019).

The vegetation here is a mix of plants from the Cerrado, Atlantic Rainforest, Amazon Rainforest, Caatinga, and the Gran Chaco (a savanna/open-forest biome of southwestern South America) (Boin et al., 2019). These plants include water hyacinths (*Eichhornia crassipes*), asthma plants (*Euphorbia hirta*), carpet and reimar grasses (*Reimarochloa*), caranday wax palms (*Copernicia alba*), and moriche palms (*Mauritia flexuosa*) (Boin et al., 2019). Many of the plants here tend to form floating mats and floating meadows as adaptations to the seasonal floods (Boin et al., 2019).

The Amazon Rainforest

The Amazon Rainforest is the largest bioregion of Brazil, being roughly the size of the contiguous US (Malhi et al., 2008). Situated about the equator with such a large area and density of vascular plants, transpiration in the Amazon accounts for 25-50% of its precipitation (Eltahir & Bras, 1994), making it very humid and warm year-round. The ITCZ and SASM are also responsible for bringing large quantities of oceanic water inland to the Amazon (Bueno et al., 2019). The Andes are responsible for stopping the trade winds from transporting this moisture any further west, which further increases the Amazon's annual rainfall (Bueno et al., 2019). These climatic conditions support a remarkable diversity of over 80,000 taxa of vascular plants (Colinvaux & De Oliveira, 2001), which can be grouped into *terra firme* forests, floodplain forests, and herbaceous areas subject to periodic flooding (Bueno et al., 2019).

Terra firme forests are the most dominant in the Amazon and form on dry soils (Bueno et al., 2019). These forests make up stratified, tall (up to 60 m) vertical habitats within the trees home to many epiphytes (Families: Orchidaceae and Areceae) and lianas (Families: Bignoniaceae,

Passifloraceae, Convolvulaceae, Hippocrateaceae, Apocynaceae, and Cucurbitaceae) (Bueno et al., 2019). Many plants in Amazonian floodplain forests have adaptations for seasonal flooding, including growth synchronized with the low-water season, loss of leaves from lower parts of the plants during floods, and fish- and water-dispersed seeds (Bueno et al., 2019). Similarly, mangroves are common around the mouth of the Amazon river in brackish waters (Bueno et al., 2019). The Amazon's herbaceous areas subject to periodic flooding are dominated by 1-9 m tall sclerophyll plants with pneumatophores that optimize gas exchange during flood events (Bueno et al., 2019).

The Cerrado

The Cerrado is a semi-humid savanna in central Brazil with dry austral winters and moist austral summers (MAP: 1200-1800 mm) (Salgado, Santos, & Paisani, 2019). Its mean annual temperature is 20-24 °C (Salgado, Santos, & Paisani, 2019) and its vegetation consists of ecotones from open forests and scrublands to open grasslands, with marshes alongside gallery forests (Salgado et al., 2019). The plants that make up this vegetation include Poaceae, *Acacia, Boscia, Byrsonima, Mimosa*-type, and *Didymopanax* distributed in grasslands and small patches of shrubs and small, gnarly trees (*cerradão* = open forest) (Salgado-Labouriau et al., 1998). The Cerrado's marshes are important areas for wetland sediment records (e.g., Cassino, Martinho, & Caminha, 2018). Also, this bioregion currently supports many charismatic Brazilian savanna fauna—including the jaguar (*Panthera onca*), giant anteater (*Myrmecophaga tridactyla*), puma (*Puma concolor*), tapir (*Tapirus terrestris*), capybara (*Hydrochoerus hydrochaeris*), and the maned wolf (*Chrysocyon brachyurus*) (Salgado et al., 2019)—and was likely suitable habitat for many Brazilian Pleistocene megafauna.

The Caatinga

The Caatinga is a semi-arid grassland/shrubland/thorn-shrub-savanna that covers 850,000 km^2 in northeastern Brazil (Behling et al., 2000). Its name is derived from the indigenous Tupi-Guarani word for white forest, which refers to the landscape's dry, washed-out appearance after the deciduous plants here shed their leaves (de Barros Corrêa et al., 2019). The Caatinga has a 6-11 month hot, dry season, with average annual precipitation often less than 250-750 mm (Behling et al., 2000). The annual amplitude of temperature change is relatively minor though, with summer and winter averages ranging from 26-28 °C and 20-26 °C, respectively (de Barros Corrêa et al., 2019). The contradictory nature of low precipitation in this equatorial bioregion comes from the South Atlantic High (an atmospheric high pressure cell) that regularly displaces the ITCZ to the north (de Barros Corrêa et al., 2019).

The vegetation adapted to this climate includes mostly Poaceae, *Borreria*, and Mimosaceae; however, patches of deciduous forest, gallery forest, and floodplain vegetation exist here too (Behling et al., 2000). These plants can be woody, herbaceous, or succulents (e.g., Family: Cactaceae), and are largely (~80%) restricted to lowlands (de Barros Corrêa et al., 2019). The presence of minor gallery forests in the Caatinga and its position between the Amazon and Atlantic rainforests have suggested to some that the Caatinga may have acted as a corridor between these two rainforests under past climatic regimes (Bouimetarhan et al., 2018) (see 'Pleistocene arc hypothesis' below).

The Cocais

The Cocais is an ecotonal landscape dominated by *Cocais* palm trees (Family: Arecaceae) between the Amazon rainforest, the Cerrado, and the Caatinga (Salgado, Santos, & Paisani, 2019). Being at the intersection of these bioregions, the Cocais has a mixed pattern of humid equatorial, semi-arid tropical, and semi-humid tropical climates (Salgado, Santos, & Paisani, 2019). Rainfall patterns in this bioregion are abnormal—instead of a spectrum between wet and dry seasons or persistent annual dry or wet conditions, the Cocais' wet season migrates from the south, to the east-central part of the bioregion, and then to the north over the span of October to July (Salgado, Santos, & Paisani, 2019). Mean annual temperatures in the eastern, semi-arid tropical Cocais range from 20-28 °C, whereas those in the humid equatorial Cocais closer to the Amazon in the west range from 26-28 °C (Salgado, Santos, & Paisani, 2019). Some workers have noted that the presence of palms interspersed by herbaceous fields in this region may be indicative of disturbance through deforestation or burns (Salgado, Santos, & Paisani, 2019). On that note, historical anthropogenic disturbance here largely occurred between the 1700s and 1800s, meaning that the current presence of palm savannas in this landscape might be a successional legacy of recent disturbance at the Amazon's edge (Salgado, Santos, & Paisani, 2019).

Quaternary paleovegetation of Brazil

In the absence of studies of non-Recent Brazilian Quaternary macroflora, genetic and palynological data have provided all of the insights regarding Brazil's Quaternary paleovegetation. Genetic studies have focused on the Amazon Rainforest's extremely high genetic diversity, especially regarding the 'Amazonian refugia hypothesis' of Haffer (1969). This hypothesis posits that during Pleistocene glacial maxima, the Amazon was isolated into patches of forest surrounded by savannas and grasslands, resulting in allopatric speciation and the resultant genetic diversity observable today (Arruda et al., 2018). A "pollen gap" for the LGM of this region precludes testing this hypothesis with palynological data (Baker & Fritz, 2015), leaving the phylogeography of the Amazon tantalizing and controversial (e.g., Da Silva & Patton, 1998; Leite et al., 2016). A similar biogeographic idea surrounding Brazil's vegetation is the 'Pleistocene arc hypothesis' of Prado and Gibbs (1993), which hypothesizes that the Amazon and Atlantic rainforests were connected in the Pleistocene through the Caatinga but have since separated, with the resultant allopatry explaining the genetic diversity and differences between the two biomes (Arruda et al., 2018).

Although existing palynological records have not resolved the history of the Amazon to the extent needed to fully understand current diversity there, the records are extremely valuable in reconstructing Quaternary vegetation in some parts of Brazil. These studies include lake sediment records from the Amazon rainforest (e.g., Hermanowski et al., 2012; Castro et al., 2013; Fontes et al., 2017; Arruda et al., 2018; and D'Apolito, Latrubesse, & Absy, 2018), two marine cores off of the northeastern coast of Brazil (Behling et al., 2000; Bouimetarhan et al., 2018), two palm swamp records from the Cerrado (Salgado-Labouriau et al., 1998; Cassino, Martinho, & Caminha, 2018), and many palynological records from the Atlantic rainforest in southern and southeastern Brazil (for a comprehensive overview, see Behling, 2002).

Archaeology of Brazil

The archaeological record of South America suggests that paleo-humans likely arrived through Central America in a singular event and then followed the Atlantic coast to Brazil ~13,000-12,000 Cal (meaning calibrated/calendar) yr BP (Goldberg, Mychajliw, & Hadly, 2016). Interestingly, many of the oldest South American archaeological sites are from the far southern reaches of Patagonia (e.g., Dillehay et al., 2015), although radiocarbon data substantiate the hypothesis that the first South Americans made their way through Central America (Goldberg, Mychajliw, & Hadly, 2016). This suggests that the first South Americans quickly passed through Brazil before establishing more persistent sites further south.

While human populations in other South American regions were expanding from the late Pleistocene through the Holocene, paleo-demographic inferences of Brazil's population suggest that it was quite stable throughout the Holocene until 2,000 Cal yr BP (Goldberg, Mychajliw, & Hadly, 2016). Goldberg, Mychajliw, & Hadly (2016) also estimated that Brazil was sparsely populated from 14,000-2,000 Cal yr BP relative to other South American regions. There have also been at least two verified Pleistocene megafaunal kill sites in Brazil—one of a disjointed and butchered *Eremotherium* at Toca da Boa Vista cave in southern Brazil and another of a *Notiomastodon platensis* ilium from Lagoa Santa in Minas Gerais, with possible butcher marks (Prous & Fogaca, 1999). However, neither of these specimens have been numerically dated, so they are not included in this study.

Methods

Paleoclimate and paleo-vegetation

Paleoclimate and paleo-vegetation records were extracted from a Web of Science search (https://clarivate.com/webofsciencegroup/solutions/web-of-science/) that focused on locating records that spanned the Pleistocene-Holocene transition and were geographically closest to megafaunal localities (Fig. 4). When possible, all radiocarbon records were re-calibrated using CALIB v. 7.1.0 (http://calib.org/calib/). For all outputs of calibrated dates, I selected only the 2σ age ranges that corresponded to the highest relative areas under each curve. For example, this means that for a given date with two possible age distributions under the calibration curve, I selected the distribution that accounted for the greatest area under the curve and did not report the other. Also, all dates were calibrated using the SHCal13 southern hemisphere calibration curve (Hogg et al., 2013) unless otherwise noted. The exceptions include marine sediment core records from Nace et al. (2014), which were calibrated using the Fairbanks0107 calibration curve (Fairbanks et al., 2005) and archaeological dates from north of the equator that were calibrated using IntCal13 (see **Humans** below). The uncalibrated values from Nace et al. (2014) were unavailable for comparison.

The Fairbanks curve is derived from radiocarbon and $^{230}Th/^{234}U/^{238}U$ dates sampled from offshore coral reefs for 50,000-0 Cal yr BP. In contrast, the SHCal13 curve is derived from southern hemisphere tree ring data for the Holocene, and the main difference between Fairbanks0107 and SHCal13 is that the former is based on a Bayesian statistical model while the latter is based on a random walk statistical model. This difference does not account for any notable variation between calibration datasets for the timeframe of the study here. For dates 50-12 ka, the SHCal13 curve is the

same as the northern hemisphere IntCal13 curve but with an average offset of 43 ∓ 13 yr (Hogg et al., 2013). This offset is to correct for southern hemisphere dates being systematically older due to an oceanic old-carbon reservoir effect (Hogg et al., 2013). The 50-12 ka dates on the IntCal13 curve in turn are derived from terrestrial plant macrofossils in varved lake sediments, U-series dated speleothems, and U-Th dates from marine records (Reimer et al., 2013).

We used the following paleo-climate proxies. For the marine sediment cores Nace et al. (2014), seawater ice-volume corrected $\delta^{18}O$ values ($\delta^{18}O_{swivc}$) provided the paleo-effective-moisture proxy. Given that global variations in both sea water temperature and ice volume can affect marine $\delta^{18}O$ values (Delaygue, 2009), Nace et al. (2014) reported $\delta^{18}O_{swivc}$ as a signal primarily of salinity. The locality where these sediments were cored is close to the Amazon River delta, such that Nace et al. (2014) attributed more negative $\delta^{18}O_{swivc}$ values in this record to freshwater isotopic dilutions during pluvial events. Therefore, these values can be used as a proxy for paleo-effective-moisture in this region.

For cave records, paleo-effective-moisture proxies came from speleothem and travertine growth-period records in northeastern Brazil (the Caatinga) (Wang et al. 2004), and from $\delta^{18}O_{VPDB}$ values from a speleothem in Botuverá Cave in southern Brazil (The *Araucaria* Plateaus) (Figures 4 & 5). For the speleothem and travertine growth period records, Wang et al. (2004) argued that growth of these formations only occurs during events where groundwater infiltration is sufficient to deposit calcite. Therefore, periods of speleothem and travertine growth are thought to represent pluvial periods as well. Lastly for paleo-effective-moisture records, the $\delta^{18}O$ record from Botuverá Cave (speleothem Bt2) is thought to primarily reflect local precipitation and upstream rainfall/transpiration (Cheng et al., 2013). These values, however, do not account for temperature effects and amount effects during the LGM. Baker & Fritz (2015) later corrected the values for those effects, so I used their measurements instead (Fig. 6).

For a paleo-temperature proxy, I used Mg/Ca-derived sea-surface temperatures (SSTs) from the Nace et al. (2014) marine sediment cores (Figures 4 & 6). The paleo-SST record of Fig. 5 is derived from Mg/Ca ratio measurements (see Higginson, 2009) on the planktonic foraminifer *Globigerinoides ruber*, extracted from the cores taken by Nace et al. (2014).

The pollen records from the paleo-vegetation reflected the regional taxa in each area, thus the taxa involved differed from site to site (e.g., *Araucaria* pollen from southern Brazil, Caatinga plant pollen from northeastern Brazil). I summarized changes in paleo-vegetation inferred from each pollen record by grouping general pollen types together (e.g., pollen types from herbaceous plants vs. those from *Araucaria* forest trees) per each locality so that they could be compared between sites more easily. The age model for each paleo-vegetation site was based on a linear interpolation between radiocarbon dates. Figures 6 and 7 compare the vegetation changes so determined, the paleo-temperature and paleo-humidity proxies, and the timing of extinction derived by the GRIWM analyses.

The analyses for selecting megafaunal/archaeological radiocarbon dates and estimating extirpation/arrival dates (Figs. 4-7) in this study were done using R (R Core Team, 2020).

Megafauna

To curate a chronology of megafaunal extirpation with locality information for Brazil, I started with 355 radiocarbon dates for South American megafauna in the ANTIGUA dataset and winnowed that down to the 25 dates reported for Brazilian megafauna specifically. I then winnowed that further down to the 13 radiocarbon dates considered robust by the rating scale reported by Barnosky and Lindsey (2010) (Table 3) All of these dates were obtained from the ANTIGUA project—a collaborative effort of more than 40 North- and South-American workers—and ranked > 10 *sensu* Lindsey & Barnosky, 2010. I confirmed with Dr. Alexander Hubbe—the ANTIGUA project expert in Brazilian archaeology and paleontology—to verify that these dates encompass all known, high-quality Brazilian Pleistocene megafauna radiocarbon dates as of October 2019. I avoided dates on bioapatite because bioapatite from both bone and enamel undergoes substantial isotopic exchange with the surrounding sediment during fossilization, which alters the isotopic ratios of interest (Zazzo & Saliège, 2011). I note that there might be more megafauna dates in the Brazilian non-English literature, but if so, I am unaware of them.

Table 3: Radiocarbon dates, Calibrated dates, and estimated extirpation date for Brazilian late-Pleistocene megafauna. Color coding follows that of Figure 4.

Bioregion	Site number from Fig. 4	Site name	Species	Lab code	^{14}C age, ∓ sd (yr BP)	2σ calibrated age range (Cal yr BP)	References
Amazon Rainforest	4	Itaituba Quarry	*Notiomastodon platensis*	Beta NA	15290, 70	18698 - 18330	Rossetti et al., 2004; Hubbe et al., 2013
			Eremotherium laurillardi	Beta "sample 2"	11340, 50	13267 - 13065	
Caatinga	7	Gruta dos Brejoes	*Nothrotherium maquinense*	NZA 6984	12200, 120	14637 - 13748	Auler et al., 2006
Cerrado	9	Lapa dos Tatus	*Catonyx cuvieri*	Beta 174688	14030, 50	17209 - 16708	Barnosky & Lindsey, 2010
				Beta 174689	13920, 50	17037 - 16552	
Araucaria Plateaus	11	Abismo do Fossil Cave	*Glyptodon clavipes*	Beta 237350	17800, 70	21786 - 21229	Hubbe et al., 2011
			Scelidotherium sp.	Beta 237349	15780, 80	19204 - 18797	Hubbe et al., 2013
			Eremotherium laurillardi	Beta 237348	12550, 60	15084 - 14304	Hubbe et al., 2013
			Toxodon platensis	Beta 237347	11850, 70	13761 - 13474	Hubbe et al., 2013
	12	Abismo do Iguatemi Cave	*Catonyx cuvieri*	Beta 230974	10800, 60	12753 - 12637	Hubbe et al., 2013

		Smilodon populator	Beta 183566	14580, 90	17956 - 17471	Hubbe et al., 2013
13	Ribeira do Iguape	*Toxodon platensis*	Beta 215330	11380, 40	13280 - 13088	Neves, Hubbe, & Karmann, 2007; Hubbe et al., 2013
			Beta 218193	11090, 40	13051 - 12780	

Because last-appearance dates (LADs) usually precede actual extinction dates (the Signor-Lipps effect; Signor III & Lipps, 1982) and vice versa for first-appearance dates (FADs), I applied the Gaussian-resampled, inversely weighted McInerny et al. (GRIWM) method (Bradshaw et al., 2012) to obtain estimates of megafaunal extirpation and human arrival. I chose GRIWM over alternatives because it is highly accurate, accounts for date uncertainties, and is not prone to Type I or II errors (Bradshaw et al., 2012) The GRIWM method works as follows: The initial, calibrated dates are first resampled in a Gaussian manner, such that the extremes of the date distribution are less likely to be resampled than the central values. Then, the temporal distance of each resampled occurrence is inversely-weighted relative to the most recent occurrence for estimating extirpation, and to estimate arrival, relative to the least recent occurrence. The shorter the time interval between a given date and the most recent one (a rough indicator suggesting relatively high population size), the further from the LAD the actual extinction date is estimated to be. The converse holds true for estimating how much earlier an actual arrival date is than the FAD.

To run the GRIWM method on my dates, I modified a script from Saltre et al. (2015) to perform the GRIWM method and created a "GRIWM" R package for reproducibility (https://github.com/sarakahanamoku/GRIWM). Because the majority of the megafauna dates come from southern Brazil (n = 8 out of 13, see Fig. 4 for locality locations), I applied the GRIWM method to this vetted radiocarbon subset and then compared the subset to a subset consisting of LADs for all other vetted Pleistocene megafauna radiocarbon dates to assess whether timing of exptirpation in southern Brazil differed from that elsewhere (Figs 6 & 7). No significant differences were found, so the following discussion is based on the complete set of 13 dates.

Humans

I filtered Brazilian archaeological dates from the ANTIGUA dataset for quality (n = 33 of 70) as I did for the megafauna dates (see *Megafauna*) above. To get a larger sample size of archaeological dates from Brazil, I also included dates from Goldberg, Mychajliw, & Hadly (2016) and McMichael & Bush (2019).

Because the Goldberg, Mychajliw, & Hadly (2016) dataset is for all of South America, I selected only those archaeological dates within Brazil. This dataset includes dates from English, Spanish, French, and Portuguese publications, and excludes dates that have been questioned in the literature. Thus, this dataset has yet to be vetted for quality *sensu* Barnosky & Lindsey (2010), but is very comprehensive. The McMichael & Bush (2019) dataset focuses on archaeological dates from the region of Amazonia, which includes some from outside of the Brazilian Amazon rainforest (e.g., those from the Peruvian Amazon Rainforest). To select only Brazilian dates from this dataset, I read a shapefile of Brazil into R and selected only those values that fell within the bounds of this shapefile. Like the Goldberg, Mychajliw, & Hadly (2016) dataset, these dates were not vetted for quality using the Barnosky and Lindsey (2010) criteria.

After obtaining a bulk archaeological dataset with 1,377 dates, I removed those that were redundant between datasets, which reduced the sample size to 1,163 dates. Of those, 1,031 of those dates are from the Goldberg, Mychajliw, & Hadly (2016) dataset and 129 dates are from the McMichael & Bush (2019) dataset. The analyzed data set included the 33 vetted dates from ANTIGUA, 30 of which also were reported in the Goldberg, Mychajilw, & Hadly (2016) and McMichael & Bush (2019 (see Appendix 1 for all 1,377 archaeological dates). I performed two GRIWM arrival estimates—one for the combined Goldberg, Mychajliw, & Hadly (2016) dataset to

estimate human arrival within Brazil as a whole, and one just on the McMichael & Bush (2019) dataset to estimate human arrival time in the Brazilian Amazon Rainforest (Table 3, Figures 3 & 4).

Table 4: Estimates for first human arrival and megafaunal extirpation in Brazil.

Arrival or extirpation	Original dataset reference	Focal region	Number of dates	Age range of GRIWM estimate (Cal yr BP)	Centroid of GRIWM estimate (Cal yr BP)
Arrival	Goldberg, Mychajliw, & Hadly, 2016	All of Brazil	1,031	22,893 - 16,005	17,950
Arrival	McMichael & Bush, 2019	Amazon Rainforest	129	8,894 - 6,642	7,781
Extirpation	ANTIGUA	All of Brazil	13	12,656 - 11,696	12,110

Results

Lumping megafaunal extirpation dates from all regions for the GRIWM analysis estimated an extirpation date of 12,656-11,696 Cal yr BP (Table 4). During this extirpation period, the paleo-effective-moisture and paleotemperature proxies of northern Brazil show no directional trends, but the loss of megafauna does correspond with an increase in effective moisture and slight decrease in temperature in northern Brazil and with a decrease in effective precipitation on the southern Brazil *Araucaria* Plateaus (Fig. 6). At the same time in the Cerrado, herb pollen increases at the expense of tree pollen (Fig. 7), indicating opening of the landscape that would be consistent with a decrease in effective moisture. In the Atlantic Rainforest, *Araucaria* forest pollen essentially disappears coincident with the lower boundary of the extinction window. Taken in concert, this pattern suggests a series of paleoenvironmental changes corresponded with the timing of extinction.

For the LADs of the megafauna taxa taken individually, no paleoclimate or paleo-vegetation events correspond with apparent losses of individual taxa, except for a decrease in *Araucaria* forest and a dry spell coinciding with the toxodon LADs (~14,000-13,000 Cal yr BP). However, the *Glyptodon*, *Notiomastodon*, *Smilodon*, and three of the seven ground sloth LADs overlap with the human arrival estimate. As for any potential trends in the relative chronology of megafauna LADs, larger herbivores seem to have earlier LADs than smaller herbivores.

For archaeological dates, the Goldberg, Mychajilw, & Hadly (2016) dataset for all of Brazil (n = 1,031 dates) yielded a human arrival estimate of 22,893-16,005 Cal yr BP, with a centroid value of 17,950 Cal yr BP (Figs 6 & 7, Table 4). The McMichael & Bush (2019) dataset focusing on the Brazilian Amazon Rainforest (n = 129) yielded a human arrival estimate of 8,894-6,642 Cal yr BP, with a centroid value of 7,781 yr BP (Table 4), which is substantially younger than the estimate for all of Brazil. This is also substantially younger than other evidence for human occupation in the Amazon ~13,000 Cal yr BP (Roosevelt, 2013).

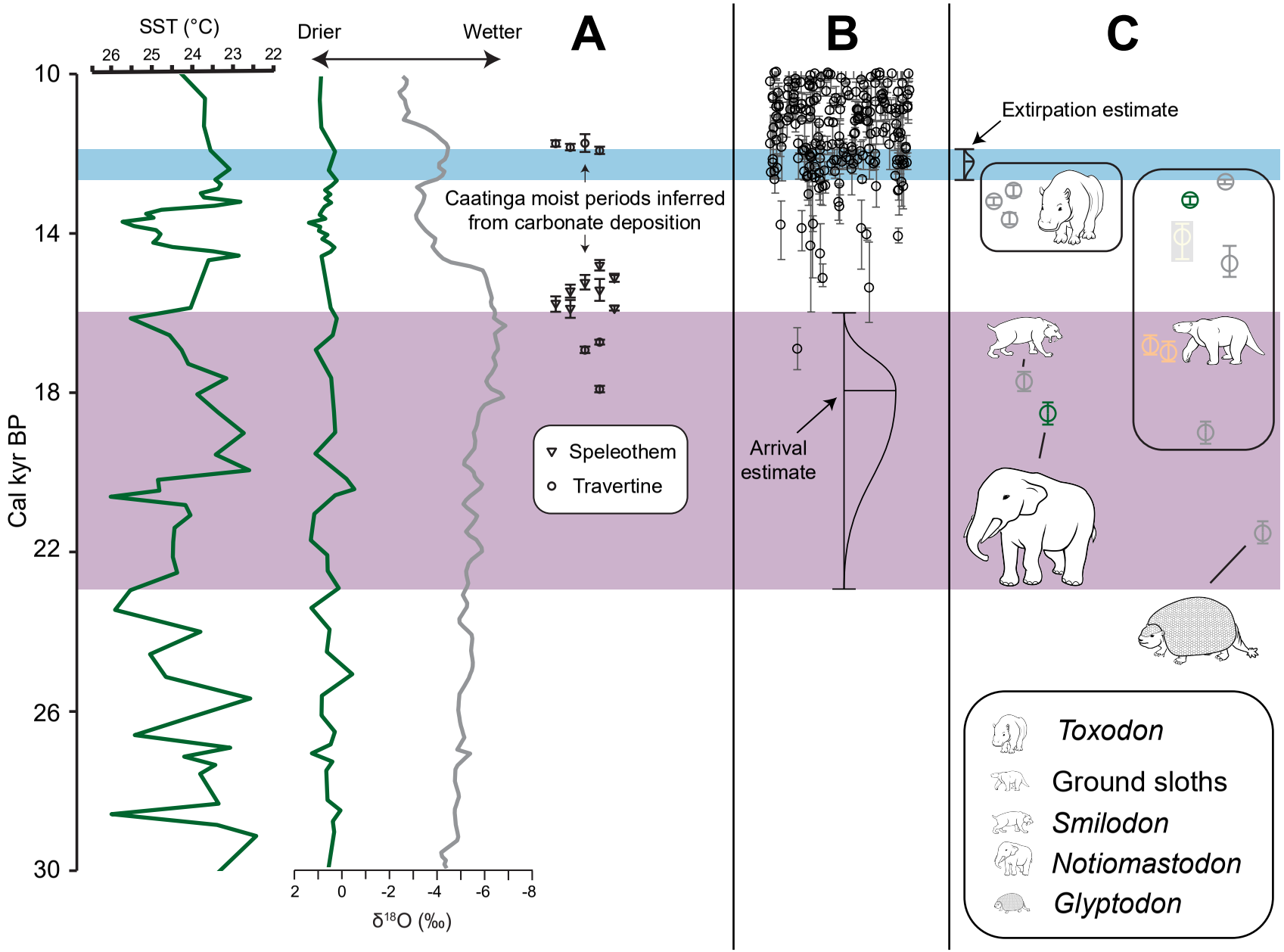
A
B
C
SST (°C)
26
25
24
23
22
Drier
Wetter
Cal kyr BP
10
14
18
22
26
30
2
0
-2
-4
-6
-8
δ18O (‰)
Caatinga moist periods inferred from carbonate deposition
Speleothem
Travertine
Arrival estimate
Extirpation estimate
Toxodon
Ground sloths
Smilodon
Notiomastodon
Glyptodon

Fig 6. Brazilian paleoclimatic changes surrounding Pleistocene human arrival and megafaunal Extirpation.

A. Paleoclimate records of Brazil. Color coding corresponds to the bioregion coloring of Fig. 3. **Left curve**—the composite Mg/Ca-derived sea surface temperature (SST) records from cores BC 82, CDH 86, and GGC 81 collected near the northeast Brazilian coast. **Middle curve**—the composite $\delta^{18}O_{swivc}$ records from cores BC 82, CDH 86, and GGC 81 collected near the northeast Brazilian coast. **Right curve**—the Baker & Fritz (2015) corrected $\delta^{18}O_{VPDB}$ record from Botuverá Cave speleothem Bt2 in southern Brazil. **Points with error bars**—growth periods from speleothems (triangles) and travertines (circles) at the Bahia locality (Caatinga bioregion).
B. Archaeological dates for Brazil from Goldberg, Mychajilw, & Hadly (2016). Confidence intervals about circles represent 2σ calibrated age ranges; circles represent the median values per each age. Purple area shows the GRIWM-estimated Brazil arrival date of 22,893-16,005 Cal yr BP, with a centroid value of 17,950 Cal yr BP (see Table 4). Only the dates younger than 10,000 Cal yr BP are shown here—193 of the 1,031 total from Goldberg, Mychajilw, & Hadly (2016). All 1,031 of these went into the GRIWM estimate however. Because none of the McMichael & Bush (2019) dates are older than 10,000 Cal yr BP, they are not shown here.
C. High-quality calibrated Pleistocene megafaunal radiocarbon dates and GRIWM-estimated extirpation date. Illustrations denote which dates correspond to which megafauna taxa. Confidence intervals about circles represent 2σ calibrated age ranges, circles represent the median values per each age, and their colors correspond to the bioregion color coding from Fig. 1. Blue area shows the GRIWM-estimated extirpation date of 12,656-11,696 Cal yr BP with a centroid value of 12,110 Cal yr BP (see Table 4).

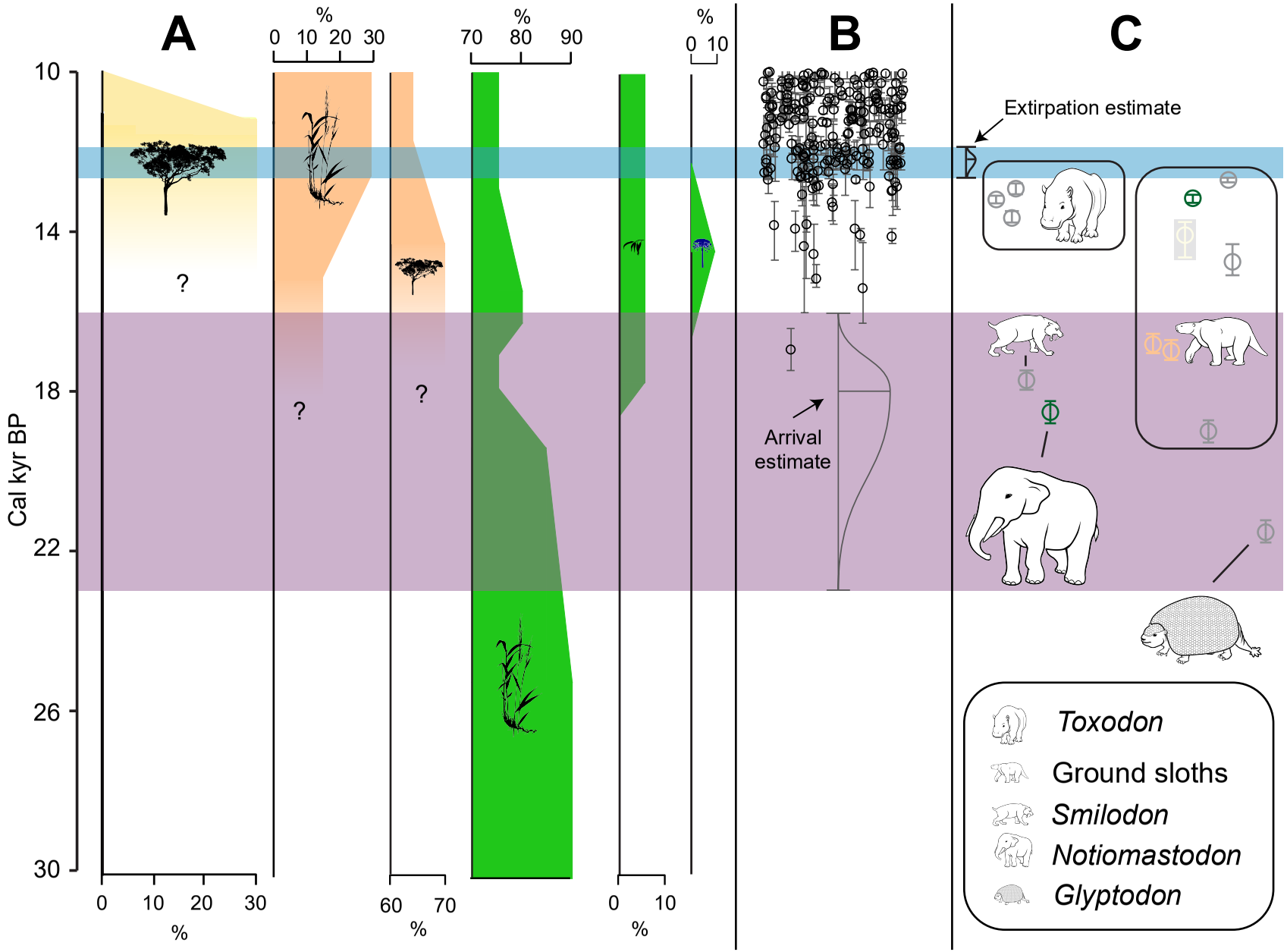
A
B
C
Cal kyr BP
10
14
18
22
26
30
0 10 20 30
%
0 10 20 30
%
60 70
%
70 80 90
%
0 10
%
?
?
?
Arrival estimate
Extirpation estimate
Toxodon
Ground sloths
Smilodon
Notiomastodon
Glyptodon

Fig. 7: Brazilian paleo-vegetational changes surrounding Pleistocene human arrival and megafaunal Extirpation.

A. Paleo-vegetation records of Brazil. Color coding corresponds to the bioregion coloring of Fig. 3. **Curves, from left to right:** Caatinga tree pollen indicators from Saquinho; herb and tree pollen indicators from the Lagoa Olhos D'Agua locality in the Atlantic Rainforest of southeastern Brazil.; and grassland, Atlantic rainforest, and *Araucaria* forest (includes trees and other plants) pollen indicators from the Morro de Itapeva locality in the Atlantic Rainforest of southern Brazil. Caatinga and Cerrado pollen indicators from SAN make up < 1% of the pollen sum, hence, were not included in this figure. Question marks and color gradients reflect that pollen relative abundances for times older than these points are unknown. See Table 2 for further locality information.
B. Same as in Fig. 6: Archaeological dates for Brazil from Goldberg, Mychajilw, & Hadly (2016). Confidence intervals about circles represent 2σ calibrated age ranges; circles represent the median values per each age. Purple area shows the GRIWM-estimated Brazil arrival date of 22,893-16,005 Cal yr BP, with a centroid value of 17,950 Cal yr BP (see Table 4). Only the dates younger than 10,000 Cal yr BP are shown here—193 of the 1,031 total from Goldberg, Mychajilw, & Hadly (2016). All 1,031 of these went into the GRIWM estimate though. Because none of the McMichael & Bush (2019) dates are older than 10,000 Cal yr BP, they are not shown here.
C. Same as in Fig. 6: High-quality calibrated Pleistocene megafaunal radiocarbon dates and GRIWM-estimated extirpation date. Illustrations denote which dates correspond to which megafauna taxa. Confidence intervals about circles represent 2σ calibrated age ranges, circles represent the median values per each age, and their colors correspond to the bioregion color coding from Fig. 3. Blue area shows the GRIWM-estimated extirpation date of 12,656-11,696 Cal yr BP with a centroid value of 12,110 Cal yr BP (see Table 4).

Discussion

Hypothesis 1: Defaunation

Regarding hypothesis 1—that megafauna extirpation caused vegetation changes—no notable vegetation change is evident directly after the estimated extirpation, except for an early-Holocene decline in Caatinga tree pollen. This postdates the minimum age of the extirpation by ~200 yr (Fig. 7). These observations lead to rejection of hypothesis 1 in a general sense. However, the Caatinga tree pollen decline that postdates the extirpation window by ~200 yr (Fig. 7) may represent a more localized defaunation signal. This is difficult to definitively claim though with only one high-quality Caatinga megafauna date (a ground sloth dated 14,637-13,748 Cal yr BP, see Table 3). If this Caatinga defaunation signal is true, however, Mimosaceae trees would have been likely most affected, given they make up most of the Caatinga's tree vegetation (see **The Caatinga** above). Interestingly, some of these Caatinga trees can survive and resprout after extreme coppicing, pollarding, and crown thinning (Figueirôa et al., 2006), suggesting that they might be adapted to Pleistocene megafaunal browsing. Though there are not any known studies that have investigated megafaunal endozoochory of Caatinga tree seeds, a lack of seed dispersal following Caatinga

megafaunal extirpation led to the observed decrease in tree pollen. However, these trees are widely used today for wood and charcoal (Figueirôa et al., 2006), so perhaps their inferred decline was due to an increase in these human behaviors at this time to some degree—the decline in Caatinga tree pollen also coincides with the aforementioned increase in archaeological dates. Altogether, Hypothesis 1 can be rejected outside of the Caatinga, but it cannot currently be resolved whether defaunation and/or anthropogenic activities might have caused the inferred Caatinga tree decline.

Hypothesis 2: Habitat loss led to megafaunal decline

The Caatinga and Atlantic Rainforest pollen records do not support Hypothesis 2, but the Cerrado and *Araucaria* Plateau records may.

In the Cerrado, the pollen record suggests a shift from forested to herbaceous landscapes. The culmination of this trade-off in pollen groups coincides with the estimated extirpation dates, particularly of toxodonts, but for all megafauna taken as a whole. *Toxodon* was a mixed C_3 feeder and C_4 grazer (Lopes et al., 2013; Pansani et al., 2019), meaning that *Toxodon* may have been more able to switch feeding habits with habitat change. If habitat loss correlates with *Toxodon* decline then, this might mask some other cause for the decline, e.g., increased competition with other species. An increase in herbaceous pollen and decrease in tree pollen suggests an opening of the landscape and less large woody vegetation, which could have been an important dietary component for some of the extinct megafauna (da Silva et al., 2019; Pansani et al., 2019; Asevedo et al., 2020). Interestingly, this vegetation shift coincided with increasing effective moisture, which would be expected to favor forest expansion over grassland, not the other way around. The estimated human arrival time precedes both of these vegetation changes, so perhaps anthropogenic landscape clearing led to these vegetation changes, an indirect pressure that eventually led to habitat loss and megafaunal decline.

The changes in *Araucaria* Plateau forest pollen from the Atlantic Rainforest of southern Brazil are interesting as well. Ledru, Mourguiart, & Riccomini (2009) noted that high abundances of *Araucaria* forest pollen tend to correlate with high effective moistures throughout the Pleistocene, and Cárdenas et al. (2019) found that initial southern Brazil *Araucaria* forest expansion in the mid-Holocene at 4,000 Cal yr BP also correlates with increased effective moisture. However, Cárdenas et al. (2019) also noted that later Holocene *Araucaria* forest expansion no longer correlated with wetter conditions. Therefore, the presence of *Araucaria* forests inferred from pollen records is not dependent upon climate alone. Robinson et al. (2018) used a neutral landscape model approach to suggest that recent *Araucaria* forest expansions from 1,410-900 Cal yr BP were due do cultivation of *Araucaria* trees for their large and nutritious *Araucaria* "pine nuts"—a legacy that can be seen in the distribution of *A. angustifolia* today. The earliest dates for *Araucaria* cultivation are unknown, but the relatively large seed size of *Araucaria* has led many authors to suggest that some form of cultivation is necessary for seed dispersal (Robinson et al., 2018). Parrots (Tella et al., 2019) and parakeets (Shepherd et al., 2008) are known to be effective *Araucaria* dispersal agents while rodents are known to be *Araucaria* seed predators (Viera et al., 2011), so a combination of human cultivation, parrots and parakeets dropping seeds, rodents forgetting or abandoning *Araucaria* seeds, and/or megafaunal endozoochory could be involved in *Araucaria* seed dispersal.

Linking back to *Araucaria* forest habitat loss, an increase in *Araucaria* forest pollen coincides with the younger bound for the human arrival window, and the inferred Pleistocene-Holocene disappearance of *Araucaria* forests lines up with the older bound for the megafaunal extirpation window. This might initially suggest that the loss of *Araucaria* forests can be implicated in the

megafaunal extirpation, but prior to ~16 kyr BP, *Araucaria* forest pollen levels at MDI (Locality 10, Fig. 4, Table 1) were 0% (Fig. 7). Perhaps a combined effect of human landscape modification superimposed on *Araucaria* forest decline was involved in the extirpation, but this cannot currently be verified.

Hypothesis 3: Climate-driven extirpation

Regarding Hypothesis 3—that climate change caused the extirpation—temperature and effective moisture in northern Brazil do not notably change preceding the extirpation period, but effective moisture does change in the Caatinga and *Araucaria* Plateaus at this time (Fig. 6). In the Caatinga, tree pollen quantity does not coincide with this, but at the *Araucaria* Plateaus, the decline in *Araucaria* forest pollen does match a dry period that interrupted a ~15+ kyr trend in increasing effective moisture (Figs 6 & 7). The extirpation window started right as this dry period ended, as inferred from *Araucaria* Plateau $\delta^{18}O$ values and resumed Caatinga carbonate growth (Fig. 6). Therefore, it is not possible to firmly reject the climate change hypothesis on the basis of these data.

Hypothesis 4: Anthropogenic extirpation

Lastly, regarding Hypothesis 4—that human pressures caused megafauna loss—it is clear that human arrival preceded megafaunal extirpation (Figs 6 & 7), and also coincided with LADs of glyptodonts, proboscideans, sloths, and *Smilodon*. If that human pressure took the form of habitat modification, competition for resources, and/or direct hunting, it may well have reduced population sizes enough to cause local population crashes. As noted in the **Results**, the LADs of larger bodied taxa are earlier than those of smaller bodied taxa, which would be consistent with animals with the smallest population sizes and longest generation times (an inverse correlate of body size) being affected earlier than smaller-bodied animals as human populations moved into the area and began to infringe on the animal populations. However, megafauna clearly persisted for at least five thousand years after humans arrived in the various areas. Therefore, while it is impossible to reject the hypothesis that humans contributed to gradual attrition of megafauna populations, it is clear that they did not cause sudden extinctions here.

Pleistocene extirpations in other regions of South America

My estimated bulk extirpation date of 12,656-11,696 Cal yr BP for Brazil is coeval with the 12,000-11,100 Cal yr BP estimate for southern Brazil based on *Sporormiella* from Raczka, Bush, & De Oliveira (2018), and overlaps that for ground sloths, equids, *Macrauchenia*, and *Toxodon* in the nearby Pampas of Argentina, all ~13,000 to 9,000 Cal yr BP (Barnosky & Lindsey, 2010). The difference on the younger end of these age ranges might be due to dietary constraints of taxa and habitat differences between these regions (see **Dietary considerations** below).

The next closest region with comparable data is southwestern Patagonia (Villavicencio et al., 2016). My estimated extirpation window of 12,656-11,696 Cal yr BP resembles that for that of Pleistocene-Holocene Patagonian felids, equids, and *Lama* cf. *owenii*, but does not overlap the extirpation estimate of ~11,000-8,000 Cal yr BP for ground sloths in Patagonia.

My 22,893-16,005 Cal yr BP estimate of human arrival in Brazil falls at least ~1,500 yr earlier than the Patagonian estimate of Villavicencio et al. (2016), but overlaps the Monte Verde ~18,500-14,500 Cal yr BP age estimate as the oldest archaeological site in Chile (Dillehay et al., 2015). Gomez-Carballa et al. (2018) used genomic data to investigate outhward dispersal from Central to South America along both the Pacific and Atlantic coasts. Therefore, my arrival estimate may suggest that there were human populations dispersing southward along the Atlantic coast as quickly as those along the Pacific coast, as prehistoric trans-Andean human dispersal is thought to be unlikely (Gómez-Carballa et al., 2018).

This is later than the estimated extirpation time of 15,800 Cal yr BP in Peru (Rozas-Dávila ~~et al.~~, Valencia, & Bush, 2016), but Rozas-Dávila, Valencia, & Bush ~~et al.~~ (2016) argue that the Peruvian extirpation was not due to human activity—15,800 Cal yr BP is much earlier than any verified archaeological dates in this region. Rather, the Peruvian extirpation is thought to coincide with warm, wet intervals that resulted in the loss of important floras and subsequent megafaunal extirpation, i.e., an example of the mosaic-nutrient hypothesis of Guthrie (1984).

Dietary considerations

C_3 plants photosynthesize sugars from water and CO_2 using phosphoglycerate—a three carbon molecule—as an intermediary, but C_4 plants are more photosynthetically efficient and dominant in Brazilian grasslands (Edwards et al., 2010). These two plant community types and their metabolic pathways can be picked up by their differences in photosynthate molecular weights, leaving distinctive $\delta^{13}C$ signatures in animal tissues, such as enamel (Koch, 2007). $\delta^{13}C$ values from South American megafauna enamel suggest that these taxa varied in their C_3/C_4 intake.

South American ground sloths tended to be C_3 browsers (Pansani et al., 2019), *Toxodon* was a mixed C_3 feeder and C_4 grazer (Lopes et al., 2013; Pansani et al., 2019), South American equids were almost exclusively C_4 grazers (Pansani et al., 2019), and *Macrauchenia* was a mixed C_3/C_4 feeder (MacFadden & Shockey, 1997). Although this may give the impression that these dietary habits are diagnostically associated with these taxa (e.g., as can be distinguished through dentition), there is growing evidence to suggest that the diets of South American herbivores were more generally dependent upon which plants were available (e.g., González-Guarda et al., 2018). For example, França et al. (2015) found a general trend $\delta^{13}C$ in Brazilian Pleistocene megafauna from north to south: C_4 grazing in the northern Cerrado (inferred to reflect the high abundance of C_4 grasses here at this time), to mixed feeding in the middle Cerrado, to C_3 feeding in the southern Cerrado, and then back to mixed feeding in southern Brazil, Uruguay, and northern Argentina—largely independent of which taxon was sampled. This means that in order to more completely understand the dynamics between megafaunal extirpation and vegetation, a finer spatial resolution needs to be analyzed (e.g., finer than that in this study), ideally with stable isotope analyses on the taxa in question.

The LAD of the ground sloths included in this study falls near the southern Brazil extirpation date maximum of 12,656 Cal yr BP. Most of the ground sloth samples included in this study are from southern Brazil, and their LAD coincided with a maximum in *Araucaria* forest pollen, a decline in Cerrado tree pollen, and an increase in Cerrado herbaceous pollen. It is unknown whether ground sloths ate *Araucaria* tissues, but the C_3 and mixed feeding habits of ground sloths and vegetation changes in this region, respectively, do not suggest that a loss of available forage or habitat caused the ground sloth extirpation here. Likewise, all of the *Toxodon* samples in this study

were from southern Brazil. If vegetation in southern Brazil changed such that C_3/C_4 plant ratios in the environment became too skewed, a mixed feeder such as *Toxodon* may have been driven to extirpation. The declines in grass and *Araucaria* forest pollen in this area coincide with the *Toxodon* LADs, but given there are only three *Toxodon* dates in this study, that means that these pollen declines also coincide with the *Toxodon* FADs, so whether vegetation change caused *Toxodon* extirpation cannot be determined here.

Archaeological considerations

Brazilian Pleistocene megafauna coexisted with humans for a long time. Goldberg, Mychajliw, & Hadly (2016) found that the density of Brazilian archaeological sites largely remained relatively low and constant until 5,000-4,000 Cal yr BP. This prehistoric Brazilian site density is also much lower than that of other South American regions—namely Peru, the northern Chilean coast, and the Southern Cone. However, Goldberg, Mychajliw, & Hadly (2016) also note that the general paucity of Brazilian archaeological sites at this time might be more of a taphonomic artifact due to low preservation potential in the Amazon and Atlantic Rainforests, and hence might underestimate the relative size of human populations. Evidence of human foraging within the Amazon Rainforest has been reported to date as far back as ~13,000 Cal yr BP (Roosevelt, 2013), and recent evidence suggests squash (*Cucurbita* sp.) cultivation in the Amazon Rainforest of Bolivia starting ~10,850 Cal yr BP (Lombardo et al., 2020). This highlights the need for further exploration of the Pleistocene peopling of the Amazon Rainforest—a large and important part of the Brazilian paleoecological story.

Conclusion

My data reject the hypothesis that megafaunal extirpation caused vegetation change, with the possible exception of a Caatinga tree pollen decline that postdates the extirpation window by ~200 yr. My second hypothesis—that vegetation change and subsequent habitat loss caused the megafaunal extirpation—is rejected by the Caatinga and Atlantic Rainforest pollen records, but may be consistent with changes in Cerrado and Atlantic Rainforest pollen records that precede the megafaunal extirpation estimate. The hypothesis that climate change caused the extirpation can be rejected for northern Brazil, but may be consistent with a wetting event that followed significant drying in southern Brazil from ~13,000 to ~11,500 Cal yr BP. My data do not reject the hypothesis that anthropogenic pressures caused the extirpation through direct and indirect pressures that reduced megafauna populations over millennia, but do reject a rapid "blitzkrieg" event.

The timing of extirpation in Brazil is mostly coeval with that for Pampean and Patagonian Pleistocene megafauna, but is much younger than that for Peru. Climate change is the leading hypothesis for megafaunal extirpation in the Pampas (Barnosky et al., 2016) and Peru (Rozas-Dávila et al., 2016) but a combination of humans, climate, and vegetation change are all implicated in the extirpation of megafauna from Patagonia (Villavicencio et al., 2015), I also found that humans, climate, and vegetation change correlate with Brazilian Pleistocene megafaunal extirpation, but in the form of gradual human population growth, regional effective moisture changes, and regional vegetation change.

Chapter 3: The effects of temperature and humidity on *Sporormiella minima* growth: Implications for historic and prehistoric records

Spano, N.[1, 2]
[1]Department of Integrative Biology, University of California, Berkeley, Berkeley, California, United States of America
[2]University of California Museum of Paleontology, University of California, Berkeley, Berkeley, California, United States of America
E-mail: spano@berkeley.edu

Keywords: *Sporormiella*, temperature, humidity, paleoecology

Abstract

A growing number of studies use the *Sporormiella* indicator to reconstruct historic and prehistoric populations of large terrestrial herbivores, but little is known about how sensitive this indicator is to environmental variables, including climate. In this study, I tested the following hypotheses: 1) *Sporormiella* has optimal growth rates at moderate temperatures; and 2) *Sporormiella* has maximum growth rates at high relative humidities. To test these hypotheses, I conducted experiments using *Sporormiella minima*—a *Sporormiella* species commonly reported in large terrestrial herbivore population reconstruction studies—, cultured it in growth chambers with constant temperatures and relative humidities, and recorded daily mycelial growth rates.

I found that *S. minima* grew optimally at 30 °C but did not differ in its growth between high (~100%) and low (89-95%) relative humidity treatments. Also, although the *S. minima* in this study formed hyphae and ascocarps under constant light, it did not eject spores.. For temperature, a contrast between presumably optimum growth substrate temperature and ambient temperatures could inhibit *Sporormiella*'s fitness and subsequent representation in historic and prehistoric records. Relative humidity above 89% may not affect *Sporormiella*'s growth directly, but high relative humidity buffers growth media against temperature swings and effective moisture as a product of relative humidity likely still has taphonomic consequences for *Sporormiella* representation. Both variables could be complicated by local adaptation in *Sporormiella* strains and populations, making comparative work necessary to understand these factors more generally. Lastly, comparing these results with

findings from paleoecological studies highlights the potential influence of paleoclimate on *Sporormiella* growth and subsequent abundance in sediment records.

Introduction

Large terrestrial herbivores are ecologically important. As ecosystem engineers (Jones, Lawton & Shachak, 1994), they substantially increase nutrient transport rates (Doughty et al., 2016), affect the distributions of other species (Estes et al., 2011), and have a pronounced influence on atmospheric methane concentrations—with considerable implications for global warming (Solomon et al., 2007). These phenomena are well documented for modern large terrestrial herbivores, but were likely even more important prior to the Late Quaternary extinction (LQE) event. This event occurred ~50-3 ka and resulted in the loss of ~65% of all large (mass > 44 kg) mammal species worldwide (Nogues-Bravo et al., 2010). The LQE was abnormal compared to background extinction rates of large animals throughout the Cenozoic (Alroy, 1999) and peaked during an age of global climate change—including glacial-interglacial cycles throughout the Pleistocene along with warming after the last glacial maximum (LGM) (Clark et al., 2009)—and human population expansion (Brook & Barnosky, 2009). The ability to quantify large terrestrial herbivore abundances through time is key for understanding their effects on ecosystems, the dynamics of the LQE, and how to better conserve the last large terrestrial herbivores left.

One increasingly popular approach (see Baker, Bhagwat, & Willis, 2013) to reconstruct past abundances of large terrestrial herbivores is to measure relative quantities of spores from the dung fungus *Sporormiella* (syn: *Preussia*, Kruys & Wedin, 2009) in historic and prehistoric sediment records (e.g., Burney, Robinson, & Burney, 2003; Robinson, Burney, & Burney, 2005; Gill et al., 2009; Wood et al., 2011; and Rule et al., 2012). *Sporormiella* (Family Sporormiaceae) is an ascomycete that generally grows and reproduces on the dung of large terrestrial herbivores (Ahmed & Cain, 1972). Regarding mammals, it has been found on mammoth (Aptroot & van Geel, 3006), savanna elephant (Ebersohn & Eicker, 1997), cow, goat, sheep, donkey, horse, moose, elk, deer, rabbit, and rodent dung (Ahmed & Cain, 1972). It can also be found on moa (Wood & Wilmshurst, 2016), partridge, pheasant, and goose dung (Ahmed & Cain, 1972) though, so it is not solely adapted to mammals. Most of the > 60 species of *Sporormiella* (Ahmed & Cain, 1972) have only been found on dung, but *S. minima*, *Preussia africana*, *P. mediterranea*, and *P. terricola* are also known to grow on vegetation, while *S. subticinensis*, *P. fleischhakii*, *P. flanaganii*, *P. aemulans,* and *P. funiculata* can use soil as a growth substrate (Kruys & Wedin, 2010). *Sporormiella* has been found in boreal and deciduous forests (Davis & Shafer, 2006), tropical (Basumatary & McDonald, 2017) and temperate grasslands (Gill et al., 2013), and tropical forests (Harvey et al., 2019) as a wide-ranging fungus. After growing vegetatively on dung for approximately six weeks (Asina, Jain, & Kain, 1977a), the fruiting bodies (ascocarps) of *Sporormiella* eject spores (ascospores) that adhere to nearby vegetation (Bell, 1983) or are ultimately incorporated into soils (e.g., Wood & Wilmshurst, 2011), wetlands (e.g., Schofield & Edwards, 2011), lake sediments (e.g., Etienne et al., 2012), and nearshore marine sediments (e.g., Byrne et al., 1982). When

the spores that adhere to vegetation are consumed by large terrestrial herbivores and later defecated, they germinate in the new dung to repeat the cycle (Bell, 2005). Those that are preserved in sediment records are commonly applied in general paleoenvironmental studies because they have been found on every continent except Antarctica (Baker, Bhagwat, & Willis, 2012), are relatively easy to identity (Gill, 2013), and are thought to be mostly obligate to the dung of large terrestrial herbivores (Gill, 2013). *Sporormiella* hyphae have not been found in the fossil record, but *Sporormiella* spores have relatively thick, chitinous, melanized, cell walls which are thought to aid in preservation (van Asperen, Kirby, & Hunt, 2016)—the oldest record of which is from a 12 Myr-old Miocene welded tuff deposit in Idaho (Davis & Ellis, 2010). However, other environmental factors—including climate—may affect *Sporormiella*'s representation in historic and prehistoric records.

Both temperature and humidity affect *Sporormiella* ascospore germination rates (Asina, Jain, & Cain, 1977a) and ascocarp production (Asina, Jain, & Cain, 1977b). Therefore, (paleo)climatic changes and ambient weather conditions may significantly influence spore production, spore ejection, and hence spore influx rates into depositional environments and sediment records. This is important because the key assumption behind *Sporormiella*'s utility is that the quantity of *Sporormiella* spores in historic and prehistoric records is predominantly a function of how much large terrestrial herbivore dung is on the surrounding landscape, which is ultimately dependent upon how many large terrestrial herbivores are present.

In this study, I sought to test how temperature and relative humidity affect *Sporormiella* abundances, with implications for reconstructing past large terrestrial herbivore abundances. I hypothesized that: 1) *Sporormiella* has optimal growth rates at moderate temperatures; and 2) at relatively high humidities (between 89-100%), *Sporormiella* has maximum growth rates at higher humidities. To test these hypotheses, I cultured *S. minima*—a *Sporormiella* species commonly reported in large terrestrial herbivore population reconstruction studies (e.g., Davis, 1987)—on potato dextrose agar (PDA) in growth chambers set to fixed temperatures with saturated salt solutions to control relative humidities (see Rockland, 1960). I used saturated salt solutions because they are a cost-effective and well-calibrated way to control relative humidity within a closed environment.

Methods

I started by ordering four unique strains of *Sporormiella* from the United States Department of Agriculture (USDA) Agricultural Research Service (ARS) Culture Collection, Mold Database on 26 November 2019 (Table 5). These strains are available free-of-cost from the USDA ARS Northern Regional Research Laboratory (NRRL) in Peoria, IL (https://nrrl.ncaur.usda.gov/). I then stored them in the dark for five days at ~2 °C before sampling. During this time, I prepared BD Difco™ PDA following the manufacturer's instructions, and poured 25 mL of PDA per 100 mm × 15 mm polystyrene Petri dish (hereafter "Petri dish(es)") using serological pipettes in a Baker E6-6252 laminar flow hood.

Table 5: *Sporormiella* strains ordered from the United States Department of Agriculture (USDA) Agricultural Research Service (ARS) Culture Collection, Mold Database, with associated collecting and growth conditions.

NRRL number	Other reported number	Strain name	Collector	Isolation information	Isolation locality	Reported optimal growth temperature [°C]	Original prepared growth medium
66943	ATCC (American Type Culture Collection) 16014	*Sporormiella minima*	Shung-Chang Jong	Unknown	Unknown	25	PDA
38181	MYC-1508	*Sporormiella minimoides*	Unknown	Unknown	Unknown	25	PDA
29282	MYC-467	*Sporormiella leporina*	Donald T. Wicklow	Growing on a preexisting black stroma (possibly that of *Hyoxylon*) on downed hardwood	Delabar State Park, Henderson County, IL, USA	25	PDA
29987	MYC-745	*Sporormiella minima*	Donald T. Wicklow	Growing on preexisting tissue of *Stereum*	A mixed hardwood forest in Warm	25	PDA

	complicatum on downed hardwood	Spring, GA, USA

As a pilot experiment, I placed initial isolates into plastic, 2.5 L Decor Tellfresh® Pastry Storer containers (hereafter "containers") with the container lids sealed to test which of the four strains under which lighting and general humidity conditions would grow well enough for my main temperature × relative humidity experiment. The pilot experiment was done in Conviron PGR15 growth chambers (hereafter "growth chambers") with: 1) full, fluorescent light, constantly on, measured with a LI-COR LI-250A Light Meter (average = 65.054 μmol of photons m^{-2} s^{-1}, see Supplemental Table 1) vs. complete darkness; and 2) growth in ambient humidity vs. high humidity (expected value of 100%), the latter condition created by adding double-distilled water to open Petri dishes placed within the containers. I used a marker on each sample's Petri dish lid to trace daily mycelial growth at roughly the same time of day for one week, and found that *S. minima* strain NRRL 66943 grew the quickest of the four strains and grew quickest under full light at ambient humidity. Using full light for my primary experiment was optimal because *Sporormiella* does not develop pigmentation without light (Asina, Jain, & Cain, 1977b), which would have made observing and recording growth rates much more difficult. Also, I only used fluorescent lighting for this experiment, as Asina, Jain, & Cain, (1977b) found that *Sporormiella* ascocarp development does not require incandescent light.

Using *S. minima* strain NRRL 66943, I sampled the Petri dish from the pilot experiment with the most vigorous growth using a ~1 cm diameter cork borer and inoculated new PDA plates in a Baker UBM-400 biosafety cabinet—prepared as noted above. The cork borer was pressed vertically through the inside edge of the mycelial growth margin and each "plug" of mycelium + PDA was placed at the center of each new PDA plate for inoculation. After one week of growth, the best growing treatment was sampled by cork borer in the same way to inoculate autoclaved crystallizing glass dishes that each had 20 mL of PDA. The crystallizing dishes then had their glass lids sealed using Micropore™ surgical tape to close them off from other microbes but allow for gas exchange. I then placed the crystalizing dishes into the containers and placed those into 2.5 gallon zipper-sealed plastic bags before placing each container in its respective growth chamber.

Sporormiella spore germination (Asina, Jain, & Cain, 1977a) and ascocarp production rates (Asina, Jain, & Cain, 1977b) have not been observed outside of 10-40 °C , so I set the growth chambers in this study to constant values of 10, 20, 30, and 40 °C. Also, *Sporormiella* spore germination is highest with freestanding water (near 100% relative humidity), and had not previously been known to occur at relative humidities lower than 92% (Kuthubutheen & Webster, 1986a). At 10-40 °C, a potassium nitrate saturated salt solution will create relative humidities from 89-95%, respectively (Rockland, 1960) (Table 6). As using potassium nitrate creates relative humidities on the lower end of the known *Sporormiella* tolerance spectrum, I therefore used potassium nitrate saturated salt solutions prepared in open Petri dishes alongside freestanding double-distilled water in open Petri dishes to create eight unique temperature × relative humidity treatment combinations, with two dishes (one replicate) per treatment. For the potassium nitrate treatments, this meant the relative humidities were expected to be 95.16% at 10 °C, 94.62% at 20 °C, 92.31% at 30 °C, and 89.03% at 40 °C (Table 6). This also meant that there was only one relative humidity per each temperature

treatment. I also included one Lascar Electronics EL-USB-2 temperature, humidity, and dew point data logger per treatment to record temperatures and relative humidities over the entire observation period (Supplemental Figs 1-8).

Table 6: Expected relative humidities for potassium nitrate at the temperatures tested in this study. All standing water treatments have expected humidity values of 100% at all temperatures.

Temperature [°C]	Expected humidity [%]	Expected humidity uncertainty [∓, %]
10	95.1	1.4
20	94.6	0.66
30	92.3	0.60
40	89.0	1.2

To document *S. minima* mycelial growth rates and spore ejection, I removed each crystalizing dish from its plastic bag treatment daily at around the same time and then photographed each sample for six weeks (see Supplemental Folder 1 for photograph files) using a Motorola g^7 cell phone camera running Android v. 9 placed at a fixed position over the edge of a 17.5 cm tall cardboard box (see Appendix 1 for camera and photograph file details). The box and dish to be photographed were placed in the same location with the same lighting to keep photograph light levels consistent while imaging. I chose a six week period because Asina, Jain, & Cain (1977a) found that maximum spore ejection rates required that long of an incubation period. I also periodically checked the samples for ascocarp development and spore ejection using a dissecting microscope. *Sporormiella* creates ~250 μm pseudothecial ascocarps that can be easily distinguished from a surrounding mycelial stroma (e.g., Kruys, 2015). After finishing photographing, I then used the "Selection Tool" in Adobe Photoshop 2020 to calculate ratios of how many pixels in each photograph showed mycelial coverage vs. how many pixels made up the bottom of each crystalizing dish. To standardize the daily growth selection process, I only selected areas in each photograph that had a distinct contact between hyphal cover and fresh agar—the margin of the mycelium. I then used these ratios to calculate growth rates as percentages of plate coverage per each day, with one replicate per treatment (Fig. 8).

Results and Discussion

Temperature and humidities achieved

Temperatures recorded were within ~3 °C of the programmed range for each experimental setup (10, 20, 30, and 40 °C; see Supplemental Figs 1-8). The humidity values for all treatments were lower than expected (95.16% at 10 °C, 94.62% at 20 °C, 92.31% at 30 °C, and 89.03% at 40 °C), but all of the potassium nitrate treatments were less humid than their freestanding water counterparts. The humidity values for the freestanding water treatments were within ~5% of the expected 100% relative humidity values and did not notably vary over the observation period (Supplemental Figs 1-8). However, the 10 °C potassium nitrate treatment was the only one that retained its humidity throughout the experiment. Although the other potassium nitrate treatments lost humidity throughout and at different rates, this did not seem to have any observable effects on growth rates compared to the constant humidity, freestanding water treatments at the same temperatures. This suggests that even with the heterogeneous relative humidities of the potassium nitrate treatments, these relatively lower humidities did not affect growth rates. Lastly, the data logger results show notable, punctuated daily temperature and humidity changes due to my photographing sessions where I needed to remove the samples from their growth chambers; however, they otherwise show mostly constant trends (Supplemental Figures 1-8).

Effects of temperature on *Sporormiella minima* growth

In general, the mycelial growth rates of the *Sporormiella minima* samples in this study were comparable between replicates, optimal at 30 °C, and absent at 40 °C (Fig. 8).

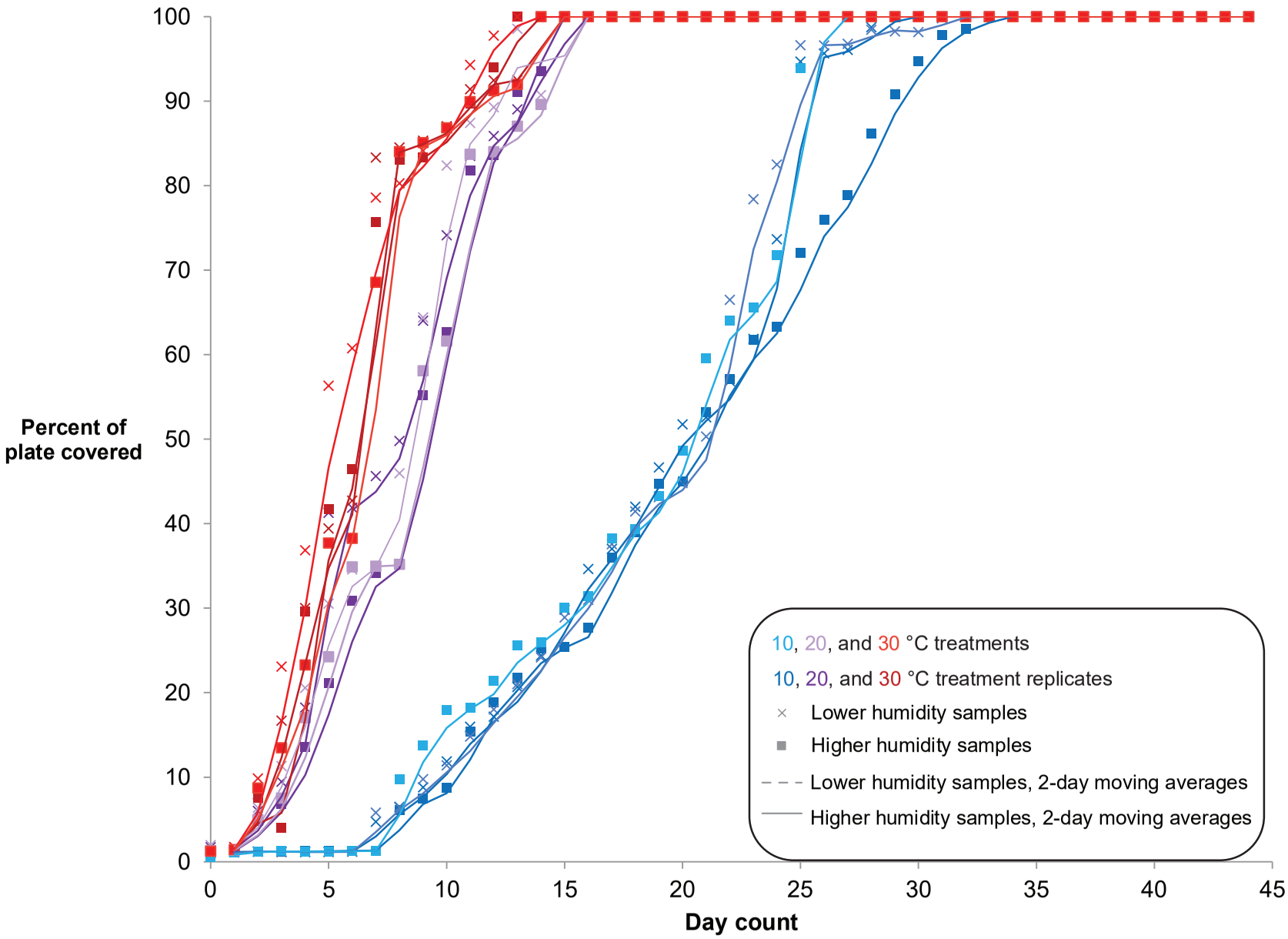
Percent of plate covered
100
90
80
70
60
50
40
30
20
10
0
0
5
10
15
20
25
30
35
40
45
Day count
10, 20, and 30 °C treatments
10, 20, and 30 °C treatment replicates
Lower humidity samples
Higher humidity samples
Lower humidity samples, 2-day moving averages
Higher humidity samples, 2-day moving averages

Figure 8: Growth rates of *Sporormiella minima* by day per each Plate 1 temperature × relative humidity treatment. Percent of plate covered refers to how much of each crystalizing dish showed visible mycelial growth. The 40 °C samples are not shown here because they did not grow. Growth varied notably between temperature treatments but not relative humidity treatments.

Although I did not test growth at 5 °C increments, the optimum I observed at 30 °C follows the observation from the USDA ARS NRRL that the *S. minima* strain in this study (NRRL 66943, ATCC 16014) grows optimally at 25 °C (Table 5). Asina, Jain, & Cain (1977a) found that *S. minima* germinates optimally at 30 °C, but they also found that *S. minima* produces a maximum mycelial mass anywhere from 15-40 °C (1977b). Wicklow & Moore (1974) likewise found that *S. minima* germination occurred anywhere from 10-37.5 °C, and that coprophilous ascomycete development in general was slower at cooler temperatures. It is not surprising then that the 10 °C samples in this study grew more slowly and that the 40 °C samples did not grow whatsoever. An important consideration for this experiment though is that constant temperature is not very representative of growth conditions in the field. An experiment with daily temperature oscillations may produce a different and more representative growth response.

Effects of relative humidity on *Sporormiella minima* growth

Coprophilous fungal growth rates are typically well known to decline in drier conditions (Kuthubutheen & Webster, 1986a), which makes the similarity between high and low relative humidity growth rates in this study quite interesting. Kuthubutheen & Webster (1986b) recorded growth rates of coprophilous fungi and found that they do not fruit at relative humidities lower than 98%; however, *Sporromiella* was not one of the fungi they investigated. The *S. minima* in this study did fruit though, suggesting that it has a relatively wide relative humidity tolerance.

As with constant temperature though, constant relative humidity is a simplification compared to field growth conditions. An experiment with a gradual reduction in relative humidity to represent aging, drying feces may be a better model to test *Sporormiella* growth (Schlüz & Shumiloskikh, 2017). Relative humidity is also not the same as effective moisture, rainfall, or overland flow, which are known to affect organic microfossil deposition (Holmes, 1994). However, high relative humidity is a prerequisite for effective moisture and rainfall, so it could have taphonomic consequences later on.

Sporormiella spore ejection and ambient light

The fact that none of the samples in this study ejected their spores is also quite interesting, as the spores are the main units of paleoecological interest (see references in the Introduction). The reproductive structures observed in this study were verified to be ascocarps and not asexual conidiophores (see Asgari & Rasoul, 2010 for *Sporormiella* conidiophores), meaning that sexual

reproduction had occurred, but the spores may not have been present within the ascocarps. Asina, Jain, & Cain (1977a) found that maximum spore ejection (no other spore ejection values were reported) occurred after their *Sporormiella* samples were incubated in six weeks of darkness, followed by a 12-hour window of full light conditions. This suggests that in field conditions, *Sporormiella* grows deep enough within dung boluses to be persistently shielded from light, and needs dung that is not disturbed and exposed to light by rainfall, scavenging insects, herbivore trampling, or other factors in order to eject spores. Once the mycelium has developed enough, *Sporormiella* then needs a cue to develop ascocarps and spores at the dung surface.

Local climatic adaptation could also affect *Sporormiella* levels

Local adaptation of *S. minima* may mean that strains from different areas could have different responses to temperature and relative humidity regimes. This complicates comparing the responses of modern *Sporormiella* to *Sporormiella* that grew during the last glacial maximum in boreal forest biomes, for example. The *S. minima* strain used in this study (NRRL 66943) does not have locality information associated with it, so no speculation can be made regarding adaptations to its environment of origin. The strain in this study may be specifically adapted to the area it came from and not be representative of general *Sporormiella minima* growth. One approach to address *Sporormiella* temperature and humidity adaptations could be to test for genetic markers of heat and humidity (in)tolerance, as has been done regarding thermal adaptation in *Candida albicans*—the yeast that causes thrush in humans (Leach et al., 2012).

In situ factors that could affect *Sporormiella* growth

Sporormiella growth could also be limited if the dung it is growing on erodes before the fungus is old enough to develop and eject spores. In a temperate conifer forest plantation in southwestern Japan, Hirata et al. (2008) found that cattle dung takes ~100-500 days to decompose to ~50-66% of its original mass, which is surprisingly slow. However, Hirata et al. (2008) note that their study plantation may have been relatively dry, and that areas with higher precipitation could have quicker dung weathering rates. Indeed, a study by Cruz et al. (2012) found that dung weathering rates in a tropical grassland in Mexico were quicker during the rainy season. Hirata et al. (2008) also noted though that an absence of dung-decomposing animals may have been responsible for the slow weathering rates they observed. In an experimental study, Horgan (2005) found that dung beetles in the eastern slopes of the Peruvian Andes removed 50-100% of pig dung samples within three days. In an experimental study on moose dung fungal diversity vs. its natural habitat in Sweden, Nyberg & Persson (2002) found that insect damage was negatively correlated with dung fungal diversity too. In sum, both high precipitation and insect damage could hinder *Sporormiella* growth by prematurely weathering and eroding dung, which would ultimately result in lower *Sporormiella* spore quantities in sediment records.

Contrasts between dung, soil, and air temperatures could also affect *Sporormiella* growth. Ashcroft & Gollan (2013) found that for soil and adjacent ground-level air samples, moisture content and the high heat capacity of water effectively buffers both soil and ground-level air from temperature swings. Air temperature was found to be more sensitive to changes in relative humidity while soil temperature depended more on vapor pressure deficit, meaning that soil requires both low humidity and high temperature to dry out and hence be more susceptible to temperature swings. At lower relative humidities, ground-level air temperature was found to be significantly correlated with topographic exposure and canopy cover, while the same held true for soils with higher vapor pressure deficits. For marked changes in ground-level and soil temperatures throughout the Quaternary (e.g., the Pleistocene - Holocene transition), this means that less humid areas would have been more susceptible to temperature swings which could have limited *Sporormiella* growth. Based on the findings in this study, this means that it is reasonable to expect that global Quaternary paleoclimatic changes could have affected ground-level microclimates and therefore could have significantly affected historic and prehistoric *Sporormiella* quantities.

Implications for interpreting paleoecological records

Changes in Quaternary (paleo)climates occur at millennial, centennial, and decadal scales, with effects that cannot be observed with diurnal time scale experiments such as this one. However, persistent temperature differences could affect *Sporormiella* growth over multiple lifecycles, which could add up to (paleo)climate timescales if those temperature differences are large enough. Table 7 shows how paleoclimate and vegetation change—a factor that could affect local microclimates—correlate with *Sporormiella* declines in select paleoecological studies.

In their study on Pleistocene *Sporormiella* declines coinciding with the formation of novel plant communities in the eastern US, Gill et al. (2009) noted that the lowering of *Sporormiella* abundances coincided with a date from a butchered mammoth bone in nearby southeastern Wisconsin. They suggest that the *Sporormiella* decline was due to a decline in large herbivore populations, and that it may have been at least partially anthropogenic. Thus, although *Sporormiella* declined in that study alongside Bølling-Allerød warming, it is consistent with the data to suggest that both climate change and large herbivore losses could have caused that *Sporormiella* decline. Gill et al. (2009) also found that *Sporormiella* decline coincided with a transition from spruce to broadleaf forest. This may also mean that large herbivore dung became more shaded by denser canopies. Nyberg & Persson (2002) found that moose dung fungal diversity was lower on dung in a spruce forest compared to a pine forest, and suggested that higher shade from the spruce branches and hence increased relative humidity was the reason. If canopy cover became greater in eastern US broadleaf forests than it was with spruce forests, the *Sporormiella* decline observed by Gill et al. (2009) coincident with this forest transition could have been at least partially due to a canopy-mediated microclimate effect as well.

Parker & Williams (2011) sought to test which factors explain *Sporormiella* quantities in modern sediments and found that county-level cattle population density and precipitation were significant predictors. They also found that precipitation was interestingly negatively correlated with *Sporormiella* spore abundance, and posited that the aerial spores could be knocked down by rainfall and therefore hindered from dispersing further. This highlighted how rainfall and precipitation could affect the dispersal and transport of *Sporormiella* spores. This is a separate mechanism from how relative humidity could affect *Sporormiella* growth, as I tested in this study. Further work is required to investigate how precipitation in a more confined experimental setting, or conversely, how relative humidity in a larger field study, could affect *Sporormiella* taphonomy.

Davis & Shafer (2006) found a correlation between *Sporormiella* declines and a transition to warm-dry conditions. This could then mean that the decline was in part due to climate change. In the Peruvian Andes, Rozas-Davila, Valencia, & Bush (2016) reported *Sporormiella* declines that coincided with warmer and wetter conditions. The warmer conditions were more generally related to post-LGM warming and the wetter conditions were inferred from an increase in benthic diatom abundances. Again, this could mean that *Sporormiella* levels lowered because they were being dispersal-limited by rainfall, but Rozas-Davila, Valencia, & Bush (2016) suggested that perhaps nearby soils became too waterlogged for palatable plants, causing a loss of food supply and subsequent large terrestrial herbivore declines.

In southeastern Brazil, Raczka, Bush, & De Oliveira (2018) observed that *Sporormiella* declines coincided with cooler and wetter conditions, but did not provide a mechanistic explanation for how that climatic transition would have affected *Sporormiella* quantities or large herbivore populations. In southern Patagonia, Musotto, Bianchinotti, & Borromei (2012) did not go into much detail regarding why *Sporormiella* quantities declined alongside a transition from forest to steppe conditions, but this could have been due to more general drying conditions. For Australia, both Rule et al. (2012) and van der Kaars et al. (2017) reported no link between Pleistocene *Sporormiella* declines and climate change. Rule et al. (2012) noted a coincident increase in grass and sclerophyll pollen, but argued that this was a consequence, not a cause of large terrestrial herbivore losses as inferred from *Sporormiella* declines. van der Kaars et al. (2017) reported a decrease in "herbaceous woody" taxa—predominantly from Asteraceae and Chenopodiae—in southwestern Australia and argued that this was due to regional drying. This means that the drying could have reduced *Sporormiella* quantities both directly at ground level and indirectly through a reduction in canopy cover, perhaps alongside large herbivore extinctions. Lastly, Robinson, Burney, & Burney (2005) did not report on the climatic conditions surrounding Holocene herbivore extinctions in Madagascar. They observed an increase in graminoid and other charcoal types, but this happened after *Sporormiella* declined.

The relationship between climate change and *Sporormiella* declines in sediment records is therefore not unidirectional and as many authors have pointed out (e.g., Cook et al., 2011; Feranec et al., 2011; Parker & Williams, 2011; Dodson & Field, 2018; Perrotti & van Asperen, 2019; and references therein) likely depends on many different factors. All of this is not to say that *Sporormiella* quantities are not influenced by large herbivore concentrations—there are many verification studies

to suggest that they are (e.g., Etiennne et al., 2012; Gill et al., 2013; Baker et al., 2016)—but more that the hypothesis that climate change causes *Sporormiella* quantity changes in sediment records cannot be rejected.

Conclusion

My first hypothesis was that *Sporormiella minima* grows optimally at medium temperatures. This is supported given the fastest *S. minima* mycelial growth rates occurred at 30 °C and were lower at temperatures outside of that (Fig. 8). My second hypothesis was that *Sporormiella* grows best at high humidities (approaching 100%), which is rejected given the mycelial growth rates I observed in *S. minima* were not notably different between relative humidity treatments as low as 89% (Fig. 8). Lastly, although I set out to test *Sporormiella* spore ejection rates as well, my samples did not eject spores whatsoever.

The temperature optimum for *S. minima* observed in this study matches that for previous studies on *S. minima* ascospore germination (Asina, Jain, & Cain, 1977a) and ascocarp production rates (Asina, Jain, & Cain,, 1977b). However, the insensitivity to humidity I observed in this study differs from other experimental studies that have observed humidity preferences in *S. minima* (e.g., Kuthubutheen & Webster, 1986a; 1986b). Local climatic adaptation might complicate comparing my findings to *Sporormiella* from other locations and times. However, while a handful of paleoecological studies on *Sporormiella* declines have found at least some correlation with climate change, others found no correlation. There is also a pronounced effect of moisture on soil and ground-level air temperature (Ashcroft & Gollan, 2013), meaning that paleo-humidity is likely important for buffering *Sporormiella* growth from detrimental temperature swings. This highlights the need for further work to assess the relative importance of paleoclimate—including paleotemperature, paleo-precipitation, and paleo-humidity—alongside large herbivore population reconstructions to better understand the *Sporormiella* indicator and its utility.

References

Ahmed, S. I., & Cain, R. F. (1972). Revision of the genera *Sporormia* and *Sporormiella*. *Canadian Journal of Botany*, *50*(3), 419–477. https://doi.org/10.1139/b72-061

Alroy, J. (1999). Putting North America's End-Pleistocene Megafaunal Extinction in Context. In *Extinctions in Near Time* (pp. 105–143). Springer US. https://doi.org/10.1007/978-1-4757-5202-1_6

Andreev, A. A., Tarasov, P. E., Wennrich, V., Raschke, E., Herzschuh, U., Nowaczyk, N. R., … Melles, M. (2014). Late Pliocene and Early Pleistocene vegetation history of northeastern Russian Arctic inferred from the Lake El'gygytgyn pollen record. *Climate of the Past*, *10*(3), 1017–1039. https://doi.org/10.5194/cp-10-1017-2014

Angel, K., & Wicklow, D. T. (1983). Coprophilous fungal communities in semiarid to mesic grasslands. *Canadian Journal of Botany*, *61*(2), 594–602. https://doi.org/10.1139/b83-067

Aptroot, A., & van Geel, B. (2006). Fungi of the colon of the Yukagir Mammoth and from stratigraphically related permafrost samples. *Review of Palaeobotany and Palynology*, *141*(1–2), 225–230. https://doi.org/10.1016/j.revpalbo.2005.04.006

Araujo, B. B. A., Oliveira-Santos, L. G. R., Lima-Ribeiro, M. S., Diniz-Filho, J. A. F., & Fernandez, F. A. S. (2017). Bigger kill than chill: The uneven roles of humans and climate on late Quaternary megafaunal extinctions. *Quaternary International*, *431*, 216–222. https://doi.org/10.1016/J.QUAINT.2015.10.045

Archibald, S., Bond, W. J., Stock, W. D., & Fairbanks, D. H. K. (2005). Shaping the landscape: Fire-grazer interactions in an African savanna. *Ecological Applications*, *15*(1), 96–109. https://doi.org/10.1890/03-5210

Arruda, D. M., Schaefer, C. E. G. R., Fonseca, R. S., Solar, R. R. C., & Fernandes-Filho, E. I. (2018). Vegetation cover of Brazil in the last 21 ka: New insights into the Amazonian refugia and Pleistocenic arc hypotheses. *Global Ecology and Biogeography*, *27*(1), 47–56. https://doi.org/10.1111/geb.12646

Asevedo, L., D'Apolito, C., Misumi, S. Y., Barros, M. A. de, Barth, O. M., & Avilla, L. dos S. (2020). Palynological analysis of dental calculus from Pleistocene proboscideans of southern Brazil: A new approach for paleodiet and paleoenvironmental reconstructions.

Palaeogeography, Palaeoclimatology, Palaeoecology, *540*, 109523. https://doi.org/10.1016/j.palaeo.2019.109523

Asgari, B., & Zare, R. (2010). Two new species of Preussia from Iran. *Nova Hedwigia*. https://doi.org/10.1127/0029-5035/2010/0090-0533

Ashcroft, M. B., & Gollan, J. R. (2013). Moisture, thermal inertia, and the spatial distributions of near-surface soil and air temperatures: Understanding factors that promote microrefugia. *Agricultural and Forest Meteorology*, *176*, 77–89. https://doi.org/10.1016/j.agrformet.2013.03.008

Asina, S., Jain, K., & Cain, R. F. (1977a). Factors influencing ascospore germination in three species of *Sporormiella*. *Canadian Journal of Botany*, *55*(14), 1908–1914. https://doi.org/10.1139/b77-218

Asina, S., Jain, K., & Cain, R. F. (1977b). Factors influencing growth and ascocarp production in three species of Sporormiella. *Canadian Journal of Botany*, *55*(14), 1915–1925. https://doi.org/10.1139/b77-219

Baker, A. G., Bhagwat, S. A., & Willis, K. J. (2013). Do dung fungal spores make a good proxy for past distribution of large herbivores? *Quaternary Science Reviews*, *62*, 21–31. https://doi.org/10.1016/j.quascirev.2012.11.018

Baker, A. G., Cornelissen, P., Bhagwat, S. A., Vera, F. W. M. M., & Willis, K. J. (2016). Quantification of population sizes of large herbivores and their long-term functional role in ecosystems using dung fungal spores. *Methods in Ecology and Evolution*, *7*(11), 1273–1281. https://doi.org/10.1111/2041-210X.12580

Baker, A. S. (2009). Acari in archaeology. *Experimental and Applied Acarology*, *49*(1–2), 147–160. https://doi.org/10.1007/s10493-009-9271-1

Baker, P. A., & Fritz, S. C. (2015). Nature and causes of Quaternary climate variation of tropical South America. *Quaternary Science Reviews*, *124*, 31–47. https://doi.org/10.1016/J.QUASCIREV.2015.06.011

Barnosky, A. D. (2004). *Biodiversity response to climate change in the middle Pleistocene : the Porcupine Cave fauna from Colorado*. University of California Press.

Barnosky, A. D., & Lindsey, E. L. (2010). Timing of Quaternary megafaunal extinction in South America in relation to human arrival and climate change. *Quaternary International*, *217*(1–2), 10–29. https://doi.org/10.1016/j.quaint.2009.11.017

Barnosky, A. D., Lindsey, E. L., Villavicencio, N. A., Bostelmann, E., Hadly, E. A., Wanket, J., & Marshall, C. R. (2016). Variable impact of late-Quaternary megafaunal extinction in causing ecological state shifts in North and South America. *Proceedings of the National Academy of Sciences*, *113*(4), 856–861. https://doi.org/10.1073/pnas.1505295112

Barnosky, E. H. (1994). Ecosystem dynamics through the past 2000 years as revealed by fossil mammals from Lamar cave in Yellowstone National Park, USA. *Historical Biology*, *8*(1–4), 71–90. https://doi.org/10.1080/10292389409380472

Bartlett, L. J., Williams, D. R., Prescott, G. W., Balmford, A., Green, R. E., Eriksson, A., … Manica, A. (2015). Robustness despite uncertainty: Regional climate data reveal the dominant role of humans in explaining global extinctions of Late Quaternary megafauna. *Ecography*, (July 2015), 152–161. https://doi.org/10.1111/ecog.01566

Basumatary, S. K., & McDonald, H. G. (2017). Coprophilous fungi from dung of the Greater One-Horned Rhino in Kaziranga National Park, India and its implication to paleoherbivory and paleoecology. *Quaternary Research (United States)*, *88*(1), 14–22. https://doi.org/10.1017/qua.2017.34

Behling, H. (2002). South and southeast Brazilian grasslands during Late Quaternary times: a synthesis. *Palaeogeography, Palaeoclimatology, Palaeoecology*, *177*(1–2), 19–27. https://doi.org/10.1016/S0031-0182(01)00349-2

Behling, H., & Oliveira, M. A. T. de. (2018). Evidence of a late glacial warming event and early Holocene cooling in the southern Brazilian coastal highlands. *Quaternary Research*, *89*(1), 90–102. https://doi.org/10.1017/qua.2017.87

Behling, H., W. Arz, H., Pätzold, J., & Wefer, G. (2000). Late Quaternary vegetational and climate dynamics in northeastern Brazil, inferences from marine core GeoB 3104-1. *Quaternary Science Reviews*, *19*(10), 981–994. https://doi.org/10.1016/S0277-3791(99)00046-3

Behrensmeyer, A. K., Damuth, J. . D., DiMichele, W. A., Potts, R., Sues, H.-D., & Wing, S. L. (Eds.). (1992). *Terrestrial Ecosystems Through Time: Evolutionary Paleoecology of Terrestrial Plants and Animals* (2nd ed.). Chicago: University of Chicago Press. Retrieved from https://books.google.com/books?hl=en&lr=&id=0piKj_X4Ua8C&oi=fnd&pg=PR13&dq=Terrestrial+ecosystems+through+time:+evolutionary+paleoecology+of+terrestrial+plants+and+animals&ots=RZ4H8Ve0yp&sig=Wjd_XJY5sGViHkHHtPnElItebYQ#v=onepage&q=Terrestrial ecosystems

Bell, A. E. (Ann E. . (1983). *Dung fungi : an illustrated guide to coprophilous fungi in New Zealand*. Victoria University Press.

BELL, & A. (2005). An illustrated guide to the coprophilous Ascomycetes of Australia. *CBS Biodivers Ser*, *3*, 1–178. Retrieved from https://ci.nii.ac.jp/naid/10019290791/

Bethell, P. H., Goad, L. J., Evershed, R. P., & Ottaway, J. (1994). The Study of Molecular Markers of Human Activity: The Use of Coprostanol in the Soil as an Indicator of Human Faecal Material. *Journal of Archaeological Science*, *21*(5), 619–632. https://doi.org/10.1006/jasc.1994.1061

Birks, H. J. B. (2005). Mind the gap: how open were European primeval forests? *Trends in Ecology & Evolution*, *20*(4), 154–156. https://doi.org/10.1016/J.TREE.2005.02.001

Blois, J. L., McGuire, J. L., & Hadly, E. A. (2010). Small mammal diversity loss in response to late-Pleistocene climatic change. *Nature*, *465*(7299), 771–774. https://doi.org/10.1038/nature09077

Boin, M. N., Martins, P. C. S., da Silva, C. A., & Salgado, A. A. R. (2019). Pantanal: The Brazilian Wetlands (pp. 75–91). Springer, Cham. https://doi.org/10.1007/978-3-030-04333-9_5

Borrero, L. A. (2009). The Elusive Evidence: The Archeological Record of the South American Extinct Megafauna (pp. 145–168). Springer, Dordrecht. https://doi.org/10.1007/978-1-4020-8793-6_8

Borsch, T. (1998). Pollen types in the Amaranthaceae. Morphology and evolutionary significance. *Grana*, *37*(3), 129–142. https://doi.org/10.1080/00173139809362658

Bouchet, F., Guidon, N., Dittmar, K., Harter, S., Ferreira, L. F., Chaves, S. M., … Araújo, A. (2003). Parasite remains in archaeological sites. *Memórias Do Instituto Oswaldo Cruz*, *98*(suppl 1), 47–52. https://doi.org/10.1590/S0074-02762003000900009

Bouimetarhan, I., Chiessi, C. M., González-Arango, C., Dupont, L., Voigt, I., Prange, M., & Zonneveld, K. (2018). Intermittent development of forest corridors in northeastern Brazil during the last deglaciation: Climatic and ecologic evidence. *Quaternary Science Reviews*, *192*, 86–96. https://doi.org/10.1016/J.QUASCIREV.2018.05.026

Bowes, K., Mercuri, A. M., Rattighieri, E., Rinaldi, R., Arnoldus-Huyzendveld, A., Ghisleni, M., … Vaccaro, E. (2015). Palaeoenvironment and land use of Roman peasant farmhouses in

southern Tuscany. *Plant Biosystems*, *149*(1), 174–184. https://doi.org/10.1080/11263504.2014.992997

Bradshaw, C. J. A., Cooper, A., Turney, C. S. M., & Brook, B. W. (2012). Robust estimates of extinction time in the geological record. *Quaternary Science Reviews*, *33*, 14–19. https://doi.org/10.1016/J.QUASCIREV.2011.11.021

Bradshaw, R. H. W., Hannon, G. E., & Lister, A. M. (2003). A long-term perspective on ungulate-vegetation interactions. *Forest Ecology and Management*, *181*(1–2), 267–280. https://doi.org/10.1016/S0378-1127(03)00138-5

Brook, B. W., & Barnosky, A. D. (2013). Quaternary extinctions and their link to climate change. In *Saving a Million Species: Extinction Risk from Climate Change* (pp. 179–198). Island Press-Center for Resource Economics . https://doi.org/10.5822/978-1-61091-182-5_11

Buckland, P. C., & Edwards, K. J. (1984). The longevity of pastoral episodes of clearance activity in pollen diagrams: the role of post-occupation grazing. *Journal of Biogeography*, *11*, 243–249. Retrieved from https://www.jstor.org/stable/pdf/2844643.pdf

Bueno, G. T., Cherem, L. F. S., Toni, F., Guimarães, F. S., & Bayer, M. (2019). Amazonia (pp. 169–197). Springer, Cham. https://doi.org/10.1007/978-3-030-04333-9_9

Burney, D. A., Robinson, G. S., & Burney, L. P. (2003). Sporormiella and the late Holocene extinctions in Madagascar. *Proceedings of the National Academy of Sciences of the United States of America*, *100*(19), 10800–10805. https://doi.org/10.1073/pnas.1534700100

BYRNE, R., ROGER, B., ED, C. J. R., ED, B. J., ED, P. L. W., ED, S. L. N., … ED, V. V. (1982). PRELIMINARY POLLEN ANALYSIS OF DEEP SEA DRILLING PROJECT LEG 64 HOLE 480 (CORES 1-11). *PRELIMINARY POLLEN ANALYSIS OF DEEP SEA DRILLING PROJECT LEG 64 HOLE 480 (CORES 1-11)*.

Cano, J., & Guarro, J. (1990). The genus Aphanoascus. *Mycological Research*, *94*(3), 355–377. https://doi.org/10.1016/S0953-7562(09)80361-4

Cárdenas, M. L., Wilson, O. J., Schorn, L. A., Mayle, F. E., & Iriarte, J. (2019). A quantitative study of modern pollen–vegetation relationships in southern Brazil's Araucaria forest. *Review of Palaeobotany and Palynology*, *265*, 27–40. https://doi.org/10.1016/J.REVPALBO.2019.03.003

Cassino, R. F., Martinho, C. T., & da Silva Caminha, S. A. F. (2018). A Late Quaternary palynological record of a palm swamp in the Cerrado of central Brazil interpreted using

modern analog data. *Palaeogeography, Palaeoclimatology, Palaeoecology*, *490*, 1–16. https://doi.org/10.1016/J.PALAEO.2017.08.036

CASTRO, D. F., OLIVEIRA, P. E. DE, ROSSETTI, D. F., PESSENDA, L. C. R., CASTRO, D. F., OLIVEIRA, P. E. DE, … PESSENDA, L. C. R. (2013). Late Quaternary landscape evolution of northeastern Amazonia from pollen and diatom records. *Anais Da Academia Brasileira de Ciências*, *85*(1), 35–55. https://doi.org/10.1590/S0001-37652013000100004

CBS, A. B.-U., & 2005, undefined. (n.d.). An Illustrated Guide to the Coprophilous Ascomycetes of Australia (CBS Biodiversity Series, No. 3).

Chan, Y. L., Anderson, C. N. K., & Hadly, E. A. (2006). Bayesian estimation of the timing and severity of a population bottleneck from ancient DNA. *PLoS Genetics*, *2*(4), 451–460. https://doi.org/10.1371/journal.pgen.0020059

Cheng, H., Sinha, A., Cruz, F. W., Wang, X., Edwards, R. L., d'Horta, F. M., … Auler, A. S. (2013). Climate change patterns in Amazonia and biodiversity. *Nature Communications*, *4*(1), 1411. https://doi.org/10.1038/ncomms2415

Chepstow-Lusty, A. J., Frogley, M. R., & Baker, A. S. (2019). Comparison of Sporormiella dung fungal spores and oribatid mites as indicators of large herbivore presence: evidence from the Cuzco region of Peru. *Journal of Archaeological Science*, *102*, 61–70. https://doi.org/10.1016/J.JAS.2018.12.006

Chepstow-Lusty, A. J., Frogley, M. R., Bauer, B. S., Leng, M. J., Cundy, A. B., Boessenkool, K. P., & Gioda, A. (2007). Evaluating socio-economic change in the Andes using oribatid mite abundances as indicators of domestic animal densities. *Journal of Archaeological Science*, *34*, 1178–1186. https://doi.org/10.1016/j.jas.2006.12.023

Clark, P. U., Dyke, A. S., Shakun, J. D., Carlson, A. E., Clark, J., Wohlfarth, B., … McCabe, A. M. (2009). The Last Glacial Maximum. *Science*, *325*(5941), 710–714. Retrieved from https://science.sciencemag.org/content/325/5941/710/tab-pdf

CLIFFORD, H. T. (1962). Insect Pollination of Plantago lanceolata L. *Nature*, *193*(4811), 196–196. https://doi.org/10.1038/193196a0

Cohen, A. S. (2003). Lakes as Archives of Earth History. In *Paleolimnology: The History and Evolution of Lake Systems* (1st ed., pp. 3–20). Oxford University Press. Retrieved from https://books.google.com/books?hl=en&lr=&id=50fZ_yue4ToC&oi=fnd&pg=PA3&dq=Paleolimnology:+The+History+and+Evolution+of+Lake+Systems&ots=M5mffIBp

Wx&sig=psJpJl2BA0vSRlacsrX3SGW1OuQ#v=onepage&q=Paleolimnology%253A%2520The%2520History%2520and%2520Evolution%2520of%2520Lake%25

Colinvaux, P. A., & De Oliveira, P. E. (2001). Amazon plant diversity and climate through the Cenozoic. *Palaeogeography, Palaeoclimatology, Palaeoecology*, *166*(1–2), 51–63. https://doi.org/10.1016/S0031-0182(00)00201-7

Cook, E. J. (2009). A record of late Quaternary environments at lunette-lakes Bolac and Turangmoroke, Western Victoria, Australia, based on pollen and a range of non-pollen palynomorphs. *Review of Palaeobotany and Palynology*, *153*(3–4), 185–224. https://doi.org/10.1016/J.REVPALBO.2008.07.001

Cook, E. J., Geel, B. van, Kaars, S. van der, & Arkel, J. van. (2011). A review of the use of non-pollen palynomorphs in palaeoecology with examples from Australia. *Palynology*, *35*(2), 155–178. https://doi.org/10.1080/gspalynol.35.2.155

Cruz, F. W., Burns, S. J., Karmann, I., Sharp, W. D., & Vuille, M. (2006). Reconstruction of regional atmospheric circulation features during the late Pleistocene in subtropical Brazil from oxygen isotope composition of speleothems. *Earth and Planetary Science Letters*, *248*(1–2), 495–507. https://doi.org/10.1016/J.EPSL.2006.06.019

Cruz, F. W., Burns, S. J., Karmann, I., Sharp, W. D., Vuille, M., Cardoso, A. O., … Viana, O. (2005). Insolation-driven changes in atmospheric circulation over the past 116,000 years in subtropical Brazil. *Nature*, *434*(7029), 63–66. https://doi.org/10.1038/nature03365

CRUZ, M., MARTÍNEZ, I., … J. L.-C.-R. C., & 2012, undefined. (2012). Degradation of cattle dung by dung beetles in tropical grassland in Veracruz, Mexico. *Revista Columbiana de Entomologica*. Retrieved from http://www.scielo.org.co/scielo.php?pid=S0120-04882012000100026&script=sci_arttext&tlng=en

D'Apolito, C., Latrubesse, E. M., & Absy, M. L. (2018). Results confirm a relatively dry setting during the last glacial (MIS 3 and LGM) in Carajás, Amazonia: A comment on Guimarães et al. *The Holocene*, *28*(2), 330–331. https://doi.org/10.1177/0959683617721333

DA SILVA, M. N. F., & PATTON, J. L. (1998). Molecular phylogeography and the evolution and conservation of Amazonian mammals. *Molecular Ecology*, *7*(4), 475–486. https://doi.org/10.1046/j.1365-294x.1998.00276.x

Dale Guthrie, R. (2006). New carbon dates link climatic change with human colonization and Pleistocene extinctions. *Nature*, *441*(7090), 207–209. https://doi.org/10.1038/nature04604

Davis, O. K. (1987). Spores of the dung fungus Sporormiella: Increased abundance in historic sediments and before Pleistocene megafaunal extinction. *Quaternary Research*, *28*(2), 290–294. https://doi.org/10.1016/0033-5894(87)90067-6

Davis, O. K., & Ellis, B. (2010). Early occurrence of sagebrush steppe, Miocene (12 Ma) on the Snake River Plain. *Review of Palaeobotany and Palynology*, *160*(3–4), 172–180. https://doi.org/10.1016/j.revpalbo.2010.02.012

Davis, O. K., & Ellis, B. (2010). Early occurrence of sagebrush steppe, Miocene (12 Ma) on the Snake River Plain. *Review of Palaeobotany and Palynology*, *160*(3–4), 172–180. https://doi.org/10.1016/J.REVPALBO.2010.02.012

Davis, O. K., & Shafer, D. S. (2006). Sporormiella fungal spores, a palynological means of detecting herbivore density. *Palaeogeography, Palaeoclimatology, Palaeoecology*, *237*(1), 40–50. https://doi.org/10.1016/j.palaeo.2005.11.028

de Barros Corrêa, A. C., de Azevêdo Cavalcanti Tavares, B., de Lira, D. R., da Silva Mutzenberg, D., & de Souza Cavalcanti, L. C. (2019). The Semi-arid Domain of the Northeast of Brazil (pp. 119–150). Springer, Cham. https://doi.org/10.1007/978-3-030-04333-9_7

Delaygue, G. (2009). Oxygen Isotopes. In *Encyclopedia of Paleoclimatology and Ancient Environments* (pp. 666–673). Dordrecht: Springer Netherlands. https://doi.org/10.1007/978-1-4020-4411-3_163

DEOCAMPO, D. M. (2002). Sedimentary Structures Generated by Hippopotamus amphibius in a Lake-margin Wetland, Ngorongoro Crater, Tanzania. *PALAIOS*, *17*(2).

DeSantis, L. R. G., Crites, J. M., Feranec, R. S., Fox-Dobbs, K., Farrell, A. B., Harris, J. M., … Cerling, T. E. (2019). Causes and Consequences of Pleistocene Megafaunal Extinctions as Revealed from Rancho La Brea Mammals. *Current Biology*, *29*(15), 2488-2495.e2. https://doi.org/10.1016/J.CUB.2019.06.059

Dillehay, T. D., Ocampo, C., Saavedra, J., Sawakuchi, A. O., Vega, R. M., Pino, M., … Dix, G. (2015). New Archaeological Evidence for an Early Human Presence at Monte Verde, Chile. *PLOS ONE*, *10*(11), e0141923. https://doi.org/10.1371/journal.pone.0141923

Dirzo, R., Young, H. S., Galetti, M., Ceballos, G., Isaac, N. J. B., & Collen, B. (2014). Defaunation in the Anthropocene. *Science*, *345*(6195), 401–406. https://doi.org/10.1126/science.1251817

Dodson, J., & Field, J. H. (2018). What does the occurrence of *Sporormiella* (*Preussia*) spores mean in Australian fossil sequences? *Journal of Quaternary Science*, *33*(4), 380–392. https://doi.org/10.1002/jqs.3020

Doughty, C. E., Roman, J., Faurby, S., Wolf, A., Haque, A., Bakker, E. S., … Svenning, J. C. (2016). Global nutrient transport in a world of giants. *Proceedings of the National Academy of Sciences of the United States of America*, *113*(4), 868–873. https://doi.org/10.1073/pnas.1502549112

Doyen, E., & Etienne, D. (2017). Ecological and human land-use indicator value of fungal spore morphotypes and assemblages. *Vegetation History and Archaeobotany*, *26*(4), 357–367. https://doi.org/10.1007/s00334-016-0599-2

Ebersohn, C., Sinica, A. E.-B. B. of A., & 1997, undefined. (n.d.). Determination of the coprophilous fungal fruit body successional phases and the delimitation of species association classes on dung substrates of African.

Edwards, E. J., Osborne, C. P., Strömberg, C. A. E., Smith, S. A., Bond, W. J., Christin, P. A., … Tipple, B. (2010, April 30). The origins of C4 Grasslands: Integrating evolutionary and ecosystem science. *Science*. American Association for the Advancement of Science. https://doi.org/10.1126/science.1177216

Ejarque, A., Miras, Y., & Riera, S. (2011). Pollen and non-pollen palynomorph indicators of vegetation and highland grazing activities obtained from modern surface and dung datasets in the eastern Pyrenees. *Review of Palaeobotany and Palynology*, *167*(1–2), 123–139. https://doi.org/10.1016/J.REVPALBO.2011.08.001

Ekblom, A., & Gillson, L. (2010). Dung fungi as indicators of past herbivore abundance, Kruger and Limpopo National Park. *Palaeogeography, Palaeoclimatology, Palaeoecology*, *296*(1–2), 14–27. https://doi.org/10.1016/j.palaeo.2010.06.009

Elhmmali, M. M., Roberts, D. J., & Evershed, R. P. (1997). Bile acids as a new class of sewage pollution indicator. *Environmental Science and Technology*, *31*(12), 3663–3668. https://doi.org/10.1021/es9704040

Eltahir, E. A. B., & Bras, R. L. (1994). Precipitation recycling in the Amazon basin. *Quarterly Journal of the Royal Meteorological Society*, *120*(518), 861–880. https://doi.org/10.1002/qj.49712051806

Estes, J. A., Terborgh, J., Brashares, J. S., Power, M. E., Berger, J., Bond, W. J., … Wardle, D. A. (2011, July 15). Trophic downgrading of planet earth. *Science*. American Association for the Advancement of Science. https://doi.org/10.1126/science.1205106

Etienne, D., Destas, M., Lyautey, E., Marti, R., Ruffaldi, P., Georges-Leroy, M., … Topp, E. (2015). Two thousand-year reconstruction of livestock production intensity in France using sediment-archived fecal Bacteroidales and source-specific mitochondrial markers. *The Holocene*, *25*(9), 1384–1393. https://doi.org/10.1177/0959683615585836

Etienne, D., Wilhelm, B., Sabatier, P., Reyss, J. L., & Arnaud, F. (2013). Influence of sample location and livestock numbers on Sporormiella concentrations and accumulation rates in surface sediments of Lake Allos, French Alps. *Journal of Paleolimnology*, *49*(2), 117–127. https://doi.org/10.1007/s10933-012-9646-x

Evershed, R. P. (1993). Biomolecular archaeology and lipids. *World Archaeology*, *25*(1), 74–93. https://doi.org/10.1080/00438243.1993.9980229

Evershed, R. P., & Bethell, P. H. (1996). Application of Multimolecular Biomarker Techniques to the Identification of Fecal Material in Archaeological Soils and Sediments. In *Archaeological Chemistry* (pp. 157–172). https://doi.org/10.1021/bk-1996-0625.ch013

Fairbanks, R. G. (1989). A 17,000-year glacio-eustatic sea level record: influence of glacial melting rates on the Younger Dryas event and deep-ocean circulation. *Nature*, *342*(6250), 637–642. https://doi.org/10.1038/342637a0

Fairbanks, R. G., Mortlock, R. A., Chiu, T.-C., Cao, L., Kaplan, A., Guilderson, T. P., … Nadeau, M.-J. (2005). Radiocarbon calibration curve spanning 0 to 50,000 years BP based on paired 230Th/234U/238U and 14C dates on pristine corals. *Quaternary Science Reviews*, *24*(16–17), 1781–1796. https://doi.org/10.1016/J.QUASCIREV.2005.04.007

Fairweather, I., & Threadgold, L. T. (1981). Hymenolepis nana: the fine structure of the embryonic envelopes. *Parasitology*, *82*(03), 429. https://doi.org/10.1017/S0031182000066968

Feranec, R. S., Miller, N. G., Lothrop, J. C., & Graham, R. W. (2011). The Sporormiella proxy and end-Pleistocene megafaunal extinction: A perspective. *Quaternary International*, *245*(2), 333–338. https://doi.org/10.1016/j.quaint.2011.06.004

Fiedel, S. J. (2018). The spore conundrum: Does a dung fungus decline signal humans' arrival in the Eastern United States? *Quaternary International*, *466*, 247–255. https://doi.org/10.1016/J.QUAINT.2015.11.130

Figueirôa, J. de, Pareyn, F., … E. de L. A.-F. E. and, & 2006, undefined. (n.d.). Effects of cutting regimes in the dry and wet season on survival and sprouting of woody species from the semi-arid caatinga of northeast Brazil. *Elsevier*. Retrieved from https://www.sciencedirect.com/science/article/pii/S0378112706002556

Florenzano, A., Marignani, M., Rosati, L., Fascetti, S., & Mercuri, A. M. (2015). Are Cichorieae an indicator of open habitats and pastoralism in current and past vegetation studies? *Plant Biosystems*, *149*(1), 154–165. https://doi.org/10.1080/11263504.2014.998311

Fogaça, E., & Prous, A. (1999). Archaeology of the Pleistocene-Holocene boundary in Brazil. *Quaternary International*, *53–54*(1), 21–41. https://doi.org/10.1016/S1040-6182(98)00005-6

Fontes, D., Cordeiro, R. C., Martins, G. S., Behling, H., Turcq, B., Sifeddine, A., … Rodrigues, R. A. (2017). Paleoenvironmental dynamics in South Amazonia, Brazil, during the last 35,000 years inferred from pollen and geochemical records of Lago do Saci. *Quaternary Science Reviews*, *173*, 161–180. https://doi.org/10.1016/J.QUASCIREV.2017.08.021

França, L. de M., de Asevedo, L., Dantas, M. A. T., Bocchiglieri, A., Avilla, L. dos S., Lopes, R. P., & da Silva, J. L. L. (2015, January 1). Review of feeding ecology data of Late Pleistocene mammalian herbivores from South America and discussions on niche differentiation. *Earth-Science Reviews*. Elsevier. https://doi.org/10.1016/j.earscirev.2014.10.006

Freire, F. das C. O., Kozakiewicz, Z., & Paterson, R. R. M. (2000). Mycoflora and mycotoxins in Brazilian black pepper, white pepper and Brazil nuts. *Mycopathologia*, *149*(1), 13–19. https://doi.org/10.1023/A:1007241827937

Galetti, M., Moleón, M., Jordano, P., Pires, M. M., Guimarães, P. R., Pape, T., … Svenning, J.-C. (2018). Ecological and evolutionary legacy of megafauna extinctions. *Biological Reviews*, *93*(2), 845–862. https://doi.org/10.1111/brv.12374

Garrison, T. S. (2012). *Oceanography: An Invitation to Marine Science*. Retrieved from https://www.google.com/books/edition/_/0cUKAAAAQBAJ?hl=en

Gauthier, E., Bichet, V., Massa, C., Petit, C., Vannière, B., & Richard, H. (2010). Pollen and non-pollen palynomorph evidence of medieval farming activities in southwestern

Greenland. *Vegetation History and Archaeobotany*, *19*(5–6), 427–438. https://doi.org/10.1007/s00334-010-0251-5

Giguet-Covex, C., Pansu, J., Arnaud, F., Rey, P.-J., Griggo, C., Gielly, L., … Taberlet, P. (2014). Long livestock farming history and human landscape shaping revealed by lake sediment DNA. *Nature Communications*, *5*(1), 3211. https://doi.org/10.1038/ncomms4211

Gill, F. L., Crump, M. P., Schouten, R., & Bull, I. D. (2009). Lipid analysis of a ground sloth coprolite. *Quaternary Research*, *72*(02), 284–288. https://doi.org/10.1016/j.yqres.2009.06.006

Gill, J. L. (2014). Ecological impacts of the late Quaternary megaherbivore extinctions. *New Phytologist*, *201*(4), 1163–1169. https://doi.org/10.1111/nph.12576

Gill, J. L., McLauchlan, K. K., Skibbe, A. M., Goring, S., Zirbel, C. R., & Williams, J. W. (2013). Linking abundances of the dung fungus *Sporormiella* to the density of bison: implications for assessing grazing by megaherbivores in palaeorecords. *Journal of Ecology*, *101*(5), 1125–1136. https://doi.org/10.1111/1365-2745.12130

Gill, J. L., Williams, J. W., Jackson, S. T., Lininger, K. B., & Robinson, G. S. (2009). Pleistocene megafaunal collapse, novel plant communities, and enhanced fire regimes in North America. *Science (New York, N.Y.)*, *326*(5956), 1100–1103. https://doi.org/10.1126/science.1179504

Ginarte, M., Pereiro Jr., M., Fernández-Redondo, V., & Toribio, J. (1996). Plantar Infection by Scopulariopsis brevicaulis. *Dermatology*, *193*(2), 149–151. https://doi.org/10.1159/000246234

Goldberg, A., Mychajliw, A. M., & Hadly, E. A. (2016). Post-invasion demography of prehistoric humans in South America. *Nature*, *532*(7598), 232–235. https://doi.org/10.1038/nature17176

Gómez-Carballa, A., Pardo-Seco, J., Brandini, S., Achilli, A., Perego, U. A., Coble, M. D., … Salas, A. (2018). The peopling of South America and the trans-Andean gene flow of the first settlers. *Genome Research*, *28*(6), 767–779. https://doi.org/10.1101/gr.234674.118

González-Guarda, E., Petermann-Pichincura, A., Tornero, C., Domingo, L., Agustí, J., Pino, M., … Rivals, F. (2018). Multiproxy evidence for leaf-browsing and closed habitats in extinct proboscideans (Mammalia, Proboscidea) from central Chile. *Proceedings of the National Academy of Sciences of the United States of America*, *115*(37), 9258–9263. https://doi.org/10.1073/pnas.1804642115

Graf, M. T., & Chmura, G. L. (2006). Development of modern analogues for natural, mowed and grazed grasslands using pollen assemblages and coprophilous fungi. *Review of Palaeobotany and Palynology*, *141*(1–2), 139–149. https://doi.org/10.1016/j.revpalbo.2006.03.018

Graham, R. W., Belmecheri, S., Choy, K., Culleton, B. J., Davies, L. J., Froese, D., … Wooller, M. J. (2016). Timing and causes of mid-Holocene mammoth extinction on St. Paul Island, Alaska. *Proceedings of the National Academy of Sciences of the United States of America*, *113*(33), 9310–9314. https://doi.org/10.1073/pnas.1604903113

Gu, F., Chiessi, C. M., Zonneveld, K. A. F., & Behling, H. (2018). Late Quaternary environmental dynamics inferred from marine sediment core GeoB6211-2 off southern Brazil. *Palaeogeography, Palaeoclimatology, Palaeoecology*, *496*, 48–61. https://doi.org/10.1016/J.PALAEO.2018.01.015

Gu, F., Zonneveld, K. A. F., Chiessi, C. M., Arz, H. W., Pätzold, J., & Behling, H. (2017). Long-term vegetation, climate and ocean dynamics inferred from a 73,500 years old marine sediment core (GeoB2107-3) off southern Brazil. *Quaternary Science Reviews*, *172*, 55–71. https://doi.org/10.1016/J.QUASCIREV.2017.06.028

Guillemot, T., Zocatelli, R., Bichet, V., Jacob, J., Massa, C., Le Milbeau, C., … Gauthier, E. (2015). *Evolution of pastoralism in Southern Greenland during the last two millennia reconstructed from bile acids and coprophilous fungal spores in lacustrine sediments*. *Organic Geochemistry* (Vol. 81). https://doi.org/10.1016/j.orggeochem.2015.01.012

Gulvik, M. (2007). Mites (Acari) as indicators of soil biodiversity and land use monitoring : a review. *Polish Journal of Ecology*, *55*(3), 415–440. Retrieved from https://yadda.icm.edu.pl/baztech/element/bwmeta1.element.baztech-article-BGPK-1801-6827;jsessionid=E0578672914B5E63EAB80EA7A765150F

Guthrie, R. D. (n.d.). Mosaics, allelochemics and nutrients: an ecological theory of late Pleistocene megafaunal extinctions. In *Quaternary Extinctions: A Prehistoric Revolution*.

Hadly, E. A., Ramakrishnan, U., Chan, Y. L., van Tuinen, M., O'Keefe, K., Spaeth, P. A., & Conroy, C. J. (2004). Genetic Response to Climatic Change: Insights from Ancient DNA and Phylochronology. *PLoS Biology*, *2*(10), e290. https://doi.org/10.1371/journal.pbio.0020290

Haffer, J. (1969). Speciation in amazonian forest birds. *Science (New York, N.Y.)*, *165*(3889), 131–137. https://doi.org/10.1126/science.165.3889.131

Halligan, J. J., Waters, M. R., Perrotti, A., Owens, I. J., Feinberg, J. M., Bourne, M. D., … Dunbar, J. S. (2016). Pre-Clovis occupation 14,550 years ago at the Page-Ladson site, Florida, and the peopling of the Americas. *Science Advances*, *2*(5), e1600375. https://doi.org/10.1126/sciadv.1600375

Hanski, I., & Cambefort, Y. (Eds.). (2014). *Dung Beetle Ecology*. Princeton University Press. Retrieved from https://books.google.com/books?hl=en&lr=&id=ekIABAAAQBAJ&oi=fnd&pg=PP1&dq=Dung+Beetle+Ecology&ots=5X00tHiift&sig=o5vz324eDxVSaL1ySiEclUnz2Mc#v=onepage&q=Dung Beetle Ecology&f=false

Harrault, L., Milek, K., Jardé, E., Jeanneau, L., Derrien, M., & Anderson, D. G. (2019). Faecal biomarkers can distinguish specific mammalian species in modern and past environments. *PLOS ONE*, *14*(2), e0211119. https://doi.org/10.1371/journal.pone.0211119

Harvey, W. J., Stansell, N., Nogué, S., & Willis, K. J. (2019). The Apparent Resilience of the Dry Tropical Forests of the Nicaraguan Region of the Central American Dry Corridor to Variations in Climate Over the Last C. 1200 Years. *Quaternary*, *2*(3), 25. https://doi.org/10.3390/quat2030025

Haskouri, F. El, Bouziane, H., del Mar Trigo, M., Kadiri, M., & Kazzaz, M. (2016). Airborne ascospores in Tetouan (NW Morocco) and meteorological parameters. *Aerobiologia*, *32*(4), 669–681. https://doi.org/10.1007/s10453-016-9440-8

Hayes, M. A. (2012). The Geomyces Fungi: Ecology and Distribution. *BioScience*, *62*(9), 819–823. https://doi.org/10.1525/bio.2012.62.9.7

Hempson, G. P., Archibald, S., Bond, W. J., Ellis, R. P., Grant, C. C., Kruger, F. J., … Vickers, K. J. (2015). Ecology of grazing lawns in Africa. *Biological Reviews*, *90*(3), 979–994. https://doi.org/10.1111/brv.12145

Hermanowski, B., da Costa, M. L., Carvalho, A. T., & Behling, H. (2012). Palaeoenvironmental dynamics and underlying climatic changes in southeast Amazonia (Serra Sul dos Carajás, Brazil) during the late Pleistocene and Holocene. *Palaeogeography, Palaeoclimatology, Palaeoecology*, *365–366*, 227–246. https://doi.org/10.1016/J.PALAEO.2012.09.030

Hernández Trejo, F., Muñoz Rodríguez, A. F., Tormo Molina, R., & Silva Palacios, I. (2012). Airborne ascospores in Mérida (SW Spain) and the effect of rain and other meteorological parameters on their concentration. *Aerobiologia*, *28*(1), 13–26. https://doi.org/10.1007/s10453-011-9207-1

Higginson, M. J. (2009). Geochemical proxies (Non-isotopic). In *Encyclopedia of Earth Sciences Series* (pp. 1203–1208). Springer Netherlands. https://doi.org/10.1007/978-1-4020-4411-3_89

Hirata, M., Hasegawa, N., Nomura, M., Ito, H., Nogami, K., & Sonoda, T. (2009). Deposition and decomposition of cattle dung in forest grazing in southern Kyushu, Japan. *Ecological Research*, *24*(1), 119–125. https://doi.org/10.1007/s11284-008-0488-y

Hjelle, K. L. (1999). Modern pollen assemblages from mown and grazed vegetation types in western Norway. *Review of Palaeobotany and Palynology*, *107*(1–2), 55–81. https://doi.org/10.1016/S0034-6667(99)00015-9

Hogg, A. G., Hua, Q., Blackwell, P. G., Niu, M., Buck, C. E., Guilderson, T. P., … Zimmerman, S. R. H. (2013). SHCal13 Southern Hemisphere Calibration, 0–50,000 Years cal BP. *Radiocarbon*, *55*(4), 1889–1903. https://doi.org/10.2458/azu_js_rc.55.16783

Holmes, P. L. (1994). The sorting of spores and pollen by water: experimental and field evidence. In A. Traverse (Ed.), *Sedimentation of Organic Particles* (p. 544). Cambridge: Cambridge University Press. Retrieved from http://ebooks.cambridge.org/ref/id/CBO9780511524875A010

Holmes, P. L. (2010). The sorting of spores and pollen by water: experimental and field evidence. In *Sedimentation of Organic Particles* (pp. 9–32). Cambridge University Press. https://doi.org/10.1017/cbo9780511524875.003

Horgan, F. G. (2005). Effects of deforestation on diversity, biomass and function of dung beetles on the eastern slopes of the Peruvian Andes. *Forest Ecology and Management*, *216*(1–3), 117–133. https://doi.org/10.1016/j.foreco.2005.05.049

Howard, D. H. (Ed.). (2002). *Pathogenic Fungi in Humans and Animals*. CRC Press. Retrieved from https://books.google.com/books?hl=en&lr=&id=my7KbbJi2b4C&oi=fnd&pg=PR5&dq=Pathogenic+fungi+in+humans+and+animals&ots=YvClHFfM8E&sig=N2khM1fkNCoq82tNzIRQzMM0rdU#v=onepage&q=Pathogenic fungi in humans and animals&f=false

Hubbe, A., Hubbe, M., & Neves, W. A. (2013). The Brazilian megamastofauna of the Pleistocene/Holocene transition and its relationship with the early human settlement of the continent. *Earth-Science Reviews*, *118*, 1–10. https://doi.org/10.1016/J.EARSCIREV.2013.01.003

Hubbe, A., Vasconcelos, A. G., Vilaboim, L., Karmann, I., & Neves, W. (2011). Chronological Distribution of Brazilian *Glyptodon* SP. Remains: A Direct ^{14} C Date for a Specimen from Iporanga, São Paulo, Brazil. *Radiocarbon*, *53*(1), 13–19. https://doi.org/10.1017/S0033822200034329

Innes, J. B., & Blackford, J. J. (2003). The ecology of Late Mesolithic woodland disturbances: Model testing with fungal spore assemblage data. *Journal of Archaeological Science*, *30*(2), 185–194. https://doi.org/10.1006/jasc.2002.0832

Ivanova, A., & Marfenina, O. (2015). Soil fungal communities as bioindicators of ancient human impacts in medieval settlements in different geographic regions of Russia and southwestern Kazakhstan. *Quaternary International*, *365*, 212–222. https://doi.org/10.1016/J.QUAINT.2014.10.016

J. T. Verweij, R., Verrelst, J., Loth, P. E., M. A. Heitkönig, I., & M. H. Brunsting, A. (2006). Grazing lawns contribute to the subsistence of mesoherbivores on dystrophic savannas. *Oikos*, *114*(1), 108–116. https://doi.org/10.1111/j.2006.0030-1299.14209.x

Jackson, J. B. C., & McClenachan, L. (2017). Historical ecology for the paleontologist. In G. P. Dietl & K. W. Flessa (Eds.), *Conservation Paleobiology: Science and Practice - Google Books* (1st ed., pp. 87–100). Chicago: University of Chicago Press. Retrieved from https://books.google.com/books?hl=en&lr=&id=u-k5DwAAQBAJ&oi=fnd&pg=PA87&dq=Historical+Ecology+for+the+Paleontologist&ots=0merLBX9NX&sig=iiBkqKaVbG1VApoaLJZQNlGCBxU#v=onepage&q=Historical Ecology for the Paleontologist&f=false

Jeng, W.-L., & Han, B.-C. (1994). Sedimentary coprostanol in Kaohsiung Harbour and the Tan-Shui Estuary, Taiwan. *Marine Pollution Bulletin*, *28*(8), 494–499. https://doi.org/10.1016/0025-326X(94)90523-1

Jimenez, B. (2007). Helminth ova removal from wastewater for agriculture and aquaculture reuse. *Water Science and Technology*, *55*(1–2), 485–493. https://doi.org/10.2166/wst.2007.046

Johnson, C. N. (2009). Ecological consequences of Late Quaternary extinctions of megafauna. *Proceedings of the Royal Society B: Biological Sciences*, *276*(1667), 2509–2519. https://doi.org/10.1098/rspb.2008.1921

Jones, C. G., Lawton, J. H., & Shachak, M. (1994). Organisms as Ecosystem Engineers. *Oikos*, *69*(3), 373. https://doi.org/10.2307/3545850

Kamino, L. H. Y., Rezende, É. A., Santos, L. J. C., Felippe, M. F., & Assis, W. L. (2019). Atlantic Tropical Brazil (pp. 41–73). Springer, Cham. https://doi.org/10.1007/978-3-030-04333-9_4

Keatley, B. E., Blais, J. M., Douglas, M. S. V., Gregory-Eaves, I., Mallory, M. L., Michelutti, N., & Smol, J. P. (2011). Historical seabird population dynamics and their effects on Arctic pond ecosystems: a multi-proxy paleolimnological study from Cape Vera, Devon Island, Arctic Canada. *Fundamental and Applied Limnology / Archiv Für Hydrobiologie*, *179*(1), 51–66. https://doi.org/10.1127/1863-9135/2011/0179-0051

Kidwell, S. M., & Flessa, K. W. (1996). THE QUALITY OF THE FOSSIL RECORD: Populations, Species, and Communities. *Annual Review of Earth and Planetary Sciences*, *24*(1), 433–464. https://doi.org/10.1146/annurev.earth.24.1.433

Kidwell, S. M., & Holland, S. M. (2002). The Quality of the Fossil Record: Implications for Evolutionary Analyses. *Annual Review of Ecology and Systematics*, *33*(1), 561–588. https://doi.org/10.1146/annurev.ecolsys.33.030602.152151

Koch, P. L. (2008). Isotopic Study of the Biology of Modern and Fossil Vertebrates. In *Stable Isotopes in Ecology and Environmental Science* (pp. 99–154). Oxford, UK: Blackwell Publishing Ltd. https://doi.org/10.1002/9780470691854.ch5

Koch, P. L., & Barnosky, A. D. (2006). Late Quaternary Extinctions: State of the Debate. *Annual Review of Ecology, Evolution, and Systematics*, *37*(1), 215–250. https://doi.org/10.1146/annurev.ecolsys.34.011802.132415

Krug, J. C., Benny, G. L., & Keller, H. W. (2004). Coprophilous fungi. In G. M. Mueller, G. F. Bills, & M. S. Foster (Eds.), *Biodiversity of Fungi: Inventory and Monitoring Methods* (pp. 467–499). Elsevier Inc. https://doi.org/https://doi.org/10.1016/B978-0-12-509551-8.X5000-4

Kruys, Å. (2015). New species of Preussia with 8-celled ascospores (Sporormiaceae, Pleosporales, Ascomycota). *Phytotaxa*, *234*(2), 143–150. https://doi.org/10.11646/phytotaxa.234.2.4

Kruys, Å., & Wedin, M. (2009). Phylogenetic relationships and an assessment of traditionally used taxonomic characters in the Sporormiaceae (Pleosporales, Dothideomycetes, Ascomycota), utilising multi-gene phylogenies. *Systematics and Biodiversity*, *7*(4), 465–478. https://doi.org/10.1017/S1477200009990119

Kuthubutheen, A. J. J., & Webster, J. (1986). Effects of water availability on germination, growth and sporulation of coprophilous fungi. *Transactions of the British Mycological Society*, *86*(1), 77–91. https://doi.org/10.1016/S0007-1536(86)80119-X

Kuthubutheen, A. J. J., & Webster, J. (1986). Water availability and the coprophilous fungus succession. *Transactions of the British Mycological Society*, *86*(1), 63–76. https://doi.org/10.1016/S0007-1536(86)80118-8

Leach, M. D., Budge, S., Walker, L., Munro, C., Cowen, L. E., & Brown, A. J. P. (2012). Hsp90 Orchestrates Transcriptional Regulation by Hsf1 and Cell Wall Remodelling by MAPK Signalling during Thermal Adaptation in a Pathogenic Yeast. *PLoS Pathogens*, *8*(12), e1003069. https://doi.org/10.1371/journal.ppat.1003069

LeBlanc, L. A., Latimer, J. S., Ellis, J. T., & Quinn, J. G. (1992). The geochemistry of coprostanol in waters and surface sediments from Narragansett Bay. *Estuarine, Coastal and Shelf Science*, *34*(5), 439–458. https://doi.org/10.1016/S0272-7714(05)80116-7

Ledger, P. M., Edwards, K. J., & Schofield, J. E. (2015). Taphonomy or signal sensitivity in palaeoecological investigations of Norse *landnám* in Vatnahverfi, southern Greenland? *Boreas*, *44*(1), 197–215. https://doi.org/10.1111/bor.12089

Ledger, P. M., Edwards, K. J., & Schofield, J. E. (2014). A multiple profile approach to the palynological reconstruction of Norse landscapes in Greenland's Eastern Settlement. *Quaternary Research*, *82*(1), 22–37. https://doi.org/10.1016/j.yqres.2014.04.003

Ledru, M.-P., Rousseau, D.-D., Cruz, F. W., Riccomini, C., Karmann, I., & Martin, L. (2005). Paleoclimate Changes during the last 100,000 yr from a Record in the Brazilian Atlantic Rainforest region and Interhemispheric Comparison. *Quaternary Research*, *64*(3), 444–450. https://doi.org/10.1016/j.yqres.2005.08.006

Ledru, M. P., Mourguiart, P., & Riccomini, C. (2009). Related changes in biodiversity, insolation and climate in the Atlantic rainforest since the last interglacial. *Palaeogeography, Palaeoclimatology, Palaeoecology*, *271*(1–2), 140–152. https://doi.org/10.1016/j.palaeo.2008.10.008

Lee Foote, A., & Rice Hornung, C. L. (2005). Odonates as biological indicators of grazing effects on Canadian prairie wetlands. *Ecological Entomology*, *30*(3), 273–283. https://doi.org/10.1111/j.0307-6946.2005.00701.x

Leite, Y. L. R., Costa, L. P., Loss, A. C., Rocha, R. G., Batalha-Filho, H., Bastos, A. C., … Pardini, R. (2016). Neotropical forest expansion during the last glacial period challenges

refuge hypothesis. *Proceedings of the National Academy of Sciences*, *113*(4), 1008–1013. https://doi.org/10.1073/PNAS.1513062113

Lombardo, U., Iriarte, J., Hilbert, L., Ruiz-Pérez, J., Capriles, J. M., & Veit, H. (2020). Early Holocene crop cultivation and landscape modification in Amazonia. *Nature*, *581*(7807), 190–193. https://doi.org/10.1038/s41586-020-2162-7

Lopes, R. P., Ribeiro, A. M., Dillenburg, S. R., & Schultz, C. L. (2013). Late middle to late Pleistocene paleoecology and paleoenvironments in the coastal plain of Rio Grande do Sul State, Southern Brazil, from stable isotopes in fossils of Toxodon and Stegomastodon. *Palaeogeography, Palaeoclimatology, Palaeoecology*, *369*, 385–394. https://doi.org/10.1016/j.palaeo.2012.10.042

López-Merino, L., López-Sáez, J. A., Alba-Sánchez, F., Pérez-Díaz, S., & Carrión, J. S. (2009). 2000 years of pastoralism and fire shaping high-altitude vegetation of Sierra de Gredos in central Spain. *Review of Palaeobotany and Palynology*, *158*(1–2), 42–51. https://doi.org/10.1016/j.revpalbo.2009.07.003

Lydolph, M. C., Jacobsen, J., Arctander, P., Gilbert, M. T. P., Gilichinsky, D. A., Hansen, A. J., … Lange, L. (2005). Beringian paleoecology inferred from permafrost-preserved fungal DNA. *Applied and Environmental Microbiology*, *71*(2), 1012–1017. https://doi.org/10.1128/AEM.71.2.1012-1017.2005

MacFadden, B., Paleobiology, B. S.-, & 1997, undefined. (n.d.). Ancient feeding ecology and niche differentiation of Pleistocene mammalian herbivores from Tarija, Bolivia: morphological and isotopic evidence. *Cambridge.Org*. Retrieved from https://www.cambridge.org/core/journals/paleobiology/article/ancient-feeding-ecology-and-niche-differentiation-of-pleistocene-mammalian-herbivores-from-tarija-bolivia-morphological-and-isotopic-evidence/B65D7F9B031BA412722AA82886442063

Mahaney, W. C., Allen, C. C. R., Pentlavalli, P., Kulakova, A., Young, J. M., Dirszowsky, R. W., … Milner, M. W. (2017). Biostratigraphic Evidence Relating to the Age-Old Question of Hannibal's Invasion of Italy, II: Chemical Biomarkers and Microbial Signatures. *Archaeometry*, *59*(1), 179–190. https://doi.org/10.1111/arcm.12228

Malhi, Y., Roberts, J. T., Betts, R. A., Killeen, T. J., Li, W., & Nobre, C. A. (2008, January 11). Climate change, deforestation, and the fate of the Amazon. *Science*. American Association for the Advancement of Science. https://doi.org/10.1126/science.1146961

Martin, F. M., & Borrero, L. A. (2017). Climate change, availability of territory, and Late Pleistocene human exploration of Ultima Esperanza, South Chile. *Quaternary International*, *428*, 86–95. https://doi.org/10.1016/J.QUAINT.2015.06.023

Mazier, F., Galop, D., Brun, C., & Buttler, A. (2006). Modern pollen assemblages from grazed vegetation in the western Pyrenees, France: a numerical tool for more precise reconstruction of past cultural landscapes. *The Holocene*, *16*(1), 91–103. https://doi.org/10.1191/0959683606hl908rp

Mcmichael, C. N. H., & Bush, M. B. (2019). Spatiotemporal patterns of pre-columbian people in amazonia. *Quaternary Research (United States)*, *92*(1), 53–69. https://doi.org/10.1017/qua.2018.152

Miller, S. E. (1983). Late Quaternary Insects of Rancho La Brea and McKittrick, California. *Quaternary Research*, *20*(01), 90–104. https://doi.org/10.1016/0033-5894(83)90067-4

Moldovan, O., Barnett, A. A., Falcon, W., Rico, P., Tella, J. L., Blanco, G., … Hiraldo, F. (2019). Overlooked Parrot Seed Dispersal in Australia and South America: Insights on the Evolution of Dispersal Syndromes and Seed Size in Araucaria Trees. *Frontiers in Ecology and Evolution | Www.Frontiersin.Org*, *1*, 82. https://doi.org/10.3389/fevo.2019.00082

Monjeau, J. A., Araujo, B., Abramson, G., Kuperman, M. N., Laguna, M. F., & Lanata, J. L. (2017). The controversy space on Quaternary megafaunal extinctions. *Quaternary International*, *431*, 194–204. https://doi.org/10.1016/J.QUAINT.2015.10.022

Moro, R. S., de Mattos Bicudo, C. E., de Melo, M. S., & Schmitt, J. (2004). Paleoclimate of the late Pleistocene and Holocene at Lagoa Dourada, Paraná State, southern Brazil. *Quaternary International*, *114*(1), 87–99. https://doi.org/10.1016/S1040-6182(03)00044-2

Mudelsee, M. (2014). Correlation. In *Climate Time Series Analysis* (pp. 271–319). Springer, Cham. https://doi.org/10.1007/978-3-319-04450-7_7

Mudelsee, M. (2014). Regression I. In *Climate Time Series Analysis* (pp. 107–167). Springer, Cham. https://doi.org/10.1007/978-3-319-04450-7_4

Müller, G., Kanazawa, A., & Teshima, S. ichi. (1979). Sedimentary record of fecal pollution in part of lake constance by coprostanol determination. *Naturwissenschaften*, *66*(10), 520–522. https://doi.org/10.1007/BF00404867

Musotto, L. L., Bianchinotti, M. V., & Borromei, A. M. (2012). Pollen and fungal remains as environmental indicators in surface sediments of Isla Grande de Tierra del Fuego,

southernmost Patagonia. *Palynology*, *36*(2), 162–179. https://doi.org/10.1080/01916122.2012.662919

Nace, T. E., Baker, P. A., Dwyer, G. S., Silva, C. G., Rigsby, C. A., Burns, S. J., … Zhu, J. (2014). The role of North Brazil Current transport in the paleoclimate of the Brazilian Nordeste margin and paleoceanography of the western tropical Atlantic during the late Quaternary. *Palaeogeography, Palaeoclimatology, Palaeoecology*, *415*, 3–13. https://doi.org/10.1016/J.PALAEO.2014.05.030

Nagaoka, L., Rick, T., & Wolverton, S. (2018). The overkill model and its impact on environmental research. *Ecology and Evolution*, *8*(19), 9683–9696. https://doi.org/10.1002/ece3.4393

Newcombe, G., Campbell, J., Griffith, D., Baynes, M., Launchbaugh, K., & Pendleton, R. (2016). Revisiting the Life Cycle of Dung Fungi, Including Sordaria fimicola. *PLOS ONE*, *11*(2), e0147425. https://doi.org/10.1371/journal.pone.0147425

Nogués-Bravo, D., Ohlemüller, R., Batra, P., & Araújo, M. B. (2010). CLIMATE PREDICTORS OF LATE QUATERNARY EXTINCTIONS. *Evolution*, *64*(8), no-no. https://doi.org/10.1111/j.1558-5646.2010.01009.x

Nyberg, Å., & Persson, I. L. (2002). Habitat differences of coprophilous fungi on moose dung. *Mycological Research*, *106*(11), 1360–1366. https://doi.org/10.1017/S0953756202006597

Oorschot, C. A. N. Van. (1980). A revision of Chrysosporium and allied genera. *Studies in Mycology*, (No. 20), 89. Retrieved from https://www.cabdirect.org/cabdirect/abstract/19801365833

Orbay-Cerrato, M. E., Oswald, W. W., Doughty, E. D., Foster, D. R., & Hall, B. R. (2017). Historic grazing in southern New England, USA, recorded by fungal spores in lake sediments. *Vegetation History and Archaeobotany*, *26*(2), 159–165. https://doi.org/10.1007/s00334-016-0577-8

Pansani, T. R., Muniz, F. P., Cherkinsky, A., Pacheco, M. L. A. F., & Dantas, M. A. T. (2019). Isotopic paleoecology (δ13C, δ18O) of Late Quaternary megafauna from Mato Grosso do Sul and Bahia States, Brazil. *Quaternary Science Reviews*, *221*, 105864. https://doi.org/10.1016/j.quascirev.2019.105864

Parducci, L., Bennett, K. D., Ficetola, G. F., Alsos, I. G., Suyama, Y., Wood, J. R., & Pedersen, M. W. (2017). Ancient plant DNA in lake sediments. *New Phytologist*, *214*(3), 924–942. https://doi.org/10.1111/nph.14470

Parker, N. E., & Williams, J. W. (2011). Influences of climate, cattle density, and lake morphology on Sporormiella abundances in modern lake sediments in the US Great Plains. *The Holocene*, *22*(4), 475–483. https://doi.org/10.1177/0959683611425550

Pedersen, M. W., Overballe-Petersen, S., Ermini, L., Sarkissian, C. Der, Haile, J., Hellstrom, M., … Willerslev, E. (2015). Ancient and modern environmental DNA. *Philosophical Transactions of the Royal Society of London. Series B, Biological Sciences*, *370*(1660), 20130383. https://doi.org/10.1098/rstb.2013.0383

Perrotti, A. G., & van Asperen, E. (2019). Dung fungi as a proxy for megaherbivores: opportunities and limitations for archaeological applications. *Vegetation History and Archaeobotany*, *28*(1), 93–104. https://doi.org/10.1007/s00334-018-0686-7

Person, B. T., Herzog, M. P., Ruess, R. W., Sedinger, J. S., Anthony, R. M., & Babcock, C. A. (2003). Feedback dynamics of grazing lawns: coupling vegetation change with animal growth. *Oecologia*, *135*(4), 583–592. https://doi.org/10.1007/s00442-003-1197-4

Pires, M. M., Galetti, M., Donatti, C. I., Pizo, M. A., Dirzo, R., & Guimarães, P. R. (2014). Reconstructing past ecological networks: the reconfiguration of seed-dispersal interactions after megafaunal extinction. *Oecologia*, *175*(4), 1247–1256. https://doi.org/10.1007/s00442-014-2971-1

Pires, M. M., Guimarães, P. R., Galetti, M., & Jordano, P. (2018). Pleistocene megafaunal extinctions and the functional loss of long-distance seed-dispersal services. *Ecography*, *41*(1), 153–163. https://doi.org/10.1111/ecog.03163

Pires, M. M., Koch, P. L., Fariña, R. A., de Aguiar, M. A. M., dos Reis, S. F., & Guimarães, P. R. (2015). Pleistocene megafaunal interaction networks became more vulnerable after human arrival. *Proceedings. Biological Sciences / The Royal Society*, *282*(1814), 20151367-. https://doi.org/10.1098/rspb.2015.1367

Prado, D. E., & Gibbs, P. E. (1993). Patterns of Species Distributions in the Dry Seasonal Forests of South America. *Annals of the Missouri Botanical Garden*, *80*(4), 902. https://doi.org/10.2307/2399937

Presbury, D. G. C., & Young, C. N. (1978). Trichophyton ajelloi isolated from a child. *Medical Mycology*, *16*(3), 233–235. https://doi.org/10.1080/00362177885380321

Press, C. I.-U., Cambridge, undefined, and, U. K., & 2007, undefined. (n.d.). The physical science basis. Contribution of working group I to the fourth assessment report of the Intergovernmental Panel on Climate Change.

Qiu, Z., Yang, Y., Shang, X., Li, W., Abuduresule, Y., Hu, X., … Jiang, H. (2014). Paleo-environment and paleo-diet inferred from Early Bronze Age cow dung at Xiaohe Cemetery, Xinjiang, NW China. *Quaternary International*, *349*, 167–177. https://doi.org/10.1016/J.QUAINT.2014.03.029

Quilès, F., Balandier, J.-Y., & Capizzi-Banas, S. (2006). In situ characterisation of a microorganism surface by Raman microspectroscopy: the shell of Ascaris eggs. *Analytical and Bioanalytical Chemistry*, *386*(2), 249–255. https://doi.org/10.1007/s00216-006-0638-4

Raczka, M. F., Bush, M. B., & De Oliveira, P. E. (2018). The collapse of megafaunal populations in southeastern Brazil. *Quaternary Research*, *89*(1), 103–118. https://doi.org/10.1017/qua.2017.60

Raine, E. H., & Slade, E. M. (2019). Dung beetle–mammal associations: methods, research trends and future directions. *Proceedings of the Royal Society B: Biological Sciences*, *286*(1897), 20182002. https://doi.org/10.1098/rspb.2018.2002

RAMAKRISHNAN, U., HADLY, E. A., & MOUNTAIN, J. L. (2005). Detecting past population bottlenecks using temporal genetic data. *Molecular Ecology*, *14*(10), 2915–2922. https://doi.org/10.1111/j.1365-294X.2005.02586.x

Rawlence, N. J., Lowe, D. J., Wood, J. R., Young, J. M., Churchman, G. J., Huang, Y. T., & Cooper, A. (2014). Using palaeoenvironmental DNA to reconstruct past environments: Progress and prospects. *Journal of Quaternary Science*, *29*(7), 610–626. https://doi.org/10.1002/jqs.2740

Reimer, P. J., Bard, E., Bayliss, A., Beck, J. W., Blackwell, P. G., Ramsey, C. B., … van der Plicht, J. (2013). IntCal13 and Marine13 Radiocarbon Age Calibration Curves 0–50,000 Years cal BP. *Radiocarbon*, *55*(4), 1869–1887. https://doi.org/10.2458/azu_js_rc.55.16947

Reinhard, K., Confalonieri, U., Herrmann, B., Ferreira, L., & Araujo, A. (1986). Recovery of Parasite Remains From Coprolites and Latrines: Aspects of Paleoparasitological Technique. *Homo*, *37*, 217–239. Retrieved from http://digitalcommons.unl.edu/anthropologyfacpub/29

Richardson, M. J. (2001). Diversity and occurrence of coprophilous fungi. *Mycological Research*, *105*(4), 387–402. https://doi.org/10.1017/S0953756201003884

Ripple, W. J., Newsome, T. M., Wolf, C., Dirzo, R., Everatt, K. T., Galetti, M., … Van Valkenburgh, B. (2015). Collapse of the world's largest herbivores. *Science Advances*, *1*(4), e1400103–e1400103. https://doi.org/10.1126/sciadv.1400103

Robinson, G. S., Pigott Burney, L., & Burney, D. A. (2005). LANDSCAPE PALEOECOLOGY AND MEGAFAUNAL EXTINCTION IN SOUTHEASTERN NEW YORK STATE. *Ecological Monographs*, *75*(3), 295–315. https://doi.org/10.1890/03-4064

Robinson, M., De Souza, J. G., Maezumi, S. Y., Cárdenas, M., Pessenda, L., Prufer, K., … Iriarte, J. (2018). Uncoupling human and climate drivers of late Holocene vegetation change in southern Brazil. *Scientific Reports*, *8*(1), 7800. https://doi.org/10.1038/s41598-018-24429-5

Rockland, L. B. (1960). Saturated Salt Solutions for Static Control of Relative Humidity between 5° and 40° C. *Analytical Chemistry*, *32*(10), 1375–1376. https://doi.org/10.1021/ac60166a055

Roosevelt, A. (n.d.). The Amazon and the Anthropocene: 13,000 years of human influence in a tropical rainforest. *Elsevier*. Retrieved from https://www.sciencedirect.com/science/article/pii/S2213305414000241

Rozas-Davila, A., Valencia, B. G., & Bush, M. B. (2016). The functional extinction of Andean megafauna. *Ecology*, *97*(10), 2533–2539. https://doi.org/10.1002/ecy.1531

Rule, S., Brook, B. W. B. B., Haberle, S. G. S. G., Turney, C. S. M. C. S. M., Kershaw, A. P. P., & Johnson, C. N. C. N. (2012). The Aftermath of Megafaunal Extinction: Ecosystem Transformation in Pleistocene Australia. *Science*, *335*(6075), 1483–1486. https://doi.org/10.1126/science.1214261

Salgado, A. A. R., Assis, W. L., Magalhães Júnior, A. P., do Carmo, F. F., de Sordi, M. V., & de Oliveira, F. S. (2019). Semi-humid: The Landscape of Central Brazil (pp. 93–117). Springer, Cham. https://doi.org/10.1007/978-3-030-04333-9_6

Salgado, A. A. R., Santos, L. J. C., & Paisani, J. C. (2019). Introduction (pp. 1–6). Springer, Cham. https://doi.org/10.1007/978-3-030-04333-9_1

Salgado-Labouriau, M. L., Barberi, M., Ferraz-Vicentini, K. R., & Parizzi, M. G. (1998). A dry climatic event during the late Quaternary of tropical Brazil. *Review of Palaeobotany and Palynology*, *99*(2), 115–129. https://doi.org/10.1016/S0034-6667(97)00045-6

Saltre, F., Brook, B. W., Rodriguez-Rey, M., Cooper, A., Johnson, C. N., Turney, C. S. M., & Bradshaw, C. J. A. (2015). Uncertainties in dating constrain model choice for inferring extinction time from fossil records. *Quaternary Science Reviews*, *112*, 128–137. https://doi.org/10.1016/j.quascirev.2015.01.022

Sandom, C. J., Ejrnæs, R., Hansen, M. D. D., & Svenning, J.-C. (2014). High herbivore density associated with vegetation diversity in interglacial ecosystems. *Proceedings of the National Academy of Sciences of the United States of America*, *111*(11), 4162–4167. https://doi.org/10.1073/pnas.1311014111

Schelvis, J. (1990). The reconstruction of local environments on the basis of remains of oribatid mites (Acari; Oribatida). *Journal of Archaeological Science*, *17*(5), 559–571. https://doi.org/10.1016/0305-4403(90)90036-5

Schelvis, J. (1992). The identification of archaeological dung deposits on the basis of remains of predatory mites (Acari; Gamasida). *Journal of Archaeological Science*, *19*(6), 677–682. https://doi.org/10.1016/0305-4403(92)90037-4

Schelvis, J. (1987). Some aspects of research on mites (Acari) in archeological samples. *Palaeohistoria*, *29*(0), 211–218. Retrieved from http://rjh.ub.rug.nl/Palaeohistoria/article/view/24881

Schlütz, F., & Shumilovskikh, L. S. (2017, April 1). Non-pollen palynomorphs notes: 1. Type HdV-368 (Podospora-type), descriptions of associated species, and the first key to related spore types. *Review of Palaeobotany and Palynology*. Elsevier B.V. https://doi.org/10.1016/j.revpalbo.2016.12.005

Schofield, J. E., & Edwards, K. J. (2011). Grazing impacts and woodland management in Eriksfjord: Betula, coprophilous fungi and the Norse settlement of Greenland. *Vegetation History and Archaeobotany*, *20*(3), 181–197. https://doi.org/10.1007/s00334-011-0281-7

Schweiger, A. H., & Svenning, J.-C. (2018). Down-sizing of dung beetle assemblages over the last 53 000 years is consistent with a dominant effect of megafauna losses. *Oikos*, *127*(9), 1243–1250. https://doi.org/10.1111/oik.04995

Setyaningsih, C. A., Behling, H., Saad, A., Shumilovskikh, L., Sabiham, S., & Biagioni, S. (2019). First palaeoecological evidence of buffalo husbandry and rice cultivation in the Kerinci Seblat National Park in Sumatra, Indonesia. *Vegetation History and Archaeobotany*, 1–16. https://doi.org/10.1007/s00334-019-00716-7

Shapiro, B., Drummond, A. J., Rambaut, A., Wilson, M. C., Matheus, P. E., Sher, A. V, … Cooper, A. (2004). Rise and fall of the Beringian steppe bison. *Science (New York, N.Y.)*, *306*(5701), 1561–1565. https://doi.org/10.1126/science.1101074

Shepherd, J. D., Ditgen, R. S., & Sanguinetti, J. (2008). *Araucaria araucana and the Austral parakeet: pre-dispersal seed predation on a masting species El pehuén y la cachaña: depredación*

predispersión de una especie "masting." Historia Natural (Vol. 81). Retrieved from https://www.redalyc.org/pdf/3699/369944287008.pdf

Sherwin, M. R., Van Vleet, E. S., Fossato, V. U., & Dolci, F. (1993). Coprostanol (5β-cholestan-3β-ol) in lagoonal sediments and mussels of Venice, Italy. *Marine Pollution Bulletin*, *26*(9), 501–507. https://doi.org/10.1016/0025-326X(93)90467-X

Signor, P. W., & Lipps, J. H. (1982). Sampling bias, gradual extinction patterns and catastrophes in the fossil record (pp. 291–296). https://doi.org/10.1130/SPE190-p291

Silva, J. de A. da, Leal, L. A., Cherkinsky, A., & Dantas, M. A. T. (2019). Late Pleistocene meso-megamammals from Anagé, Bahia, Brazil: Taxonomy and isotopic paleoecology (δ13C). *Journal of South American Earth Sciences*, *96*, 102362. https://doi.org/10.1016/j.jsames.2019.102362

Sistiaga, A., Berna, F., Laursen, R., & Goldberg, P. (2014). Steroidal biomarker analysis of a 14,000 years old putative human coprolite from Paisley Cave, Oregon. *Journal of Archaeological Science*, *41*, 813–817. https://doi.org/10.1016/J.JAS.2013.10.016

Smith, F. A., Tomé, C. P., Elliott Smith, E. A., Lyons, S. K., Newsome, S. D., & Stafford, T. W. (2016). Unraveling the consequences of the terminal Pleistocene megafauna extinction on mammal community assembly. *Ecography*, *39*(2), 223–239. https://doi.org/10.1111/ecog.01779

Solhøy, T. (2001). Oribatid Mites. In *Tracking Environmental Change Using Lake Sediments* (pp. 81–104). Springer, Dordrecht. https://doi.org/10.1007/0-306-47671-1_5

Steele, J. (2010). Radiocarbon dates as data: quantitative strategies for estimating colonization front speeds and event densities. *Journal of Archaeological Science*, *37*(8), 2017–2030. https://doi.org/10.1016/J.JAS.2010.03.007

Summerbell, R. C. (2004). Fungi Associated with Vertebrates. In *Biodiversity of Fungi: Inventory and Monitoring Methods* (Vol. 21, pp. 451–465). Elsevier Inc. https://doi.org/10.1016/B978-0-12-509551-8.50023-4

Svenning, J. (2002). A review of natural vegetation openness in north-western Europe. *Biological Conservation*, *104*(2), 133–148. https://doi.org/10.1016/S0006-3207(01)00162-8

TAUBER, H. (1974). A STATIC NON-OVERLOAD POLLEN COLLECTOR. *New Phytologist*, *73*(2), 359–369. https://doi.org/10.1111/j.1469-8137.1974.tb04770.x

Taylor, C. R., Caldwell, S. L., & Rowntree, V. J. (1972). Running up and down hills: some consequences of size. *Science (New York, N.Y.)*, *178*(4065), 1096–1097. https://doi.org/10.1126/SCIENCE.178.4065.1096

Terry, R. C. (2008). Modeling the Effects of Predation, Prey Cycling, and Time Averaging on Relative Abundance in Raptor-Generated Small Mammal Death Assemblages. *PALAIOS*, *23*(6), 402–410. https://doi.org/10.2110/palo.2007.p07-071r

Tkach, N. V., Hoffmann, M. H., Röser, M., Korobkov, A. A., & von Hagen, K. B. (2007). PARALLEL EVOLUTIONARY PATTERNS IN MULTIPLE LINEAGES OF ARCTIC ARTEMISIA L. (ASTERACEAE). *Evolution*, *0*(0), 071101082849002-??? https://doi.org/10.1111/j.1558-5646.2007.00270.x

Università degli Studi di Roma "La Sapienza". Dipartimento di Biologia Ambientale., A., Mercuri, A. M., & Carter, J. C. (2013). *ECONOMY AND ENVIRONMENT OF THE GREEK COLONIAL SYSTEM IN SOUTHERN ITALY: POLLEN AND NPPS EVIDENCE OF GRAZING FROM THE RURAL SITE OF FATTORIA FABRIZIO (6th - 4th CENT. BC; METAPONTO, BASILICATA). Annali di Botanica* (Vol. 3). Università degli Studi di Roma "La Sapienza." Retrieved from https://statusquaestionis.uniroma1.it/index.php/Annalidibotanica/article/view/10248/10205

van Asperen, E. N. (2017). Fungal diversity on dung of tropical animals in temperate environments: Implications for reconstructing past megafaunal populations. *Fungal Ecology*, *28*, 25–32. https://doi.org/10.1016/J.FUNECO.2016.12.006

van Asperen, E. N., Kirby, J. R., & Hunt, C. O. (2016). The effect of preparation methods on dung fungal spores: Implications for recognition of megafaunal populations. *Review of Palaeobotany and Palynology*, *229*, 1–8. https://doi.org/10.1016/J.REVPALBO.2016.02.004

Van Der Kaars, S., Miller, G. H., Turney, C. S. M. M., Cook, E. J., Nürnberg, D., Schönfeld, J., … Lehman, S. J. (2017). Humans rather than climate the primary cause of Pleistocene megafaunal extinction in Australia. *Nature Communications*, *8*(1), 14142. https://doi.org/10.1038/ncomms14142

van Geel, B., Buurman, J., Brinkkemper, O., Schelvis, J., Aptroot, A., van Reenen, G., & Hakbijl, T. (2003). Environmental reconstruction of a Roman Period settlement site in Uitgeest (The Netherlands), with special reference to coprophilous fungi. *Journal of Archaeological Science*, *30*(7), 873–883. https://doi.org/10.1016/S0305-4403(02)00265-0

Velázquez, N. J., & Burry, L. S. (2012). Palynological analysis of Lama guanicoe modern feces and its importance for the study of coprolites from Patagonia, Argentina. *Review of Palaeobotany and Palynology*, *184*, 14–23. https://doi.org/10.1016/j.revpalbo.2012.07.012

Vera, F. W. M. (Ed.). (2000). *Grazing ecology and forest history*. Wallingford: CABI. https://doi.org/10.1079/9780851994420.0000

Verdum, R., Vieira, L. de F. dos S., Caneppele, J. C. G., & Gass, S. L. B. (2019). Pampa: The South Brazil (pp. 7–20). Springer, Cham. https://doi.org/10.1007/978-3-030-04333-9_2

Vieira, E. M., Ribeiro, J. F., & Iob, G. (2011). Seed predation of *Araucaria angustifolia* (Araucariaceae) by small rodents in two areas with contrasting seed densities in the Brazilian *Araucaria* forest. *Journal of Natural History*, *45*(13–14), 843–854. https://doi.org/10.1080/00222933.2010.536265

Villavicencio, N. A., Lindsey, E. L., Martin, F. M., Borrero, L. A., Moreno, P. I., Marshall, C. R., & Barnosky, A. D. (2016). Combination of humans, climate, and vegetation change triggered Late Quaternary megafauna extinction in the Última Esperanza region, southern Patagonia, Chile. *Ecography*, *39*(2), 125–140. https://doi.org/10.1111/ecog.01606

Walker, R. W., Wun, C. K., & Litsky, W. (1982). Coprostanol as an Indicator of Fecal Pollution. *C R C Critical Reviews in Environmental Control*, *12*(2), 91–112. https://doi.org/10.1080/10643388209381695

Wall, J., Douglas-Hamilton, I., & Vollrath, F. (2006). Elephants avoid costly mountaineering. *Current Biology*, *16*(14), R527–R529. https://doi.org/10.1016/J.CUB.2006.06.049

Wang, X., Auler, A. S., Edwards, R. L., Cheng, H., Cristalli, P. S., Smart, P. L., … Shen, C.-C. (2004). Wet periods in northeastern Brazil over the past 210 kyr linked to distant climate anomalies. *Nature*, *432*(7018), 740–743. https://doi.org/10.1038/nature03067

Western, D., & Behrensmeyer, A. K. (2009). Bone assemblages track animal community structure over 40 years in an African savanna ecosystem. *Science (New York, N.Y.)*, *324*(5930), 1061–1064. https://doi.org/10.1126/science.1171155

Wicklow, D. T., & Moore, V. (1974). Effect of incubation temperature on the coprophilous fungal succession. *Transactions of the British Mycological Society*, *62*(2), 411–415. https://doi.org/10.1016/s0007-1536(74)80051-3

Williams, A. P., Gordon, H., Jones, D. L., Strachan, N. J. C., Avery, L. M., & Killham, K. (2008). Leaching of bioluminescent Escherichia coli O157:H7 from sheep and cattle

faeces during simulated rainstorm events. *Journal of Applied Microbiology*, *105*(5), 1452–1460. https://doi.org/10.1111/j.1365-2672.2008.03898.x

Wood, J. R., & Wilmshurst, J. M. (2016). A protocol for subsampling Late Quaternary coprolites for multi-proxy analysis. *Quaternary Science Reviews*, *138*, 1–5. https://doi.org/10.1016/j.quascirev.2016.02.018

Wood, J. R., & Wilmshurst, J. M. (2012). Wetland soil moisture complicates the use of Sporormiella to trace past herbivore populations. *Journal of Quaternary Science*, *27*(3), 254–259. https://doi.org/10.1002/jqs.1539

Wood, J. R., Wilmshurst, J. M., Turney, C. S. M., & Fogwill, C. J. (2016). Palaeoecological signatures of vegetation change induced by herbivory regime shifts on subantarctic Enderby Island. *Quaternary Science Reviews*, *134*, 51–58. https://doi.org/10.1016/j.quascirev.2015.12.018

Wood, J. R., Wilmshurst, J. M., Worthy, T. H., & Cooper, A. (2011). Sporormiella as a proxy for non-mammalian herbivores in island ecosystems. *Quaternary Science Reviews*, *30*(7–8), 915–920. https://doi.org/10.1016/J.QUASCIREV.2011.01.007

Woodward, F. I. (1987). *Climate and Plant Distribution*. Cambridge University Press. Retrieved from https://books.google.com/books?hl=en&lr=&id=0Ld1h0MT3oIC&oi=fnd&pg=PR9&dq=Climate+and+Plant+Distribution&ots=QgGJtc6i_R&sig=a4NeTqn8NjlcPapHJZ141aSumTE#v=onepage&q=Climate and Plant Distribution&f=false

Wroe, S., Field, J., Fullagar, R., & Jermin, L. S. (2004). Megafaunal extinction in the late Quaternary and the global overkill hypothesis. *Alcheringa: An Australasian Journal of Palaeontology*, *28*(1), 291–331. https://doi.org/10.1080/03115510408619286

Wubah, D. A., Fuller, M. S., & Akin, D. E. (1991). Resistant Body Formation in *Neocallimastix* Sp., An Anaerobic Fungus from the Rumen of a Cow. *Mycologia*, *83*(1), 40–47. https://doi.org/10.1080/00275514.1991.12025977

Wubah, D. A. (2004). Anaerobic Zoosporic Fungi Associated with Animals. In G. M. Mueller, G. F. Bills, & M. S. Foster (Eds.), *Biodiversity of Fungi: Inventory and Monitoring Methods* (1st ed., pp. 501–510). Elsevier Inc. https://doi.org/10.1016/B978-0-12-509551-8.50025-8

Young, H. S., McCauley, D. J., Galetti, M., & Dirzo, R. (2016). Patterns, Causes, and Consequences of Anthropocene Defaunation. *Annual Review of Ecology, Evolution, and Systematics*, *47*(1), 333–358. https://doi.org/10.1146/annurev-ecolsys-112414-054142

Zazzo, A., & Saliège, J. F. (2011). Radiocarbon dating of biological apatites: A review. *Palaeogeography, Palaeoclimatology, Palaeoecology*, *310*(1–2), 52–61. https://doi.org/10.1016/j.palaeo.2010.12.004

Zhang, N., O'Donnell, K., Sutton, D. A., Nalim, F. A., Summerbell, R. C., Padhye, A. A., & Geiser, D. M. (2006). Members of the Fusarium solani Species Complex That Cause Infections in Both Humans and Plants Are Common in the Environment. *Journal of Clinical Microbiology*, *44*(6), 2186–2190. https://doi.org/10.1128/JCM.00120-06

Zimmermann, G. (2008). The entomopathogenic fungi Isaria farinosa (formerly Paecilomyces farinosus) and the Isaria fumosorosea species complex (formerly Paecilomyces fumosoroseus): biology, ecology and use in biological control. *Biocontrol Science and Technology*, *18*(9), 865–901. https://doi.org/10.1080/09583150802471812

Zimov, S. A., Zimov, N. S., & Chapin, F. S. (2012). The Past and Future of the Mammoth Steppe Ecosystem. In *Paleontology in Ecology and Conservation* (pp. 193–225). Berlin, Heidelberg: Springer Berlin Heidelberg. https://doi.org/10.1007/978-3-642-25038-5_10

Bibliography

Kahanamoku-Meyer, S., 2020, GRIWM at https://github.com/sarakahanamoku/GRIWM accessed 2020-05-24

R Core Team, 2020. R: A language and environment for statistical computing. R Foundation for Statistical Computing, Vienna, Austria. URL http://www.R-project.org/

Stuiver, M., Reimer, P.J., and Reimer, R.W., 2020, CALIB 7.1 [WWW program] at http://calib.org, accessed 2020-5-24

United States Department of Agriculture Agricultural Research Service Northern Regional Research Laboratory, 2020, https://nrrl.ncaur.usda.gov/ accessed 2020-05-24

Web of Science, 2020, https://clarivate.com/webofsciencegroup/solutions/web-of-science/ accessed 2019-10-16

Appendix 1: Archaeological localities and dates for Brazil.

Date ID	Dataset	Latitude, longitude (°)	Radiocarbon age ∓ 1σ (yr BP)	2σ calibrated age range (Cal yr BP)	Calibration curve
an_sh_0004	ANTIGUA	-19, -43	140, 40	1 - 153	shcal13
an_sh_0020	ANTIGUA	unknown, unknown	2970, 170	2923 - 3230	shcal13
an_sh_0021	ANTIGUA	-15.4667, -56.8	2710, 60	2705 - 2949	shcal13
gb_sh_0001	Goldberg, Mychajliw, & Hadly, 2016	unknown, unknown	3775, 130	3718 - 4436	shcal13
gb_sh_0002	Goldberg, Mychajliw, & Hadly, 2016	-24.15, -46.9	4636, 100	4971 - 5488	shcal13
gb_sh_0003	Goldberg, Mychajliw, & Hadly, 2016	-24.0003, -46.4339	4520, 130	4829 - 5472	shcal13
gb_sh_0004	Goldberg, Mychajliw, & Hadly, 2016	-7.78923, -35.5813	2200, 80	1996 - 2343	shcal13
gb_sh_0005	Goldberg, Mychajliw, & Hadly, 2016	-11.1149, -42.0863	2712, 60	2707 - 2950	shcal13
gb_sh_0006	Goldberg, Mychajliw, & Hadly, 2016	-29.4167, -53.25	2945, 85	2842 - 3255	shcal13
gb_sh_0007	Goldberg, Mychajliw, & Hadly, 2016	-21.3295, -52.2104	2760, 60	2744 - 2955	shcal13
gb_sh_0008	Goldberg, Mychajliw, & Hadly, 2016	-21.3295, -52.2104	9370, 70	10288 - 10709	shcal13
gb_sh_0009	Goldberg, Mychajliw, & Hadly, 2016	-21.3295, -52.2104	10405, 100	11824 - 12451	shcal13

gb_sh_0010	Goldberg, Mychajliw, & Hadly, 2016	-11.2616, -42.0184	8790, 80	9543 - 9953	shcal13
gb_sh_0011	Goldberg, Mychajliw, & Hadly, 2016	-11.2616, -42.0184	8860, 115	9560 - 10180	shcal13
gb_sh_0012	Goldberg, Mychajliw, & Hadly, 2016	-11.2616, -42.0184	9390, 90	10252 - 10785	shcal13
gb_sh_0013	Goldberg, Mychajliw, & Hadly, 2016	-11.2616, -42.0184	9450, 90	10375 - 10879	shcal13
gb_sh_0014	Goldberg, Mychajliw, & Hadly, 2016	-11.2616, -42.0184	9610, 90	10655 - 11186	shcal13
gb_sh_0015	Goldberg, Mychajliw, & Hadly, 2016	-11.2616, -42.0184	9650, 90	10697 - 11203	shcal13
gb_sh_0016	Goldberg, Mychajliw, & Hadly, 2016	-30.5014, -56.2819	8270, 70	9019 - 9406	shcal13
gb_sh_0017	Goldberg, Mychajliw, & Hadly, 2016	-30.5014, -56.2819	8370, 60	9135 - 9474	shcal13
gb_sh_0018	Goldberg, Mychajliw, & Hadly, 2016	-8.93958, -38.7382	2780, 170	2376 - 3251	shcal13
gb_sh_0019	Goldberg, Mychajliw, & Hadly, 2016	-25.0441, -48.5725	5310, 50	5922 - 6185	shcal13
gb_sh_0020	Goldberg, Mychajliw, & Hadly, 2016	-15.4667, -56.8	3600, 60	3451 - 4295	shcal13
gb_sh_0021	Goldberg, Mychajliw, & Hadly, 2016	-22.5429, -42.8051	3530, 30	3682 - 3856	shcal13
gb_sh_0022	Goldberg, Mychajliw, & Hadly, 2016	-22.5429, -42.8051	3540, 70	3587 - 3931	shcal13

gb_sh_0023	Goldberg, Mychajliw, & Hadly, 2016	-22.5429, -42.8051	3800, 40	3977 - 4249	shcal13
gb_sh_0024	Goldberg, Mychajliw, & Hadly, 2016	-7.8009, -35.5759	4758, 90	5280 - 5645	shcal13
gb_sh_0025	Goldberg, Mychajliw, & Hadly, 2016	-7.8009, -35.5759	4769, 90	5284 - 5652	shcal13
gb_sh_0026	Goldberg, Mychajliw, & Hadly, 2016	-25.0181, -48.0514	3790, 110	3828 - 4427	shcal13
gb_sh_0027	Goldberg, Mychajliw, & Hadly, 2016	-25.0181, -48.0514	4175, 100	4406 - 4875	shcal13
gb_sh_0028	Goldberg, Mychajliw, & Hadly, 2016	-22.6047, -42.9569	2800, 60	2751 - 3001	shcal13
gb_sh_0029	Goldberg, Mychajliw, & Hadly, 2016	-22.6047, -42.9569	3340, 70	3377 - 3694	shcal13
gb_sh_0030	Goldberg, Mychajliw, & Hadly, 2016	-22.6047, -42.9569	3460, 70	3479 - 3850	shcal13
gb_sh_0031	Goldberg, Mychajliw, & Hadly, 2016	-24.1342, -46.9189	4630, 140	4951 - 5585	shcal13
gb_sh_0032	Goldberg, Mychajliw, & Hadly, 2016	unknown, unknown	2840, 60	2766 - 3065	shcal13
gb_sh_0033	Goldberg, Mychajliw, & Hadly, 2016	-27.7944, -48.5445	2670, 90	2432 - 2951	shcal13
gb_sh_0034	Goldberg, Mychajliw, & Hadly, 2016	-13.73, -44	8865, 110	9582 - 10183	shcal13
gb_sh_0035	Goldberg, Mychajliw, & Hadly, 2016	-8.854, -42.6078	3800, 70	3920 - 4300	shcal13

gb_sh_0036	Goldberg, Mychajliw, & Hadly, 2016	-8.854, -42.6078	4920, 70	5464 - 5753	shcal13
gb_sh_0037	Goldberg, Mychajliw, & Hadly, 2016	-8.854, -42.6078	5200, 80	5715 - 6126	shcal13
gb_sh_0038	Goldberg, Mychajliw, & Hadly, 2016	-8.854, -42.6078	6420, 120	6999 - 7509	shcal13
gb_sh_0039	Goldberg, Mychajliw, & Hadly, 2016	-15.4667, -56.8	7010, 70	7557 - 8074	shcal13
gb_sh_0040	Goldberg, Mychajliw, & Hadly, 2016	-8.854, -42.6078	7350, 180	7755 - 8442	shcal13
gb_sh_0041	Goldberg, Mychajliw, & Hadly, 2016	-8.854, -42.6078	9540, 170	10371 - 11217	shcal13
gb_sh_0042	Goldberg, Mychajliw, & Hadly, 2016	-28.8, -50.49	6620, 175	7155 - 7797	shcal13
gb_sh_0043	Goldberg, Mychajliw, & Hadly, 2016	-24.9047, -48.1207	4145, 212	4070 - 5083	shcal13
gb_sh_0044	Goldberg, Mychajliw, & Hadly, 2016	-24.9047, -48.1207	4920, 100	5447 - 5774	shcal13
gb_sh_0045	Goldberg, Mychajliw, & Hadly, 2016	-24.9047, -48.1207	9050, 100	9764 - 10412	shcal13
gb_sh_0047	Goldberg, Mychajliw, & Hadly, 2016	-22.9259, -42.547	3800, 190	3627 - 4629	shcal13
gb_sh_0048	Goldberg, Mychajliw, & Hadly, 2016	-22.9259, -42.547	4160, 180	4140 - 5065	shcal13
gb_sh_0049	Goldberg, Mychajliw, & Hadly, 2016	-22.9259, -42.547	4300, 190	4287 - 5323	shcal13

gb_sh_0050	Goldberg, Mychajliw, & Hadly, 2016	-22.9259, -42.547	4520, 190	4783 - 5589	shcal13
gb_sh_0051	Goldberg, Mychajliw, & Hadly, 2016	-8.62, -43.363	3480, 100	3453 - 3930	shcal13
gb_sh_0052	Goldberg, Mychajliw, & Hadly, 2016	-8.62, -43.363	5090, 110	5584 - 6014	shcal13
gb_sh_0053	Goldberg, Mychajliw, & Hadly, 2016	-8.62, -43.363	7730, 140	8190 - 8792	shcal13
gb_sh_0054	Goldberg, Mychajliw, & Hadly, 2016	-8.62, -43.363	9160, 170	9730 - 10714	shcal13
gb_sh_0055	Goldberg, Mychajliw, & Hadly, 2016	-8.62, -43.363	9650, 100	10672 - 11213	shcal13
gb_sh_0056	Goldberg, Mychajliw, & Hadly, 2016	-8.62, -43.363	9730, 140	10586 - 11396	shcal13
gb_sh_0057	Goldberg, Mychajliw, & Hadly, 2016	-8.62, -43.363	10530, 110	12023 - 12666	shcal13
gb_sh_0058	Goldberg, Mychajliw, & Hadly, 2016	-8.644, -42.3808	9700, 120	10656 - 11265	shcal13
gb_sh_0059	Goldberg, Mychajliw, & Hadly, 2016	-8.644, -42.3808	9850, 120	10768 - 11627	shcal13
gb_sh_0060	Goldberg, Mychajliw, & Hadly, 2016	-22.8198, -42.961	3760, 190	3566 - 4583	shcal13
gb_sh_0061	Goldberg, Mychajliw, & Hadly, 2016	-24.9683, -47.8844	3080, 55	3066 - 3378	shcal13
gb_sh_0062	Goldberg, Mychajliw, & Hadly, 2016	-24.9833, -47.8833	4120, 110	4287 - 4850	shcal13

gb_sh_0063	Goldberg, Mychajliw, & Hadly, 2016	-24.9833, -47.8833	4160, 100	4404 - 4866	shcal13
gb_sh_0064	Goldberg, Mychajliw, & Hadly, 2016	-24.9678, -47.8519	3090, 110	2924 - 3479	shcal13
gb_sh_0065	Goldberg, Mychajliw, & Hadly, 2016	-24.9678, -47.8519	3220, 90	3163 - 3613	shcal13
gb_sh_0066	Goldberg, Mychajliw, & Hadly, 2016	-8.85, -42.5556	6150, 50	6849 - 7162	shcal13
gb_sh_0067	Goldberg, Mychajliw, & Hadly, 2016	-8.85, -42.5556	6160, 130	6670 - 7279	shcal13
gb_sh_0068	Goldberg, Mychajliw, & Hadly, 2016	-8.85, -42.5556	7220, 80	7847 - 8173	shcal13
gb_sh_0069	Goldberg, Mychajliw, & Hadly, 2016	-8.85, -42.5556	7230, 80	7912 - 8177	shcal13
gb_sh_0070	Goldberg, Mychajliw, & Hadly, 2016	-8.85, -42.5556	7640, 160	8021 - 8775	shcal13
gb_sh_0071	Goldberg, Mychajliw, & Hadly, 2016	-8.85, -42.5556	7750, 80	8357 - 8647	shcal13
gb_sh_0072	Goldberg, Mychajliw, & Hadly, 2016	-8.85, -42.5556	8050, 170	8454 - 9309	shcal13
gb_sh_0073	Goldberg, Mychajliw, & Hadly, 2016	-8.85, -42.5556	8080, 120	8591 - 9280	shcal13
gb_sh_0074	Goldberg, Mychajliw, & Hadly, 2016	-8.85, -42.5556	8170, 90	8747 - 9320	shcal13
gb_sh_0075	Goldberg, Mychajliw, & Hadly, 2016	-8.85, -42.5556	8170, 80	8767 - 9310	shcal13

gb_sh_0076	Goldberg, Mychajliw, & Hadly, 2016	-8.85, -42.5556	8450, 80	9239 - 9541	shcal13
gb_sh_0077	Goldberg, Mychajliw, & Hadly, 2016	-8.85, -42.5556	8600, 60	9457 - 9675	shcal13
gb_sh_0078	Goldberg, Mychajliw, & Hadly, 2016	-8.85, -42.5556	9506, 135	10386 - 11181	shcal13
gb_sh_0079	Goldberg, Mychajliw, & Hadly, 2016	-8.85, -42.5556	9800, 60	11070 - 11290	shcal13
gb_sh_0080	Goldberg, Mychajliw, & Hadly, 2016	-8.85, -42.5556	10040, 80	11240 - 11803	shcal13
gb_sh_0081	Goldberg, Mychajliw, & Hadly, 2016	-8.85, -42.5556	10050, 80	11241 - 11819	shcal13
gb_sh_0082	Goldberg, Mychajliw, & Hadly, 2016	-8.85, -42.5556	10400, 180	11599 - 12672	shcal13
gb_sh_0083	Goldberg, Mychajliw, & Hadly, 2016	-8.85, -42.5556	10454, 114	11937 - 12647	shcal13
gb_sh_0084	Goldberg, Mychajliw, & Hadly, 2016	-8.85, -42.5556	13989, 167	16378 - 17421	shcal13
gb_sh_0085	Goldberg, Mychajliw, & Hadly, 2016	-25.1453, -48.0325	3750, 50	3894 - 4163	shcal13
gb_sh_0086	Goldberg, Mychajliw, & Hadly, 2016	-25.1453, -48.0325	3760, 50	3904 - 4184	shcal13
gb_sh_0088	Goldberg, Mychajliw, & Hadly, 2016	-25.1453, -48.0325	4060, 50	4385 - 4646	shcal13
gb_sh_0089	Goldberg, Mychajliw, & Hadly, 2016	-25.1453, -48.0325	4140, 50	4511 - 4822	shcal13

gb_sh_0090	Goldberg, Mychajliw, & Hadly, 2016	-25.1453, -48.0325	4400, 110	4796 - 5308	shcal13
gb_sh_0091	Goldberg, Mychajliw, & Hadly, 2016	-25.1453, -48.0325	4590, 90	4956 - 5469	shcal13
gb_sh_0092	Goldberg, Mychajliw, & Hadly, 2016	-3.755, -49.6219	9570, 70	10649 - 11130	shcal13
gb_sh_0093	Goldberg, Mychajliw, & Hadly, 2016	-3.7611, -49.565	9510, 60	10555 - 10879	shcal13
gb_sh_0094	Goldberg, Mychajliw, & Hadly, 2016	-23.2867, -49.5139	3920, 60	4143 - 4440	shcal13
gb_sh_0095	Goldberg, Mychajliw, & Hadly, 2016	-23.2867, -49.5139	4260, 60	4566 - 4872	shcal13
gb_sh_0096	Goldberg, Mychajliw, & Hadly, 2016	-15.4667, -56.8	5080, 230	5645 - 5915	shcal13
gb_sh_0097	Goldberg, Mychajliw, & Hadly, 2016	-23.2867, -49.5139	7020, 70	7677 - 7944	shcal13
gb_sh_0098	Goldberg, Mychajliw, & Hadly, 2016	-25.0147, -47.9267	3900, 450	3168 - 5470	shcal13
gb_sh_0099	Goldberg, Mychajliw, & Hadly, 2016	-25.0147, -47.9267	3360, 330	2768 - 4419	shcal13
gb_sh_0100	Goldberg, Mychajliw, & Hadly, 2016	unknown, unknown	2050, 100	1725 - 2182	shcal13
gb_sh_0101	Goldberg, Mychajliw, & Hadly, 2016	-28.4283, -48.8294	4120, 220	3972 - 5079	shcal13
gb_sh_0102	Goldberg, Mychajliw, & Hadly, 2016	unknown, unknown	5020, 20	5640 - 5750	shcal13

gb_sh_0103	Goldberg, Mychajliw, & Hadly, 2016	-25.1686, -47.9914	4630, 50	5049 - 5194	shcal13
gb_sh_0104	Goldberg, Mychajliw, & Hadly, 2016	-25.1686, -47.9914	4715, 95	5257 - 5597	shcal13
gb_sh_0105	Goldberg, Mychajliw, & Hadly, 2016	-23.3596, -46.7536	2270, 100	1994 - 2490	shcal13
gb_sh_0106	Goldberg, Mychajliw, & Hadly, 2016	-23.3596, -46.7536	3210, 150	2960 - 3722	shcal13
gb_sh_0107	Goldberg, Mychajliw, & Hadly, 2016	-23.3596, -46.7536	3230, 155	2990 - 3731	shcal13
gb_sh_0108	Goldberg, Mychajliw, & Hadly, 2016	-23.3596, -46.7536	3310, 150	3140 - 3885	shcal13
gb_sh_0109	Goldberg, Mychajliw, & Hadly, 2016	-23.3596, -46.7536	3370, 160	3167 - 3982	shcal13
gb_sh_0110	Goldberg, Mychajliw, & Hadly, 2016	-19.5333, -44.0667	9500, 200	10245 - 11218	shcal13
gb_sh_0111	Goldberg, Mychajliw, & Hadly, 2016	-8.825, -42.5744	7610, 80	8197 - 8522	shcal13
gb_sh_0112	Goldberg, Mychajliw, & Hadly, 2016	-8.825, -42.5744	9480, 170	10276 - 11173	shcal13
gb_sh_0113	Goldberg, Mychajliw, & Hadly, 2016	-23.4812, -48.267	2060, 230	1424 - 2498	shcal13
gb_sh_0114	Goldberg, Mychajliw, & Hadly, 2016	-23.4812, -48.267	4650, 170	4851 - 5646	shcal13
gb_sh_0115	Goldberg, Mychajliw, & Hadly, 2016	-22.9588, -43.0476	2328, 135	2007 - 2717	shcal13

gb_sh_0116	Goldberg, Mychajliw, & Hadly, 2016	-22.9588, -43.0476	2562, 139	2305 - 2894	shcal13
gb_sh_0117	Goldberg, Mychajliw, & Hadly, 2016	-22.9588, -43.0476	4475, 160	4783 - 5475	shcal13
gb_sh_0118	Goldberg, Mychajliw, & Hadly, 2016	-22.9588, -43.0476	7958, 224	8342 - 9333	shcal13
gb_sh_0119	Goldberg, Mychajliw, & Hadly, 2016	-25.1323, -47.9324	5620, 60	6277 - 6493	shcal13
gb_sh_0120	Goldberg, Mychajliw, & Hadly, 2016	-25.1323, -47.9324	5730, 60	6387 - 6637	shcal13
gb_sh_0121	Goldberg, Mychajliw, & Hadly, 2016	-24.855, -47.475	3710, 140	3681 - 4413	shcal13
gb_sh_0122	Goldberg, Mychajliw, & Hadly, 2016	-24.855, -47.475	3780, 110	3827 - 4422	shcal13
gb_sh_0123	Goldberg, Mychajliw, & Hadly, 2016	-24.855, -47.475	4300, 140	4492 - 5088	shcal13
gb_sh_0124	Goldberg, Mychajliw, & Hadly, 2016	-24.855, -47.475	4340, 110	4566 - 5085	shcal13
gb_sh_0125	Goldberg, Mychajliw, & Hadly, 2016	-28.407, -49.1115	3370, 70	3386 - 3721	shcal13
gb_sh_0126	Goldberg, Mychajliw, & Hadly, 2016	-28.407, -49.11	3500, 50	3584 - 3855	shcal13
gb_sh_0127	Goldberg, Mychajliw, & Hadly, 2016	-24.8466, -48.239	6090, 40	6777 - 7009	shcal13
gb_sh_0128	Goldberg, Mychajliw, & Hadly, 2016	-24.8466, -48.239	8500, 70	9302 - 9545	shcal13

gb_sh_0129	Goldberg, Mychajliw, & Hadly, 2016	-24.8466, -48.239	8795, 100	9543 - 9964	shcal13
gb_sh_0130	Goldberg, Mychajliw, & Hadly, 2016	-24.8466, -48.239	8860, 60	9658 - 10165	shcal13
gb_sh_0132	Goldberg, Mychajliw, & Hadly, 2016	-24.8466, -48.239	9250, 50	10244 - 10510	shcal13
gb_sh_0133	Goldberg, Mychajliw, & Hadly, 2016	-24.8466, -48.239	5000, 70	5588 - 5798	shcal13
gb_sh_0134	Goldberg, Mychajliw, & Hadly, 2016	-24.8466, -48.239	4500, 40	4958 - 5292	shcal13
gb_sh_0135	Goldberg, Mychajliw, & Hadly, 2016	-24.8466, -48.239	4530, 50	4960 - 5312	shcal13
gb_sh_0136	Goldberg, Mychajliw, & Hadly, 2016	-10.136, -48.437	8980, 70	9881 - 10234	shcal13
gb_sh_0137	Goldberg, Mychajliw, & Hadly, 2016	-10.136, -48.437	9410, 60	10396 - 10755	shcal13
gb_sh_0138	Goldberg, Mychajliw, & Hadly, 2016	-10.136, -48.437	9850, 70	11075 - 11404	shcal13
gb_sh_0140	Goldberg, Mychajliw, & Hadly, 2016	-28.4414, -48.9603	3780, 40	3971 - 4237	shcal13
gb_sh_0142	Goldberg, Mychajliw, & Hadly, 2016	-21.3859, -44.0801	2400, 100	2285 - 2722	shcal13
gb_sh_0143	Goldberg, Mychajliw, & Hadly, 2016	-21.3859, -44.0801	2460, 110	2300 - 2752	shcal13
gb_sh_0144	Goldberg, Mychajliw, & Hadly, 2016	-21.3859, -44.0801	2550, 100	2348 - 2771	shcal13

gb_sh_0145	Goldberg, Mychajliw, & Hadly, 2016	-21.3859, -44.0801	3040, 50	3004 - 3277	shcal13
gb_sh_0147	Goldberg, Mychajliw, & Hadly, 2016	-21.3859, -44.0801	3275, 125	3156 - 3731	shcal13
gb_sh_0148	Goldberg, Mychajliw, & Hadly, 2016	-21.3859, -44.0801	3300, 150	3137 - 3868	shcal13
gb_sh_0150	Goldberg, Mychajliw, & Hadly, 2016	-21.3859, -44.0801	3350, 150	3171 - 3925	shcal13
gb_sh_0151	Goldberg, Mychajliw, & Hadly, 2016	-21.3859, -44.0801	3370, 110	3340 - 3858	shcal13
gb_sh_0152	Goldberg, Mychajliw, & Hadly, 2016	-21.3859, -44.0801	3400, 150	3229 - 3984	shcal13
gb_sh_0153	Goldberg, Mychajliw, & Hadly, 2016	-21.3859, -44.0801	3875, 125	3863 - 4574	shcal13
gb_sh_0154	Goldberg, Mychajliw, & Hadly, 2016	-19.528, -44.0367	7970, 40	8627 - 8818	shcal13
gb_sh_0155	Goldberg, Mychajliw, & Hadly, 2016	-23.8833, -46.3839	4300, 180	4377 - 5319	shcal13
gb_sh_0156	Goldberg, Mychajliw, & Hadly, 2016	-19.521, -44.003	6470, 60	7247 - 7463	shcal13
gb_sh_0157	Goldberg, Mychajliw, & Hadly, 2016	-19.5219, -44.0019	8230, 50	9009 - 9295	shcal13
gb_sh_0158	Goldberg, Mychajliw, & Hadly, 2016	-19.5219, -44.0019	8240, 40	9021 - 9286	shcal13
gb_sh_0159	Goldberg, Mychajliw, & Hadly, 2016	-19.5219, -44.0019	9020, 120	9682 - 10412	shcal13

gb_sh_0160	Goldberg, Mychajliw, & Hadly, 2016	-19.5219, -44.0019	9130, 60	10158 - 10433	shcal13
gb_sh_0161	Goldberg, Mychajliw, & Hadly, 2016	-19.5219, -44.0019	9720, 128	10651 - 11326	shcal13
gb_sh_0162	Goldberg, Mychajliw, & Hadly, 2016	-25.6721, -49.1249	2670, 80	2460 - 2929	shcal13
gb_sh_0163	Goldberg, Mychajliw, & Hadly, 2016	-25.6721, -49.1249	3705, 130	3688 - 4359	shcal13
gb_sh_0164	Goldberg, Mychajliw, & Hadly, 2016	-18.2853, -43.8539	2025, 95	1707 - 2159	shcal13
gb_sh_0165	Goldberg, Mychajliw, & Hadly, 2016	-18.2853, -43.8539	2620, 90	2376 - 2847	shcal13
gb_sh_0166	Goldberg, Mychajliw, & Hadly, 2016	-18.2853, -43.8539	2900, 95	2764 - 3231	shcal13
gb_sh_0167	Goldberg, Mychajliw, & Hadly, 2016	-18.2853, -43.8539	3450, 160	3328 - 4091	shcal13
gb_sh_0168	Goldberg, Mychajliw, & Hadly, 2016	-18.2853, -43.8539	3450, 100	3442 - 3910	shcal13
gb_sh_0169	Goldberg, Mychajliw, & Hadly, 2016	-18.2853, -43.8539	3650, 115	3607 - 4244	shcal13
gb_sh_0170	Goldberg, Mychajliw, & Hadly, 2016	-18.2853, -43.8539	4460, 100	4829 - 5317	shcal13
gb_sh_0171	Goldberg, Mychajliw, & Hadly, 2016	-18.2853, -43.8539	4515, 115	4837 - 5332	shcal13
gb_sh_0172	Goldberg, Mychajliw, & Hadly, 2016	-18.2853, -43.8539	4590, 100	4946 - 5470	shcal13

gb_sh_0173	Goldberg, Mychajliw, & Hadly, 2016	-18.2853, -43.8539	5600, 130	6168 - 6645	shcal13
gb_sh_0174	Goldberg, Mychajliw, & Hadly, 2016	-18.2853, -43.8539	5603, 100	6179 - 6574	shcal13
gb_sh_0175	Goldberg, Mychajliw, & Hadly, 2016	-18.2853, -43.8539	5935, 135	6401 - 7028	shcal13
gb_sh_0176	Goldberg, Mychajliw, & Hadly, 2016	-18.2853, -43.8539	6085, 120	6638 - 7183	shcal13
gb_sh_0177	Goldberg, Mychajliw, & Hadly, 2016	-18.2853, -43.8539	6225, 125	6748 - 7329	shcal13
gb_sh_0178	Goldberg, Mychajliw, & Hadly, 2016	-18.2853, -43.8539	6600, 150	7161 - 7703	shcal13
gb_sh_0179	Goldberg, Mychajliw, & Hadly, 2016	-18.2853, -43.8539	6630, 125	7262 - 7675	shcal13
gb_sh_0180	Goldberg, Mychajliw, & Hadly, 2016	-18.2853, -43.8539	6820, 190	7307 - 7978	shcal13
gb_sh_0181	Goldberg, Mychajliw, & Hadly, 2016	-18.2853, -43.8539	6900, 135	7484 - 7951	shcal13
gb_sh_0182	Goldberg, Mychajliw, & Hadly, 2016	-18.2853, -43.8539	7152, 140	7658 - 8201	shcal13
gb_sh_0183	Goldberg, Mychajliw, & Hadly, 2016	-18.2853, -43.8539	7300, 140	7826 - 8374	shcal13
gb_sh_0184	Goldberg, Mychajliw, & Hadly, 2016	-18.2853, -43.8539	7820, 150	8325 - 9011	shcal13
gb_sh_0185	Goldberg, Mychajliw, & Hadly, 2016	-18.2853, -43.8539	8100, 135	8588 - 9315	shcal13

gb_sh_0186	Goldberg, Mychajliw, & Hadly, 2016	-18.2853, -43.8539	8400, 200	8703 - 9787	shcal13
gb_sh_0187	Goldberg, Mychajliw, & Hadly, 2016	-18.2853, -43.8539	9520, 160	10372 - 11200	shcal13
gb_sh_0188	Goldberg, Mychajliw, & Hadly, 2016	-18.2853, -43.8539	11000, 250	12384 - 13378	shcal13
gb_sh_0190	Goldberg, Mychajliw, & Hadly, 2016	-22.9798, -42.0288	4190, 130	4287 - 4979	shcal13
gb_sh_0191	Goldberg, Mychajliw, & Hadly, 2016	-28.5137, -49.0081	2115, 50	1914 - 2159	shcal13
gb_sh_0192	Goldberg, Mychajliw, & Hadly, 2016	-28.5137, -49.0081	2705, 85	2651 - 2976	shcal13
gb_sh_0193	Goldberg, Mychajliw, & Hadly, 2016	-28.5137, -49.0081	2740, 70	2716 - 2993	shcal13
gb_sh_0194	Goldberg, Mychajliw, & Hadly, 2016	-28.5137, -49.0081	2835, 95	2748 - 3161	shcal13
gb_sh_0195	Goldberg, Mychajliw, & Hadly, 2016	-28.5137, -49.0081	3165, 55	3179 - 3454	shcal13
gb_sh_0196	Goldberg, Mychajliw, & Hadly, 2016	-28.5137, -49.0081	3270, 200	2926 - 3929	shcal13
gb_sh_0197	Goldberg, Mychajliw, & Hadly, 2016	-28.5137, -49.0081	3350, 85	3360 - 3727	shcal13
gb_sh_0198	Goldberg, Mychajliw, & Hadly, 2016	unknown, unknown	2120, 220	1562 - 2542	shcal13
gb_sh_0199	Goldberg, Mychajliw, & Hadly, 2016	unknown, unknown	4070, 220	3866 - 5056	shcal13

gb_sh_0200	Goldberg, Mychajliw, & Hadly, 2016	-19.5381, -43.951	10460, 60	12031 - 12438	shcal13
gb_sh_0201	Goldberg, Mychajliw, & Hadly, 2016	-22.8282, -42.0801	3010, 80	2924 - 3359	shcal13
gb_sh_0202	Goldberg, Mychajliw, & Hadly, 2016	-22.8282, -42.0801	3215, 90	3159 - 3612	shcal13
gb_sh_0203	Goldberg, Mychajliw, & Hadly, 2016	-22.8282, -42.0801	3720, 90	3814 - 4291	shcal13
gb_sh_0204	Goldberg, Mychajliw, & Hadly, 2016	-22.8282, -42.0801	4205, 111	4411 - 4973	shcal13
gb_sh_0205	Goldberg, Mychajliw, & Hadly, 2016	-22.8282, -42.0801	4265, 75	4527 - 4893	shcal13
gb_sh_0206	Goldberg, Mychajliw, & Hadly, 2016	-23.8435, -46.3566	2590, 80	2363 - 2774	shcal13
gb_sh_0208	Goldberg, Mychajliw, & Hadly, 2016	-23.8435, -46.3566	4210, 90	4434 - 4869	shcal13
gb_sh_0210	Goldberg, Mychajliw, & Hadly, 2016	-28.5518, -49.0628	3640, 50	3814 - 4011	shcal13
gb_sh_0211	Goldberg, Mychajliw, & Hadly, 2016	-28.5487, -49.0537	3180, 50	3210 - 3464	shcal13
gb_sh_0212	Goldberg, Mychajliw, & Hadly, 2016	unknown, unknown	3350, 135	3215 - 3887	shcal13
gb_sh_0213	Goldberg, Mychajliw, & Hadly, 2016	unknown, unknown	8115, 80	8695 - 9152	shcal13
gb_sh_0214	Goldberg, Mychajliw, & Hadly, 2016	-15.4667, -56.8	9460, 90	10501 - 10785	shcal13

gb_sh_0215	Goldberg, Mychajliw, & Hadly, 2016	unknown, unknown	2030, 155	1606 - 2325	shcal13
gb_sh_0216	Goldberg, Mychajliw, & Hadly, 2016	-28.624, -48.9157	3930, 50	4150 - 4439	shcal13
gb_sh_0217	Goldberg, Mychajliw, & Hadly, 2016	-28.624, -48.9157	4160, 50	4517 - 4827	shcal13
gb_sh_0218	Goldberg, Mychajliw, & Hadly, 2016	-28.624, -48.9157	4290, 50	4782 - 4892	shcal13
gb_sh_0219	Goldberg, Mychajliw, & Hadly, 2016	-28.6157, -48.9149	4320, 40	4808 - 4970	shcal13
gb_sh_0220	Goldberg, Mychajliw, & Hadly, 2016	-28.6157, -48.9149	4420, 50	4841 - 5066	shcal13
gb_sh_0221	Goldberg, Mychajliw, & Hadly, 2016	-26.3014, -48.8439	2220, 240	1692 - 2753	shcal13
gb_sh_0224	Goldberg, Mychajliw, & Hadly, 2016	-25.05, -48.05	3490, 80	3545 - 3910	shcal13
gb_sh_0225	Goldberg, Mychajliw, & Hadly, 2016	-25.1321, -48.8804	3655, 26	3835 - 3989	shcal13
gb_sh_0226	Goldberg, Mychajliw, & Hadly, 2016	-25.1321, -48.8804	4124, 27	4508 - 4653	shcal13
gb_sh_0227	Goldberg, Mychajliw, & Hadly, 2016	unknown, unknown	3960, 100	4076 - 4628	shcal13
gb_sh_0228	Goldberg, Mychajliw, & Hadly, 2016	-25.52, -42.472	2010, 75	1731 - 2096	shcal13
gb_sh_0229	Goldberg, Mychajliw, & Hadly, 2016	unknown, unknown	4350, 250	4236 - 5489	shcal13

gb_sh_0230	Goldberg, Mychajliw, & Hadly, 2016	-20, -44	4670, 130	4959 - 5600	shcal13
gb_sh_0231	Goldberg, Mychajliw, & Hadly, 2016	-24.1379, -51.9939	2110, 120	1805 - 2339	shcal13
gb_sh_0233	Goldberg, Mychajliw, & Hadly, 2016	-24.1379, -51.9939	3620, 60	3696 - 4006	shcal13
gb_sh_0234	Goldberg, Mychajliw, & Hadly, 2016	-24.1379, -51.9939	4610, 60	5037 - 5333	shcal13
gb_sh_0235	Goldberg, Mychajliw, & Hadly, 2016	-28.6518, -48.9741	4240, 190	4235 - 5305	shcal13
gb_sh_0236	Goldberg, Mychajliw, & Hadly, 2016	-26.2997, -48.5684	2240, 70	2044 - 2345	shcal13
gb_sh_0237	Goldberg, Mychajliw, & Hadly, 2016	-26.2997, -48.5684	2320, 55	2148 - 2433	shcal13
gb_sh_0238	Goldberg, Mychajliw, & Hadly, 2016	-26.2997, -48.5684	3618, 130	3556 - 4247	shcal13
gb_sh_0239	Goldberg, Mychajliw, & Hadly, 2016	-26.2997, -48.5684	3815, 50	3976 - 4299	shcal13
gb_sh_0240	Goldberg, Mychajliw, & Hadly, 2016	-26.2997, -48.5684	3940, 140	3960 - 4709	shcal13
gb_sh_0241	Goldberg, Mychajliw, & Hadly, 2016	-26.2997, -48.5684	4330, 140	4516 - 5299	shcal13
gb_sh_0242	Goldberg, Mychajliw, & Hadly, 2016	-26.2997, -48.5684	4910, 55	5569 - 5733	shcal13
gb_sh_0243	Goldberg, Mychajliw, & Hadly, 2016	-26.2997, -48.5684	5270, 80	5874 - 6211	shcal13

gb_sh_0244	Goldberg, Mychajliw, & Hadly, 2016	-26.2997, -48.5684	5520, 120	5985 - 6500	shcal13
gb_sh_0247	Goldberg, Mychajliw, & Hadly, 2016	-25.5869, -54.4105	2035, 70	1809 - 2148	shcal13
gb_sh_0248	Goldberg, Mychajliw, & Hadly, 2016	-25.5869, -54.4105	2850, 60	2765 - 3076	shcal13
gb_sh_0249	Goldberg, Mychajliw, & Hadly, 2016	-25.5869, -54.4105	4035, 150	4080 - 4847	shcal13
gb_sh_0250	Goldberg, Mychajliw, & Hadly, 2016	-25.5869, -54.4105	6265, 80	6908 - 7312	shcal13
gb_sh_0251	Goldberg, Mychajliw, & Hadly, 2016	-25.5869, -54.4105	6505, 105	7230 - 7566	shcal13
gb_sh_0252	Goldberg, Mychajliw, & Hadly, 2016	-25.5869, -54.4105	6910, 75	7578 - 7856	shcal13
gb_sh_0253	Goldberg, Mychajliw, & Hadly, 2016	-8.13333, -36.3667	8495, 70	9299 - 9544	shcal13
gb_sh_0254	Goldberg, Mychajliw, & Hadly, 2016	-8.13333, -36.3667	9150, 140	9885 - 10608	shcal13
gb_sh_0255	Goldberg, Mychajliw, & Hadly, 2016	-8.13333, -36.3667	9150, 70	10169 - 10497	shcal13
gb_sh_0256	Goldberg, Mychajliw, & Hadly, 2016	-8.13333, -36.3667	11060, 90	12727 - 13058	shcal13
gb_sh_0257	Goldberg, Mychajliw, & Hadly, 2016	-28.5538, -48.7877	3090, 70	3023 - 3400	shcal13
gb_sh_0258	Goldberg, Mychajliw, & Hadly, 2016	-28.5541, -48.7886	4400, 60	4829 - 5069	shcal13

gb_sh_0259	Goldberg, Mychajliw, & Hadly, 2016	-28.5447, -48.7964	4530, 70	4951 - 5314	shcal13
gb_sh_0260	Goldberg, Mychajliw, & Hadly, 2016	-28.6137, -48.8926	2705, 240	2296 - 3365	shcal13
gb_sh_0261	Goldberg, Mychajliw, & Hadly, 2016	-28.6137, -48.8926	2840, 70	2757 - 3077	shcal13
gb_sh_0262	Goldberg, Mychajliw, & Hadly, 2016	-28.6137, -48.8926	3780, 70	3886 - 4299	shcal13
gb_sh_0263	Goldberg, Mychajliw, & Hadly, 2016	-28.6137, -48.8926	4110, 70	4418 - 4821	shcal13
gb_sh_0264	Goldberg, Mychajliw, & Hadly, 2016	unknown, unknown	5230, 350	5213 - 6730	shcal13
gb_sh_0265	Goldberg, Mychajliw, & Hadly, 2016	unknown, unknown	5270, 300	5317 - 6659	shcal13
gb_sh_0266	Goldberg, Mychajliw, & Hadly, 2016	-22.779, -41.9044	5150, 110	5606 - 6029	shcal13
gb_sh_0268	Goldberg, Mychajliw, & Hadly, 2016	-17.381, -48.6676	2280, 60	2094 - 2353	shcal13
gb_sh_0269	Goldberg, Mychajliw, & Hadly, 2016	-16.1609, -52.002	4560, 150	4838 - 5488	shcal13
gb_sh_0270	Goldberg, Mychajliw, & Hadly, 2016	-16.166, -52.0024	2920, 75	2837 - 3215	shcal13
gb_sh_0271	Goldberg, Mychajliw, & Hadly, 2016	-16.166, -52.0024	4100, 65	4415 - 4730	shcal13
gb_sh_0272	Goldberg, Mychajliw, & Hadly, 2016	-16.1805, -51.9911	4455, 115	4810 - 5325	shcal13

gb_sh_0273	Goldberg, Mychajliw, & Hadly, 2016	-18.2864, -52.0477	6690, 90	7415 - 7680	shcal13
gb_sh_0274	Goldberg, Mychajliw, & Hadly, 2016	-18.2864, -52.0477	7395, 80	8006 - 8347	shcal13
gb_sh_0275	Goldberg, Mychajliw, & Hadly, 2016	-18.2864, -52.0477	7420, 80	8022 - 8361	shcal13
gb_sh_0276	Goldberg, Mychajliw, & Hadly, 2016	-18.2864, -52.0477	8740, 90	9521 - 9949	shcal13
gb_sh_0277	Goldberg, Mychajliw, & Hadly, 2016	-18.2864, -52.0477	8805, 100	9546 - 9966	shcal13
gb_sh_0278	Goldberg, Mychajliw, & Hadly, 2016	-18.2864, -52.0477	8915, 115	9605 - 10227	shcal13
gb_sh_0279	Goldberg, Mychajliw, & Hadly, 2016	-18.2864, -52.0477	9020, 70	9887 - 10254	shcal13
gb_sh_0280	Goldberg, Mychajliw, & Hadly, 2016	-18.2864, -52.0477	9060, 65	9910 - 10288	shcal13
gb_sh_0281	Goldberg, Mychajliw, & Hadly, 2016	-18.2864, -52.0477	9195, 75	10194 - 10515	shcal13
gb_sh_0283	Goldberg, Mychajliw, & Hadly, 2016	-18.2864, -52.0477	9765, 75	11058 - 11258	shcal13
gb_sh_0284	Goldberg, Mychajliw, & Hadly, 2016	-18.2864, -52.0477	10400, 130	11713 - 12567	shcal13
gb_sh_0285	Goldberg, Mychajliw, & Hadly, 2016	-18.2864, -52.0477	10580, 115	12248 - 12695	shcal13
gb_sh_0286	Goldberg, Mychajliw, & Hadly, 2016	-15.4667, -56.8	10120, 60	11312 - 11970	shcal13

gb_sh_0287	Goldberg, Mychajliw, & Hadly, 2016	-18.4447, -52.0004	5720, 50	6387 - 6570	shcal13
gb_sh_0288	Goldberg, Mychajliw, & Hadly, 2016	-18.4472, -52.0055	10740, 85	12540 - 12741	shcal13
gb_sh_0289	Goldberg, Mychajliw, & Hadly, 2016	-16.1747, -51.9156	2140, 55	1928 - 2184	shcal13
gb_sh_0290	Goldberg, Mychajliw, & Hadly, 2016	-16.1747, -51.9156	2345, 55	2154 - 2485	shcal13
gb_sh_0291	Goldberg, Mychajliw, & Hadly, 2016	-16.1747, -51.9156	2475, 70	2349 - 2717	shcal13
gb_sh_0292	Goldberg, Mychajliw, & Hadly, 2016	-16.1747, -51.9156	2740, 60	2738 - 2948	shcal13
gb_sh_0293	Goldberg, Mychajliw, & Hadly, 2016	-16.1747, -51.9156	2900, 50	2850 - 3084	shcal13
gb_sh_0294	Goldberg, Mychajliw, & Hadly, 2016	-16.1747, -51.9156	3000, 50	2956 - 3253	shcal13
gb_sh_0295	Goldberg, Mychajliw, & Hadly, 2016	-16.1747, -51.9156	4505, 55	4956 - 5298	shcal13
gb_sh_0296	Goldberg, Mychajliw, & Hadly, 2016	-18.4447, -52.0369	8370, 85	9088 - 9500	shcal13
gb_sh_0297	Goldberg, Mychajliw, & Hadly, 2016	-18.4447, -52.0369	8880, 90	9611 - 10189	shcal13
gb_sh_0298	Goldberg, Mychajliw, & Hadly, 2016	-14.4833, -49.4667	10750, 300	11619 - 13193	shcal13
gb_sh_0299	Goldberg, Mychajliw, & Hadly, 2016	-30.4333, -50.5	2980, 130	2784 - 3383	shcal13

gb_sh_0300	Goldberg, Mychajliw, & Hadly, 2016	-30.4333, -50.5	3000, 90	2916 - 3358	shcal13
gb_sh_0301	Goldberg, Mychajliw, & Hadly, 2016	-30.4333, -50.5	3300, 95	3237 - 3710	shcal13
gb_sh_0302	Goldberg, Mychajliw, & Hadly, 2016	-30.4333, -50.5	3365, 85	3372 - 3730	shcal13
gb_sh_0304	Goldberg, Mychajliw, & Hadly, 2016	-30.4333, -50.5	4790, 95	5285 - 5663	shcal13
gb_sh_0305	Goldberg, Mychajliw, & Hadly, 2016	-6, -50	8260, 50	9021 - 9315	shcal13
gb_sh_0306	Goldberg, Mychajliw, & Hadly, 2016	-19.7148, -42.9878	4380, 70	4812 - 5076	shcal13
gb_sh_0307	Goldberg, Mychajliw, & Hadly, 2016	-6.042, -50.201	6905, 50	7592 - 7798	shcal13
gb_sh_0308	Goldberg, Mychajliw, & Hadly, 2016	-6.042, -50.201	7925, 45	8576 - 8799	shcal13
gb_sh_0309	Goldberg, Mychajliw, & Hadly, 2016	-6.042, -50.201	8065, 360	8150 - 9708	shcal13
gb_sh_0310	Goldberg, Mychajliw, & Hadly, 2016	-6.042, -50.201	8140, 130	8627 - 9329	shcal13
gb_sh_0312	Goldberg, Mychajliw, & Hadly, 2016	-20.4, -45.813	9610, 60	10704 - 11150	shcal13
gb_sh_0313	Goldberg, Mychajliw, & Hadly, 2016	-6.0875, -50.12	8119, 50	8760 - 9136	shcal13
gb_sh_0314	Goldberg, Mychajliw, & Hadly, 2016	-6.0875, -50.12	8340, 50	9128 - 9453	shcal13

gb_sh_0315	Goldberg, Mychajliw, & Hadly, 2016	-6.0875, -50.12	8520, 50	9409 - 9545	shcal13
gb_sh_0316	Goldberg, Mychajliw, & Hadly, 2016	-6.0875, -50.12	9000, 50	9913 - 10101	shcal13
gb_sh_0317	Goldberg, Mychajliw, & Hadly, 2016	-6.04, -50.27	8470, 50	9393 - 9532	shcal13
gb_sh_0318	Goldberg, Mychajliw, & Hadly, 2016	-9.42207, -40.6296	2200, 110	1871 - 2363	shcal13
gb_sh_0319	Goldberg, Mychajliw, & Hadly, 2016	-9.42207, -40.6296	2360, 50	2291 - 2490	shcal13
gb_sh_0320	Goldberg, Mychajliw, & Hadly, 2016	-9.42207, -40.6296	3630, 70	3692 - 4089	shcal13
gb_sh_0321	Goldberg, Mychajliw, & Hadly, 2016	-9.42207, -40.6296	4590, 70	4968 - 5333	shcal13
gb_sh_0322	Goldberg, Mychajliw, & Hadly, 2016	-9.42207, -40.6296	5280, 120	5740 - 6283	shcal13
gb_sh_0323	Goldberg, Mychajliw, & Hadly, 2016	-9.42207, -40.6296	7580, 410	7606 - 9313	shcal13
gb_sh_0324	Goldberg, Mychajliw, & Hadly, 2016	-24.9167, -47.8667	4310, 105	4520 - 5069	shcal13
gb_sh_0325	Goldberg, Mychajliw, & Hadly, 2016	-24.9167, -47.8667	4920, 110	5446 - 5799	shcal13
gb_sh_0326	Goldberg, Mychajliw, & Hadly, 2016	-15.4667, -56.8	5110, 230	5592 - 6003	shcal13
gb_sh_0327	Goldberg, Mychajliw, & Hadly, 2016	-25.6747, -48.5082	4128, 134	4220 - 4878	shcal13

gb_sh_0328	Goldberg, Mychajliw, & Hadly, 2016	-25.6747, -48.5082	4220, 200	4220 - 5300	shcal13
gb_sh_0329	Goldberg, Mychajliw, & Hadly, 2016	-25.05, -48.0167	2285, 45	2153 - 2346	shcal13
gb_sh_0330	Goldberg, Mychajliw, & Hadly, 2016	-8.90566, -38.8893	2900, 170	2698 - 3449	shcal13
gb_sh_0331	Goldberg, Mychajliw, & Hadly, 2016	-8.90566, -38.8893	3140, 70	3136 - 3457	shcal13
gb_sh_0332	Goldberg, Mychajliw, & Hadly, 2016	-8.90566, -38.8893	3250, 180	2954 - 3870	shcal13
gb_sh_0333	Goldberg, Mychajliw, & Hadly, 2016	-22.7035, -42.1164	3110, 60	3102 - 3401	shcal13
gb_sh_0334	Goldberg, Mychajliw, & Hadly, 2016	-22.7035, -42.1164	3210, 50	3234 - 3484	shcal13
gb_sh_0335	Goldberg, Mychajliw, & Hadly, 2016	-22.7035, -42.1164	3410, 60	3452 - 3729	shcal13
gb_sh_0337	Goldberg, Mychajliw, & Hadly, 2016	-22.6936, -42.1163	2060, 60	1834 - 2112	shcal13
gb_sh_0338	Goldberg, Mychajliw, & Hadly, 2016	-22.6936, -42.1163	3670, 80	3700 - 4155	shcal13
gb_sh_0339	Goldberg, Mychajliw, & Hadly, 2016	-22.6811, -42.0522	2820, 200	2377 - 3368	shcal13
gb_sh_0340	Goldberg, Mychajliw, & Hadly, 2016	-22.6862, -42.046	3650, 40	3826 - 4010	shcal13
gb_sh_0341	Goldberg, Mychajliw, & Hadly, 2016	-22.6862, -42.046	3740, 110	3820 - 4407	shcal13

gb_sh_0342	Goldberg, Mychajliw, & Hadly, 2016	-22.6862, -42.046	3850, 140	3826 - 4583	shcal13
gb_sh_0343	Goldberg, Mychajliw, & Hadly, 2016	-25.4234, -48.6732	2480, 110	2304 - 2758	shcal13
gb_sh_0344	Goldberg, Mychajliw, & Hadly, 2016	-25.4234, -48.6732	2500, 110	2307 - 2772	shcal13
gb_sh_0345	Goldberg, Mychajliw, & Hadly, 2016	-25.4234, -48.6732	3150, 110	3000 - 3569	shcal13
gb_sh_0346	Goldberg, Mychajliw, & Hadly, 2016	-22.8934, -41.9809	2219, 32	2092 - 2311	shcal13
gb_sh_0348	Goldberg, Mychajliw, & Hadly, 2016	-22.9966, -41.9943	2360, 40	2298 - 2470	shcal13
gb_sh_0349	Goldberg, Mychajliw, & Hadly, 2016	-22.8934, -41.9809	3074, 33	3140 - 3356	shcal13
gb_sh_0350	Goldberg, Mychajliw, & Hadly, 2016	-22.8934, -41.9809	3302, 40	3383 - 3579	shcal13
gb_sh_0351	Goldberg, Mychajliw, & Hadly, 2016	-2.60488, -44.2865	2495, 10	2363 - 2542	shcal13
gb_sh_0352	Goldberg, Mychajliw, & Hadly, 2016	-2.60488, -44.2865	2655, 10	2727 - 2766	shcal13
gb_sh_0353	Goldberg, Mychajliw, & Hadly, 2016	-25.1666, -47.9143	4340, 50	4809 - 4985	shcal13
gb_sh_0354	Goldberg, Mychajliw, & Hadly, 2016	-25.1666, -47.9143	4360, 60	4807 - 5055	shcal13
gb_sh_0355	Goldberg, Mychajliw, & Hadly, 2016	-22.9549, -44.6522	2830, 50	2765 - 3007	shcal13

gb_sh_0356	Goldberg, Mychajliw, & Hadly, 2016	-22.9549, -44.6522	3060, 40	3073 - 3350	shcal13
gb_sh_0357	Goldberg, Mychajliw, & Hadly, 2016	-23.1314, -44.2462	2650, 350	1874 - 3514	shcal13
gb_sh_0358	Goldberg, Mychajliw, & Hadly, 2016	-23.1314, -44.2462	2910, 90	2775 - 3235	shcal13
gb_sh_0360	Goldberg, Mychajliw, & Hadly, 2016	-28.3965, -48.9645	5170, 60	5710 - 6000	shcal13
gb_sh_0361	Goldberg, Mychajliw, & Hadly, 2016	-28.3965, -48.9645	5270, 60	5891 - 6191	shcal13
gb_sh_0362	Goldberg, Mychajliw, & Hadly, 2016	-15.4667, -56.8	2600, 60	2428 - 2779	shcal13
gb_sh_0363	Goldberg, Mychajliw, & Hadly, 2016	-27.2708, -52.5083	5930, 140	6398 - 7029	shcal13
gb_sh_0364	Goldberg, Mychajliw, & Hadly, 2016	-22.9732, -43.0245	2290, 170	1893 - 2731	shcal13
gb_sh_0365	Goldberg, Mychajliw, & Hadly, 2016	unknown, unknown	6715, 135	7304 - 7793	shcal13
gb_sh_0366	Goldberg, Mychajliw, & Hadly, 2016	-27.1833, -53.75	7145, 120	7689 - 8166	shcal13
gb_sh_0367	Goldberg, Mychajliw, & Hadly, 2016	-19, -43	7560, 110	7981 - 8609	shcal13
gb_sh_0368	Goldberg, Mychajliw, & Hadly, 2016	-27.1833, -53.75	7600, 160	8004 - 8664	shcal13
gb_sh_0369	Goldberg, Mychajliw, & Hadly, 2016	-27.1833, -53.75	8095, 90	8634 - 9146	shcal13

gb_sh_0370	Goldberg, Mychajliw, & Hadly, 2016	-27.1833, -53.75	8640, 180	9243 - 10181	shcal13
gb_sh_0371	Goldberg, Mychajliw, & Hadly, 2016	-27.1833, -53.75	8640, 95	9432 - 9898	shcal13
gb_sh_0373	Goldberg, Mychajliw, & Hadly, 2016	-24.8667, -47.8833	3900, 100	3970 - 4529	shcal13
gb_sh_0374	Goldberg, Mychajliw, & Hadly, 2016	-24.8667, -47.8833	3635, 90	3681 - 4149	shcal13
gb_sh_0375	Goldberg, Mychajliw, & Hadly, 2016	-25.8833, -47.8833	4685, 105	5038 - 5593	shcal13
gb_sh_0376	Goldberg, Mychajliw, & Hadly, 2016	-25.8833, -47.8833	5070, 100	5588 - 5948	shcal13
gb_sh_0377	Goldberg, Mychajliw, & Hadly, 2016	-25.8833, -47.8833	5245, 125	5710 - 6221	shcal13
gb_sh_0378	Goldberg, Mychajliw, & Hadly, 2016	unknown, unknown	3270, 70	3329 - 3633	shcal13
gb_sh_0379	Goldberg, Mychajliw, & Hadly, 2016	-29.5275, -53.584	2190, 80	1994 - 2339	shcal13
gb_sh_0380	Goldberg, Mychajliw, & Hadly, 2016	-28.5615, -48.9827	2430, 125	2152 - 2749	shcal13
gb_sh_0381	Goldberg, Mychajliw, & Hadly, 2016	-28.5615, -48.9827	2655, 110	2360 - 2929	shcal13
gb_sh_0382	Goldberg, Mychajliw, & Hadly, 2016	-28.5615, -48.9827	3995, 85	4147 - 4643	shcal13
gb_sh_0383	Goldberg, Mychajliw, & Hadly, 2016	-28.5615, -48.9827	4185, 90	4433 - 4853	shcal13

gb_sh_0384	Goldberg, Mychajliw, & Hadly, 2016	-28.579, -48.9603	2020, 40	1836 - 2009	shcal13
gb_sh_0385	Goldberg, Mychajliw, & Hadly, 2016	-28.579, -48.9603	2060, 85	1785 - 2161	shcal13
gb_sh_0386	Goldberg, Mychajliw, & Hadly, 2016	-28.579, -48.9603	2070, 60	1864 - 2151	shcal13
gb_sh_0387	Goldberg, Mychajliw, & Hadly, 2016	-28.579, -48.9603	2075, 65	1833 - 2155	shcal13
gb_sh_0388	Goldberg, Mychajliw, & Hadly, 2016	-28.579, -48.9603	2115, 65	1888 - 2183	shcal13
gb_sh_0389	Goldberg, Mychajliw, & Hadly, 2016	-28.579, -48.9603	2165, 75	1986 - 2318	shcal13
gb_sh_0390	Goldberg, Mychajliw, & Hadly, 2016	-28.579, -48.9603	2170, 95	1913 - 2340	shcal13
gb_sh_0391	Goldberg, Mychajliw, & Hadly, 2016	-28.579, -48.9603	2170, 45	2004 - 2188	shcal13
gb_sh_0392	Goldberg, Mychajliw, & Hadly, 2016	-28.579, -48.9603	2180, 105	1891 - 2348	shcal13
gb_sh_0393	Goldberg, Mychajliw, & Hadly, 2016	-28.579, -48.9603	2210, 60	2038 - 2325	shcal13
gb_sh_0394	Goldberg, Mychajliw, & Hadly, 2016	-28.579, -48.9603	2240, 170	1831 - 2623	shcal13
gb_sh_0395	Goldberg, Mychajliw, & Hadly, 2016	-28.579, -48.9603	2270, 75	2037 - 2358	shcal13
gb_sh_0396	Goldberg, Mychajliw, & Hadly, 2016	-28.579, -48.9603	2280, 80	2011 - 2381	shcal13

gb_sh_0398	Goldberg, Mychajliw, & Hadly, 2016	-28.579, -48.9603	2295, 90	2008 - 2491	shcal13
gb_sh_0399	Goldberg, Mychajliw, & Hadly, 2016	-15.4667, -56.8	2310, 70	2084 - 2468	shcal13
gb_sh_0400	Goldberg, Mychajliw, & Hadly, 2016	-28.579, -48.9603	2320, 50	2149 - 2379	shcal13
gb_sh_0401	Goldberg, Mychajliw, & Hadly, 2016	-28.579, -48.9603	2335, 35	2295 - 2360	shcal13
gb_sh_0402	Goldberg, Mychajliw, & Hadly, 2016	-28.579, -48.9603	2340, 50	2156 - 2440	shcal13
gb_sh_0403	Goldberg, Mychajliw, & Hadly, 2016	-28.579, -48.9603	2345, 105	2083 - 2623	shcal13
gb_sh_0404	Goldberg, Mychajliw, & Hadly, 2016	-28.579, -48.9603	2365, 45	2296 - 2490	shcal13
gb_sh_0405	Goldberg, Mychajliw, & Hadly, 2016	-28.579, -48.9603	2370, 35	2303 - 2471	shcal13
gb_sh_0406	Goldberg, Mychajliw, & Hadly, 2016	-28.579, -48.9603	2470, 55	2351 - 2621	shcal13
gb_sh_0407	Goldberg, Mychajliw, & Hadly, 2016	-28.579, -48.9603	2490, 35	2358 - 2549	shcal13
gb_sh_0408	Goldberg, Mychajliw, & Hadly, 2016	-28.579, -48.9603	2500, 155	2148 - 2866	shcal13
gb_sh_0409	Goldberg, Mychajliw, & Hadly, 2016	-28.579, -48.9603	2655, 105	2362 - 2895	shcal13
gb_sh_0410	Goldberg, Mychajliw, & Hadly, 2016	-28.579, -48.9603	2795, 35	2768 - 2945	shcal13

gb_sh_0411	Goldberg, Mychajliw, & Hadly, 2016	-28.579, -48.9603	2855, 105	2747 - 3211	shcal13
gb_sh_0412	Goldberg, Mychajliw, & Hadly, 2016	-28.579, -48.9603	2880, 75	2779 - 3163	shcal13
gb_sh_0413	Goldberg, Mychajliw, & Hadly, 2016	-28.579, -48.9603	2890, 55	2842 - 3083	shcal13
gb_sh_0414	Goldberg, Mychajliw, & Hadly, 2016	-28.6033, -49.0215	3080, 80	2990 - 3404	shcal13
gb_sh_0415	Goldberg, Mychajliw, & Hadly, 2016	-24.6333, -47.7022	5240, 150	5649 - 6285	shcal13
gb_sh_0416	Goldberg, Mychajliw, & Hadly, 2016	-23.3284, -52.7633	5241, 306	5288 - 6673	shcal13
gb_sh_0417	Goldberg, Mychajliw, & Hadly, 2016	-23.3284, -52.7633	6683, 355	6731 - 8184	shcal13
gb_sh_0418	Goldberg, Mychajliw, & Hadly, 2016	-25.0846, -48.0197	4130, 100	4382 - 4849	shcal13
gb_sh_0419	Goldberg, Mychajliw, & Hadly, 2016	-25.0846, -48.0197	4350, 110	4570 - 5093	shcal13
gb_sh_0420	Goldberg, Mychajliw, & Hadly, 2016	-25.0846, -48.0197	4380, 100	4796 - 5295	shcal13
gb_sh_0421	Goldberg, Mychajliw, & Hadly, 2016	-25.0846, -48.0197	4970, 110	5463 - 5915	shcal13
gb_sh_0422	Goldberg, Mychajliw, & Hadly, 2016	-25.0846, -48.0197	5010, 115	5468 - 5943	shcal13
gb_sh_0424	Goldberg, Mychajliw, & Hadly, 2016	-9.597, -37.8661	2500, 10	2376 - 2545	shcal13

gb_sh_0425	Goldberg, Mychajliw, & Hadly, 2016	-9.597, -37.8661	3270, 135	3138 - 3734	shcal13
gb_sh_0426	Goldberg, Mychajliw, & Hadly, 2016	-9.597, -37.8661	4340, 10	4830 - 4879	shcal13
gb_sh_0427	Goldberg, Mychajliw, & Hadly, 2016	-9.597, -37.8661	8950, 70	9762 - 10221	shcal13
gb_sh_0428	Goldberg, Mychajliw, & Hadly, 2016	-3.27962, -45.1403	2520, 10	2457 - 2718	shcal13
gb_sh_0429	Goldberg, Mychajliw, & Hadly, 2016	-28.5367, -48.7904	4320, 50	4797 - 4976	shcal13
gb_sh_0430	Goldberg, Mychajliw, & Hadly, 2016	-28.5314, -48.7885	4070, 50	4403 - 4652	shcal13
gb_sh_0431	Goldberg, Mychajliw, & Hadly, 2016	-28.5303, -48.7871	4130, 50	4491 - 4728	shcal13
gb_sh_0432	Goldberg, Mychajliw, & Hadly, 2016	-28.5347, -48.7879	2040, 50	1834 - 2063	shcal13
gb_sh_0433	Goldberg, Mychajliw, & Hadly, 2016	-19.6355, -43.8773	6660, 50	7431 - 7577	shcal13
gb_sh_0434	Goldberg, Mychajliw, & Hadly, 2016	-19.6355, -43.8773	7250, 60	7936 - 8170	shcal13
gb_sh_0435	Goldberg, Mychajliw, & Hadly, 2016	-9.75, -48.3716	10300, 60	11750 - 12176	shcal13
gb_sh_0436	Goldberg, Mychajliw, & Hadly, 2016	-28.543, -49.0748	5470, 60	6091 - 6318	shcal13
gb_sh_0437	Goldberg, Mychajliw, & Hadly, 2016	-11.9074, -52.9384	7070, 40	7753 - 7955	shcal13

gb_sh_0438	Goldberg, Mychajliw, & Hadly, 2016	-11.9074, -52.9384	8040, 40	8701 - 9009	shcal13
gb_sh_0439	Goldberg, Mychajliw, & Hadly, 2016	-19.516, -44.0675	7500, 60	8169 - 8392	shcal13
gb_sh_0440	Goldberg, Mychajliw, & Hadly, 2016	-27.1833, -53.75	7560, 160	8152 - 8544	shcal13
gb_sh_0441	Goldberg, Mychajliw, & Hadly, 2016	-19, -43	8190, 40	9002 - 9150	shcal13
gb_sh_0442	Goldberg, Mychajliw, & Hadly, 2016	-19.516, -44.0675	8240, 50	9010 - 9305	shcal13
gb_sh_0443	Goldberg, Mychajliw, & Hadly, 2016	-19.516, -44.0675	8280, 50	9030 - 9326	shcal13
gb_sh_0444	Goldberg, Mychajliw, & Hadly, 2016	-19.516, -44.0675	8300, 50	9084 - 9423	shcal13
gb_sh_0445	Goldberg, Mychajliw, & Hadly, 2016	-19, -43	8360, 50	9194 - 9465	shcal13
gb_sh_0446	Goldberg, Mychajliw, & Hadly, 2016	-19.516, -44.0675	8420, 100	9119 - 9539	shcal13
gb_sh_0447	Goldberg, Mychajliw, & Hadly, 2016	-19.516, -44.0675	8510, 60	9397 - 9547	shcal13
gb_sh_0448	Goldberg, Mychajliw, & Hadly, 2016	-19, -43	8730, 110	9492 - 9956	shcal13
gb_sh_0449	Goldberg, Mychajliw, & Hadly, 2016	-19.516, -44.0675	8750, 150	9479 - 10181	shcal13
gb_sh_0450	Goldberg, Mychajliw, & Hadly, 2016	-19.516, -44.0675	8810, 60	9552 - 9949	shcal13

gb_sh_0451	Goldberg, Mychajliw, & Hadly, 2016	-19, -43	8820, 150	9530 - 10203	shcal13
gb_sh_0452	Goldberg, Mychajliw, & Hadly, 2016	-19.516, -44.0675	8980, 60	9886 - 10232	shcal13
gb_sh_0453	Goldberg, Mychajliw, & Hadly, 2016	-19.516, -44.0675	9210, 130	10119 - 10699	shcal13
gb_sh_0454	Goldberg, Mychajliw, & Hadly, 2016	-19.516, -44.0675	9420, 60	10404 - 10764	shcal13
gb_sh_0455	Goldberg, Mychajliw, & Hadly, 2016	-19.516, -44.0675	9600, 60	10692 - 11145	shcal13
gb_sh_0456	Goldberg, Mychajliw, & Hadly, 2016	-19.516, -44.0675	9640, 50	10749 - 11161	shcal13
gb_sh_0457	Goldberg, Mychajliw, & Hadly, 2016	-19.516, -44.0675	9650, 60	10745 - 11175	shcal13
gb_sh_0458	Goldberg, Mychajliw, & Hadly, 2016	-19.516, -44.0675	10150, 130	11240 - 12102	shcal13
gb_sh_0459	Goldberg, Mychajliw, & Hadly, 2016	-19.516, -44.0675	12240, 50	13907 - 14276	shcal13
gb_sh_0460	Goldberg, Mychajliw, & Hadly, 2016	-19.6525, -44.011	7870, 40	8511 - 8769	shcal13
gb_sh_0461	Goldberg, Mychajliw, & Hadly, 2016	-19.6525, -44.011	8520, 40	9436 - 9537	shcal13
gb_sh_0462	Goldberg, Mychajliw, & Hadly, 2016	-19.55, -43.9928	8830, 50	9594 - 9955	shcal13
gb_sh_0463	Goldberg, Mychajliw, & Hadly, 2016	-19.8167, -43.95	9350, 80	10262 - 10698	shcal13

gb_sh_0464	Goldberg, Mychajliw, & Hadly, 2016	-15.1166, -44.2166	9870, 260	10496 - 12113	shcal13
gb_sh_0465	Goldberg, Mychajliw, & Hadly, 2016	-15.1166, -44.2166	10000, 232	10746 - 12174	shcal13
gb_sh_0466	Goldberg, Mychajliw, & Hadly, 2016	-15.1166, -44.2166	10200, 250	11171 - 12570	shcal13
gb_sh_0467	Goldberg, Mychajliw, & Hadly, 2016	-15.1166, -44.2166	10250, 345	11063 - 12725	shcal13
gb_sh_0468	Goldberg, Mychajliw, & Hadly, 2016	-15.1166, -44.2166	10910, 140	12556 - 13063	shcal13
gb_sh_0469	Goldberg, Mychajliw, & Hadly, 2016	-15.1166, -44.2166	11000, 232	12400 - 13338	shcal13
gb_sh_0470	Goldberg, Mychajliw, & Hadly, 2016	-15.1166, -44.2166	11250, 150	12737 - 13325	shcal13
gb_sh_0471	Goldberg, Mychajliw, & Hadly, 2016	-15.1166, -44.2166	11440, 240	12780 - 13714	shcal13
gb_sh_0472	Goldberg, Mychajliw, & Hadly, 2016	-15.1166, -44.2166	12000, 300	13202 - 14934	shcal13
gb_sh_0473	Goldberg, Mychajliw, & Hadly, 2016	-15.1166, -44.2166	12070, 170	13460 - 14474	shcal13
gb_sh_0474	Goldberg, Mychajliw, & Hadly, 2016	-19.5916, -43.9419	9780, 70	11062 - 11269	shcal13
gb_sh_0475	Goldberg, Mychajliw, & Hadly, 2016	-18.2853, -43.8539	10380, 60	11947 - 12422	shcal13
gb_sh_0476	Goldberg, Mychajliw, & Hadly, 2016	-18.2853, -43.8539	10560, 40	12405 - 12569	shcal13

gb_sh_0477	Goldberg, Mychajliw, & Hadly, 2016	-20.2011, -55.267	2200, 50	2040 - 2311	shcal13
gb_sh_0478	Goldberg, Mychajliw, & Hadly, 2016	-14.45, -44.44	10000, 255	10734 - 12319	shcal13
gb_sh_0479	Goldberg, Mychajliw, & Hadly, 2016	-14.45, -44.44	11000, 300	12059 - 13430	shcal13
gb_sh_0480	Goldberg, Mychajliw, & Hadly, 2016	-16.2617, -46.0486	8595, 215	9080 - 10175	shcal13
gb_sh_0481	Goldberg, Mychajliw, & Hadly, 2016	-16.2617, -46.0486	9580, 200	10252 - 11291	shcal13
gb_sh_0482	Goldberg, Mychajliw, & Hadly, 2016	-18.303, -43.7419	10210, 60	11600 - 12046	shcal13
gb_sh_0483	Goldberg, Mychajliw, & Hadly, 2016	-19.4772, -44.0392	3810, 50	3972 - 4298	shcal13
gb_sh_0484	Goldberg, Mychajliw, & Hadly, 2016	-15.4667, -56.8	3830, 90	4066 - 4298	shcal13
gb_sh_0485	Goldberg, Mychajliw, & Hadly, 2016	-19.4772, -44.0392	3930, 40	4220 - 4423	shcal13
gb_sh_0486	Goldberg, Mychajliw, & Hadly, 2016	-19.4772, -44.0392	3950, 40	4227 - 4440	shcal13
gb_sh_0487	Goldberg, Mychajliw, & Hadly, 2016	-19.4772, -44.0392	3960, 40	4230 - 4445	shcal13
gb_sh_0488	Goldberg, Mychajliw, & Hadly, 2016	-19.4772, -44.0392	4010, 130	4086 - 4828	shcal13
gb_sh_0489	Goldberg, Mychajliw, & Hadly, 2016	-19.4772, -44.0392	4070, 60	4380 - 4660	shcal13

gb_sh_0490	Goldberg, Mychajliw, & Hadly, 2016	-19.4772, -44.0392	4140, 40	4513 - 4729	shcal13
gb_sh_0491	Goldberg, Mychajliw, & Hadly, 2016	-19.4772, -44.0392	4290, 90	4520 - 5046	shcal13
gb_sh_0492	Goldberg, Mychajliw, & Hadly, 2016	-19.4772, -44.0392	4470, 40	4868 - 5080	shcal13
gb_sh_0493	Goldberg, Mychajliw, & Hadly, 2016	-19.4772, -44.0392	5990, 40	6670 - 6889	shcal13
gb_sh_0494	Goldberg, Mychajliw, & Hadly, 2016	-19.4772, -44.0392	7400, 40	8037 - 8224	shcal13
gb_sh_0495	Goldberg, Mychajliw, & Hadly, 2016	-19.4772, -44.0392	7700, 40	8387 - 8542	shcal13
gb_sh_0496	Goldberg, Mychajliw, & Hadly, 2016	-19.4772, -44.0392	7890, 40	8538 - 8780	shcal13
gb_sh_0497	Goldberg, Mychajliw, & Hadly, 2016	-15.4667, -56.8	7940, 70	8591 - 8814	shcal13
gb_sh_0498	Goldberg, Mychajliw, & Hadly, 2016	-19.4772, -44.0392	8170, 50	8979 - 9276	shcal13
gb_sh_0500	Goldberg, Mychajliw, & Hadly, 2016	-19.4772, -44.0392	8230, 40	9019 - 9275	shcal13
gb_sh_0501	Goldberg, Mychajliw, & Hadly, 2016	-19.4772, -44.0392	8530, 40	9443 - 9539	shcal13
gb_sh_0502	Goldberg, Mychajliw, & Hadly, 2016	-19.4772, -44.0392	8540, 50	9432 - 9547	shcal13
gb_sh_0503	Goldberg, Mychajliw, & Hadly, 2016	-19.4772, -44.0392	8580, 50	9442 - 9564	shcal13

gb_sh_0504	Goldberg, Mychajliw, & Hadly, 2016	-19.4772, -44.0392	8600, 160	9192 - 9954	shcal13
gb_sh_0505	Goldberg, Mychajliw, & Hadly, 2016	-19.4772, -44.0392	8600, 50	9465 - 9631	shcal13
gb_sh_0506	Goldberg, Mychajliw, & Hadly, 2016	-19.4772, -44.0392	8620, 40	9481 - 9631	shcal13
gb_sh_0507	Goldberg, Mychajliw, & Hadly, 2016	-19.4772, -44.0392	8660, 50	9497 - 9699	shcal13
gb_sh_0508	Goldberg, Mychajliw, & Hadly, 2016	-19.4772, -44.0392	8670, 40	9528 - 9688	shcal13
gb_sh_0509	Goldberg, Mychajliw, & Hadly, 2016	-19.4772, -44.0392	8690, 40	9532 - 9701	shcal13
gb_sh_0510	Goldberg, Mychajliw, & Hadly, 2016	-19.4772, -44.0392	8700, 40	9534 - 9706	shcal13
gb_sh_0511	Goldberg, Mychajliw, & Hadly, 2016	-19.4772, -44.0392	8710, 80	9493 - 9914	shcal13
gb_sh_0512	Goldberg, Mychajliw, & Hadly, 2016	-19.4772, -44.0392	8710, 40	9537 - 9736	shcal13
gb_sh_0513	Goldberg, Mychajliw, & Hadly, 2016	-19.4772, -44.0392	8730, 50	9538 - 9798	shcal13
gb_sh_0514	Goldberg, Mychajliw, & Hadly, 2016	-19.4772, -44.0392	8750, 40	9546 - 9799	shcal13
gb_sh_0515	Goldberg, Mychajliw, & Hadly, 2016	-19.4772, -44.0392	8790, 40	9560 - 9901	shcal13
gb_sh_0517	Goldberg, Mychajliw, & Hadly, 2016	-19.4772, -44.0392	8800, 40	9557 - 9912	shcal13

gb_sh_0518	Goldberg, Mychajliw, & Hadly, 2016	-19.4772, -44.0392	8810, 90	9548 - 9963	shcal13
gb_sh_0519	Goldberg, Mychajliw, & Hadly, 2016	-19.4772, -44.0392	8820, 40	9582 - 9934	shcal13
gb_sh_0520	Goldberg, Mychajliw, & Hadly, 2016	-19.4772, -44.0392	8840, 60	9600 - 9965	shcal13
gb_sh_0521	Goldberg, Mychajliw, & Hadly, 2016	-19.4772, -44.0392	8870, 100	9595 - 10187	shcal13
gb_sh_0522	Goldberg, Mychajliw, & Hadly, 2016	-19.4772, -44.0392	8880, 50	9701 - 10159	shcal13
gb_sh_0523	Goldberg, Mychajliw, & Hadly, 2016	-19.4772, -44.0392	8890, 40	9736 - 10161	shcal13
gb_sh_0524	Goldberg, Mychajliw, & Hadly, 2016	-19.4772, -44.0392	8900, 40	9762 - 10168	shcal13
gb_sh_0525	Goldberg, Mychajliw, & Hadly, 2016	-19.4772, -44.0392	8930, 40	9885 - 10186	shcal13
gb_sh_0526	Goldberg, Mychajliw, & Hadly, 2016	-19.4772, -44.0392	8980, 40	9913 - 10205	shcal13
gb_sh_0527	Goldberg, Mychajliw, & Hadly, 2016	-19.4772, -44.0392	9100, 40	10163 - 10287	shcal13
gb_sh_0528	Goldberg, Mychajliw, & Hadly, 2016	-19.4772, -44.0392	9150, 40	10196 - 10305	shcal13
gb_sh_0529	Goldberg, Mychajliw, & Hadly, 2016	-19.4772, -44.0392	9370, 40	10398 - 10683	shcal13
gb_sh_0530	Goldberg, Mychajliw, & Hadly, 2016	-19.4772, -44.0392	9470, 50	10508 - 10788	shcal13

gb_sh_0531	Goldberg, Mychajliw, & Hadly, 2016	-19.4772, -44.0392	9520, 60	10567 - 10883	shcal13
gb_sh_0532	Goldberg, Mychajliw, & Hadly, 2016	-19.4772, -44.0392	9650, 50	10758 - 11168	shcal13
gb_sh_0533	Goldberg, Mychajliw, & Hadly, 2016	-19.4772, -44.0392	9680, 50	10775 - 11039	shcal13
gb_sh_0534	Goldberg, Mychajliw, & Hadly, 2016	-19.4772, -44.0392	9720, 40	11066 - 11212	shcal13
gb_sh_0535	Goldberg, Mychajliw, & Hadly, 2016	-19.4772, -44.0392	9900, 40	11198 - 11356	shcal13
gb_sh_0536	Goldberg, Mychajliw, & Hadly, 2016	-19.4772, -44.0392	10070, 100	11243 - 11841	shcal13
gb_sh_0537	Goldberg, Mychajliw, & Hadly, 2016	-19.4772, -44.0392	10130, 60	11387 - 11850	shcal13
gb_sh_0538	Goldberg, Mychajliw, & Hadly, 2016	-19.4772, -44.0392	10490, 50	12057 - 12240	shcal13
gb_sh_0539	Goldberg, Mychajliw, & Hadly, 2016	-19.5415, -43.9414	4300, 300	4072 - 5587	shcal13
gb_sh_0540	Goldberg, Mychajliw, & Hadly, 2016	-19.5415, -43.9414	7650, 50	8340 - 8539	shcal13
gb_sh_0541	Goldberg, Mychajliw, & Hadly, 2016	-19.5415, -43.9414	7680, 40	8377 - 8524	shcal13
gb_sh_0542	Goldberg, Mychajliw, & Hadly, 2016	-22.05, -42.675	8310, 40	9118 - 9426	shcal13
gb_sh_0543	Goldberg, Mychajliw, & Hadly, 2016	-19.5415, -43.9414	8960, 50	9886 - 10220	shcal13

gb_sh_0544	Goldberg, Mychajliw, & Hadly, 2016	-15.1358, -44.2442	8640, 90	9439 - 9832	shcal13
gb_sh_0545	Goldberg, Mychajliw, & Hadly, 2016	-15.1358, -44.2442	8890, 90	9623 - 10197	shcal13
gb_sh_0546	Goldberg, Mychajliw, & Hadly, 2016	-15.1358, -44.2442	9140, 90	10120 - 10517	shcal13
gb_sh_0547	Goldberg, Mychajliw, & Hadly, 2016	-15.1358, -44.2442	9390, 160	10228 - 11100	shcal13
gb_sh_0548	Goldberg, Mychajliw, & Hadly, 2016	-15.1358, -44.2442	9500, 130	10388 - 11175	shcal13
gb_sh_0549	Goldberg, Mychajliw, & Hadly, 2016	-15.1358, -44.2442	10450, 70	12008 - 12442	shcal13
gb_sh_0550	Goldberg, Mychajliw, & Hadly, 2016	-19.6064, -43.7344	8080, 40	8721 - 9031	shcal13
gb_sh_0554	Goldberg, Mychajliw, & Hadly, 2016	-19.6064, -43.7344	8730, 40	9539 - 9782	shcal13
gb_sh_0555	Goldberg, Mychajliw, & Hadly, 2016	-19.6064, -43.7344	8910, 40	9772 - 10174	shcal13
gb_sh_0556	Goldberg, Mychajliw, & Hadly, 2016	-19.6064, -43.7344	9040, 40	10123 - 10243	shcal13
gb_sh_0557	Goldberg, Mychajliw, & Hadly, 2016	-19.6064, -43.7344	9540, 90	10553 - 11143	shcal13
gb_sh_0558	Goldberg, Mychajliw, & Hadly, 2016	-19.6064, -43.7344	9550, 60	10644 - 10910	shcal13
gb_sh_0559	Goldberg, Mychajliw, & Hadly, 2016	-19.6064, -43.7344	9620, 40	10736 - 11110	shcal13

gb_sh_0560	Goldberg, Mychajliw, & Hadly, 2016	-19.6388, -43.976	7190, 50	7845 - 8054	shcal13
gb_sh_0561	Goldberg, Mychajliw, & Hadly, 2016	-19.6388, -43.976	8290, 40	9081 - 9332	shcal13
gb_sh_0562	Goldberg, Mychajliw, & Hadly, 2016	-19.6388, -43.976	8350, 40	9194 - 9444	shcal13
gb_sh_0563	Goldberg, Mychajliw, & Hadly, 2016	-19.6388, -43.976	8810, 50	9554 - 9938	shcal13
gb_sh_0564	Goldberg, Mychajliw, & Hadly, 2016	-19.6388, -43.976	9760, 70	11061 - 11250	shcal13
gb_sh_0565	Goldberg, Mychajliw, & Hadly, 2016	-19.6388, -43.976	11990, 50	13591 - 13978	shcal13
gb_sh_0566	Goldberg, Mychajliw, & Hadly, 2016	-19.6064, -43.8966	3070, 110	2921 - 3455	shcal13
gb_sh_0567	Goldberg, Mychajliw, & Hadly, 2016	-19.6064, -43.8966	3260, 110	3158 - 3713	shcal13
gb_sh_0569	Goldberg, Mychajliw, & Hadly, 2016	-19.6064, -43.8966	3430, 130	3354 - 3982	shcal13
gb_sh_0570	Goldberg, Mychajliw, & Hadly, 2016	-19.6064, -43.8966	3580, 130	3478 - 4157	shcal13
gb_sh_0571	Goldberg, Mychajliw, & Hadly, 2016	-19.6064, -43.8966	3660, 110	3631 - 4246	shcal13
gb_sh_0572	Goldberg, Mychajliw, & Hadly, 2016	-19.6064, -43.8966	3720, 120	3700 - 4317	shcal13
gb_sh_0574	Goldberg, Mychajliw, & Hadly, 2016	-19.6064, -43.8966	3750, 110	3823 - 4412	shcal13

gb_sh_0575	Goldberg, Mychajliw, & Hadly, 2016	-19.6064, -43.8966	4170, 120	4292 - 4892	shcal13
gb_sh_0576	Goldberg, Mychajliw, & Hadly, 2016	-19.6064, -43.8966	4350, 120	4568 - 5289	shcal13
gb_sh_0577	Goldberg, Mychajliw, & Hadly, 2016	-19.6064, -43.8966	4400, 120	4783 - 5313	shcal13
gb_sh_0578	Goldberg, Mychajliw, & Hadly, 2016	-19.6064, -43.8966	4550, 130	4844 - 5474	shcal13
gb_sh_0579	Goldberg, Mychajliw, & Hadly, 2016	-19.6064, -43.8966	5120, 130	5587 - 6127	shcal13
gb_sh_0580	Goldberg, Mychajliw, & Hadly, 2016	-19.6064, -43.8966	6830, 150	7424 - 7936	shcal13
gb_sh_0581	Goldberg, Mychajliw, & Hadly, 2016	-19.6064, -43.8966	6950, 140	7554 - 8000	shcal13
gb_sh_0582	Goldberg, Mychajliw, & Hadly, 2016	-19.6064, -43.8966	8490, 160	9012 - 9797	shcal13
gb_sh_0583	Goldberg, Mychajliw, & Hadly, 2016	-19.6064, -43.8966	9330, 60	10267 - 10604	shcal13
gb_sh_0585	Goldberg, Mychajliw, & Hadly, 2016	-19.6064, -43.8966	10200, 220	11206 - 12447	shcal13
gb_sh_0586	Goldberg, Mychajliw, & Hadly, 2016	-19.6064, -43.8966	12960, 300	14243 - 16244	shcal13
gb_sh_0587	Goldberg, Mychajliw, & Hadly, 2016	-25.0814, -48.5684	6980, 90	7614 - 7942	shcal13
gb_sh_0588	Goldberg, Mychajliw, & Hadly, 2016	-9.38854, -40.4572	6390, 80	7154 - 7430	shcal13

gb_sh_0590	Goldberg, Mychajliw, & Hadly, 2016	-22.8829, -42.0001	3050, 80	2958 - 3382	shcal13
gb_sh_0591	Goldberg, Mychajliw, & Hadly, 2016	-22.8829, -42.0001	3725, 75	3827 - 4248	shcal13
gb_sh_0592	Goldberg, Mychajliw, & Hadly, 2016	-22.8829, -42.0001	4020, 80	4222 - 4649	shcal13
gb_sh_0593	Goldberg, Mychajliw, & Hadly, 2016	-22.8829, -42.0001	5140, 180	5575 - 6280	shcal13
gb_sh_0594	Goldberg, Mychajliw, & Hadly, 2016	-23.9525, -46.1847	4400, 130	4574 - 5317	shcal13
gb_sh_0595	Goldberg, Mychajliw, & Hadly, 2016	-23.9027, -46.2048	3865, 95	3963 - 4445	shcal13
gb_sh_0596	Goldberg, Mychajliw, & Hadly, 2016	-23.9027, -46.2048	3925, 145	3897 - 4655	shcal13
gb_sh_0597	Goldberg, Mychajliw, & Hadly, 2016	-9.80306, -48.3936	9940, 60	11202 - 11499	shcal13
gb_sh_0598	Goldberg, Mychajliw, & Hadly, 2016	unknown, unknown	4400, 280	4223 - 5612	shcal13
gb_sh_0599	Goldberg, Mychajliw, & Hadly, 2016	-28.5208, -48.9687	2245, 60	2077 - 2345	shcal13
gb_sh_0600	Goldberg, Mychajliw, & Hadly, 2016	-28.5208, -48.9687	2535, 165	2153 - 2929	shcal13
gb_sh_0601	Goldberg, Mychajliw, & Hadly, 2016	-28.5182, -48.9707	4685, 160	4872 - 5650	shcal13
gb_sh_0602	Goldberg, Mychajliw, & Hadly, 2016	-22.8299, -42.9226	5180, 80	5660 - 6024	shcal13

gb_sh_0603	Goldberg, Mychajliw, & Hadly, 2016	-21.657, -52.553	8215, 120	8760 - 9462	shcal13
gb_sh_0604	Goldberg, Mychajliw, & Hadly, 2016	-21.657, -52.553	8620, 110	9371 - 9909	shcal13
gb_sh_0605	Goldberg, Mychajliw, & Hadly, 2016	-21.657, -52.553	10190, 190	11228 - 12427	shcal13
gb_sh_0606	Goldberg, Mychajliw, & Hadly, 2016	-15.8, -44.1	8845, 90	9583 - 10162	shcal13
gb_sh_0608	Goldberg, Mychajliw, & Hadly, 2016	-15.7097, -44.0175	9135, 105	10111 - 10524	shcal13
gb_sh_0609	Goldberg, Mychajliw, & Hadly, 2016	-9.6375, -48.4138	9397, 80	10268 - 10772	shcal13
gb_sh_0610	Goldberg, Mychajliw, & Hadly, 2016	-9.6375, -48.4138	9456, 95	10376 - 10892	shcal13
gb_sh_0611	Goldberg, Mychajliw, & Hadly, 2016	-9.6375, -48.4138	9670, 60	10760 - 11186	shcal13
gb_sh_0612	Goldberg, Mychajliw, & Hadly, 2016	-9.6375, -48.4138	9790, 70	11064 - 11291	shcal13
gb_sh_0613	Goldberg, Mychajliw, & Hadly, 2016	-9.6375, -48.4138	9890, 80	11104 - 11510	shcal13
gb_sh_0614	Goldberg, Mychajliw, & Hadly, 2016	-9.6375, -48.4138	9990, 60	11229 - 11629	shcal13
gb_sh_0615	Goldberg, Mychajliw, & Hadly, 2016	-9.6375, -48.4138	10530, 90	12057 - 12650	shcal13
gb_sh_0616	Goldberg, Mychajliw, & Hadly, 2016	-6.7, -36.6	9640, 100	10660 - 11207	shcal13

gb_sh_0617	Goldberg, Mychajliw, & Hadly, 2016	-24.6847, -47.6181	4790, 115	5267 - 5735	shcal13
gb_sh_0618	Goldberg, Mychajliw, & Hadly, 2016	-28.5094, -49.0209	3240, 70	3233 - 3582	shcal13
gb_sh_0619	Goldberg, Mychajliw, & Hadly, 2016	-28.5094, -49.0209	3360, 70	3381 - 3717	shcal13
gb_sh_0620	Goldberg, Mychajliw, & Hadly, 2016	-24.5629, -47.7403	4511, 32	4971 - 5292	shcal13
gb_sh_0621	Goldberg, Mychajliw, & Hadly, 2016	-24.5629, -47.7403	4985, 35	5594 - 5747	shcal13
gb_sh_0622	Goldberg, Mychajliw, & Hadly, 2016	-24.5629, -47.7403	5420, 30	6171 - 6282	shcal13
gb_sh_0623	Goldberg, Mychajliw, & Hadly, 2016	-24.5629, -47.7403	5895, 45	6529 - 6786	shcal13
gb_sh_0624	Goldberg, Mychajliw, & Hadly, 2016	-28.5026, -48.9753	3230, 70	3226 - 3575	shcal13
gb_sh_0625	Goldberg, Mychajliw, & Hadly, 2016	-28.5026, -48.9753	4480, 60	4869 - 5145	shcal13
gb_sh_0627	Goldberg, Mychajliw, & Hadly, 2016	-22.7853, -42.3636	2020, 70	1777 - 2096	shcal13
gb_sh_0628	Goldberg, Mychajliw, & Hadly, 2016	-22.7853, -42.3636	2600, 160	2303 - 3007	shcal13
gb_sh_0629	Goldberg, Mychajliw, & Hadly, 2016	-28.5362, -48.9624	2075, 110	1781 - 2213	shcal13
gb_sh_0630	Goldberg, Mychajliw, & Hadly, 2016	-19.583, -52.66	10090, 70	11269 - 11830	shcal13

gb_sh_0631	Goldberg, Mychajliw, & Hadly, 2016	-19.583, -52.66	10340, 110	11692 - 12437	shcal13
gb_sh_0632	Goldberg, Mychajliw, & Hadly, 2016	-19.583, -52.66	10480, 80	12011 - 12559	shcal13
gb_sh_0633	Goldberg, Mychajliw, & Hadly, 2016	-15.4667, -56.8	2970, 50	2871 - 3253	shcal13
gb_sh_0634	Goldberg, Mychajliw, & Hadly, 2016	-15.3785, -54.7266	3470, 75	3542 - 3876	shcal13
gb_sh_0635	Goldberg, Mychajliw, & Hadly, 2016	-16.9507, -55.6165	2110, 65	1884 - 2181	shcal13
gb_sh_0636	Goldberg, Mychajliw, & Hadly, 2016	-15.9216, -54.378	8160, 60	8951 - 9278	shcal13
gb_sh_0637	Goldberg, Mychajliw, & Hadly, 2016	-15.9216, -54.378	8180, 80	8850 - 9314	shcal13
gb_sh_0638	Goldberg, Mychajliw, & Hadly, 2016	-15.9216, -54.378	8210, 80	8975 - 9420	shcal13
gb_sh_0639	Goldberg, Mychajliw, & Hadly, 2016	-15.9216, -54.378	8270, 80	9014 - 9422	shcal13
gb_sh_0640	Goldberg, Mychajliw, & Hadly, 2016	-15.9216, -54.378	8390, 80	9127 - 9521	shcal13
gb_sh_0641	Goldberg, Mychajliw, & Hadly, 2016	-15.9216, -54.378	10080, 80	11256 - 11832	shcal13
gb_sh_0642	Goldberg, Mychajliw, & Hadly, 2016	-16.9507, -55.7154	2570, 70	2377 - 2754	shcal13
gb_sh_0643	Goldberg, Mychajliw, & Hadly, 2016	-16.793, -56.7041	2560, 80	2364 - 2751	shcal13

gb_sh_0644	Goldberg, Mychajliw, & Hadly, 2016	-16.9507, -55.8582	5750, 80	6314 - 6669	shcal13
gb_sh_0645	Goldberg, Mychajliw, & Hadly, 2016	-16.9507, -55.858	2390, 60	2299 - 2542	shcal13
gb_sh_0646	Goldberg, Mychajliw, & Hadly, 2016	-24.1336, -46.9503	4575, 110	4866 - 5470	shcal13
gb_sh_0647	Goldberg, Mychajliw, & Hadly, 2016	-5.966, -50.5333	8050, 70	8628 - 9032	shcal13
gb_sh_0648	Goldberg, Mychajliw, & Hadly, 2016	-5.966, -50.5333	8110, 60	8702 - 9137	shcal13
gb_sh_0649	Goldberg, Mychajliw, & Hadly, 2016	-5.95, -50.6	8240, 90	8979 - 9457	shcal13
gb_sh_0650	Goldberg, Mychajliw, & Hadly, 2016	-5.95, -50.616	8310, 60	9078 - 9434	shcal13
gb_sh_0651	Goldberg, Mychajliw, & Hadly, 2016	-14.4631, -48.4435	10605, 125	12250 - 12709	shcal13
gb_sh_0652	Goldberg, Mychajliw, & Hadly, 2016	-25, -47.9181	2840, 225	2357 - 3413	shcal13
gb_sh_0653	Goldberg, Mychajliw, & Hadly, 2016	-25, -47.9181	4380, 160	4513 - 5325	shcal13
gb_sh_0654	Goldberg, Mychajliw, & Hadly, 2016	-5.933, -50.666	8680, 40	9531 - 9693	shcal13
gb_sh_0655	Goldberg, Mychajliw, & Hadly, 2016	-5.933, -50.666	8850, 40	9672 - 9961	shcal13
gb_sh_0656	Goldberg, Mychajliw, & Hadly, 2016	-8.902, -38.708	3840, 180	3696 - 4647	shcal13

gb_sh_0657	Goldberg, Mychajliw, & Hadly, 2016	-24.6183, -47.7181	5035, 140	5450 - 6016	shcal13
gb_sh_0658	Goldberg, Mychajliw, & Hadly, 2016	-27.7743, -48.516	3735, 100	3819 - 4300	shcal13
gb_sh_0660	Goldberg, Mychajliw, & Hadly, 2016	-27.7743, -48.516	3850, 105	3897 - 4444	shcal13
gb_sh_0662	Goldberg, Mychajliw, & Hadly, 2016	-27.7743, -48.516	4460, 110	4816 - 5325	shcal13
gb_sh_0663	Goldberg, Mychajliw, & Hadly, 2016	-27.7743, -48.516	4515, 100	4848 - 5325	shcal13
gb_sh_0664	Goldberg, Mychajliw, & Hadly, 2016	-24.7947, -48.1113	3530, 70	3577 - 3928	shcal13
gb_sh_0665	Goldberg, Mychajliw, & Hadly, 2016	-8.61206, -37.1671	2780, 190	2359 - 3265	shcal13
gb_sh_0666	Goldberg, Mychajliw, & Hadly, 2016	-8.61206, -37.1671	3870, 200	3717 - 4729	shcal13
gb_sh_0667	Goldberg, Mychajliw, & Hadly, 2016	-8.61206, -37.1671	4390, 200	4421 - 5472	shcal13
gb_sh_0668	Goldberg, Mychajliw, & Hadly, 2016	-8.61206, -37.1671	6240, 110	6792 - 7326	shcal13
gb_sh_0669	Goldberg, Mychajliw, & Hadly, 2016	-8.61206, -37.1671	6640, 95	7318 - 7625	shcal13
gb_sh_0670	Goldberg, Mychajliw, & Hadly, 2016	-8.0387, -34.9973	2130, 400	1259 - 3007	shcal13
gb_sh_0671	Goldberg, Mychajliw, & Hadly, 2016	-7.79157, -35.5579	2266, 110	1929 - 2493	shcal13

gb_sh_0672	Goldberg, Mychajliw, & Hadly, 2016	-7.79157, -35.5579	2802, 110	2701 - 3212	shcal13
gb_sh_0673	Goldberg, Mychajliw, & Hadly, 2016	-17.198, -47.6189	2620, 60	2455 - 2797	shcal13
gb_sh_0674	Goldberg, Mychajliw, & Hadly, 2016	-17.198, -47.6189	2860, 25	2843 - 3007	shcal13
gb_sh_0675	Goldberg, Mychajliw, & Hadly, 2016	-17.198, -47.6189	2890, 25	2869 - 3062	shcal13
gb_sh_0676	Goldberg, Mychajliw, & Hadly, 2016	-17.198, -47.6189	4160, 70	4506 - 4833	shcal13
gb_sh_0677	Goldberg, Mychajliw, & Hadly, 2016	-17.198, -47.6189	4710, 25	5314 - 5471	shcal13
gb_sh_0678	Goldberg, Mychajliw, & Hadly, 2016	-17.198, -47.6189	5790, 60	6403 - 6677	shcal13
gb_sh_0679	Goldberg, Mychajliw, & Hadly, 2016	-17.198, -47.6189	8280, 30	9081 - 9316	shcal13
gb_sh_0681	Goldberg, Mychajliw, & Hadly, 2016	-17.198, -47.6189	9400, 35	10490 - 10697	shcal13
gb_sh_0682	Goldberg, Mychajliw, & Hadly, 2016	-17.198, -47.6189	9400, 90	10257 - 10789	shcal13
gb_sh_0683	Goldberg, Mychajliw, & Hadly, 2016	-29.6522, -54.1121	2795, 55	2752 - 2980	shcal13
gb_sh_0684	Goldberg, Mychajliw, & Hadly, 2016	-9.72283, -38.4354	2245, 110	1913 - 2488	shcal13
gb_sh_0685	Goldberg, Mychajliw, & Hadly, 2016	-9.72283, -38.4354	2709, 110	2432 - 3062	shcal13

gb_sh_0686	Goldberg, Mychajliw, & Hadly, 2016	-9.72283, -38.4354	2915, 130	2756 - 3275	shcal13
gb_sh_0687	Goldberg, Mychajliw, & Hadly, 2016	-2.045, -54.1445	10000, 60	11236 - 11643	shcal13
gb_sh_0688	Goldberg, Mychajliw, & Hadly, 2016	-2.045, -54.1445	10110, 60	11318 - 11835	shcal13
gb_sh_0689	Goldberg, Mychajliw, & Hadly, 2016	-18.3111, -52.0369	10120, 80	11323 - 11849	shcal13
gb_sh_0690	Goldberg, Mychajliw, & Hadly, 2016	-2.045, -54.1445	10190, 50	11600 - 12022	shcal13
gb_sh_0693	Goldberg, Mychajliw, & Hadly, 2016	-2.045, -54.1445	10230, 60	11604 - 12064	shcal13
gb_sh_0694	Goldberg, Mychajliw, & Hadly, 2016	-2.045, -54.1445	10250, 70	11601 - 12118	shcal13
gb_sh_0695	Goldberg, Mychajliw, & Hadly, 2016	-2.045, -54.1445	10260, 60	11687 - 12093	shcal13
gb_sh_0696	Goldberg, Mychajliw, & Hadly, 2016	-2.045, -54.1445	10261, 62	11618 - 12105	shcal13
gb_sh_0697	Goldberg, Mychajliw, & Hadly, 2016	-2.045, -54.1445	10275, 275	11202 - 12678	shcal13
gb_sh_0698	Goldberg, Mychajliw, & Hadly, 2016	-2.045, -54.1445	10280, 70	11692 - 12172	shcal13
gb_sh_0699	Goldberg, Mychajliw, & Hadly, 2016	-2.045, -54.1445	10290, 80	11698 - 12315	shcal13
gb_sh_0700	Goldberg, Mychajliw, & Hadly, 2016	-2.045, -54.1445	10290, 70	11703 - 12180	shcal13

gb_sh_0702	Goldberg, Mychajliw, & Hadly, 2016	-2.045, -54.1445	10305, 275	11228 - 12683	shcal13
gb_sh_0703	Goldberg, Mychajliw, & Hadly, 2016	-2.045, -54.1445	10310, 70	11756 - 12312	shcal13
gb_sh_0704	Goldberg, Mychajliw, & Hadly, 2016	-2.045, -54.1445	10320, 70	11767 - 12311	shcal13
gb_sh_0705	Goldberg, Mychajliw, & Hadly, 2016	-2.045, -54.1445	10330, 60	11814 - 12310	shcal13
gb_sh_0706	Goldberg, Mychajliw, & Hadly, 2016	-2.045, -54.1445	10330, 70	11802 - 12407	shcal13
gb_sh_0707	Goldberg, Mychajliw, & Hadly, 2016	-2.045, -54.1445	10350, 70	11912 - 12412	shcal13
gb_sh_0708	Goldberg, Mychajliw, & Hadly, 2016	-2.045, -54.1445	10360, 50	11944 - 12406	shcal13
gb_sh_0709	Goldberg, Mychajliw, & Hadly, 2016	-2.045, -54.1445	10360, 60	11934 - 12414	shcal13
gb_sh_0710	Goldberg, Mychajliw, & Hadly, 2016	-2.045, -54.1445	10370, 60	11943 - 12418	shcal13
gb_sh_0711	Goldberg, Mychajliw, & Hadly, 2016	-2.045, -54.1445	10390, 70	11938 - 12430	shcal13
gb_sh_0713	Goldberg, Mychajliw, & Hadly, 2016	-2.045, -54.1445	10390, 60	11964 - 12423	shcal13
gb_sh_0714	Goldberg, Mychajliw, & Hadly, 2016	-2.045, -54.1445	10392, 78	11926 - 12433	shcal13
gb_sh_0715	Goldberg, Mychajliw, & Hadly, 2016	-2.045, -54.1445	10450, 60	12018 - 12436	shcal13

gb_sh_0717	Goldberg, Mychajliw, & Hadly, 2016	-2.045, -54.1445	10470, 70	12026 - 12454	shcal13
gb_sh_0719	Goldberg, Mychajliw, & Hadly, 2016	-2.045, -54.1445	10480, 70	12034 - 12554	shcal13
gb_sh_0720	Goldberg, Mychajliw, & Hadly, 2016	-2.045, -54.1445	10490, 80	12024 - 12560	shcal13
gb_sh_0721	Goldberg, Mychajliw, & Hadly, 2016	-2.045, -54.1445	10510, 60	12356 - 12560	shcal13
gb_sh_0722	Goldberg, Mychajliw, & Hadly, 2016	-2.045, -54.1445	10560, 60	12381 - 12656	shcal13
gb_sh_0723	Goldberg, Mychajliw, & Hadly, 2016	-2.045, -54.1445	10655, 285	11601 - 13074	shcal13
gb_sh_0724	Goldberg, Mychajliw, & Hadly, 2016	-2.045, -54.1445	10683, 80	12431 - 12711	shcal13
gb_sh_0725	Goldberg, Mychajliw, & Hadly, 2016	-2.045, -54.1445	10875, 295	11926 - 13310	shcal13
gb_sh_0726	Goldberg, Mychajliw, & Hadly, 2016	-2.045, -54.1445	10905, 295	11950 - 13359	shcal13
gb_sh_0727	Goldberg, Mychajliw, & Hadly, 2016	-2.045, -54.1445	11110, 310	12380 - 13566	shcal13
gb_sh_0728	Goldberg, Mychajliw, & Hadly, 2016	-2.045, -54.1445	11145, 135	12719 - 13198	shcal13
gb_sh_0729	Goldberg, Mychajliw, & Hadly, 2016	-25.0833, -48.0167	3330, 125	3216 - 3839	shcal13
gb_sh_0730	Goldberg, Mychajliw, & Hadly, 2016	-25.0628, -47.9242	3170, 95	3073 - 3566	shcal13

gb_sh_0731	Goldberg, Mychajliw, & Hadly, 2016	-25.0628, -47.9242	3250, 90	3208 - 3641	shcal13
gb_sh_0732	Goldberg, Mychajliw, & Hadly, 2016	-25.06, -47.9257	3660, 70	3717 - 4098	shcal13
gb_sh_0733	Goldberg, Mychajliw, & Hadly, 2016	-25.06, -47.9257	3700, 70	3824 - 4161	shcal13
gb_sh_0734	Goldberg, Mychajliw, & Hadly, 2016	-25.06, -47.9257	3770, 70	3867 - 4296	shcal13
gb_sh_0735	Goldberg, Mychajliw, & Hadly, 2016	-8.55, -36.8656	2030, 50	1828 - 2060	shcal13
gb_sh_0736	Goldberg, Mychajliw, & Hadly, 2016	-25.4704, -48.4803	4481, 110	4827 - 5326	shcal13
gb_sh_0737	Goldberg, Mychajliw, & Hadly, 2016	-25.4704, -48.4803	4890, 110	5318 - 5761	shcal13
gb_sh_0738	Goldberg, Mychajliw, & Hadly, 2016	-25.4704, -48.4803	4930, 100	5452 - 5893	shcal13
gb_sh_0739	Goldberg, Mychajliw, & Hadly, 2016	-24.65, -47.4833	3090, 120	2919 - 3484	shcal13
gb_sh_0740	Goldberg, Mychajliw, & Hadly, 2016	-23.4101, -49.2301	3600, 160	3559 - 4161	shcal13
gb_sh_0741	Goldberg, Mychajliw, & Hadly, 2016	-22.964, -42.0311	2080, 40	1897 - 2098	shcal13
gb_sh_0743	Goldberg, Mychajliw, & Hadly, 2016	-27.5922, -48.4592	2220, 250	1594 - 2756	shcal13
gb_sh_0744	Goldberg, Mychajliw, & Hadly, 2016	-27.5922, -48.4592	2400, 250	1807 - 2980	shcal13

gb_sh_0745	Goldberg, Mychajliw, & Hadly, 2016	-27.5922, -48.4592	3690, 100	3691 - 4255	shcal13
gb_sh_0746	Goldberg, Mychajliw, & Hadly, 2016	-27.5922, -48.4592	4280, 400	3705 - 5736	shcal13
gb_sh_0747	Goldberg, Mychajliw, & Hadly, 2016	-1.35093, -48.829	3490, 195	3228 - 4249	shcal13
gb_sh_0748	Goldberg, Mychajliw, & Hadly, 2016	-1.35093, -48.829	4090, 95	4288 - 4831	shcal13
gb_sh_0749	Goldberg, Mychajliw, & Hadly, 2016	-1.35093, -48.829	4500, 90	4857 - 5314	shcal13
gb_sh_0750	Goldberg, Mychajliw, & Hadly, 2016	-23.1733, -44.2583	2880, 40	2843 - 3076	shcal13
gb_sh_0751	Goldberg, Mychajliw, & Hadly, 2016	unknown, unknown	3870, 100	3961 - 4449	shcal13
gb_sh_0752	Goldberg, Mychajliw, & Hadly, 2016	-22.8873, -42.5808	2270, 190	1827 - 2742	shcal13
gb_sh_0753	Goldberg, Mychajliw, & Hadly, 2016	-15.0874, -43.1443	4340, 235	4241 - 5477	shcal13
gb_sh_0754	Goldberg, Mychajliw, & Hadly, 2016	-15.0874, -43.1443	4380, 80	4807 - 5090	shcal13
gb_sh_0755	Goldberg, Mychajliw, & Hadly, 2016	-15.0874, -43.1443	4610, 55	5038 - 5333	shcal13
gb_sh_0756	Goldberg, Mychajliw, & Hadly, 2016	-15.0874, -43.1443	4695, 80	5262 - 5587	shcal13
gb_sh_0757	Goldberg, Mychajliw, & Hadly, 2016	-15.0874, -43.1443	4740, 80	5282 - 5602	shcal13

gb_sh_0758	Goldberg, Mychajliw, & Hadly, 2016	-15.0874, -43.1443	4750, 65	5316 - 5584	shcal13
gb_sh_0759	Goldberg, Mychajliw, & Hadly, 2016	-15.0874, -43.1443	5045, 95	5584 - 5938	shcal13
gb_sh_0760	Goldberg, Mychajliw, & Hadly, 2016	-15.0874, -43.1443	5050, 85	5596 - 5915	shcal13
gb_sh_0761	Goldberg, Mychajliw, & Hadly, 2016	-15.0874, -43.1443	5070, 95	5590 - 5941	shcal13
gb_sh_0762	Goldberg, Mychajliw, & Hadly, 2016	-15.0874, -43.1443	5115, 195	5461 - 6280	shcal13
gb_sh_0763	Goldberg, Mychajliw, & Hadly, 2016	-25.2891, -48.1359	4540, 90	4863 - 5326	shcal13
gb_sh_0764	Goldberg, Mychajliw, & Hadly, 2016	-25.2891, -48.1359	4760, 80	5288 - 5610	shcal13
gb_sh_0765	Goldberg, Mychajliw, & Hadly, 2016	-25.2891, -48.1359	6030, 130	6504 - 7166	shcal13
gb_sh_0766	Goldberg, Mychajliw, & Hadly, 2016	-28.5831, -49.0013	3610, 70	3687 - 4012	shcal13
gb_sh_0767	Goldberg, Mychajliw, & Hadly, 2016	-24.0873, -54.2784	4065, 75	4287 - 4727	shcal13
gb_sh_0768	Goldberg, Mychajliw, & Hadly, 2016	-26.9327, -48.6372	3815, 145	3718 - 4529	shcal13
gb_sh_0769	Goldberg, Mychajliw, & Hadly, 2016	-26.9327, -48.6372	4990, 210	5275 - 6211	shcal13
gb_sh_0770	Goldberg, Mychajliw, & Hadly, 2016	unknown, unknown	3920, 100	3982 - 4569	shcal13

gb_sh_0771	Goldberg, Mychajliw, & Hadly, 2016	unknown, unknown	5040, 90	5588 - 5920	shcal13
gb_sh_0772	Goldberg, Mychajliw, & Hadly, 2016	unknown, unknown	6540, 105	7242 - 7582	shcal13
gb_sh_0773	Goldberg, Mychajliw, & Hadly, 2016	unknown, unknown	4260, 210	4217 - 5321	shcal13
gb_sh_0774	Goldberg, Mychajliw, & Hadly, 2016	-28.5133, -48.8917	2390, 70	2297 - 2546	shcal13
gb_sh_0775	Goldberg, Mychajliw, & Hadly, 2016	-24.0675, -46.8	5970, 140	6445 - 7033	shcal13
gb_sh_0776	Goldberg, Mychajliw, & Hadly, 2016	-28.5595, -49.0988	5410, 50	6090 - 6280	shcal13
gb_sh_0777	Goldberg, Mychajliw, & Hadly, 2016	-28.5595, -49.0988	6590, 60	7409 - 7569	shcal13
gb_sh_0778	Goldberg, Mychajliw, & Hadly, 2016	-24.4522, -47.2178	4560, 110	4862 - 5336	shcal13
gb_sh_0779	Goldberg, Mychajliw, & Hadly, 2016	unknown, unknown	3300, 100	3228 - 3721	shcal13
gb_sh_0780	Goldberg, Mychajliw, & Hadly, 2016	-24.4686, -47.9672	4710, 145	4958 - 5658	shcal13
gb_sh_0781	Goldberg, Mychajliw, & Hadly, 2016	-24.4686, -47.9672	4750, 110	5256 - 5652	shcal13
gb_sh_0782	Goldberg, Mychajliw, & Hadly, 2016	-24.4686, -47.9672	4860, 100	5312 - 5748	shcal13
gb_sh_0783	Goldberg, Mychajliw, & Hadly, 2016	-22.631, -42.9435	3170, 70	3156 - 3484	shcal13

gb_sh_0784	Goldberg, Mychajliw, & Hadly, 2016	unknown, unknown	4400, 200	4425 - 5472	shcal13
gb_sh_0785	Goldberg, Mychajliw, & Hadly, 2016	unknown, unknown	4240, 150	4379 - 5077	shcal13
gb_sh_0786	Goldberg, Mychajliw, & Hadly, 2016	unknown, unknown	3550, 150	3443 - 4160	shcal13
gb_sh_0787	Goldberg, Mychajliw, & Hadly, 2016	-15.3785, -54.7266	2970, 70	2735 - 3513	shcal13
gb_sh_0788	Goldberg, Mychajliw, & Hadly, 2016	-29.6167, -50.2875	4280, 180	4338 - 5312	shcal13
gb_sh_0789	Goldberg, Mychajliw, & Hadly, 2016	-29.6167, -50.2875	5680, 240	5908 - 7007	shcal13
gb_sh_0790	Goldberg, Mychajliw, & Hadly, 2016	-29.6167, -50.2875	5950, 190	6311 - 7175	shcal13
gb_sh_0791	Goldberg, Mychajliw, & Hadly, 2016	-26.2289, -51.0126	3110, 140	2916 - 3573	shcal13
gb_sh_0792	Goldberg, Mychajliw, & Hadly, 2016	-23.094, -53.5411	5380, 110	5898 - 6322	shcal13
gb_sh_0793	Goldberg, Mychajliw, & Hadly, 2016	unknown, unknown	2970, 180	2741 - 3481	shcal13
gb_sh_0794	Goldberg, Mychajliw, & Hadly, 2016	unknown, unknown	3030, 170	2768 - 3510	shcal13
gb_sh_0795	Goldberg, Mychajliw, & Hadly, 2016	-24.1358, -46.9	4635, 100	4970 - 5488	shcal13
gb_sh_0796	Goldberg, Mychajliw, & Hadly, 2016	-29.3835, -51.596	7800, 50	8422 - 8627	shcal13

gb_sh_0797	Goldberg, Mychajliw, & Hadly, 2016	-29.527, -51.7443	5655, 140	6174 - 6739	shcal13
gb_sh_0798	Goldberg, Mychajliw, & Hadly, 2016	-29.5126, -51.7278	3000, 40	2965 - 3240	shcal13
gb_sh_0799	Goldberg, Mychajliw, & Hadly, 2016	-29.5126, -51.7278	6180, 50	6881 - 7173	shcal13
gb_sh_0800	Goldberg, Mychajliw, & Hadly, 2016	-29.5126, -51.7278	8030, 50	8692 - 9007	shcal13
gb_sh_0801	Goldberg, Mychajliw, & Hadly, 2016	-29.5126, -51.7278	8150, 50	8969 - 9260	shcal13
gb_sh_0802	Goldberg, Mychajliw, & Hadly, 2016	-29.5126, -51.7278	8430, 50	9282 - 9520	shcal13
gb_sh_0803	Goldberg, Mychajliw, & Hadly, 2016	-29.7181, -56.6638	10810, 275	11823 - 13205	shcal13
gb_sh_0804	Goldberg, Mychajliw, & Hadly, 2016	-29.7892, -57.075	9230, 145	10110 - 10752	shcal13
gb_sh_0805	Goldberg, Mychajliw, & Hadly, 2016	-29.7892, -57.075	9840, 105	11057 - 11505	shcal13
gb_sh_0806	Goldberg, Mychajliw, & Hadly, 2016	-29.7892, -57.075	10010, 190	11062 - 12110	shcal13
gb_sh_0807	Goldberg, Mychajliw, & Hadly, 2016	-29.6133, -56.93	9620, 110	10647 - 11202	shcal13
gb_sh_0808	Goldberg, Mychajliw, & Hadly, 2016	-29.6133, -56.93	10200, 125	11273 - 12154	shcal13
gb_sh_0809	Goldberg, Mychajliw, & Hadly, 2016	-29.6133, -56.93	10240, 80	11586 - 12113	shcal13

gb_sh_0810	Goldberg, Mychajliw, & Hadly, 2016	-29.6133, -56.93	10400, 110	11797 - 12554	shcal13
gb_sh_0811	Goldberg, Mychajliw, & Hadly, 2016	-29.6133, -56.93	10800, 150	12387 - 13034	shcal13
gb_sh_0812	Goldberg, Mychajliw, & Hadly, 2016	-29.6133, -56.93	10985, 100	12698 - 13035	shcal13
gb_sh_0813	Goldberg, Mychajliw, & Hadly, 2016	-29.7456, -57.048	9120, 340	9471 - 11185	shcal13
gb_sh_0814	Goldberg, Mychajliw, & Hadly, 2016	-29.5322, -56.865	9450, 115	10293 - 10901	shcal13
gb_sh_0815	Goldberg, Mychajliw, & Hadly, 2016	-29.7797, -57.1285	9605, 120	10572 - 11205	shcal13
gb_sh_0816	Goldberg, Mychajliw, & Hadly, 2016	-29.7371, -57.0756	10180, 275	11083 - 12658	shcal13
gb_sh_0817	Goldberg, Mychajliw, & Hadly, 2016	-29.287, -56.5589	9035, 100	9739 - 10303	shcal13
gb_sh_0818	Goldberg, Mychajliw, & Hadly, 2016	-28.9505, -56.3052	3525, 145	3440 - 4103	shcal13
gb_sh_0819	Goldberg, Mychajliw, & Hadly, 2016	-29.7892, -57.075	8585, 115	9274 - 9898	shcal13
gb_sh_0820	Goldberg, Mychajliw, & Hadly, 2016	-29.7892, -57.075	9595, 175	10373 - 11265	shcal13
gb_sh_0821	Goldberg, Mychajliw, & Hadly, 2016	-29.7892, -57.075	9855, 130	10763 - 11653	shcal13
gb_sh_0822	Goldberg, Mychajliw, & Hadly, 2016	-28.6117, -56.0049	11555, 230	12835 - 13791	shcal13

gb_sh_0823	Goldberg, Mychajliw, & Hadly, 2016	-32.5699, -52.4322	2000, 120	1609 - 2163	shcal13
gb_sh_0824	Goldberg, Mychajliw, & Hadly, 2016	-32.5699, -52.4322	2160, 80	1927 - 2319	shcal13
gb_sh_0825	Goldberg, Mychajliw, & Hadly, 2016	-32.1034, -52.4761	2435, 85	2305 - 2738	shcal13
gb_sh_0826	Goldberg, Mychajliw, & Hadly, 2016	-32.5757, -52.428	2020, 50	1823 - 2055	shcal13
gb_sh_0827	Goldberg, Mychajliw, & Hadly, 2016	-29.6854, -52.463	2920, 120	2763 - 3268	shcal13
gb_sh_0828	Goldberg, Mychajliw, & Hadly, 2016	-29.7725, -50.5622	3730, 60	3847 - 4161	shcal13
gb_sh_0829	Goldberg, Mychajliw, & Hadly, 2016	-15.4667, -56.8	3970, 60	4235 - 4449	shcal13
gb_sh_0831	Goldberg, Mychajliw, & Hadly, 2016	-29.7725, -50.5622	4610, 140	4870 - 5488	shcal13
gb_sh_0832	Goldberg, Mychajliw, & Hadly, 2016	-29.7725, -50.5622	4690, 40	5297 - 5476	shcal13
gb_sh_0833	Goldberg, Mychajliw, & Hadly, 2016	-29.7725, -50.5622	7390, 40	8026 - 8220	shcal13
gb_sh_0835	Goldberg, Mychajliw, & Hadly, 2016	-29.8038, -51.585	5230, 40	5885 - 6022	shcal13
gb_sh_0836	Goldberg, Mychajliw, & Hadly, 2016	-29.8038, -51.585	6215, 30	6957 - 7168	shcal13
gb_sh_0837	Goldberg, Mychajliw, & Hadly, 2016	-29.8038, -51.585	7240, 40	7940 - 8068	shcal13

gb_sh_0838	Goldberg, Mychajliw, & Hadly, 2016	-29.5939, -51.7278	7250, 350	7417 - 8780	shcal13
gb_sh_0839	Goldberg, Mychajliw, & Hadly, 2016	-29.5939, -51.7278	8020, 150	8506 - 9262	shcal13
gb_sh_0840	Goldberg, Mychajliw, & Hadly, 2016	-29.5939, -51.7278	8290, 130	8971 - 9527	shcal13
gb_sh_0841	Goldberg, Mychajliw, & Hadly, 2016	-29.5939, -51.7278	9430, 360	9601 - 11652	shcal13
gb_sh_0845	Goldberg, Mychajliw, & Hadly, 2016	unknown, unknown	3540, 50	3632 - 3909	shcal13
gb_sh_0846	Goldberg, Mychajliw, & Hadly, 2016	-22.8689, -41.9954	4340, 70	4782 - 5054	shcal13
gb_sh_0847	Goldberg, Mychajliw, & Hadly, 2016	-22.8689, -41.9954	4490, 40	4951 - 5093	shcal13
gb_sh_0848	Goldberg, Mychajliw, & Hadly, 2016	-29.7007, -51.9665	4490, 136	4810 - 5471	shcal13
gb_sh_0849	Goldberg, Mychajliw, & Hadly, 2016	-29.7007, -51.9665	4859, 64	5445 - 5662	shcal13
gb_sh_0850	Goldberg, Mychajliw, & Hadly, 2016	-29.7007, -51.9665	4877, 64	5450 - 5715	shcal13
gb_sh_0851	Goldberg, Mychajliw, & Hadly, 2016	-29.7007, -51.9665	4885, 65	5455 - 5725	shcal13
gb_sh_0852	Goldberg, Mychajliw, & Hadly, 2016	-22.9169, -42.5506	2250, 60	2081 - 2346	shcal13
gb_sh_0853	Goldberg, Mychajliw, & Hadly, 2016	-22.9169, -42.5506	3280, 60	3344 - 3614	shcal13

gb_sh_0854	Goldberg, Mychajliw, & Hadly, 2016	-22.9169, -42.5506	3858, 60	4077 - 4415	shcal13
gb_sh_0855	Goldberg, Mychajliw, & Hadly, 2016	-22.9169, -42.5506	3905, 67	4084 - 4442	shcal13
gb_sh_0856	Goldberg, Mychajliw, & Hadly, 2016	-22.9169, -42.5506	3965, 66	4149 - 4529	shcal13
gb_sh_0857	Goldberg, Mychajliw, & Hadly, 2016	-22.9169, -42.5506	4056, 73	4280 - 4662	shcal13
gb_sh_0858	Goldberg, Mychajliw, & Hadly, 2016	-22.9169, -42.5506	4069, 66	4340 - 4712	shcal13
gb_sh_0859	Goldberg, Mychajliw, & Hadly, 2016	-22.9169, -42.5506	4071, 73	4294 - 4728	shcal13
gb_sh_0860	Goldberg, Mychajliw, & Hadly, 2016	-22.9169, -42.5506	4218, 63	4528 - 4848	shcal13
gb_sh_0861	Goldberg, Mychajliw, & Hadly, 2016	-22.9169, -42.5506	4256, 62	4566 - 4870	shcal13
gb_sh_0862	Goldberg, Mychajliw, & Hadly, 2016	-22.9169, -42.5506	4320, 62	4784 - 4985	shcal13
gb_sh_0863	Goldberg, Mychajliw, & Hadly, 2016	-22.9169, -42.5506	4430, 65	4841 - 5082	shcal13
gb_sh_0864	Goldberg, Mychajliw, & Hadly, 2016	-4.59513, -56.3281	5570, 125	5998 - 6567	shcal13
gb_sh_0865	Goldberg, Mychajliw, & Hadly, 2016	-22.93, -44.3467	3350, 80	3363 - 3723	shcal13
gb_sh_0866	Goldberg, Mychajliw, & Hadly, 2016	-22.93, -44.3467	7860, 80	8420 - 8795	shcal13

gb_sh_0867	Goldberg, Mychajliw, & Hadly, 2016	-25.444, -48.4551	3271, 48	3359 - 3573	shcal13
gb_sh_0868	Goldberg, Mychajliw, & Hadly, 2016	-25.444, -48.4551	3284, 61	3348 - 3617	shcal13
gb_sh_0869	Goldberg, Mychajliw, & Hadly, 2016	-25.444, -48.4551	3306, 61	3366 - 3636	shcal13
gb_sh_0870	Goldberg, Mychajliw, & Hadly, 2016	-25.444, -48.4551	3344, 61	3388 - 3647	shcal13
gb_sh_0871	Goldberg, Mychajliw, & Hadly, 2016	-25.444, -48.4551	3361, 70	3381 - 3718	shcal13
gb_sh_0872	Goldberg, Mychajliw, & Hadly, 2016	-25.444, -48.4551	3373, 58	3441 - 3704	shcal13
gb_sh_0873	Goldberg, Mychajliw, & Hadly, 2016	-25.444, -48.4551	3424, 62	3463 - 3734	shcal13
gb_sh_0874	Goldberg, Mychajliw, & Hadly, 2016	-25.444, -48.4551	3496, 56	3574 - 3866	shcal13
gb_sh_0875	Goldberg, Mychajliw, & Hadly, 2016	-25.444, -48.4551	3500, 60	3572 - 3882	shcal13
gb_sh_0876	Goldberg, Mychajliw, & Hadly, 2016	-25.444, -48.4551	4970, 95	5569 - 5907	shcal13
gb_sh_0877	Goldberg, Mychajliw, & Hadly, 2016	-22.9742, -42.4851	3610, 190	3445 - 4413	shcal13
gb_sh_0879	Goldberg, Mychajliw, & Hadly, 2016	-22.9742, -42.4851	3960, 200	3827 - 4863	shcal13
gb_sh_0881	Goldberg, Mychajliw, & Hadly, 2016	-30.2223, -50.3926	4620, 100	4960 - 5485	shcal13

gb_sh_0882	Goldberg, Mychajliw, & Hadly, 2016	-30.2223, -50.3926	4640, 80	5036 - 5482	shcal13
gb_sh_0883	Goldberg, Mychajliw, & Hadly, 2016	-30.2223, -50.3926	4740, 90	5270 - 5609	shcal13
gb_sh_0887	Goldberg, Mychajliw, & Hadly, 2016	-22.5278, -41.9394	3172, 33	3238 - 3413	shcal13
gb_sh_0888	Goldberg, Mychajliw, & Hadly, 2016	-22.5278, -41.9394	3391, 26	3544 - 3645	shcal13
gb_sh_0889	Goldberg, Mychajliw, & Hadly, 2016	-22.5278, -41.9394	3420, 61	3458 - 3732	shcal13
gb_sh_0890	Goldberg, Mychajliw, & Hadly, 2016	-22.5278, -41.9394	3473, 25	3589 - 3732	shcal13
gb_sh_0891	Goldberg, Mychajliw, & Hadly, 2016	-22.5278, -41.9394	3479, 38	3591 - 3829	shcal13
gb_sh_0892	Goldberg, Mychajliw, & Hadly, 2016	-22.5278, -41.9394	3507, 22	3679 - 3831	shcal13
gb_sh_0893	Goldberg, Mychajliw, & Hadly, 2016	-22.5278, -41.9394	3510, 36	3631 - 3845	shcal13
gb_sh_0894	Goldberg, Mychajliw, & Hadly, 2016	-22.5278, -41.9394	3533, 29	3685 - 3859	shcal13
gb_sh_0895	Goldberg, Mychajliw, & Hadly, 2016	-22.5278, -41.9394	3561, 53	3677 - 3928	shcal13
gb_sh_0896	Goldberg, Mychajliw, & Hadly, 2016	-22.5278, -41.9394	3567, 50	3683 - 3930	shcal13
gb_sh_0897	Goldberg, Mychajliw, & Hadly, 2016	-22.5278, -41.9394	3567, 27	3699 - 3891	shcal13

gb_sh_0898	Goldberg, Mychajliw, & Hadly, 2016	-22.5278, -41.9394	3588, 65	3676 - 3988	shcal13
gb_sh_0899	Goldberg, Mychajliw, & Hadly, 2016	-22.5278, -41.9394	3620, 30	3820 - 3980	shcal13
gb_sh_0900	Goldberg, Mychajliw, & Hadly, 2016	-22.5278, -41.9394	3654, 32	3831 - 3996	shcal13
gb_sh_0901	Goldberg, Mychajliw, & Hadly, 2016	-22.5278, -41.9394	3660, 30	3835 - 3995	shcal13
gb_sh_0902	Goldberg, Mychajliw, & Hadly, 2016	-22.5278, -41.9394	3662, 64	3813 - 4096	shcal13
gb_sh_0903	Goldberg, Mychajliw, & Hadly, 2016	-22.5278, -41.9394	3662, 66	3811 - 4097	shcal13
gb_sh_0904	Goldberg, Mychajliw, & Hadly, 2016	-22.5278, -41.9394	3670, 30	3840 - 4001	shcal13
gb_sh_0905	Goldberg, Mychajliw, & Hadly, 2016	-22.5278, -41.9394	3692, 68	3822 - 4157	shcal13
gb_sh_0906	Goldberg, Mychajliw, & Hadly, 2016	-22.5278, -41.9394	3710, 68	3828 - 4183	shcal13
gb_sh_0907	Goldberg, Mychajliw, & Hadly, 2016	-22.5278, -41.9394	3720, 30	3897 - 4094	shcal13
gb_sh_0908	Goldberg, Mychajliw, & Hadly, 2016	-22.5278, -41.9394	3729, 35	3901 - 4100	shcal13
gb_sh_0909	Goldberg, Mychajliw, & Hadly, 2016	-22.5278, -41.9394	3740, 30	3957 - 4104	shcal13
gb_sh_0910	Goldberg, Mychajliw, & Hadly, 2016	-22.5278, -41.9394	3743, 26	3962 - 4103	shcal13

gb_sh_0911	Goldberg, Mychajliw, & Hadly, 2016	-22.5278, -41.9394	3747, 62	3869 - 4238	shcal13
gb_sh_0913	Goldberg, Mychajliw, & Hadly, 2016	-22.5278, -41.9394	3800, 49	3966 - 4295	shcal13
gb_sh_0914	Goldberg, Mychajliw, & Hadly, 2016	-22.5278, -41.9394	3810, 30	4066 - 4244	shcal13
gb_sh_0915	Goldberg, Mychajliw, & Hadly, 2016	-22.5278, -41.9394	3810, 40	3982 - 4259	shcal13
gb_sh_0916	Goldberg, Mychajliw, & Hadly, 2016	-22.5278, -41.9394	3820, 40	3985 - 4295	shcal13
gb_sh_0917	Goldberg, Mychajliw, & Hadly, 2016	-22.5278, -41.9394	3852, 31	4086 - 4300	shcal13
gb_sh_0918	Goldberg, Mychajliw, & Hadly, 2016	-22.5278, -41.9394	3860, 40	4089 - 4359	shcal13
gb_sh_0919	Goldberg, Mychajliw, & Hadly, 2016	-22.5278, -41.9394	3910, 30	4223 - 4414	shcal13
gb_sh_0920	Goldberg, Mychajliw, & Hadly, 2016	-22.5278, -41.9394	3968, 31	4243 - 4441	shcal13
gb_sh_0921	Goldberg, Mychajliw, & Hadly, 2016	-22.5278, -41.9394	3979, 35	4245 - 4447	shcal13
gb_sh_0922	Goldberg, Mychajliw, & Hadly, 2016	-22.5278, -41.9394	4043, 26	4412 - 4533	shcal13
gb_sh_0923	Goldberg, Mychajliw, & Hadly, 2016	-22.5278, -41.9394	4127, 24	4513 - 4652	shcal13
gb_sh_0924	Goldberg, Mychajliw, & Hadly, 2016	-29.6058, -50.025	3420, 60	3458 - 3732	shcal13

gb_sh_0925	Goldberg, Mychajliw, & Hadly, 2016	-29.3541, -49.7812	3350, 50	3441 - 3644	shcal13
gb_sh_0926	Goldberg, Mychajliw, & Hadly, 2016	-22.6974, -42.9429	3290, 70	3339 - 3641	shcal13
gb_sh_0927	Goldberg, Mychajliw, & Hadly, 2016	-22.6974, -42.9429	3720, 40	3888 - 4102	shcal13
gb_sh_0928	Goldberg, Mychajliw, & Hadly, 2016	-22.6974, -42.9429	3730, 70	3836 - 4239	shcal13
gb_sh_0929	Goldberg, Mychajliw, & Hadly, 2016	-15.4667, -56.8	2350, 60	2152 - 2492	shcal13
gb_sh_0931	Goldberg, Mychajliw, & Hadly, 2016	-15.4667, -56.8	2990, 60	2924 - 3257	shcal13
gb_sh_0932	Goldberg, Mychajliw, & Hadly, 2016	-23.55, -49.65	3600, 120	3687 - 3991	shcal13
gb_sh_0933	Goldberg, Mychajliw, & Hadly, 2016	-19.4772, -44.0392	3830, 40	3915 - 4420	shcal13
gb_sh_0934	Goldberg, Mychajliw, & Hadly, 2016	-29.7725, -50.5622	3970, 40	4220 - 4525	shcal13
gb_sh_0935	Goldberg, Mychajliw, & Hadly, 2016	-23.2867, -49.5139	5080, 60	5288 - 6310	shcal13
gb_sh_0936	Goldberg, Mychajliw, & Hadly, 2016	-24.9167, -47.8667	5110, 100	5308 - 6313	shcal13
gb_sh_0937	Goldberg, Mychajliw, & Hadly, 2016	-15.4667, -56.8	5690, 70	6298 - 6568	shcal13
gb_sh_0938	Goldberg, Mychajliw, & Hadly, 2016	-15.4667, -56.8	5860, 60	6466 - 6755	shcal13

gb_sh_0939	Goldberg, Mychajliw, & Hadly, 2016	-15.4667, -56.8	5890, 70	6474 - 6803	shcal13
gb_sh_0940	Goldberg, Mychajliw, & Hadly, 2016	-15.4667, -56.8	5920, 70	6500 - 6861	shcal13
gb_sh_0941	Goldberg, Mychajliw, & Hadly, 2016	-15.4667, -56.8	5980, 70	6616 - 6952	shcal13
gb_sh_0942	Goldberg, Mychajliw, & Hadly, 2016	-15.4667, -56.8	6040, 70	6661 - 7013	shcal13
gb_sh_0943	Goldberg, Mychajliw, & Hadly, 2016	-15.4667, -56.8	6060, 80	6668 - 7030	shcal13
gb_sh_0944	Goldberg, Mychajliw, & Hadly, 2016	-15.4667, -56.8	6410, 60	7230 - 7422	shcal13
gb_sh_0945	Goldberg, Mychajliw, & Hadly, 2016	-16.33, -56.7638	6750, 230	7156 - 8020	shcal13
gb_sh_0946	Goldberg, Mychajliw, & Hadly, 2016	-8.854, -42.6078	7010, 170	7671 - 7940	shcal13
gb_sh_0947	Goldberg, Mychajliw, & Hadly, 2016	-15.4667, -56.8	7050, 55	7704 - 7948	shcal13
gb_sh_0948	Goldberg, Mychajliw, & Hadly, 2016	-19.4772, -44.0392	7940, 50	8576 - 8990	shcal13
gb_sh_0949	Goldberg, Mychajliw, & Hadly, 2016	-16.33, -56.7638	9320, 20	10375 - 10571	shcal13
gb_sh_0950	Goldberg, Mychajliw, & Hadly, 2016	-16.33, -56.7638	9340, 20	10402 - 10582	shcal13
gb_sh_0951	Goldberg, Mychajliw, & Hadly, 2016	-16.33, -56.7638	9340, 70	10267 - 10672	shcal13

gb_sh_0952	Goldberg, Mychajliw, & Hadly, 2016	-3.2, -60.3275	9460, 50	10392 - 10891	shcal13
gb_sh_0953	Goldberg, Mychajliw, & Hadly, 2016	-16.33, -56.7638	9580, 20	10945 - 11075	shcal13
gb_sh_0954	Goldberg, Mychajliw, & Hadly, 2016	-16.33, -56.7638	9635, 20	10763 - 11107	shcal13
gb_sh_0955	Goldberg, Mychajliw, & Hadly, 2016	-16.33, -56.7638	9705, 20	11070 - 11195	shcal13
gb_sh_0956	Goldberg, Mychajliw, & Hadly, 2016	-16.33, -56.7638	9790, 20	11146 - 11233	shcal13
gb_sh_0957	Goldberg, Mychajliw, & Hadly, 2016	-2.045, -54.1445	10120, 70	11330 - 11840	shcal13
gb_sh_0958	Goldberg, Mychajliw, & Hadly, 2016	-28.5914, -48.8306	3200, 60	3212 - 3498	shcal13
gb_sh_0959	Goldberg, Mychajliw, & Hadly, 2016	-28.589, -48.8219	5240, 50	5886 - 6122	shcal13
gb_sh_0960	Goldberg, Mychajliw, & Hadly, 2016	-28.584, -48.8228	4040, 50	4287 - 4622	shcal13
gb_sh_0961	Goldberg, Mychajliw, & Hadly, 2016	-28.5834, -48.8362	2530, 50	2420 - 2736	shcal13
gb_sh_0962	Goldberg, Mychajliw, & Hadly, 2016	-28.5834, -48.8362	2620, 50	2485 - 2787	shcal13
gb_sh_0963	Goldberg, Mychajliw, & Hadly, 2016	-28.5822, -48.8368	2090, 50	1894 - 2150	shcal13
gb_sh_0964	Goldberg, Mychajliw, & Hadly, 2016	-28.5822, -48.8368	4110, 50	4421 - 4709	shcal13

gb_sh_0965	Goldberg, Mychajliw, & Hadly, 2016	-28.5849, -48.8375	3510, 50	3606 - 3869	shcal13
gb_sh_0966	Goldberg, Mychajliw, & Hadly, 2016	-19.1284, -43.7272	2310, 50	2150 - 2358	shcal13
gb_sh_0967	Goldberg, Mychajliw, & Hadly, 2016	-19.1284, -43.7272	5350, 60	5935 - 6215	shcal13
gb_sh_0968	Goldberg, Mychajliw, & Hadly, 2016	-19.1284, -43.7272	5680, 70	6292 - 6567	shcal13
gb_sh_0969	Goldberg, Mychajliw, & Hadly, 2016	-19.1284, -43.7272	7820, 60	8414 - 8715	shcal13
gb_sh_0971	Goldberg, Mychajliw, & Hadly, 2016	-19.1284, -43.7272	8150, 150	8625 - 9424	shcal13
gb_sh_0972	Goldberg, Mychajliw, & Hadly, 2016	-19.1284, -43.7272	8185, 110	8722 - 9423	shcal13
gb_sh_0973	Goldberg, Mychajliw, & Hadly, 2016	-19.1284, -43.7272	8230, 150	8701 - 9484	shcal13
gb_sh_0974	Goldberg, Mychajliw, & Hadly, 2016	-19.1284, -43.7272	8280, 40	9071 - 9322	shcal13
gb_sh_0975	Goldberg, Mychajliw, & Hadly, 2016	-19.1284, -43.7272	8381, 280	8582 - 9950	shcal13
gb_sh_0976	Goldberg, Mychajliw, & Hadly, 2016	-19.1284, -43.7272	8400, 300	8591 - 9967	shcal13
gb_sh_0977	Goldberg, Mychajliw, & Hadly, 2016	-19.1284, -43.7272	8840, 130	9548 - 10183	shcal13
gb_sh_0978	Goldberg, Mychajliw, & Hadly, 2016	-19.1284, -43.7272	9460, 110	10372 - 11098	shcal13

gb_sh_0979	Goldberg, Mychajliw, & Hadly, 2016	-19.1284, -43.7272	11960, 250	13235 - 14674	shcal13
gb_sh_0980	Goldberg, Mychajliw, & Hadly, 2016	-19.1284, -43.7272	12760, 70	14797 - 15369	shcal13
gb_sh_0981	Goldberg, Mychajliw, & Hadly, 2016	-25.5, -49.5	4070, 105	4235 - 4832	shcal13
gb_sh_0982	Goldberg, Mychajliw, & Hadly, 2016	-25.5, -49.5	4665, 90	5043 - 5493	shcal13
gb_sh_0983	Goldberg, Mychajliw, & Hadly, 2016	-25.5, -49.5	4810, 100	5291 - 5731	shcal13
gb_sh_0984	Goldberg, Mychajliw, & Hadly, 2016	-25.5, -49.5	4960, 110	5460 - 5911	shcal13
gb_sh_0985	Goldberg, Mychajliw, & Hadly, 2016	unknown, unknown	2050, 50	1863 - 2091	shcal13
gb_sh_0986	Goldberg, Mychajliw, & Hadly, 2016	unknown, unknown	3800, 50	3966 - 4295	shcal13
gb_sh_0987	Goldberg, Mychajliw, & Hadly, 2016	unknown, unknown	4010, 50	4244 - 4539	shcal13
gb_sh_0988	Goldberg, Mychajliw, & Hadly, 2016	unknown, unknown	4050, 60	4287 - 4648	shcal13
gb_sh_0989	Goldberg, Mychajliw, & Hadly, 2016	unknown, unknown	4440, 50	4851 - 5073	shcal13
gb_sh_0990	Goldberg, Mychajliw, & Hadly, 2016	unknown, unknown	2040, 60	1822 - 2103	shcal13
gb_sh_0991	Goldberg, Mychajliw, & Hadly, 2016	-27.743, -49.1886	3000, 120	2841 - 3394	shcal13

gb_sh_0992	Goldberg, Mychajliw, & Hadly, 2016	-27.1716, -53.7519	7260, 100	7837 - 8215	shcal13
gb_sh_0993	Goldberg, Mychajliw, & Hadly, 2016	-22.6414, -42.9757	2160, 60	1994 - 2309	shcal13
gb_sh_0994	Goldberg, Mychajliw, & Hadly, 2016	-22.6414, -42.9757	2290, 60	2094 - 2357	shcal13
gb_sh_0995	Goldberg, Mychajliw, & Hadly, 2016	-22.6414, -42.9757	2510, 60	2360 - 2720	shcal13
gb_sh_0996	Goldberg, Mychajliw, & Hadly, 2016	-7.79564, -35.5738	4650, 150	4872 - 5595	shcal13
gb_sh_0997	Goldberg, Mychajliw, & Hadly, 2016	unknown, unknown	9040, 400	9190 - 11208	shcal13
gb_sh_0998	Goldberg, Mychajliw, & Hadly, 2016	unknown, unknown	6240, 250	6503 - 7519	shcal13
gb_sh_0999	Goldberg, Mychajliw, & Hadly, 2016	-22.8574, -42.9575	3200, 190	2917 - 3829	shcal13
gb_sh_1000	Goldberg, Mychajliw, & Hadly, 2016	-25.0333, -47.9833	3960, 90	4083 - 4589	shcal13
gb_sh_1001	Goldberg, Mychajliw, & Hadly, 2016	-25.0333, -47.9833	4010, 110	4144 - 4728	shcal13
gb_sh_1002	Goldberg, Mychajliw, & Hadly, 2016	-2.46911, -54.2813	5705, 80	6300 - 6637	shcal13
gb_sh_1003	Goldberg, Mychajliw, & Hadly, 2016	-2.46911, -54.2813	6300, 90	6944 - 7335	shcal13
gb_sh_1004	Goldberg, Mychajliw, & Hadly, 2016	-2.46911, -54.2813	6590, 100	7266 - 7597	shcal13

gb_sh_1005	Goldberg, Mychajliw, & Hadly, 2016	-2.46911, -54.2813	6640, 80	7410 - 7614	shcal13
gb_sh_1006	Goldberg, Mychajliw, & Hadly, 2016	-2.46911, -54.2813	6860, 100	7492 - 7860	shcal13
gb_sh_1007	Goldberg, Mychajliw, & Hadly, 2016	-2.46911, -54.2813	6880, 80	7564 - 7852	shcal13
gb_sh_1008	Goldberg, Mychajliw, & Hadly, 2016	-2.46911, -54.2813	6930, 80	7586 - 7868	shcal13
gb_sh_1009	Goldberg, Mychajliw, & Hadly, 2016	-2.46911, -54.2813	6980, 80	7650 - 7936	shcal13
gb_sh_1010	Goldberg, Mychajliw, & Hadly, 2016	-2.46911, -54.2813	7000, 80	7655 - 7953	shcal13
gb_sh_1011	Goldberg, Mychajliw, & Hadly, 2016	-2.46911, -54.2813	7010, 90	7652 - 7963	shcal13
gb_sh_1012	Goldberg, Mychajliw, & Hadly, 2016	-2.46911, -54.2813	7080, 80	7693 - 7998	shcal13
gb_sh_1013	Goldberg, Mychajliw, & Hadly, 2016	-2.46911, -54.2813	7090, 80	7697 - 8006	shcal13
gb_sh_1014	Goldberg, Mychajliw, & Hadly, 2016	-24.7461, -47.9644	3990, 70	4152 - 4582	shcal13
gb_sh_1015	Goldberg, Mychajliw, & Hadly, 2016	-24.7389, -48.0273	5740, 50	6394 - 6639	shcal13
gb_sh_1016	Goldberg, Mychajliw, & Hadly, 2016	-8.787, -42.515	8670, 60	9490 - 9764	shcal13
gb_sh_1017	Goldberg, Mychajliw, & Hadly, 2016	-8.787, -42.515	8800, 60	9548 - 9943	shcal13

gb_sh_1018	Goldberg, Mychajliw, & Hadly, 2016	-8.86717, -43.0424	7940, 90	8537 - 9007	shcal13
gb_sh_1019	Goldberg, Mychajliw, & Hadly, 2016	-8.86717, -43.0424	8700, 90	9478 - 9921	shcal13
gb_sh_1020	Goldberg, Mychajliw, & Hadly, 2016	-8.859, -42.588	8160, 70	8847 - 9287	shcal13
gb_sh_1021	Goldberg, Mychajliw, & Hadly, 2016	-8.859, -42.588	8190, 60	8977 - 9305	shcal13
gb_sh_1022	Goldberg, Mychajliw, & Hadly, 2016	-8.859, -42.588	8820, 70	9555 - 9957	shcal13
gb_sh_1023	Goldberg, Mychajliw, & Hadly, 2016	-8.80747, -42.8831	6990, 70	7660 - 7938	shcal13
gb_sh_1024	Goldberg, Mychajliw, & Hadly, 2016	-11.0333, -42.1167	2020, 130	1695 - 2211	shcal13
gb_sh_1025	Goldberg, Mychajliw, & Hadly, 2016	-11.0333, -42.1167	3570, 60	3677 - 3975	shcal13
gb_sh_1026	Goldberg, Mychajliw, & Hadly, 2016	-11.0333, -42.1167	3820, 340	3329 - 5054	shcal13
gb_sh_1028	Goldberg, Mychajliw, & Hadly, 2016	-11.0333, -42.1167	6030, 80	6636 - 7027	shcal13
gb_sh_1029	Goldberg, Mychajliw, & Hadly, 2016	-11.0333, -42.1167	6330, 150	6841 - 7475	shcal13
gb_sh_1030	Goldberg, Mychajliw, & Hadly, 2016	-11.0333, -42.1167	6450, 150	6967 - 7578	shcal13
gb_sh_1031	Goldberg, Mychajliw, & Hadly, 2016	-8.90517, -42.6916	2960, 60	2872 - 3234	shcal13

gb_sh_1032	Goldberg, Mychajliw, & Hadly, 2016	-8.90517, -42.6916	3100, 50	3138 - 3383	shcal13
gb_sh_1033	Goldberg, Mychajliw, & Hadly, 2016	-8.90517, -42.6916	3130, 50	3159 - 3407	shcal13
gb_sh_1035	Goldberg, Mychajliw, & Hadly, 2016	-8.90517, -42.6916	4290, 110	4510 - 5064	shcal13
gb_sh_1036	Goldberg, Mychajliw, & Hadly, 2016	-8.90517, -42.6916	4730, 110	5210 - 5614	shcal13
gb_sh_1037	Goldberg, Mychajliw, & Hadly, 2016	-8.8025, -42.4169	6270, 140	6794 - 7422	shcal13
gb_sh_1038	Goldberg, Mychajliw, & Hadly, 2016	-8.8025, -42.4169	9670, 140	10557 - 11275	shcal13
gb_sh_1039	Goldberg, Mychajliw, & Hadly, 2016	-8.87045, -42.9886	10480, 50	12251 - 12443	shcal13
gb_sh_1040	Goldberg, Mychajliw, & Hadly, 2016	-7.99365, -42.2199	2000, 300	1306 - 2544	shcal13
gb_sh_1041	Goldberg, Mychajliw, & Hadly, 2016	-7.99365, -42.2199	10900, 900	10206 - 15133	shcal13
gb_sh_1043	Goldberg, Mychajliw, & Hadly, 2016	-8.86583, -42.5858	10390, 80	11921 - 12433	shcal13
gb_sh_1044	Goldberg, Mychajliw, & Hadly, 2016	-7.48058, -36.6847	3010, 60	2955 - 3272	shcal13
gb_sh_1045	Goldberg, Mychajliw, & Hadly, 2016	-7.48058, -36.6847	3320, 60	3375 - 3641	shcal13
gb_sh_1046	Goldberg, Mychajliw, & Hadly, 2016	-9.00182, -42.7628	7180, 90	7786 - 8171	shcal13

gb_sh_1048	Goldberg, Mychajliw, & Hadly, 2016	-9.00182, -42.7628	8080, 170	8537 - 9418	shcal13
gb_sh_1049	Goldberg, Mychajliw, & Hadly, 2016	-9.00182, -42.7628	9080, 170	9622 - 10585	shcal13
gb_sh_1050	Goldberg, Mychajliw, & Hadly, 2016	-9.00182, -42.7628	9700, 200	10414 - 11629	shcal13
gb_sh_1051	Goldberg, Mychajliw, & Hadly, 2016	-11.1432, -42.1288	3230, 210	2859 - 3901	shcal13
gb_sh_1052	Goldberg, Mychajliw, & Hadly, 2016	-8.844, -42.5616	10270, 35	11796 - 12046	shcal13
gb_sh_1053	Goldberg, Mychajliw, & Hadly, 2016	-7.71324, -42.727	2090, 110	1802 - 2316	shcal13
gb_sh_1054	Goldberg, Mychajliw, & Hadly, 2016	-8.92472, -42.6083	12210, 40	13905 - 14196	shcal13
gb_sh_1055	Goldberg, Mychajliw, & Hadly, 2016	-8.738, -42.743	10400, 100	11819 - 12450	shcal13
gb_sh_1056	Goldberg, Mychajliw, & Hadly, 2016	-8.738, -42.743	10570, 80	12364 - 12673	shcal13
gb_sh_1057	Goldberg, Mychajliw, & Hadly, 2016	-8.738, -42.743	10800, 70	12614 - 12762	shcal13
gb_sh_1058	Goldberg, Mychajliw, & Hadly, 2016	-8.1569, -42.64	2840, 100	2745 - 3179	shcal13
gb_sh_1059	Goldberg, Mychajliw, & Hadly, 2016	-8.1569, -42.64	9180, 40	10219 - 10423	shcal13
gb_sh_1060	Goldberg, Mychajliw, & Hadly, 2016	-8.1569, -42.64	9200, 40	10230 - 10430	shcal13

gb_sh_1061	Goldberg, Mychajliw, & Hadly, 2016	-8.41667, -42.3331	7000, 100	7613 - 7964	shcal13
gb_sh_1062	Goldberg, Mychajliw, & Hadly, 2016	-8.41667, -42.3331	8600, 100	9394 - 9821	shcal13
gb_sh_1063	Goldberg, Mychajliw, & Hadly, 2016	-8.41667, -42.3331	8670, 120	9424 - 9955	shcal13
gb_sh_1064	Goldberg, Mychajliw, & Hadly, 2016	-8.41667, -42.3331	8780, 120	9535 - 9975	shcal13
gb_sh_1065	Goldberg, Mychajliw, & Hadly, 2016	-9.4051, -42.0249	7380, 50	8017 - 8222	shcal13
gb_sh_1066	Goldberg, Mychajliw, & Hadly, 2016	-9.4051, -42.0249	7430, 50	8149 - 8343	shcal13
gb_sh_1067	Goldberg, Mychajliw, & Hadly, 2016	-9.4051, -42.0249	7730, 60	8390 - 8588	shcal13
gb_sh_1068	Goldberg, Mychajliw, & Hadly, 2016	-9.52972, -41.4921	7400, 60	8024 - 8327	shcal13
gb_sh_1069	Goldberg, Mychajliw, & Hadly, 2016	-9.52972, -41.4921	7930, 30	8590 - 8788	shcal13
gb_sh_1070	Goldberg, Mychajliw, & Hadly, 2016	-9.52972, -41.4921	8610, 60	9465 - 9682	shcal13
gb_sh_1072	Goldberg, Mychajliw, & Hadly, 2016	-9.14715, -43.1891	8910, 50	9760 - 10178	shcal13
gb_sh_1075	Goldberg, Mychajliw, & Hadly, 2016	-8.83917, -42.5639	8960, 70	9770 - 10226	shcal13
gb_sh_1076	Goldberg, Mychajliw, & Hadly, 2016	-8.83917, -42.5639	9200, 60	10222 - 10497	shcal13

gb_sh_1077	Goldberg, Mychajliw, & Hadly, 2016	-8.83917, -42.5639	12200, 600	12860 - 15986	shcal13
gb_sh_1078	Goldberg, Mychajliw, & Hadly, 2016	-8.83917, -42.5639	12440, 230	13781 - 15250	shcal13
gb_sh_1079	Goldberg, Mychajliw, & Hadly, 2016	-8.66, -42.725	2790, 110	2698 - 3181	shcal13
gb_sh_1080	Goldberg, Mychajliw, & Hadly, 2016	-8.66, -42.725	2880, 100	2755 - 3218	shcal13
gb_sh_1081	Goldberg, Mychajliw, & Hadly, 2016	-8.66, -42.725	2950, 110	2791 - 3274	shcal13
gb_sh_1082	Goldberg, Mychajliw, & Hadly, 2016	-8.66, -42.725	8500, 60	9395 - 9543	shcal13
gb_sh_1084	Goldberg, Mychajliw, & Hadly, 2016	-8.86889, -42.613	9920, 70	11179 - 11504	shcal13
gb_sh_1085	Goldberg, Mychajliw, & Hadly, 2016	-8.85556, -42.59	9870, 50	11169 - 11355	shcal13
gb_sh_1086	Goldberg, Mychajliw, & Hadly, 2016	-8.85556, -42.59	10640, 50	12512 - 12674	shcal13
gb_sh_1087	Goldberg, Mychajliw, & Hadly, 2016	-8.88392, -42.6321	6900, 70	7577 - 7844	shcal13
gb_sh_1088	Goldberg, Mychajliw, & Hadly, 2016	-8.8519, -41.2998	7330, 50	7981 - 8191	shcal13
gb_sh_1091	Goldberg, Mychajliw, & Hadly, 2016	-22.35, -41.8167	3635, 135	3560 - 4296	shcal13
gb_sh_1092	Goldberg, Mychajliw, & Hadly, 2016	-22.35, -41.8167	3975, 160	3968 - 4831	shcal13

gb_sh_1093	Goldberg, Mychajliw, & Hadly, 2016	-23.0046, -42.0033	2068, 31	1903 - 2060	shcal13
gb_sh_1094	Goldberg, Mychajliw, & Hadly, 2016	-23.0046, -42.0033	3180, 40	3236 - 3449	shcal13
gb_sh_1095	Goldberg, Mychajliw, & Hadly, 2016	-22.986, -42.0139	2440, 40	2341 - 2540	shcal13
gb_sh_1096	Goldberg, Mychajliw, & Hadly, 2016	-22.986, -42.0139	3060, 50	3058 - 3364	shcal13
gb_sh_1099	Goldberg, Mychajliw, & Hadly, 2016	-24.8692, -47.8856	4070, 100	4242 - 4827	shcal13
gb_sh_1100	Goldberg, Mychajliw, & Hadly, 2016	-24.8833, -47.885	4440, 80	4843 - 5145	shcal13
gb_sh_1101	Goldberg, Mychajliw, & Hadly, 2016	-24.8833, -47.885	4680, 110	5034 - 5592	shcal13
gb_sh_1103	Goldberg, Mychajliw, & Hadly, 2016	-23.0107, -43.5767	2260, 160	1880 - 2712	shcal13
mc_in_0001	McMichael & Bush, 2019	-0.794, -63.097	1150, 25	980 - 1098	intcal13
mc_in_0002	McMichael & Bush, 2019	-0.794, -63.097	1290, 25	1221 - 1284	intcal13
mc_in_0003	McMichael & Bush, 2019	-0.794, -63.097	1310, 30	1224 - 1294	intcal13
mc_in_0004	McMichael & Bush, 2019	-2.47, -60	470, 130	275 - 685	intcal13
mc_in_0005	McMichael & Bush, 2019	-2.47, -60	520, 120	308 - 681	intcal13

mc_in_0006	McMichael & Bush, 2019	-2.47, -60	580, 120	423 - 738	intcal13
mc_in_0007	McMichael & Bush, 2019	-2.47, -60	890, 170	618 - 1152	intcal13
mc_in_0008	McMichael & Bush, 2019	-2.49, -60	970, 140	666 - 1181	intcal13
mc_in_0009	McMichael & Bush, 2019	-2.49, -60	980, 120	684 - 1095	intcal13
mc_in_0010	McMichael & Bush, 2019	-2.47, -60	1050, 220	636 - 1368	intcal13
mc_in_0011	McMichael & Bush, 2019	-2.49, -60	1080, 140	739 - 1275	intcal13
mc_in_0012	McMichael & Bush, 2019	-2.49, -60	1140, 130	890 - 1293	intcal13
mc_in_0013	McMichael & Bush, 2019	-2.5, -60	1170, 120	901 - 1305	intcal13
mc_in_0014	McMichael & Bush, 2019	-2.45, -60	1170, 280	632 - 1622	intcal13
mc_in_0015	McMichael & Bush, 2019	-2.49, -60	1270, 120	937 - 1382	intcal13
mc_in_0017	McMichael & Bush, 2019	-2.49, -60	1280, 150	921 - 1424	intcal13
mc_in_0018	McMichael & Bush, 2019	-2.45, -60	1280, 120	953 - 1396	intcal13
mc_in_0019	McMichael & Bush, 2019	-2.46, -60	1400, 120	1059 - 1553	intcal13

mc_in_0020	McMichael & Bush, 2019	-2.49, -60	1430, 130	1062 - 1607	intcal13
mc_in_0021	McMichael & Bush, 2019	-2.45, -60	1430, 140	1054 - 1621	intcal13
mc_in_0022	McMichael & Bush, 2019	-2.48, -60	1470, 160	1053 - 1724	intcal13
mc_in_0023	McMichael & Bush, 2019	-2.5, -60	1480, 240	924 - 1904	intcal13
mc_in_0024	McMichael & Bush, 2019	-2.48, -60	1510, 190	1053 - 1829	intcal13
mc_in_0025	McMichael & Bush, 2019	-2.48, -60	1530, 120	1256 - 1709	intcal13
mc_in_0026	McMichael & Bush, 2019	-2.45, -60	1670, 140	1308 - 1874	intcal13
mc_in_0027	McMichael & Bush, 2019	-2.45, -60	1750, 230	1258 - 2182	intcal13
mc_in_0028	McMichael & Bush, 2019	-2.45, -60	1800, 190	1312 - 2151	intcal13
mc_in_0029	McMichael & Bush, 2019	-2.45, -60	2410, 120	2298 - 2751	intcal13
mc_in_0030	McMichael & Bush, 2019	-1.98, -58.4	910, 60	724 - 931	intcal13
mc_in_0031	McMichael & Bush, 2019	-2.15, -58.95	1040, 70	788 - 1088	intcal13
mc_in_0032	McMichael & Bush, 2019	-1.98, -58.5	1050, 70	794 - 1090	intcal13

mc_in_0033	McMichael & Bush, 2019	-2.45, -58.57	1190, 70	969 - 1268	intcal13
mc_in_0034	McMichael & Bush, 2019	-2.1, -58.5	1200, 70	976 - 1273	intcal13
mc_in_0035	McMichael & Bush, 2019	-2.1, -58.5	1230, 80	981 - 1290	intcal13
mc_in_0036	McMichael & Bush, 2019	-2.1, -58.55	1240, 70	1049 - 1293	intcal13
mc_in_0038	McMichael & Bush, 2019	-2.45, -58.57	1290, 70	1058 - 1327	intcal13
mc_in_0039	McMichael & Bush, 2019	-1.6, -58.55	1320, 70	1070 - 1346	intcal13
mc_in_0040	McMichael & Bush, 2019	-2.2, -58.55	1360, 90	1061 - 1416	intcal13
mc_in_0041	McMichael & Bush, 2019	-2.15, -58.95	1490, 80	1284 - 1547	intcal13
mc_in_0042	McMichael & Bush, 2019	-2.2, -58.55	1640, 130	1301 - 1824	intcal13
mc_in_0043	McMichael & Bush, 2019	-2.2, -58.55	1800, 60	1594 - 1868	intcal13
mc_in_0044	McMichael & Bush, 2019	1.7, -67.4	250, 50	261 - 343	intcal13
mc_in_0045	McMichael & Bush, 2019	1.8, -67.7	250, 60	255 - 482	intcal13
mc_in_0046	McMichael & Bush, 2019	1.65, -67.3	260, 50	267 - 467	intcal13

mc_in_0047	McMichael & Bush, 2019	1.05, -67.7	350, 70	286 - 517	intcal13
mc_in_0048	McMichael & Bush, 2019	1.8, -67.7	400, 80	292 - 547	intcal13
mc_in_0049	McMichael & Bush, 2019	1.65, -67.3	430, 60	420 - 544	intcal13
mc_in_0050	McMichael & Bush, 2019	1.6, -67.3	480, 50	451 - 561	intcal13
mc_in_0051	McMichael & Bush, 2019	1.05, -67.7	500, 50	474 - 564	intcal13
mc_in_0052	McMichael & Bush, 2019	1.25, -67.5	530, 50	502 - 568	intcal13
mc_in_0053	McMichael & Bush, 2019	1.7, -67.4	640, 50	545 - 672	intcal13
mc_in_0054	McMichael & Bush, 2019	1.6, -67.3	670, 50	551 - 685	intcal13
mc_in_0055	McMichael & Bush, 2019	1.25, -67.5	740, 50	639 - 762	intcal13
mc_in_0056	McMichael & Bush, 2019	1.6, -67.3	920, 90	677 - 980	intcal13
mc_in_0057	McMichael & Bush, 2019	1.25, -67.5	1040, 50	899 - 1062	intcal13
mc_in_0058	McMichael & Bush, 2019	1.6, -67.3	1100, 90	899 - 1188	intcal13
mc_in_0059	McMichael & Bush, 2019	1.6, -67.3	1100, 50	928 - 1093	intcal13

mc_in_0060	McMichael & Bush, 2019	1.25, -67.5	1170, 50	964 - 1185	intcal13
mc_in_0061	McMichael & Bush, 2019	1.7, -67.4	1180, 90	951 - 1278	intcal13
mc_in_0062	McMichael & Bush, 2019	1.7, -67.4	1220, 80	978 - 1287	intcal13
mc_in_0063	McMichael & Bush, 2019	1.25, -67.5	1230, 90	968 - 1296	intcal13
mc_in_0064	McMichael & Bush, 2019	1.65, -67.3	1240, 50	1060 - 1282	intcal13
mc_in_0065	McMichael & Bush, 2019	1.7, -67.4	1260, 80	1046 - 1305	intcal13
mc_in_0066	McMichael & Bush, 2019	1.05, -67.7	1290, 80	1052 - 1344	intcal13
mc_in_0068	McMichael & Bush, 2019	1.25, -67.5	1340, 60	1172 - 1367	intcal13
mc_in_0069	McMichael & Bush, 2019	1.8, -67.7	1400, 140	1045 - 1570	intcal13
mc_in_0070	McMichael & Bush, 2019	1.65, -67.3	1410, 80	1180 - 1424	intcal13
mc_in_0071	McMichael & Bush, 2019	1.63, -67.45	1430, 60	1261 - 1419	intcal13
mc_in_0072	McMichael & Bush, 2019	1.05, -67.7	1540, 80	1298 - 1571	intcal13
mc_in_0073	McMichael & Bush, 2019	1.7, -67.4	1560, 60	1327 - 1564	intcal13

mc_in_0074	McMichael & Bush, 2019	1.7, -67.4	1700, 60	1516 - 1740	intcal13
mc_in_0075	McMichael & Bush, 2019	1.63, -67.45	2070, 80	1870 - 2186	intcal13
mc_in_0076	McMichael & Bush, 2019	1.6, -67.3	6260, 110	6912 - 7420	intcal13
mc_in_0077	McMichael & Bush, 2019	-3.412, -64.562	430, 25	462 - 523	intcal13
mc_in_0078	McMichael & Bush, 2019	-3.434, -64.624	470, 30	494 - 540	intcal13
mc_in_0079	McMichael & Bush, 2019	-3.4, -64.6	970, 25	796 - 875	intcal13
mc_in_0080	McMichael & Bush, 2019	-3.414, -64.617	1700, 30	1544 - 1637	intcal13
mc_in_0081	McMichael & Bush, 2019	-3.408, -64.562	1970, 50	1817 - 2050	intcal13
mc_in_0082	McMichael & Bush, 2019	-3.407, -64.614	2580, 30	2699 - 2762	intcal13
mc_sh_0001	McMichael & Bush, 2019	-3.191, -60.346	1590, 40	1354 - 1534	shcal13
mc_sh_0002	McMichael & Bush, 2019	-3.191, -60.346	1610, 90	1302 - 1617	shcal13
mc_sh_0003	McMichael & Bush, 2019	-3.191, -60.346	1800, 80	1511 - 1884	shcal13
mc_sh_0004	McMichael & Bush, 2019	-3.191, -60.346	2280, 100	1997 - 2494	shcal13

mc_sh_0005	McMichael & Bush, 2019	-3.549, -59.2	1800, 40	1571 - 1748	shcal13
mc_sh_0006	McMichael & Bush, 2019	-3.549, -59.2	2370, 30	2305 - 2462	shcal13
mc_sh_0038	McMichael & Bush, 2019	-14.555, -60.217	2315, 54	2147 - 2379	shcal13
mc_sh_0043	McMichael & Bush, 2019	-3.11, -60.06	350, 40	300 - 473	shcal13
mc_sh_0044	McMichael & Bush, 2019	-3.11, -60.06	570, 40	502 - 563	shcal13
mc_sh_0045	McMichael & Bush, 2019	-3.11, -60.06	890, 120	622 - 965	shcal13
mc_sh_0046	McMichael & Bush, 2019	-3.11, -60.06	910, 40	684 - 822	shcal13
mc_sh_0047	McMichael & Bush, 2019	-3.11, -60.06	960, 40	746 - 919	shcal13
mc_sh_0048	McMichael & Bush, 2019	-3.11, -60.06	960, 30	760 - 918	shcal13
mc_sh_0049	McMichael & Bush, 2019	-3.11, -60.06	980, 40	765 - 927	shcal13
mc_sh_0050	McMichael & Bush, 2019	-3.11, -60.06	1000, 40	773 - 932	shcal13
mc_sh_0052	McMichael & Bush, 2019	-3.11, -60.06	1010, 80	725 - 991	shcal13
mc_sh_0053	McMichael & Bush, 2019	-3.11, -60.06	1070, 70	773 - 1065	shcal13

mc_sh_0054	McMichael & Bush, 2019	-3.11, -60.06	1070, 50	800 - 993	shcal13
mc_sh_0055	McMichael & Bush, 2019	-3.11, -60.06	1080, 40	901 - 994	shcal13
mc_sh_0056	McMichael & Bush, 2019	-3.11, -60.06	1250, 80	962 - 1275	shcal13
mc_sh_0057	McMichael & Bush, 2019	-3.11, -60.06	1300, 40	1074 - 1271	shcal13
mc_sh_0058	McMichael & Bush, 2019	-3.11, -60.06	2310, 120	2003 - 2545	shcal13
mc_sh_0059	McMichael & Bush, 2019	-3.09, -60.07	950, 40	740 - 915	shcal13
mc_sh_0060	McMichael & Bush, 2019	-3.09, -60.07	950, 30	744 - 908	shcal13
mc_sh_0062	McMichael & Bush, 2019	-3.09, -60.07	1050, 40	799 - 967	shcal13
mc_sh_0063	McMichael & Bush, 2019	-3.09, -60.07	1100, 30	921 - 990	shcal13
mc_sh_0064	McMichael & Bush, 2019	-3.09, -60.07	1130, 40	929 - 1061	shcal13
mc_sh_0065	McMichael & Bush, 2019	-3.09, -60.07	1150, 40	928 - 1074	shcal13
mc_sh_0066	McMichael & Bush, 2019	-3.09, -60.07	1260, 40	1055 - 1192	shcal13
mc_sh_0067	McMichael & Bush, 2019	-3.09, -60.07	1940, 60	1709 - 1939	shcal13

mc_sh_0068	McMichael & Bush, 2019	-3.08, -60.08	1290, 40	1069 - 1197	shcal13
mc_sh_0069	McMichael & Bush, 2019	-3.08, -60.08	1290, 30	1072 - 1192	shcal13
mc_sh_0070	McMichael & Bush, 2019	-3.08, -60.08	1310, 40	1086 - 1274	shcal13
mc_sh_0071	McMichael & Bush, 2019	-3.08, -60.08	1320, 60	1066 - 1298	shcal13
mc_sh_0072	McMichael & Bush, 2019	-3.08, -60.08	1330, 40	1158 - 1294	shcal13
mc_sh_0073	McMichael & Bush, 2019	-3.08, -60.08	1340, 40	1166 - 1299	shcal13
mc_sh_0074	McMichael & Bush, 2019	-3.08, -60.08	1350, 40	1171 - 1303	shcal13
mc_sh_0075	McMichael & Bush, 2019	-3.08, -60.08	1350, 30	1181 - 1294	shcal13
mc_sh_0076	McMichael & Bush, 2019	-3.08, -60.08	1360, 50	1159 - 1309	shcal13
mc_sh_0077	McMichael & Bush, 2019	-3.08, -60.08	1370, 40	1177 - 1309	shcal13
mc_sh_0078	McMichael & Bush, 2019	-3.08, -60.08	1440, 70	1176 - 1433	shcal13
mc_sh_0079	McMichael & Bush, 2019	-3.08, -60.08	1550, 40	1311 - 1488	shcal13
mc_sh_0080	McMichael & Bush, 2019	-3.08, -60.08	1730, 90	1400 - 1754	shcal13

mc_sh_0081	McMichael & Bush, 2019	-3.08, -60.08	1980, 80	1705 - 2085	shcal13
mc_sh_0082	McMichael & Bush, 2019	-3.08, -60.08	2120, 40	1985 - 2154	shcal13
mc_sh_0084	McMichael & Bush, 2019	-3.11, -60.06	1250, 70	973 - 1271	shcal13
mc_sh_0156	McMichael & Bush, 2019	-8.863, -64.062	1250, 30	1056 - 1185	shcal13
mc_sh_0157	McMichael & Bush, 2019	-8.863, -64.062	1550, 30	1313 - 1476	shcal13
mc_sh_0158	McMichael & Bush, 2019	-8.863, -64.062	2730, 75	2699 - 2998	shcal13
mc_sh_0159	McMichael & Bush, 2019	-8.863, -64.062	3170, 30	3237 - 3409	shcal13